Modeling and Control of a Hot Micro-Embossing Machine

By

Grant T. Shoji

B.S., Mechanical Engineering
University of California, Berkeley, 2004

Submitted to the Department of Mechanical Engineering
in Partial Fulfillment of the Requirements for the Degree of

Master of Science in Mechanical Engineering

at the

Massachusetts Institute of Technology

June 2006

Signature of Author . . . .
Department of Mechanical Engineering
May 12, 2006

Certified by . . . .
David E. Hardt
Professor of Mechanical Engineering
Thesis Supervisor

Accepted by . . . .
Lallit Anand
Chairman, Department Committee on Graduate Students

This page intentionally left blank

Modeling and Control of a Hot Micro-Embossing Machine

by

Grant T. Shoji

Submitted to the Department of Mechanical Engineering on May 12, 2006
in Partial Fulfillment of the Requirements for the Degree of
Master of Science in Mechanical Engineering

ABSTRACT

As the market for polymer micro- and nano-devices expands there is an ever-present need for a manufacturing standard to mass produce these parts. A number of techniques for fabricating these devices are soft lithography, micro-injection molding, and micro-embossing. Micro-embossing shows great promise in terms of versatility in creating various structures, but its shortcoming is a relatively long cycle time. Therefore, it is imperative to find efficient ways of heating and cooling in addition to having good control of critical processing parameters. This thesis will address the modeling and control of a hot micro-embossing system which utilizes oil as the heating and cooling medium. There were three thermal requirements addressed for the system: steady state temperatures within ± 1 °C, fast as possible heating and cooling cycles, and being robust to various embossing and de-embossing processing temperatures. A model of the major thermal components in the system was developed and correlated well with experimental data. It was confirmed with simulation and experimentation that a lower flow rate achieved faster heating and a higher flow rate produced faster cooling. In order to address the steady state temperature requirement a variable gain PI controller was implemented. During heating the feedback signal was the platen temperature and during cooling the feedback signal was the mixing valve fluid outlet temperature. This variable gain PI controller in combination with the variable flow rates produced steady state temperatures for both platens from 55 to 120 °C within ± 1 °C in 138 seconds. Cooling for both platens from 120 to 55 °C was achieved in 190 seconds. This controller worked for a variety of processing temperatures. A Labview interface was developed to automate this process for temperature step changes. Polymer microfluidic channels were successfully fabricated using this hot micro-embossing system with automated thermal control in a short cycle time.

Thesis supervisor: David E. Hardt
Title: Professor of Mechanical Engineering

This page intentionally left blank

Acknowledgements

First and foremost, I would like to thank my parents and family for their undying love and support. I could not have realized most of my dreams without you all in my life. My experience at MIT will always be cherished.

I would like to thank Professor Dave Hardt for taking me into his research group. Before I joined the group I had heard from his previous students that not only was he a great advisor but an even better person. As I have worked under your guidance you have surpassed all of these expectations. I am grateful for the knowledge and guidance you have provided me with throughout my graduate studies.

I would like to thank Kunal Thaker for working with me on so many aspects of this project. Your help with the design and construction of the machine, metrology study, and daily advice is much appreciated. Matthew Dirckx has helped with the design and modeling of the machine. I would also like to thank Wang Qi and Adam Rzepniewski for their help in the lab. Thank you to Catherine Nichols and Erica McDaniel for processing purchase orders and providing us with ample free food.

Thanks to Hayden Taylor for his help in making our lab DRIE silicon tools. Dan Burns has helped me with AFM measurements for the metrology study. Thank you to Gerry Wentworth for helping me out in the machine shop. I would also like to thank my friends in 35-135 for making everyday at work fun.

Finally, I would like to thank the SMA for funding this research and making my work at MIT possible.

This page intentionally left blank

Table of contents

List of Figures

List of Tables

Nomenclature

Symbol	Description
A	Contact surface area between the fluid and platen
A_{fm}	Area of heat transfer between the fluid and thermal mass
A_s	Total heat transfer surface area
c_p	Specific heat of the fluid into the platen
c_{pa}	Specific heat of the average heater fluid temperature
c_{pc}	Specific heat of the fluid on the cold side of the mixing valve
c_{ph}	Specific heat of the fluid on the hot side of the mixing valve
c_{pi}	Specific heat of the fluid at the heater inlet temperature
c_{pm}	Specific heat of the thermal mass
c_{po}	Specific heat of the fluid at the heater outlet temperature
C_h	Hot capacity rate
C_{min}	Minimum capacity rate
C_{max}	Maximum capacity rate
C_v	Flow coefficient
C^*	Capacitance ratio
D	Diameter of the platen channel
D_e	Effective diameter
D_h	Hydraulic diameter
$\dot{E}_g$	Energy generated
$\dot{E}_{in}$	Energy into the system
$\dot{E}_{out}$	Energy out of the system
$\dot{E}_{st}$	Energy stored in the system
f	Friction factor
h	Heat transfer coefficient between the fluid and the platen
h_c	Smaller channel dimension
h_{fm}	Heat transfer coefficient between the fluid in the heater and thermal mass
H	Pressure head
HP	Horsepower
k	Thermal conductivity of the fluid
k_m	Thermal conductivity of the fluid at the heater inlet temperature
K	Constant for the 1st order system
L	Length of channel
$\dot{m}$	Mass flow rate of fluid through the platen
$MP_{Efficiency}$	Motor and pump efficiency
N	Valve authority
NTU	Number of transfer units
N_u	Nusselt number
OD_T	Diameter of the heater coils
P	Perimeter of the platen channel
Pr	Prandtl number
P_T	Heater coil pitch
q	Heat transfer rate

Q	Flow rate
Q_h	Flow rate of the fluid on the hot side of the mixing valve
Q_p	Flow rate of the fluid on the outlet of the mixing valve
Re	Reynolds number
s	Laplace transform of a derivative
SG	Specific gravity
T_a	Average of the fluid inlet and outlet temperatures
T_c	Temperature of the fluid on the cold side of the mixing valve
$T_{c,i}$	Cold fluid inlet temperature
T_h	Temperature of the fluid on the hot side of the mixing valve
$T_{h,i}$	Hot fluid inlet temperature
$T_{h,o}$	Hot fluid outlet temperature
T_i	Temperature of the heater inlet fluid
T_{ip}	Temperature of the fluid into the platen
T_m	Temperature of the thermal mass
T_{median}	Median temperature of the fluid in the platen
T_o	Temperature of the heater outlet fluid
T_{op}	Temperature of the fluid out of the platen
T_p	Temperature of the fluid out of the mixing valve
T_s	Surface temperature of the platen
$\overline{U}$	Overall heat transfer coefficient
V	Fluid volume of the heater
Vel	Velocity of the fluid
V_m	Volume of the thermal mass
w	Larger channel dimension
ΔP_1	Pressure drop across a fully opened valve
ΔP_2	Pressure drop across the remainder of the system
ε	Effectiveness
μ	Dynamic viscosity
ξ	Damping ratio
ρ	Density of the fluid
ρ_a	Density of the fluid at the average heater temperature
ρ_h	Density of the fluid on the hot side of the mixing valve
ρ_i	Density of the fluid at the heater inlet temperature
ρ_m	Density of the thermal mass
ρ_o	Density of the fluid at the heater outlet temperature
ρ_p	Density of the fluid on the outlet side of the mixing valve
τ	Time constant
ω_n	Natural frequency

CHAPTER

1 Introduction

1.1 Overview of Thesis

As part of the SMA II Manufacturing Systems and Technology Research Program at MIT, significant research is being conducted to "develop engineering-science-based processing procedures for producing polymer based micro- and nano-structures" [1]. As quoted from the SMA II research proposal, this program has three specific research tasks [1]:

1. Develop engineering-science-based processing procedures for producing polymer-based micro- and nano-structures
2. Develop fundamental methods for design of high-throughput machines for micro-casting, micro-forging and micro-injection molding suitable for commercial scale production
3. Develop methods for ensuring optimal process performance in a large scale, high volume, high flexibility manufacturing environment

This thesis will address task 2 of this research program regarding the modeling and control of a hot micro-embossing machine. The remainder of this chapter will comment on motivating factors driving this research program. Chapter 2 discusses various methods for creating polymer based micro- and nano-structures with an in-depth focus on micro-embossing. Chapter 3 details the design and construction of the second generation hot micro-embossing machine (HME II) in the Manufacturing Process Control Laboratory (MPCL). Thermal modeling and system characterization of the HME II is discussed in Chapter 4, followed by its temperature controller design in Chapter 5. Chapter 6 covers automation of the thermal system and development of the graphical user-interface (GUI). Plastic parts were created on the HME II and the results with regards to process control are analyzed in Chapter 7. Finally, Chapter 8 summarizes the thermal performance of the HME II and provides suggestions for future work modifying or creating the next generation HME machine.

1.2 Move toward Micro/Nano Plastic Devices

Popularity of the PC and electronic hand-held devices has fueled the semiconductor market since the late 20th century. As these consumer products got more sophisticated and compact, the need to manufacture smaller and faster IC chips became imperative. Recently, growth in the semiconductor industry has slowed down due to the dot-com bubble burst in 2001. On the contrary, a sector recently evoking investor's interest with supporting technology mirroring the evolution of the IC chip is the biotechnology industry [2]. Smaller and more complex microfluidic systems in the biotechnology sector are becoming ubiquitous as companies desire to use smaller amounts of reagents, execute high throughput screening, integrate numerous steps on a chip, and reduce costs [3]. Although silicon and glass are still widely used for microfluidic applications, there is a noticeable shift toward creating these devices using plastics because of its favorable properties and cost [4].

1.2.1 Potential Applications and Devices

Biological applications seem to be the major growth area for polymer micro- and nano-structures. These applications range anywhere from biomolecular separation, bioassays, polymerase chain reaction (PCR), micro-total analysis system (μTAS) or lab-on-a-chip [5,6,7]. The most common devices for these applications are microchannels, microfluidics devices, microarrays and microreactors [8].

Another potential hot-bed for polymer micro- and nano-structures is micro-optical devices. Currently, most of the applications for these devices stem from the telecommunications and data communications industry [9]. Common micro-optical devices are optical gratings, micro-lenses, and micro-prisms [10,11].

1.2.2 Existing Processes to Create these Devices

During early development of microfluidic devices the most common fabrication techniques were ones adopted from the IC industry. Silicon or glass was typically patterned using lithographic techniques and then etched to define features [12,13]. A prevalent and simple method to create a microfluidic device is isotropic wet etching [14]. Another accepted method using silicon or glass as a substrate is e-beam lithography.

Although IC fabrication techniques are well established, the downside is that these processes are very costly and time consuming. Therefore, industry and research is moving toward using different processes to replicate features in plastic. Established techniques for manufacturing micro- and nano-devices in plastic include micro-casting, micro-injection molding, and micro-embossing. These techniques will be covered in more detail in Section 2.1.

1.2.3 Advantages of Plastic

The most evident advantage for using plastic as a substrate over traditional silicon or glass is cost. One of the most commonly used plastic in microfluidic devices is polydimethylsiloxane (PDMS), which is quoted to be 50 times cheaper than silicon on a per volume basis. Other plastics such as polymethylmethacrylate (PMMA) cost 0.2-2 cents/cm^2, compared with boro-float glass (10-20 cents/cm^2), boro-silicate glass (5-15 cents/cm^2), and photostructurable glass (20-40 cents/cm^2) [14]. Direct cost is not the only benefit to using plastic, but its affordability and shortened time to produce a device opens restrictions to allow a lot more people to work on this technology accelerating innovation [4].

Another favorable property of plastic is its surface properties enabling it to be compatible with a lot of microfluidic applications. Silicon has the tendency to attract biomolecules making them stick to the wall surface and hindering flow in fluid applications [14]. Plastics such as PMMA are hydrophobic, meaning it repels water making it conducive for flow applications [15].

Plastics also have superior optical properties compared to silicon. Many applications require optical clarity for DNA detection using high powered laser microscopes [16]. Plastics are also widely used for microphotonic applications, where tunable optical properties via various methods are essential for device success [17].

1.3 Manufacturing of Polymer Micro- and Nano-Devices

Currently, a wealth of research related to polymer micro- and nano-devices deal with creating innovative devices. Novel designs will potentially create new applications broadening the market for plastic devices. An article from The Industrial Physicist mentions the fact that, "although microfluidics devices are entering the marketplace, no industry standard exists, even for the simplest components [18]." As the volume of fabricated parts increases, standardization of manufacturing practices becomes imperative.

1.3.1 Market Analysis

There are many indicators that suggest the market for polymer micro- and nano-devices is growing. Biotechnology companies are the primary users of microfluidics devices. Speculation in 1997 estimated the market for disposable DNA biomedical diagnostic devices to be over one billion parts per year [19]. This number should increase as pharmaceutical companies expect the need for drugs to grow because of the increase in the aging population where globally the over-60 crowd is expected to increase from 66 million in 2000 to close to 2 billion by the year 2050 [20]. In order to quantify the market growth potential, an analysis by Ducre suggests microfluidic applications in the life sciences have a global market of roughly 500 million euros, which could grow to 1.4 billion euros by 2008 [21].

The other large market for polymer micro- and nano-devices is micro-optics. The main industries utilizing this technology are telecommunication and datacommunication companies. MIT's Microphotonics Center summarized the markets and potential for plastic devices in Table 1-1. As the market grows and more parts need to be fabricated manufacturing issues also grow in importance.

Table 1-1 Market drivers for plastics in optoelectronics [9]

Industry	Application	Product Examples	Requirements	What Organics Offer	Technology Needed	Timing of Market Need
Telecom	Optical signal routing, switching, and power level control (Long-haul, Metro)	•ROADM •Wavelength blocker •WSS •OXC •Protection switches •VOA arrays •VMUX •DCE •DGE	• Low cost (CapEx & OpEx for OEM & carrier) • High reliability • Small size • Low power dissipation • Ease of scalability • Simple fiber management	Meet all requirements. Unique attributes: • Lowest power consumption dynamic thermo-optic components • Practical hybrid integration enabling complex functionality PLCs today in material with state-of-the-art performance	Cost-effective 'pick-and-place' assembly technology	Now
	Optical signal distribution (Access, FTTx)	•Splitters •Athermal mux/demux	• Low CapEx for OEM & carrier • Low OpEx for OEM & carrier • High reliability • Athermal passive behavior	Meet all requirements. Unique attributes: • Low cost, high volume replication techniques (stamping, etc.) • Athermal AWG with substrate of proper CTE	Low cost fiber arrays	Now
Datacom (Computer, Automotive, Aerospace, Security)	Short reach data links for entertainment and control systems in Digital Home and Vehicles	•Plastic Optical Fiber (POF)	• Ease of splicing and connecting • Light weight • Low bending loss • Resiliency to mechanical impact	Meet all requirements. Unique attributes: • Multimode graded index POF meeting all requirements. • With transparency windows at 850, 670, and 530 nm, it is compatible with silicon or polymer photodetectors, and with silica or polymer waveguide circuits.		Now
	Computing	•Optical interconnects on backplanes/boards/MCM for workstations and servers, and eventually personal computers	• Low cost • Low loss • Ease of connecting • PCB lamination (temperature & pressure) compatibility	Unique attributes: • Easy to manufacture and cost effective large area optics (larger than common photomasks)	Dust-resistant connectors	5-10 years
	Computing	•On-chip optical interconnects for workstations and servers, and eventually personal computers	• Low cost • Low loss • Ease of connecting • Light weight • Low bending loss • CMOS compatibility	Unique attributes: • Ease of coating on CMOS chips • Processability with reduced temperature excursions • Rapid and cost-effective manufacturing	Compact and inexpensive integrated transceivers, amplifiers, etc.	20-30 years
Display, Imaging, Scanning, Learning	Information display	•Displays in consumer products (cell phones, digital cameras, electronic newspapers, etc.) •Signage •Light collection waveguide arrays in optical scanners	• Low cost (eventually enabling omnipresent displays, disposable displays, etc.) • Light weight • Flexibility • Impact resistance • Wide viewing angle	Meet all requirements. Unique attributes: • Flexibility • Impact resistance		Now
Military, Medical	Sensing, Monitoring	•OEIC in your shirt	• Sensing fabrics • Light weight	Unique attributes: • Organic sensing fibers can be woven into comfortable, lightweight clothing	Further development of sensing fibers	5-10 years

1.3.2 Importance of Manufacturing

A number of applications for polymer micro- and nano-devices could possibly have stringent dimensional requirements. Rectangular microfluidic channels with certain aspect ratios for flowing Newtonian fluids in the laminar regime are governed by the Hagan-Poiseuille equation where the fluid resistance is shown in Equation 1-1 [22]. Where μ is the fluid viscosity, L is the length of the channel, w is the larger channel dimension, and h_c is the smaller channel dimension. This equation shows the flow is extremely sensitive to the smaller dimension of the channel. If the device is manufactured incorrectly, it could drastically alter the predicted flow performance.

$$R = \frac{12\mu L}{wh_c^{\,3}}$$

Equation 1-1

Dimensional accuracy is also essential for micro-optical components. A paper by Rossi [11] outlined a number of fabrication specifications needed to create high fidelity micro-optical modules. Alignment needed to be within ± 2 μm over the replicated area and the planarity needed to be better than ± 5 μm. Manufacturing practice based on fundamental understanding will reduce the number of devices that are out of compliance and cut down on costs.

1.3.3 Prior Research on Manufacturing

With any manufacturing process it is important to understand the sources of process variation and learn how to reduce variation by changing the appropriate processing conditions. The number of studies regarding manufacturing issues for polymer micro-devices is limited and non-standardized. A few research groups' initial characterization tests for micro-embossing are presented in this section.

A study by Lin's [23] research group compared hot embossed micro structures in a laboratory and commercial environment. Micro pyramid structures were created and their quality was evaluated based on qualitative SEM images and AFM surface roughness measurements. They found a noticeable difference between the parts created in a laboratory environment versus a commercial environment, lending to the fact that quality control was an important issue when these micro devices were created at high rates.

Another study by Lin's [24] group characterized micro-embossed microlenses under various processing conditions such as pressure, temperature, and time. The height and radius of curvature of the lens were used as a metric for quantifying the quality of the part. It was found that processing temperature was the dominant parameter affecting the final outcome of the part.

A paper by Chen [25] characterized the micro hot embossing process for polymer splitters using the Taguchi method. The typical characteristic feature dimensions were 50 μm in depth with a choose ratio of 33. These features were embossed using a 4" silicon wafer tool. Using a micro hot embossing system from Jenoptik Mikrotechnik model HEX 03, it was found that the optimal process parameters was an embossing temperature of 120 °C, embossing force of 32,500 N, embossing time of 270 seconds, and de-molding temperature of 70 °C. This paper gave a solid foundation for defining target processing parameters for the micro-embossing process.

A similar study by Hardt et. al. [26] and Qi [27] was conducted in the Laboratory for Manufacturing and Productivity (LMP) to investigate process window characterization for the micro-embossing process. A copper tool with features 50 μm tall and 500 μm wide was embossed in PMMA under various processing conditions. It was found that an embossing temperature of 110 °C produced the best replicated parts.

CHAPTER

2 Background

2.1 Various Types of Plastic Micro-Manufacturing

A number of techniques used to create plastic micro-devices have been established with the most common being soft lithography, micro injection molding, and micro embossing. Some techniques are tailored for specific materials and each has their pros and cons. The aforementioned techniques will be detailed in the following sections.

2.1.1 Soft Lithography

Soft lithography is a process where a base and curing agent is mixed, degassed, poured over a mold, and baked at an elevated temperature. The resulting part, usually made of PDMS, is then removed from the mold (Figure 2-1). There are a number of advantages to using soft lithography including the ability to utilize common wafer fabrication equipment to create parts, the material's ability to diffuse gas, and the material's good chemical stability. Its disadvantages are shrinkage upon curing, difficulty achieving accurate dimensional replication over a large area, and inability to create high fidelity extremely low and high aspect ratio features [28]. This technique shows great promise for laboratory prototyping, but might not be the best for mass production of parts.

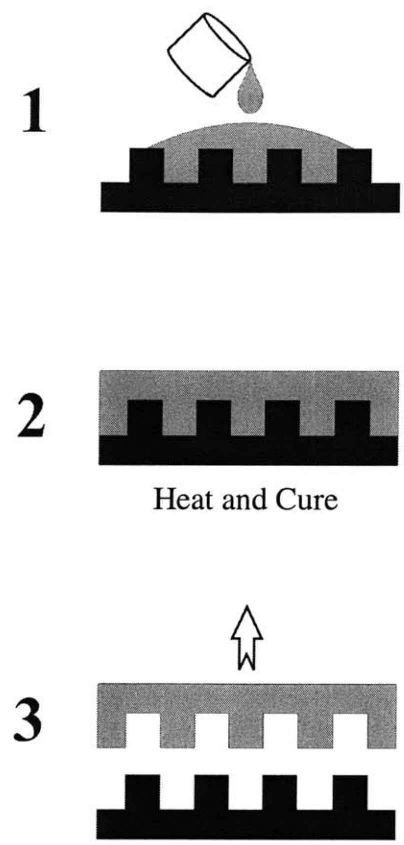

Figure 2-1 Schematic of the soft lithography process [29]

2.1.2 Micro Injection Molding

In micro-injection molding a mold is heated above the plastic glass transition temperature, molten plastic is injected into the mold, the mold and part is then cooled and separated to release the plastic part (Figure 2-2) [30]. One of the advantages to using micro-injection molding is that it has one of the fastest cycle times out of all the polymer fabrication methods. However, this process is limited by its inability to easily replicate high aspect ratio parts (>10) [31].

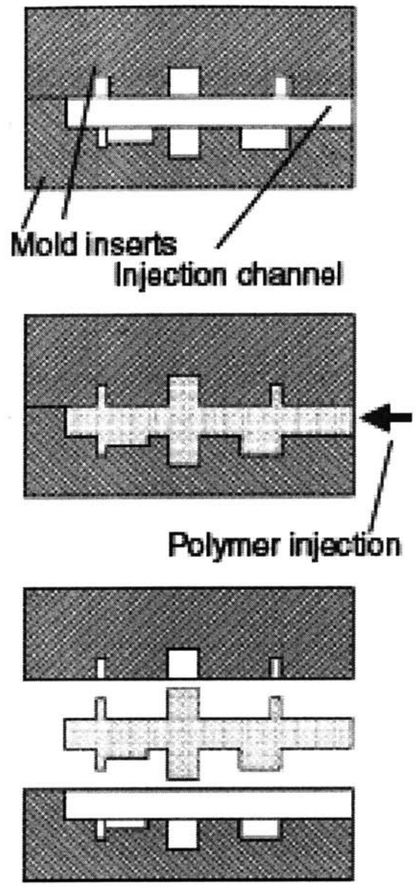

Figure 2-2 Schematic of the micro-injection molding process [30]

2.1.3 Micro-Embossing

The micro-embossing process involves heating a tool and work piece above the glass transition temperature of the plastic, then applying a force to deform the plastic, the stack is then cooled under a constant force, once the platens and work piece are at the de-embossing temperature the part is released (Figure 2-3). Typical temperature and force profiles for the micro-embossing process are shown in Figure 2-4. The advantages to using micro-embossing are its relative ease at creating high aspect ratio devices, quick cycle times to switch out tools, ability to emboss any substrate thickness and minimal shrinkage. The disadvantage to using micro-embossing is its long cycle time relative to injection molding [30,31]. In micro-injection molding, for low aspect ratio devices the mold does not have to be heated above the work piece glass transition temperature and there is a constant supply of molten plastic available. However, if the cycle time for micro-embossing can be on the same order as micro-injection molding it would be the most flexible manufacturing technique for polymer micro- and nano- devices. Therefore, the focus for the rest of the thesis will be on the micro-embossing process and figuring out ways to drive down the cycle time, while maintaining control of the critical processing parameters.

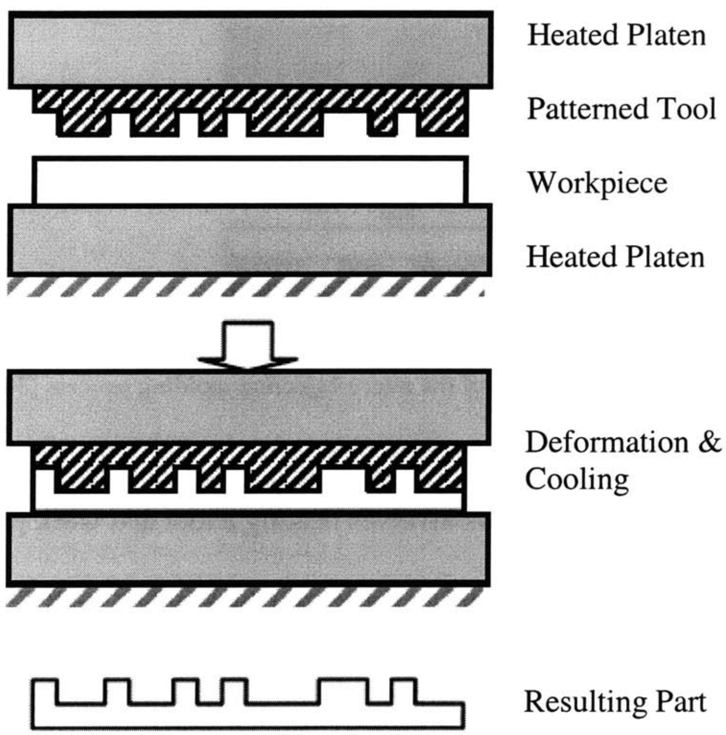

Figure 2-3 Schematic of the micro-embossing process [32]

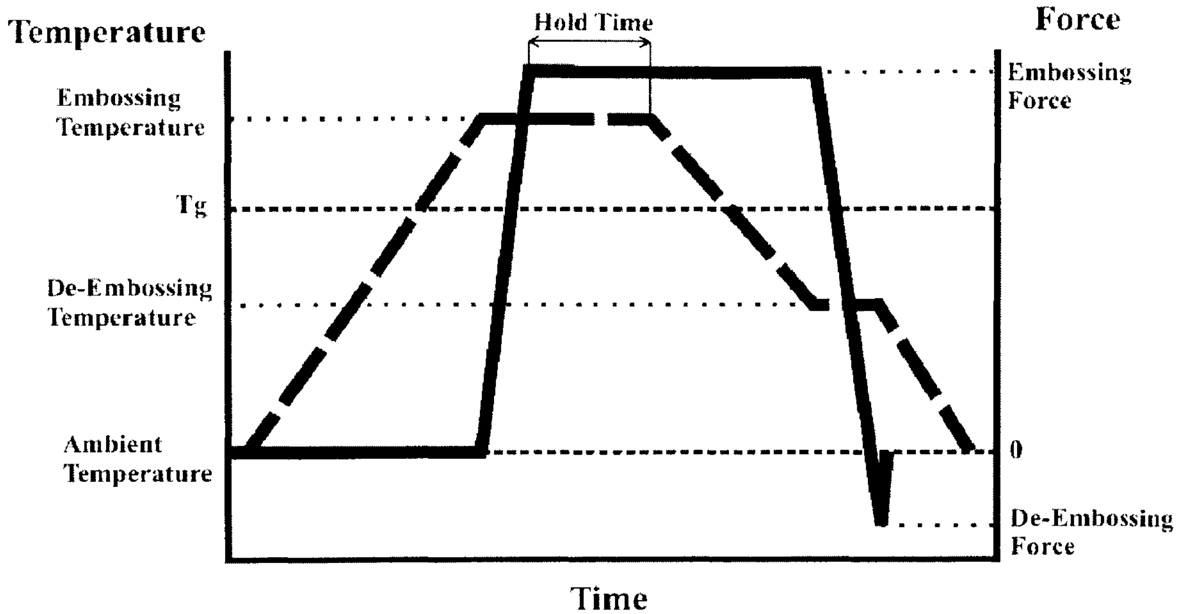

Figure 2-4 Typical temperature and force profiles for the micro-embossing process [29]

2.2 Types of Heating for Micro-Embossing Machines

The rate limiting factor for the micro-embossing process lies in the heating and cooling cycles. A variety of mechanisms for heating and cooling have been investigated by a number of research groups and companies. Techniques for cooling were usually limited to using air, water, or oil. Heating was done in a wider variety of ways. Some techniques prove to be faster, but usually at the expense of the control of critical processing parameters. The following section will outline existing heating techniques for micro-embossing machines.

2.2.1 Electric Heating

Electric resistive heating was a technique explored in a thesis by Ganesan [33]. Two 200 W cartridge heaters were placed within each copper platen and a reported heating time from room temperature to 135 °C took roughly 10 minutes. This slow thermal response was mainly caused by the large mass of the copper platens necessary to achieve good surface temperature uniformity.

2.2.2 Laser/IR Heating

A paper by Lu [34] mentioned the concept of laser/IR assisted micro-embossing. This technique focuses lasers on the surface of the substrate to heat it locally and rapidly. A cycle time of less than 5 seconds has been reported, but there was no data on temperature uniformity across the work piece or stability of the embossing temperature. Although, the cycle time was remarkably fast, accurate control of the temperature and the effect of non-isothermal forming conditions were not addressed.

2.2.3 Ultrasonic Heating

Another technique used for rapid heating was ultrasonic heating reported in a paper by Liu [35]. This technique utilizes ultrasonic vibrations to move the plastic molecules violently against each other causing friction heating. Heating to an acceptable embossing temperature within 1-2 seconds has been reported. Although the heating rate was extremely fast, there was no indication that the temperature could have been controlled well and no information was provided regarding the effect of non-isothermal forming conditions.

2.2.4 Steam Heating

Chang [36] investigated steam as a means for heating and force application and water for cooling. A heating time from 25 °C to 130 °C in 30 seconds was reported with an embossing pressure of 3 MPa. The total cycle time with cooling takes approximately 2 minutes. Although this technique was fast, they reported the inability to control the temperature directly since the steam temperature was a function of the pressure.

2.2.5 Oil Heating

Another heating method investigated by Chang [36] was using hot oil for heating and water for cooling. He reports a heating time from 25 to 130 °C in 3.5 minutes. This was slower than other reported techniques; however it had the advantage of accurate temperature control and uniformity across the work piece. There was only a limited amount of information regarding control of the de-embossing temperature with water cooling.

2.3 State of the Art Commercial Embossing Systems

Aside from just looking at what research has been done on micro-embossing machines, it is important to know the capabilities of commercially available systems. A lot of commercially available micro-embossing machines are modified wafer bonders initially developed for the semiconductor industry. Wafer bonders are used to fuse two wafers together or seal a device at elevated temperatures with high precision alignment and often in a vacuum environment. These characteristics make this machine well suited for micro-embossing. The available commercial systems vary in terms of wafer size capacity, maximum processing parameters, and control of these parameters.

2.3.1 Commercial Embossing Systems

Obducat, a Swedish company commercializing Nano Imprint Lithography machines, has a number of micro-embossing systems with the capacity for 2.5" to 8" diameter wafers [37]. The model with the best thermal performance is the NIL 6" which can reach a maximum temperature of 300 °C. Its temperature uniformity is ± 3 % and it can settle to a temperature of ± 2 °C. The maximum heating ramp is 100 K/min and maximum cooling ramp is 50 K/min. This specification does not necessarily imply these heating rates can be sustained for a long period of time. Therefore, an accurate estimate for a typical cycle time is difficult to discern.

Jenoptik Mikrotechnique recently released their top of the line hot embossing/nano imprinting system called HEX 04 [38]. This system has an automated substrate handler capable of moving 300 mm wafers. It can achieve a maximum temperature of 500 °C with a steady state temperature of ± 1 °C. Since it has the same thermal capabilities as the HEX 03 it should be able to heat up from 60 to 180 °C in roughly 7 minutes. It can also cool from 180 to 60 °C in roughly 7 minutes.

EV Group has a micro-embossing machine model EVG 520 HE with the capability to handle 200 mm substrates [39]. It can reach a maximum temperature of 550 °C with temperature stability of ± 1 °C and temperature uniformity of ± 1 %. Its specified heating from 60 to 180 °C takes 6 minutes and cooling from 180 to 60 °C takes 5 minutes.

2.3.2 Best Performing Commercial System

None of these systems outperform the others in all thermal specifications. It is also difficult to analyze each of the system's actual performance as companies tend to specify only the most favorable characteristics of the machine. A typical cycle time cannot be calculated since limited information is available from the companies. Table 2-1 summarizes the best thermal specifications from all of the abovementioned machines. Many of these systems do not have transparent temperature control systems which can be altered or programmed by the user. A thorough understanding of the micro-embossing process requires full knowledge of most of the processing parameters, therefore full control of the machine states was desired and a machine was built from scratch.

Table 2-1 Specifications for the best thermal performance of all mentioned commercial embossing machines

Specification	Performance
Substrate Size	300 mm
Maximum Temperature	550 °C
Temperature Uniformity	± 1 %
Temperature Stability	± 1 °C
Heating Time (60 °C to 180 °C)	6 minutes
Cooling Time (180 °C to 60 °C)	5 minutes

CHAPTER

3 Design and Construction of Second Generation HME Machine

This chapter and any corresponding appendices were co-authored with Thaker. A hot micro-embossing machine was constructed instead of purchasing a commercially available one to give the user full control of the design and processing capabilities.

3.1 Background-First Generation HME System

The first generation HME system built in the MPCL by Ganesan [33] has four main subsystems: (1) force and position actuation; (2) platens; (3) temperature actuation; and (4) control. An Instron model 5869 load frame provided force and position actuation. The platens, used to hold the work piece and tool, are made of copper. The platens are heated with two 200W cartridge heaters and cooled by running city water and/or pressurized air through tubing connected to the platens. The temperature is monitored by two thermocouples (one each in the top and bottom platen) and controlled with Chromalox 2110 controllers and the Instron is controlled with a hardware controller via its proprietary FastTrack and Merlin softwares. See Figure 3-1 for a close-up of the platen assembly.

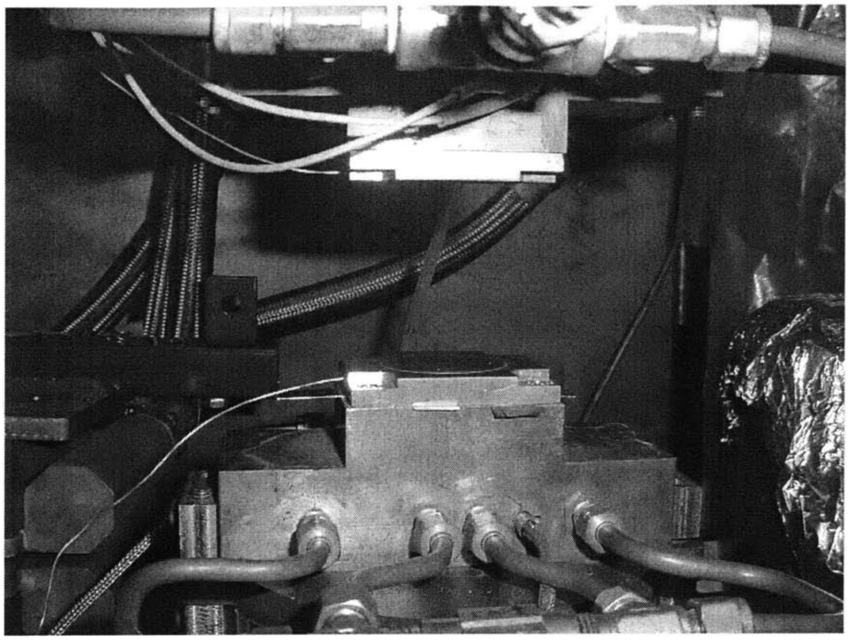

Figure 3-1 Close-up of the first generation HME system platens

The maximum force capacity is 50kN and temperatures up to 300°C are possible [29]. The Instron crosshead has a resolution of 0.0625 μm and can be controlled to speeds from 0.001 mm/min to 500 mm/min [40]. Typical heating time from ambient to 130°C is 15 minutes and cooling time back to ambient is 5 minutes [29]. The largest work piece that could be embossed was on the order of 40-45 mm [29]. Both copper and silicon tools can be used with this system.

The system has three main drawbacks: (1) large thermal mass and the resulting slow thermal cycle time; (2) limited control of key processing parameters; and (3) limited to small part sizes. These drawbacks led to a second generation HME system, designed by Dirckx [29], a graduate student in the MPCL.

3.2 Second Generation HME Subsystems

3.2.1 Platen Subsystem

Dirckx [29] designed and machined the platen subsystem, one of the three subsystems that underwent major changes. The main objectives of this platen design were to: (1) increase the work piece area to 100mm diameter; (2) accommodate a thermal-oil heat transfer system for rapid and uniform heating; and (3) provide more reliable platen alignment and flexible tool and work piece fixturing. Figure 3-2 to Figure 3-4 shows the various pieces in the platen assembly. For further details on the platen subsystem design and fabrication refer to Dirckx's SM thesis: D*esign of a Fast Cycle-Time Hot Micro-Embossing Machine* [29].

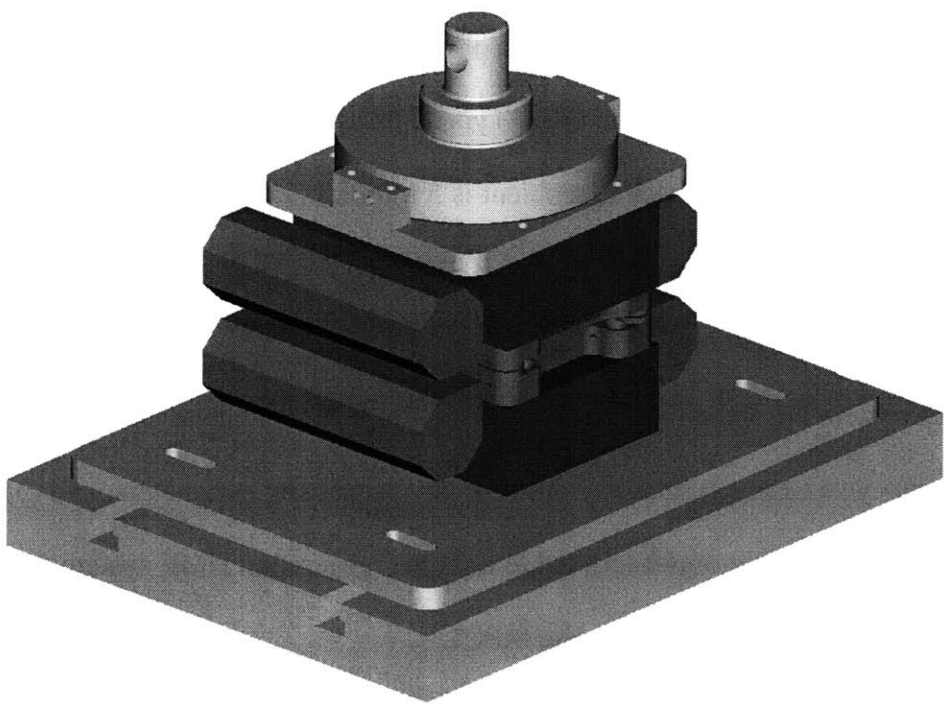

Figure 3-2 Three-dimensional view of the full platen assembly [29]

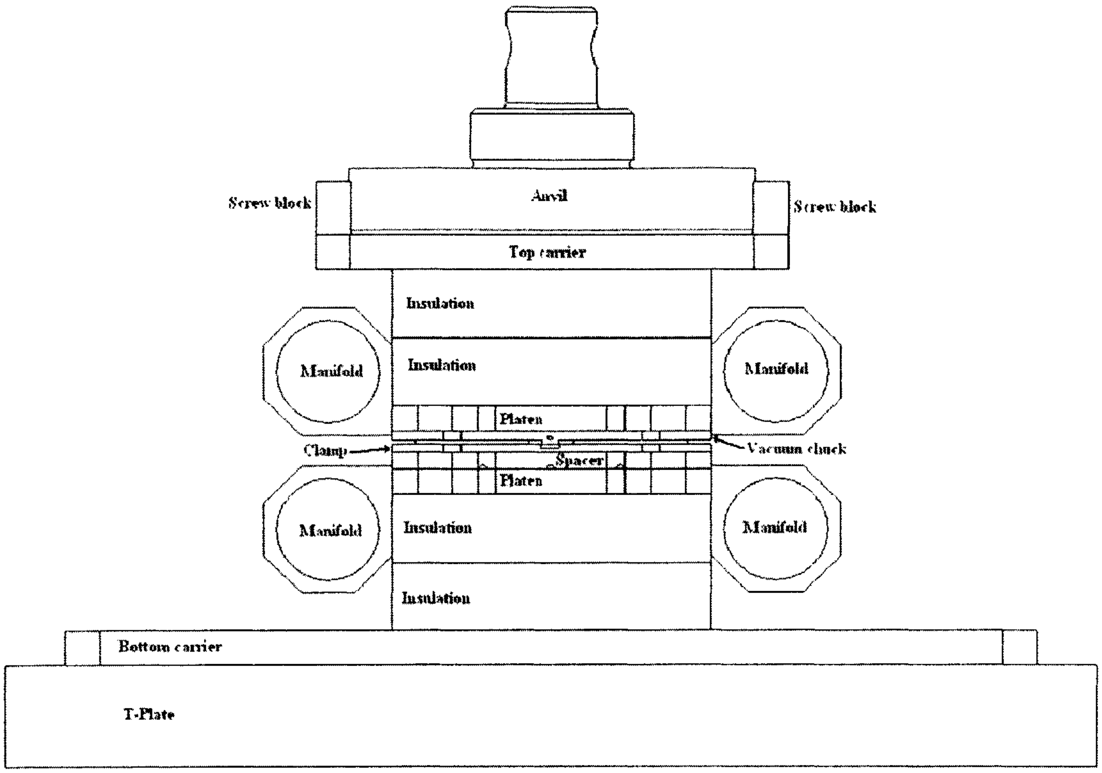

Figure 3-3 The full platen assembly [29]

Three major changes were made to the platen subsystem after initial construction. Omegatherm thermally conductive silicone paste Model OT-201 (Appendix A.1) was placed between the top platen and top spacer plate and between the bottom spacer plate and additional bottom spacer plate. This reduced the thermal resistance by eliminating the air gap between layers. Given difficulties with de-embossing using a silicon tool, Wang Qi, a graduate student in the MPCL designed a top spacer plate that could be used to affix copper tools. This plate was also needed when embossing a part with an unsecured silicon tool to keep the top and bottom manifolds from contacting one another prior to forming the part (see Figure 3-4). A vacuum pump to integrate with the vacuum chuck was also added.

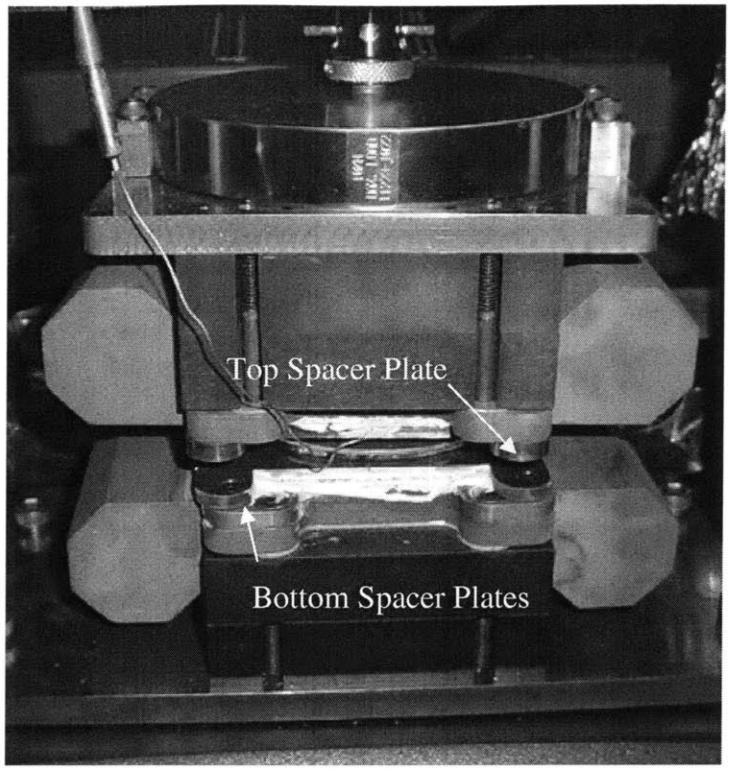

Figure 3-4 The platen assembly without the vacuum chuck and with the top and bottom spacer plates

A vacuum pump was needed to apply a holding force on the tool in contact with the vacuum chuck. The suction force on the tool is proportional to the vacuum level of the pump. The theoretical limitation of any vacuum pump is 0 Torr (pure vacuum). No pump is capable of achieving this; however, several turbo molecular pumps can achieve 10^{-10} Torr. The objective is to maximize holding force, thus there is no need for a high vacuum pump, which would add unreasonable cost with minimal (fractions of a Torr) benefit. Therefore, the focus was on vacuum pumps with ~99% vacuum.

The important parameters to consider when specifying the vacuum pump are: (1) absolute pressure; (2) flowrate; (3) pump speed; (4) weight; (5) dimensions; (6) noise level; and (6) power requirements.

The most suitable vacuum pump for small volume evacuation is a roughing single-stage rotary vane pump. Other pumps offer higher vacuum but at much higher costs with negligible improvement in holding force. The rotary vane pump is the most common and economical mechanical pump for the transport of clean, dry, non-reactive gases, such as air. Oil lubrication, as opposed to dry lubrication, is recommended for a longer life and lower initial cost.

A 0.5HP Kinney-Tuthill KVO-5 capable of 3.1 cfm and an absolute pressure of 7.5 Torr was chosen because it met the aforementioned requirements at the most reasonable cost. The pump was wired to a switch mounted on the computer stand. A flexible stainless steel hose connects the vacuum pump to a brass barb epoxied with Duralco 4461 to the vacuum chuck (Figure 3-5). For further detail, see the vacuum pump user manual.

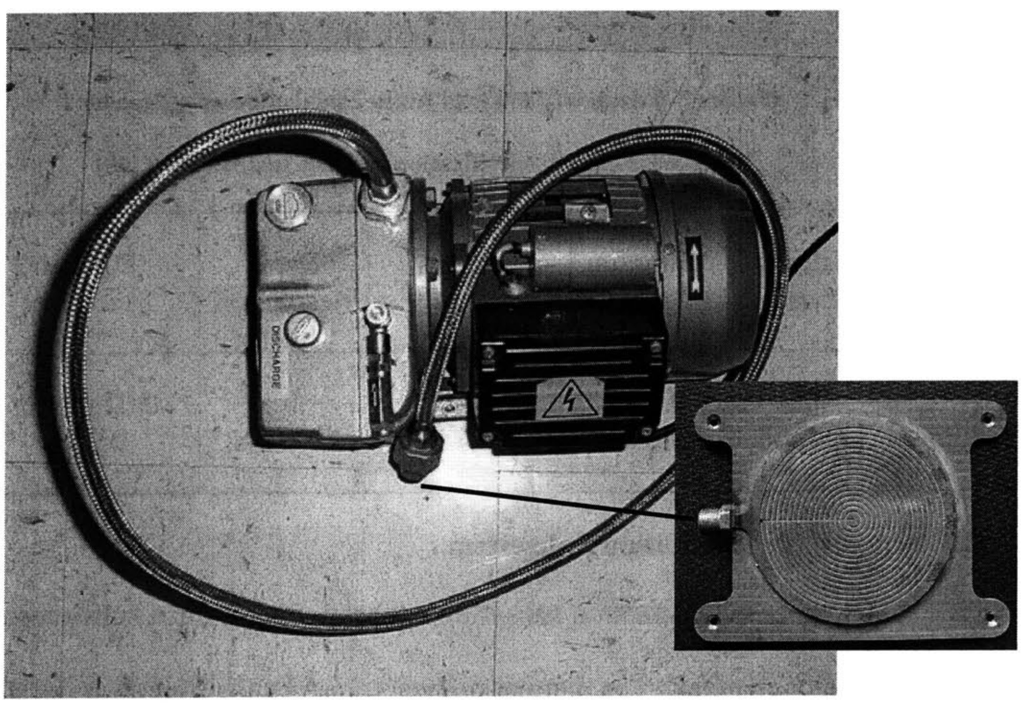

Figure 3-5 Vacuum pump and hose shown with vacuum chuck and barb

3.2.2 Force and Position Actuation Subsystem

The force and position actuation subsystem did not change from the first to the second generation HME system. The parameters for the Instron 5869 (Figure 3-6) shown in Table 3-1 are sufficient for the demands of the new 100 mm system. Refer to the Instron 5869 manual for further detail.

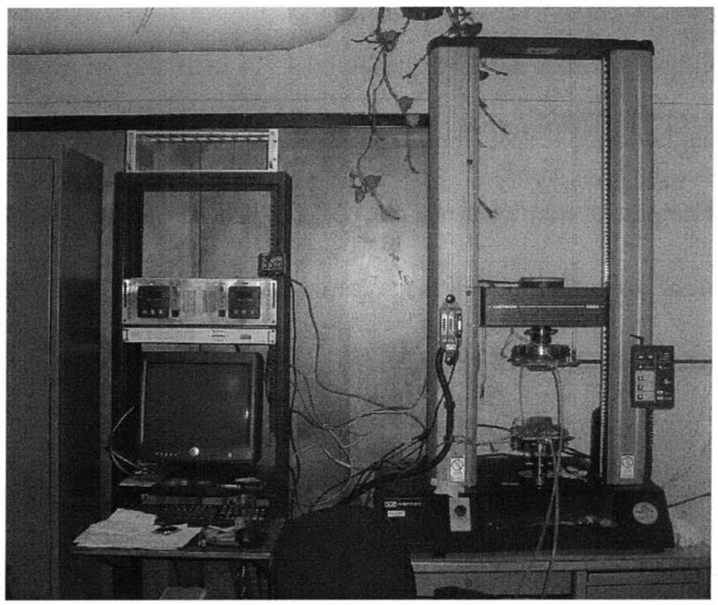

Figure 3-6 Instron 5869 load frame and computer controller

Table 3-1 General specifications for the Instron 5869 [40]

Load Rating	Maximum Speed	Minimum Speed	Force Accuracy	Force Resolution	Position Accuracy	Position Resolution
50kN	500 mm/min	0.001 mm/min	0.4 -0.5%	0.001 N	0.02 mm or 0.05%	0.0625 μm

3.2.3 Temperature Actuation Subsystem

The temperature actuation subsystem is the second of three subsystems that underwent major changes. The thermal-oil heat transfer subsystem was designed by

Dirckx [29] and integrated and constructed by the author and Thaker. This subsystem will be discussed in detail in the following chapter.

3.2.4 Software Control Subsystem

The third subsystem to undergo major changes is the control subsystem. The first generation HME system relied on hardware controllers to reach the desired platen temperature. Given the major changes in temperature actuation, the author developed a new software program in LabView. Force and position are still controlled with the Instron hardware via its proprietary FastTrack and Merlin softwares. Figure 3-7 is a screen capture of the new user interface used to control the system temperature.

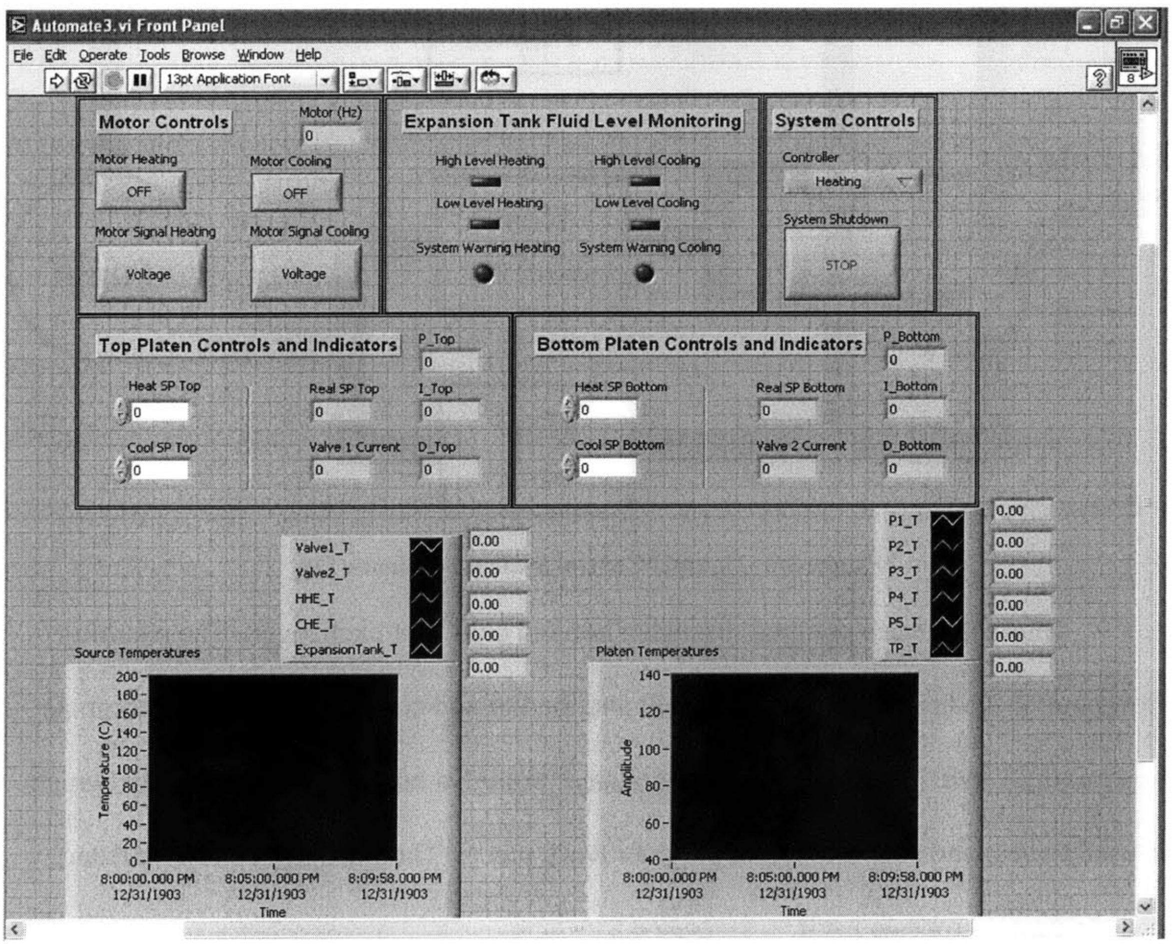

Figure 3-7 Screen capture of the LabView interface used to control the HME system temperature

3.3 Temperature Actuation Subsystem

3.3.1 Overview of the Temperature Actuation System

The temperature actuation system designed by Dirckx [29] utilizes heat transfer fluid flowing through mixing valves, heat exchangers, and a pump to command a certain temperature of a platen assembly. A layout of the system is shown in Figure 3-8.

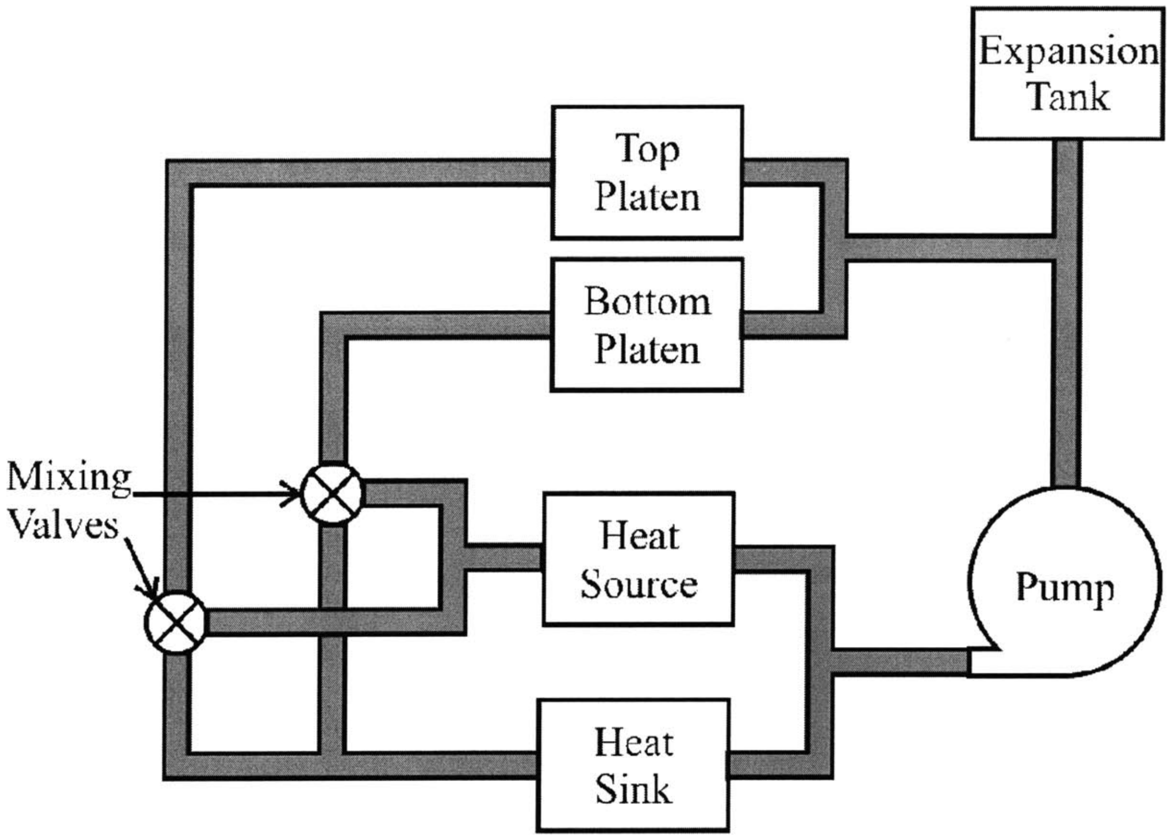

Figure 3-8 Thermal Control System Schematic [29]

Thermal fluid is pumped through a hot and cold heat exchanger. The resulting flows out of the heat exchangers are split and the hot and cold streams of fluid combine in a mixing valve. This fluid is then circulated through a copper platen assembly, which is used to heat and cool a tool and polymer work piece. The fluid is then re-circulated and the process repeats itself.

3.3.2 Heat Transfer Fluid

A heat transfer fluid for the thermal system was selected based on good thermal properties, chemical and thermal stability in air, and non-toxicity. Dirckx [29] chose Paratherm MR, a paraffinic hydrocarbon oil, to be the working fluid. It has low viscosity, relatively high thermal conductivity, and a boiling point much higher than the system's maximum temperature. Other favorable characteristics of the fluid are low toxicity, low odor, and stability in air. The last point enables the fluid to be used in a non-pressurized system. A complete list of Paratherm MR fluid properties can be found in Appendix A.2.

3.3.3 Hot Heat Exchanger

The hot heat exchanger selected by Dirckx [29] is a 30 kW circulation heater from Vulcan Electric Company (Figure 3-9). Internal to the heater are 18 U-tube heater elements enclosed within a 44" long and 8" diameter chamber. There are also baffles located in the heater to induce turbulence. A specifications drawing of the hot heat exchanger is in Appendix B.1.

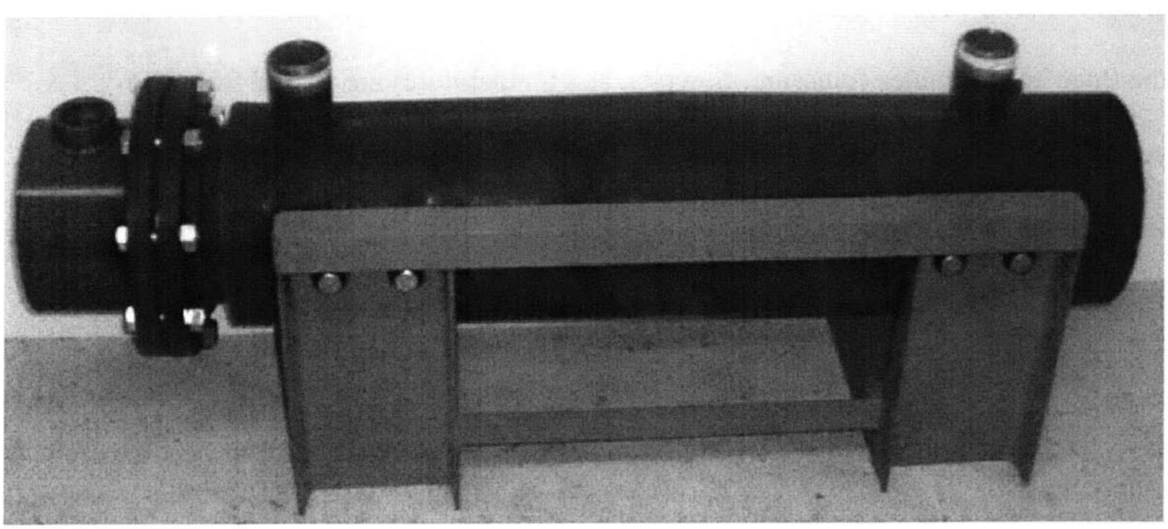

Figure 3-9 Photo of the Circulation Heater [29]

3.3.4 Cold Heat Exchanger

The cold heat exchanger selected by Dirckx [29] is a plate and frame MaxChanger model MX-22 from Tranter PHE (Figure 3-10). This is a counter-flow heat exchanger with city water flowing in one direction and oil flowing in the other direction. A specifications drawing of the cold heat exchanger is in Appendix B.2.

Figure 3-10 Photo of the Maxchanger model MX-22 cold heat exchanger [29]

3.3.5 Fluid Flow Model

In order to specify the requirements on the major components of the system, a preliminary model needs to be developed to approximate the thermal-fluid properties. According to ANSYS simulations [29], the system requires a flowrate of 40 GPM and a temperature to T=200°C. The specified operating temperature range, however, is room temperature to 180°C. Each major component in the system was modeled in Matlab and the three key variables (pressure, flowrate, and temperature) are passed from one component to the next to find the pressure drop in the whole system for a desired platen temperature. This pressure drop was needed to select both the pump and the mixing valves. The model operates on the following assumptions:

1. Constant flow rate pump
2. The hot/cold heat exchangers and platens are the only sites for heat transfer
3. Estimated pipe length is 21 feet with a diameter of 1.5 inches

4. Pressure drop is considered in piping, cold/hot heat exchangers, and platens

The pressure drop in the platens was found by curve fitting data from Dirckx's ANSYS simulations [29]. The pressure drop in the cold heat exchanger was obtained from manufacturer's data and the pressure drop in the hot heat exchanger was calculated based on dimensional specifications obtained from the manufacturer. From this model, the required pressure drop in the mixing valve was calculated and then the pump was specified. The model was run for desired platen temperatures of T=30°C and T=179°C. Table 3-2 shows the estimated pressure drop in the system for these two temperatures. As expected, the pressure drop is lower for the high temperature simulation because of the lower viscosity of the Paratherm MR and lower pressure drop through the heating subcircuit compared to the cooling subcircuit.

Table 3-2 Pressure drops from a preliminary model used to specify pump and mixing valves

Temperature	System pressure drop-Valves
30°C	30.0 psi
179°C	13.7 psi

As construction progressed, the Matlab model was modified to include the pressure drop in the: (1) Y-strainer; (2) an updated platen model; (3) flow meters; and (4) more accurate lengths, diameters, and fittings of pipe. This model was used to select pipe lengths and diameters to try to minimize the pressure drop of the system. Figure 3-11 shows the flowchart behind this model. Minor pipe losses and fittings between the major components were also included in the model. Appendix E outlines the subsections and equations used to generate this model.

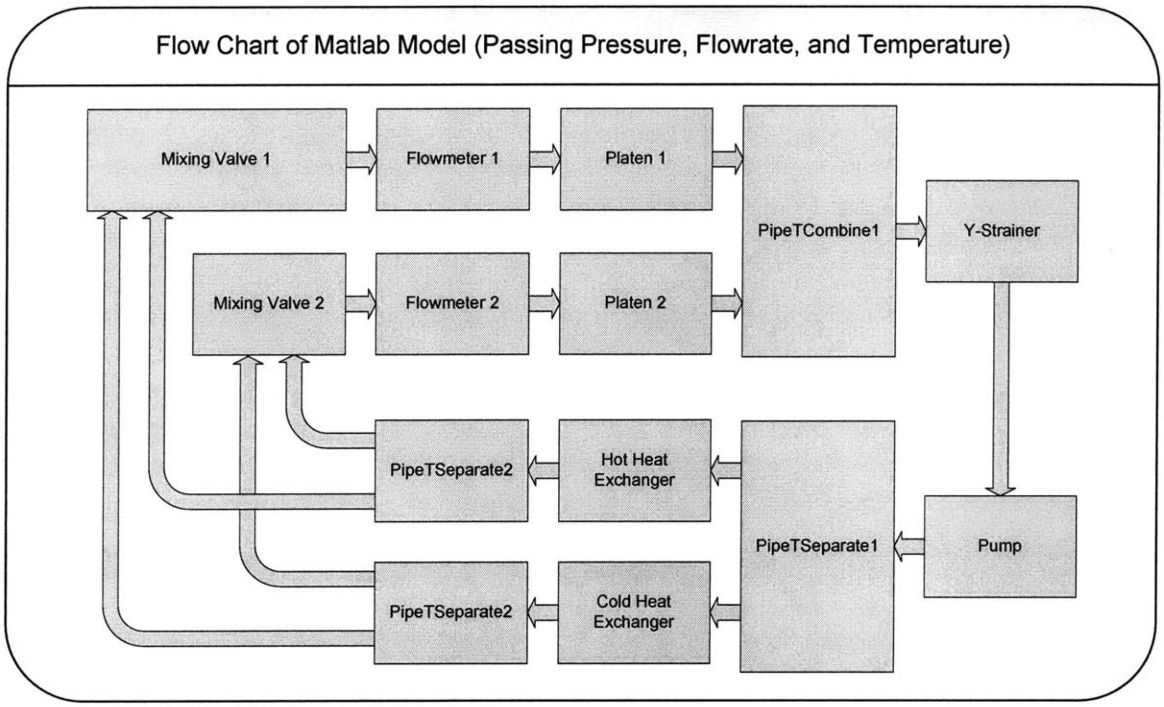

Figure 3-11 Flow chart of the updated Matlab model

3.3.6 Mixing Valve Assembly

The mixing valve assembly consists of a mixing valve, actuator, and positioner. A photo of the mixing valve assembly is shown in Figure 3-12. The selection and sizing of these components are described in the following sections. A specification chart is listed in Appendix B.3.

Figure 3-12 Photo of the mixing valve, actuator, and positioner [29]

3.3.6.1. Mixing Valve

An initial design consideration for the control element in the thermal system involved using four individual globe style valves to mix hot and cold fluid streams to heat up two individual platens. This particular design allows flexible control of the flow rates through the platens. However, simulating and controlling the system with four valves can be quite complicated. A simpler way to control the fluid temperature is using two mixing valves. One of the downsides to using mixing valves is little to no flexibility with regards to changing the flow rate of fluid through a platen. However, this problem can potentially be eliminated by: (1) installing throttling valves or simple ball valves upstream from the mixing valves; or (2) varying the pump speed with a motor controller. Therefore, mixing valves were chosen as the control element in the thermal control system.

Proper sizing of the mixing valves was essential for optimal performance and ease of controllability. If the valve was too small, minute changes in valve position may cause the flows to drastically change. On the other hand, a valve too large might have unpredictable and little effect on temperature with changes in position [41]. Equation 3-1 is a valve authority equation used for sizing valves, where ΔP_1 is the pressure drop across a fully opened valve, ΔP_2 is the pressure drop across the remainder of the system, and N is the valve authority.

$$N = \frac{\Delta P_1}{\Delta P_1 + \Delta P_2}$$

Equation 3-1

It is good practice to design a system with a valve authority between 0.2 and 0.5, with better performance closer to 0.5 [41]. This ensures that with every increment in valve movement there will be a similar corresponding change in flow rate. Using the system simulation presented in Section 3.3.5, ΔP_2 was calculated for cases where 179 °C and 30 ° C fluid flows through both platens. The pressure drop for the system excluding the mixing valves comes out to 13.7 psi and 30 psi, respectively. Given this range of pressures and choosing a valve authority of $N = 0.5$, the pressure drop across the valve should be between 13.7 psi and 30 psi.

Once the pressure drop across the valve was known, the flow coefficient (C_v) for the valve was calculated using Equation 3-2.

$$C_v = Q\sqrt{\frac{SG}{\Delta P_1}}$$

Equation 3-2 [42]

The flow coefficient, C_v, is defined as the flow of water through a valve at 60 °F in gal/min at a pressure drop of 1 psi, Q is the flow rate in gal/min, SG is the specific gravity of the fluid, and ΔP_1 is the pressure drop across the valve. Assuming a target flow rate through a single platen is 20 GPM, a SG ranging between 0.68-0.8, and ΔP_1 between 13.7 psi and 30 psi, the C_v of the valve should be between 3.38 and 4.4. After consultation with Paxton Corporation, a control products and valve distributor, they recommended a ½" C_v =6.3, model 2830 three-way mixing valve from Warren Controls. The justification for going with a higher C_v was the fear of the total system pressure getting too high and a smaller valve might induce fluid velocities high enough to approach a point where it may damage the valve seating. The valve has a linear trim meaning that given equal fluid inlet pressures, the flows should be proportional to the position of the valve stem.

3.3.6.2. Pneumatic Actuator

One of the goals of the system was to reduce cycle time, so having the ability to move the mixing valve stem quickly is essential for a successful system. A pneumatic actuator has the response time necessary for quick and efficient control of the valve stem. A DL49 spring-diaphragm actuator 49 in^2 was selected, which uses air pressure to move the valve stem in one direction and a spring to retract it back. More information on the DL49 can be found in the product specification manual [43].

3.3.6.3. Positioner

Another component necessary for controlling the mixing valves is an electro-pneumatic positioner. This gives the user the capability to control the mixing valves via computer. A Moore 760E positioner was selected with some of its properties shown in Table 3-3. The positioner accepts a 4-20 mA current signal over its full range and is assumed to be linear throughout. Mechanical feedback from the positioner actuator stem is provided by a feedback lever through a characterized cam to the spool valve which controls pressure to the actuator. Detailed information with regards to the Moore 760E positioner can be found in Appendix B.4.

Table 3-3 Performance parameters of the Moore 760E Positioner

Parameter	Specification
Linearity	0.75% of normal span
Hysteresis	1.0% of normal span
Deadband	Less than 0.25% of span
Repeatability	Within 0.5% valve travel

3.3.7 Positive Displacement Pump

Based on the system requirements, the pump must be capable of delivering 40 GPM of fluid in a temperature range of 25°C-200°C. The pump was specified based on the highest system pressure drop expected (at lowest temperatures). The fluid model described in Section 3.3.5 indicated that a system pressure drop of 30 psi can be expected, not including the valves and other minor pipe losses. The mixing valve specification described in Section 3.3.6 showed that they would add another 30 psi. This puts the full system pressure drop estimate at 60 psi. However, given possible inaccuracies in the model and other design additions that could raise the pressure drop of the system, the pump was specified based on a possible 100 psi system pressure drop (safety factor of 1.8). Given that there is no downside in over specifying the pump (except for slightly higher initial capital costs), it was advisable to be cautious in selecting an adequately sized pump that can handle future pumping requirements.

Based on this number, two main types of pumps were investigated: centrifugal and positive displacement. Centrifugal pumps were considered first because they are much safer. As opposed to a positive displacement pump, which is essentially constant flow rate regardless of system pressure, according to a typical curve (see Figure 3-13), a

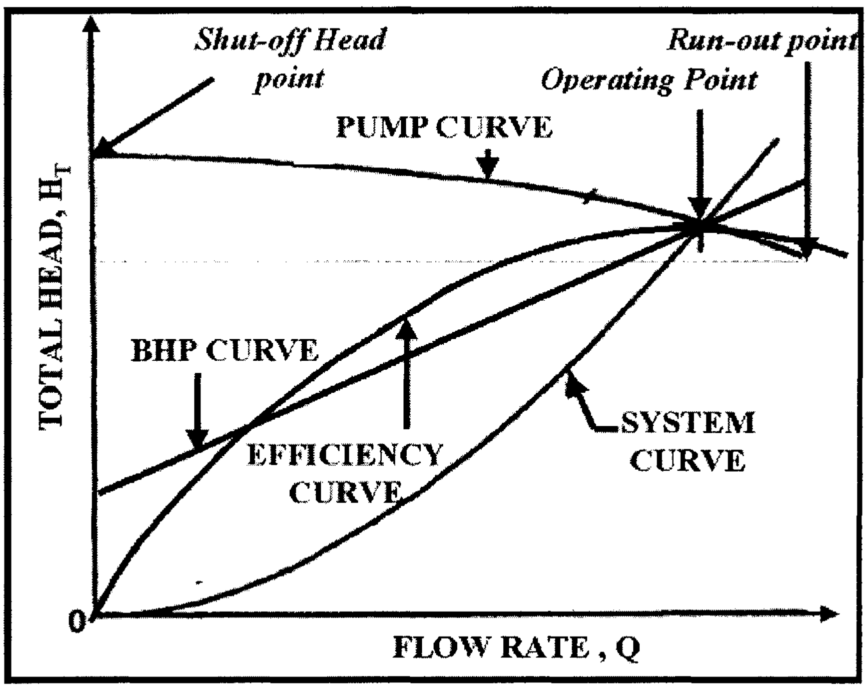

Figure 3-13 Typical centrifugal pump curve [44]

centrifugal pump will not blow-out and cause physical injury because the pump flow diminishes with increasing system head. System head in feet (*H*) is equivalent to pressure (psi) according to Equation 3-3.

$$P(psi) = \frac{H * SG}{2.31}$$

Equation 3-3

A positive displacement pump, however, can over pressurize and possibly explode under high pressure situations. Figure 3-13 also suggests that centrifugal pump flow rates are dependent on the change in the pressure of the system. As seen in the Matlab model in Section 3.3.5, the pressure drop in the system changes significantly with temperature. Therefore, centrifugal pumps pose a very difficult control problem. The flow rate would have to be controlled closed loop with a motor controller or a pressure regulating valve to ensure a constant flow rate as the process temperature cycles. Positive displacement pumps, on the contrary, have pump curves more similar to Figure 3-14. The flow rate is almost constant with changes in the system curve (with the exception of some slip at higher pressures).

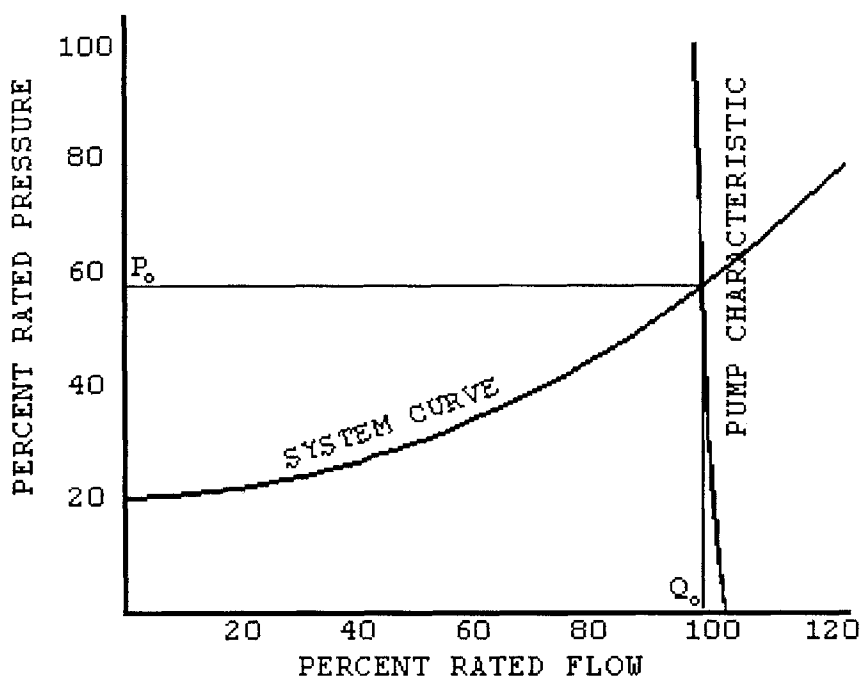

Figure 3-14 Typical positive displacement pump curve [45]

Based on this information, a positive displacement pump was specified. To ensure safe operating conditions, a pressure relief valve set below the pumps rated capacity was placed immediately downstream of the pump to avoid over-pressurization. Several pump manufacturers were investigated. However, based on advice from Paratherm corporation, Roper pumps was selected because of their compatibility with hot oil-systems and all steel and cast iron construction. The Roper model 3711W series of positive displacement pumps operate on a gear principle (see Figure 3-15) that forces the fluid from inlet to outlet through a series of gear teeth.

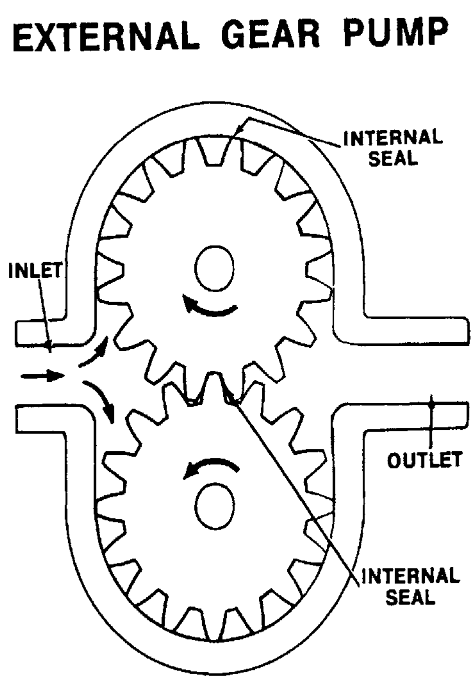

Figure 3-15 Schematic of gear pump operation [46]

To size the pump, the required pump RPM for the pump was calculated. This calculation was done with the pump performance curves found in Appendix B.5. The first step was to determine the viscosity of the Paratherm MR. Based on the chart in Appendix A.2, the viscosity of Paratherm from 25°C to 180°C is ~5-0.5 centistokes. Given this viscosity, the slip GPM for the pump at its rated pressure of 100 psi was found to be ~6 GPM. Given this, the pump was specified for 46 GPM (40 GPM required plus 6

GPM slip). From this, the appropriate RPM was found to be ~400 RPM. The next step was to calculate the motor size required. Based on a 400 RPM speed and 100 psi pressure, a base 2.5 HP was required in addition to another 0.5 HP for viscosity effects for a total of at least 3 HP. Given start-up torque requirements a minimum of 4 HP motor would be required to power this pump. However, the manufacturer only had 5 HP pumps on hand, so a 5 HP motor unit was installed. A check of this calculation is Equation 3-4, which equates required pump horsepower to the flow rate (40 GPM), pressure head (100 psi), specific gravity (~0.8) at 30°C and (Motor and Pump)$_{Efficiency}$~0.5. This standard efficiency for the motor-gearbox-pump assembly was recommended as a rule of thumb by the pump manufacturer (Roper pumps).

$$HP = \frac{Q(GPM) * H(feet) * SpecificGravity}{3960 * MP_{Efficency}}$$

Equation 3-4 [47]

The selected pump has 2" NPT fittings and comes mounted to a painted steel base with a coupling and guard connected to the motor through a gear reduction box. The motor is a three-phase 230-460V Totally Enclosed Fan Cooled (TEFC) inverter grade motor that is compatible with motor controllers, which will be required to change the flow rate of the system. The gear-reduction box has a 4.6:1 ratio and steps down the 1760 RPM motor to ~382 RPM (as close as possible to the rated 400 RPM given the discrete gear-box ratios). The pump is rated for the high temperature option and also has an in-built relief valve (RV) style pressure relief valve that bypasses the pump outlet if the pressure exceeds a user defined value 30-125 psi. The current installation of the valve is set to 125 psi. The motor-pump assembly rests on a PVC/fiber-reinforced vibration damping pad to keep it from vibrating during operation.

Another important consideration is the Net Positive Suction Head (NPSH) of the pump inlet. Cavitation could occur at the pump inlet if there is insufficient pressure head. This is not of concern in this application because a 4-6 foot head of fluid is present on the pump inlet. For further detail on maintenance and specifications, refer to the pump, gearbox, and motor manuals.

3.3.8 Motor Controller

Based on the positive displacement pump specified, a motor controller was required to control the speed of the motor to allow for variable flow rate. A variable flow rate is required to: (1) soft start the pump to ensure the motor does not overload caused by high start-up torque; and (2) change the flow rate through the platens at different points in the process cycle to maximize cycle time and reduce temperature non-uniformity at the platens. The minimum requirements for the motor controller were:

1. Variable power input to a 5 HP three-phase 460 V motor
2. Manual speed control and on/off capability
3. Analog inputs to control motor speed and emergency on/off from a remote site
4. Capable of handling moderate vibration and robust to environmental changes found near a thermal-oil system
5. Full load amp delivery of at least 8.1 amps- given 5 HP (3.7 kW) motor and its 460V three phase power

Based on these requirements, several options were investigated and the Hitachi L100 was selected because it satisfied all the requirements at the most reasonable cost. Figure 3-16 below shows a front view of the motor controller.

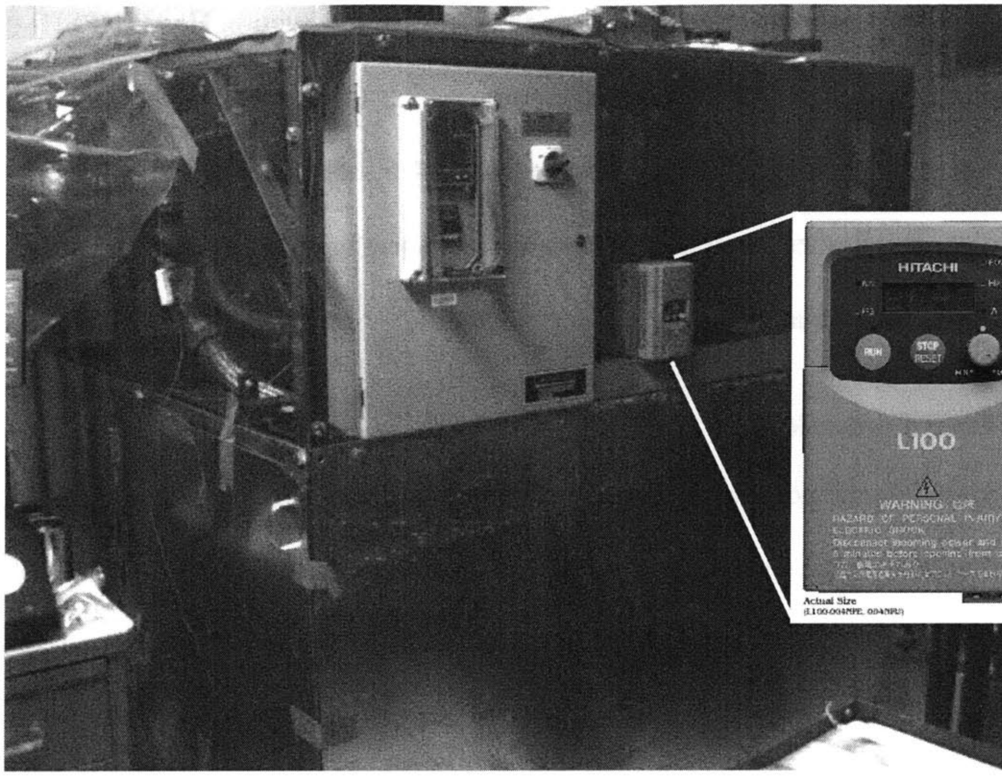

Figure 3-16 Picture of the motor controller in the HME System [48]

The motor controller operates on the principle of sine wave Pulse Width Modulation (PWM) to convert the 60 Hz three-phase 480 V input to a variable frequency (0-60 Hz) three-phase 460 V output. The output frequency from the motor controller is approximately proportional to the motor speed and thus the flow rate of the pump. Every 1.3 Hz set on the motor controller corresponds to approximately 1 GPM of flow from the pump. The power wiring from the three-phase 480 V 10 amp fuse box to the motor controller and the motor controller to the pump motor was done by the MIT facilities department.

The motor controller also has the ability to direct the motor to move in the forward and reverse direction, which may be useful in breaking up an obstruction, should debris clog the system. Moreover, the motor controller has dynamic braking and soft starting (to reduce the power spike to the motor and increase the motor and pump lifetime). Constant or reduced motor torque settings as a function of motor controller frequency are also possible. This setting determines whether the full amp rating or a reduced amp rating will be permitted to be transmitted to the motor while running at reduced speeds. Several other more advanced features, such as the remote and local programming of preset trajectories of the motor, are possible with this motor controller. Reference the motor controller manuals for further detail.

3.3.9 Heater Controller

Based on the electric circulation heater specified, a heater controller to select the set point temperature of the fluid exiting the heater is required to ensure maximum flexibility when designing the micro-embossing process cycle. The minimum requirements for the heater controller are:

1. Variable power input to a 480V three-phase delta 30kW electric circulation heater
2. Two temperature inputs
    a. Set point output fluid temperature- feedback control
    b. Heater coil temperature (type J thermocouple)- auto shutoff
3. Analog and emergency remote inputs
    a. Alarm situations from the computer
    b. Startup/shutdown routines from the computer
4. Manual controls
    a. On/off switch
    b. Set point temperature
    c. Coil temperature shutoff

5. Analog output

a. Set point temperature

A review of the market of heater controllers showed that all the required functions listed above were not possible in one product, but rather, required the integration of three products: (1) a process controller; (2) an over-temperature controller; and (3) a power controller. These three products can be sold separately or combined in a power control box. These boxes have pre-wired communications and power in a NEMA 1 enclosure (well-insulated from ambient).

A Chromalox 4268 Silicon Controlled Rectified (SCR) Power Controller Box was chosen because it satisfied all the requirements at the most reasonable cost. This unit houses a 2104 Process Controller, a 1600 Over-temperature Controller and an SCR power controller. The SCR is a zero voltage switched unit that proportionally turns on and off a full cycle of the power line. The unit varies power to the heater by varying the number of AC power line cycles [49]. Figure 3-17 shows a front view of the heater controller installed on the system. The power wiring from the three-phase 480 V 100 amp fuse box to the heater controller and the heater controller to the heater was done by the MIT facilities department. Reference the heater controller manuals for further detail.

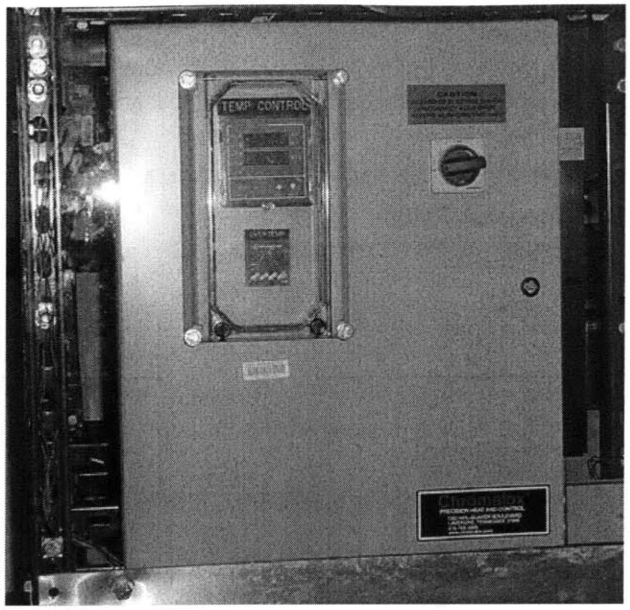

Figure 3-17 Heater Controller with Process and Over-temperature displays visible

3.3.10 Expansion Tank

The expansion tank serves as a multipurpose safety device found in thermal fluid systems allowing for thermal expansion of fluid, venting of vapor pressure, and maintaining a positive pressure into the entrance of the pump. Depending on the type of fluid used in the system there are a variety of designs for optimal performance and prevention of fluid degradation. Paratherm MR, the working fluid in the system, has a very low vapor pressure allowing the system to not be pressurized. A liquid phase systems design guide by Therminol detailed the most commonly used expansion tank designs and design rules [50]. The expansion tank can either have a single leg or double leg, the latter being more effective in venting non-condensable and purging of air/water upon start-up of the system. A cold seal tank used in conjunction with the double leg expansion tank is the best design to preserve the integrity of the fluid. Figure 3-18 details the final design used in the system.

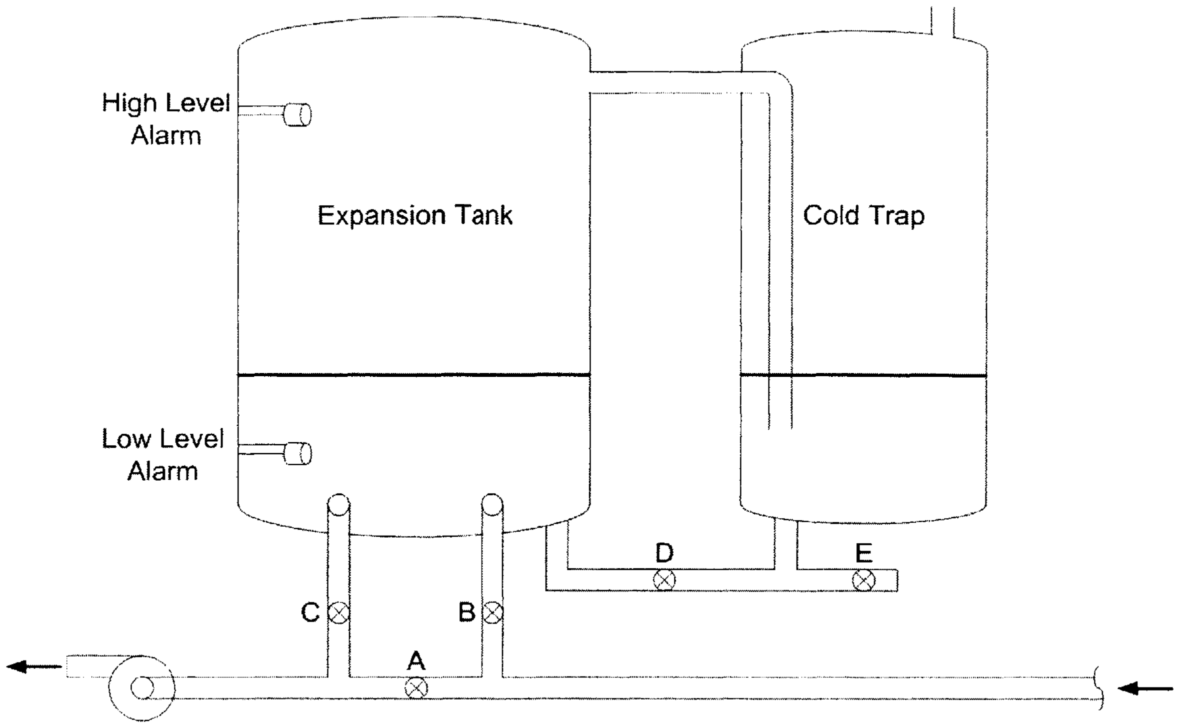

Figure 3-18 Expansion tank diagram

Upon the initial charging of the fluid in the system, it is recommended to run the fluid through the expansion tank at a low flow rate to expel any entrapped air. This requires all of the valves to be opened except valve A. During normal operation of the system all of the valves should be opened except valve C. This will prevent the bulk of the fluid from entering the expansion tank and unnecessarily heating up the fluid and air which may result in oxidation of the fluid. The hose connection between the expansion tank and cold trap serves to mitigate air contact in the expansion tank, while allowing hot air within the expansion tank to exhaust. Another function of this design is to eliminate any non-condensables, such as water. The pipes branching from the main pipe to the expansion tank are raised 1" from the bottom of the tank, so water can settle out below into the piping between the expansion tank and cold trap. Disposing of the non-condensables requires shutting off valve D and E, then opening the cap on the right side of valve E. Proper sizing of the expansion tank and cold trap is recommended for system safety and keeping costs down. If the tank is too small, it may overflow during heating. If it is too large, a significant amount of the fluid needs to be purchased. Standard design rules suggest having the fluid level in the tank at 25% when the fluid is at room temperature and 75% when the fluid is at the highest system temperature. These conditions are taking into account the worst possible scenario, so the fluid level should typically operate between 25% and 50%. In the case of a system failure, either a backup in the system causing fluid levels to rise or a catastrophic loss of fluid, level sensors should be placed within the expansion tank to send a signal to shut down the pump and heater. A technical representative from Therminol suggested that the low level sensor should be placed at 10% of the tank capacity and the high level sensor at 90% of the tank capacity.

An initial calculation of the fluid volume within the system excluding the expansion tank was 10.7 gallons. This calculation is detailed in Appendix G.1. Assuming a system temperature ranging between 20 °C and 180 °C, a properly sized expansion tank using the rules stated above comes out to roughly 4.5 gallons. Staying on the conservative side of the design and using more fluid, a six gallon steel pail sealed with a lug cover serves as the expansion tank and a three gallon tin-plated steel pail is the cold trap. The dimensions of the expansion tank are 16" in height and 11.5" in diameter. The dimensions of the cold trap are 13.75" in height and 9" in diameter. Given some restrictions regarding the height differential between the expansion tank and cold trap, the side mounted stainless steel fluid level sensors from Madison Company were placed at heights of 3.5" and 11" in the expansion tank. An aluminum flexible-sight liquid-level gauge 12" center-to-center with a 10.5" sight length was attached to the cold trap enabling the user to visually monitor the liquid level in the tanks. A flexible hose connected from the expansion tank into the cold trap exhausts gases and pressure from the system. A K-type thermocouple was also attached to the outside of the tank monitoring the temperature of the fluid in the tank.

3.3.11 Sensor Communication

When designing an automatic control system, the selection and placement of sensors, actuators, and data acquisition are critical to the performance of the system. A layout of the communication between the computer and components within the system is shown in Figure 3-19.

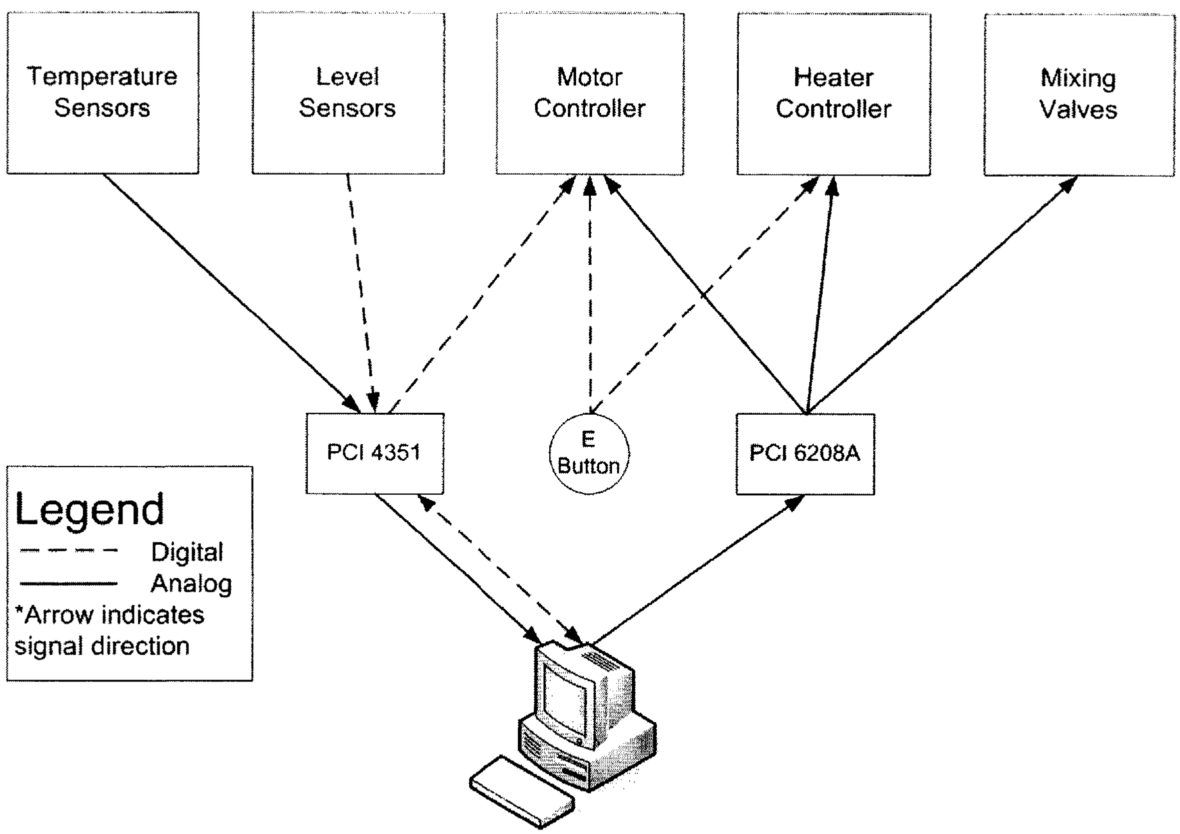

Figure 3-19 Communication between the computer and system components

A total of 11 analog inputs were needed for the system, all of them thermocouple measurements. The locations of these temperature measurements are detailed in Table 3-4.

Table 3-4 List of analog inputs needed in the system

Number of Analog Inputs	Description of Measurement
1	Outlet of the Hot Heat Exchanger Fluid Temperature
1	Outlet of the Cold Heat Exchanger Fluid Temperature
2	Outlet of the Mixing Valve Fluid Temperature
5	Different Locations on Bottom Platen Temperature
1	Top Platen Temperature
1	Expansion Tank Temperature
Total=11	

Four analog current outputs (4-20 mA) in the system are described in Table 3-5.

Table 3-5 List of current outputs needed in the system

Number of Analog Outputs (4)	Description of Control
1	Controls the speed of the pump motor
1	Controls the hot heat exchanger set point temperature
2	Controls the positions of the mixing valves

The system also required a number of digital inputs and outputs for the fluid level sensors and motor controller. Two digital input lines were needed to monitor the fluid level sensors in the expansion tank. They need to be integrated with a simple electrical circuit, which will be detailed in Section 3.3.14.6. Two digital output lines were used for switching the motor on and off and also switching the type of signal sent to the motor controller. The digital outputs needed to be integrated with an additional electric circuit described in Section 3.3.14.1.

3.3.12 Computer Hardware

A National Instruments PCI-4351 card specifically designed for thermocouple measurements is the main sensor interface for the entire system. This board has 14 differential thermocouple inputs, an auto zero channel, and cold junction compensation. Its 24-bit ADC resolution and onboard signal conditioning provide extremely high precision temperature measurements; however, the trade-off being a slow maximum sampling rate of only 60 readings/second. In addition to the analog inputs, the board has 8 TTL digital I/O lines. The PCI-4351 was interfaced with a TC-2190 shielded isothermal rack mount with thermocouple mini-connector ports for ease of use. This board was sufficient for the 11 thermocouple readings and 4 digital I/Os needed for the system.

In addition to measuring analog inputs, the system required four analog current outputs to control two mixing valves, a pump motor, and heater. The NI PCI-4351 does not have any analog output channels, so an Adlinktech PCI-6208A card was selected. The Adlinktech PCI-6208A provides 8 current outputs, 4 digital inputs and 4 digital outputs. The pin assignment for the card is shown in Figure 3-20. Current sourcing is possible because of additional onboard high-precision voltage to current transducers. Performance of the board is adequate with a 4-20 mA range and current signals settling within 17 μs at a 15-bit resolution. Interfaced with the board is a DIN-37D terminal board with a 37-pin D-sub Connector and DIN-Rail Mounting.

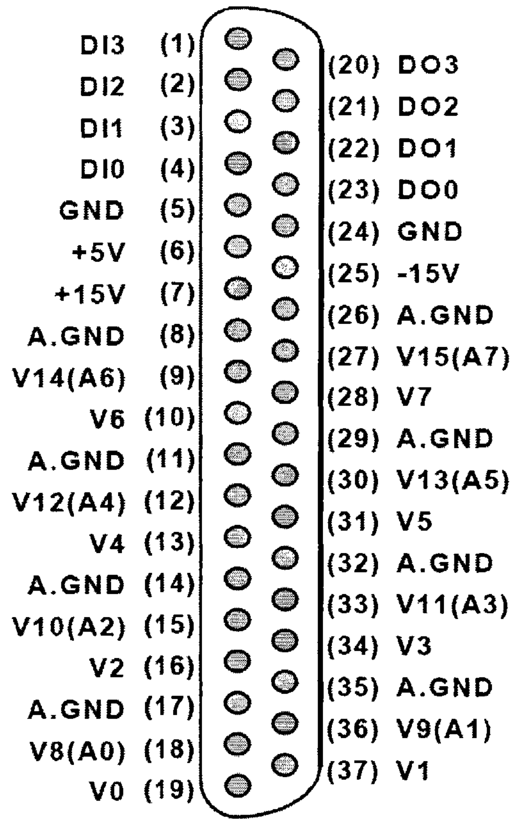

Figure 3-20 Pin assignment for the PCI 6208A [51]

3.3.13 Sensors

3.3.13.1. Thermocouples

A variety of thermocouples were selected for measuring the temperature at different locations in the system. Directly measuring the temperature of the fluid required a thermocouple that could handle a substantial amount of pressure, since the fluid itself is pressurized. Therefore, rugged pipe plug probe K-type thermocouples with ¼" NPT connections were placed after the two mixing valves and at the outlet of the cold heat exchanger. A dual K-type thermocouple with 1/8" NPT connection was placed at the outlet of the hot heat exchanger. Transition junction style K-type thermocouple probes 6" in length and 0.032" in diameter were used in all other locations. The bottom spacer plate, machined by Dirckx, has five channels and ports where the thermocouples can measure the temperature of the PMMA directly (Figure 3-21). High temperature ceramic cement from Omega was used to mount the thermocouples in the bottom spacer plate. See Appendix A.3 for properties of the adhesive. A hole was drilled into the side of the top spacer plate deep enough so that there are no thermal edge effects for the thermocouple reading. The last thermocouple was secured to the side of the expansion tank to monitor the temperature of the fluid.

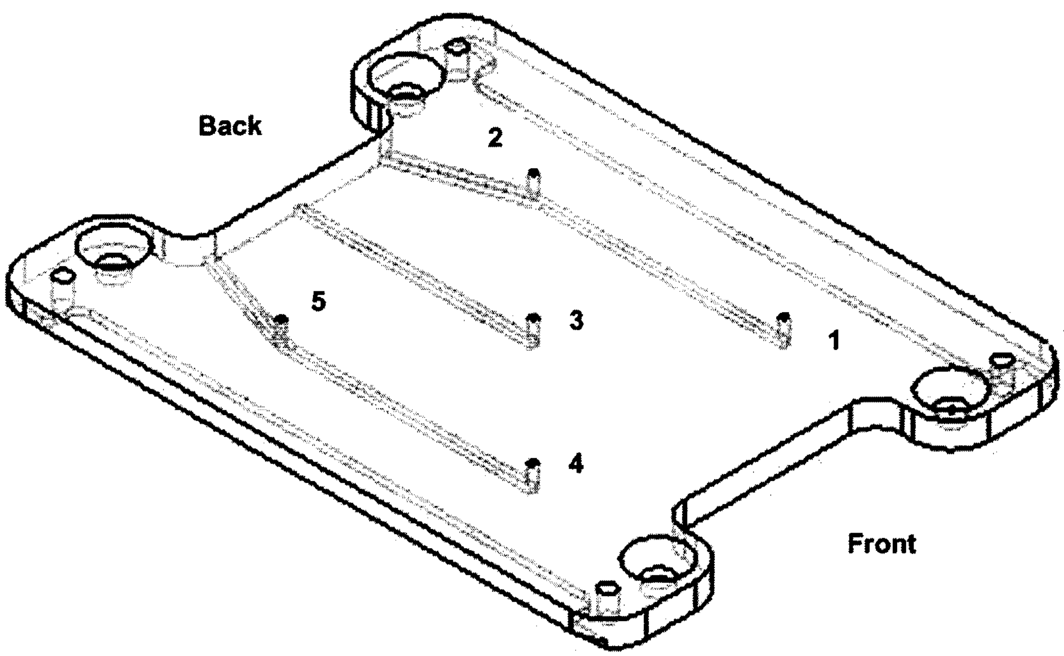

Figure 3-21 Bottom spacer plate with five thermocouple ports designed and machined by Dirckx [29]

3.3.13.2. Level Sensors

Level sensors monitor the fluid level in the expansion tank to prevent overflow or catastrophic loss of fluid. A horizontally mounted stainless steel float type level sensor from Madison was used for the expansion tank. The basic operation of the sensor is to close a circuit when the fluid brings the float horizontal and breaks the circuit when the float is in air. These sensors can work in fluids with specific gravity down to 0.7, which corresponds to a Paratherm MR bulk fluid temperature of 150 °C. The temperature of the Paratherm MR within the expansion tank should never reach a temperature of 150 °C, because the temperature will typically be cycling between 55 °C and 150 °C. The sensors can also tolerate a temperature of up to 200 °C, so they should operate properly when the machine is running for an extended period of time.

Integrating the level sensors to work with the PCI-4351 digital inputs required some additional circuitry. Figure 3-22 shows the electric circuit used to get the sensors functioning properly. The PCI 4351 has a +5 V supply and a digital ground. The PCI 4351 requirement for a digital input is a maximum low level input of 0.8 V and a minimum high level input of 2.0 V with a current between -10 μA and 10 μA. Therefore, a 10 kohm resistor between the +5 V supply and digital input port will drop the high level by 0.1 V, which would not affect the range of voltages needed to detect a low and high level. Without the resistor, the voltage read by the digital input port would mostly be a high level reading whether or not the circuit is closed.

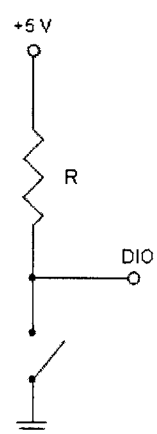

Figure 3-22 Electrical circuit integrated with the level sensors

3.3.14 System Wiring

3.3.14.1. Motor Controller Wiring

Three functions that needed wiring of the motor controller were: (1) turning the motor on/off; (2) analog input to control the speed of the motor; and (3) analog current or voltage input signal switching. A diagram of the wire terminals on the motor controller is shown in Figure 3-23.

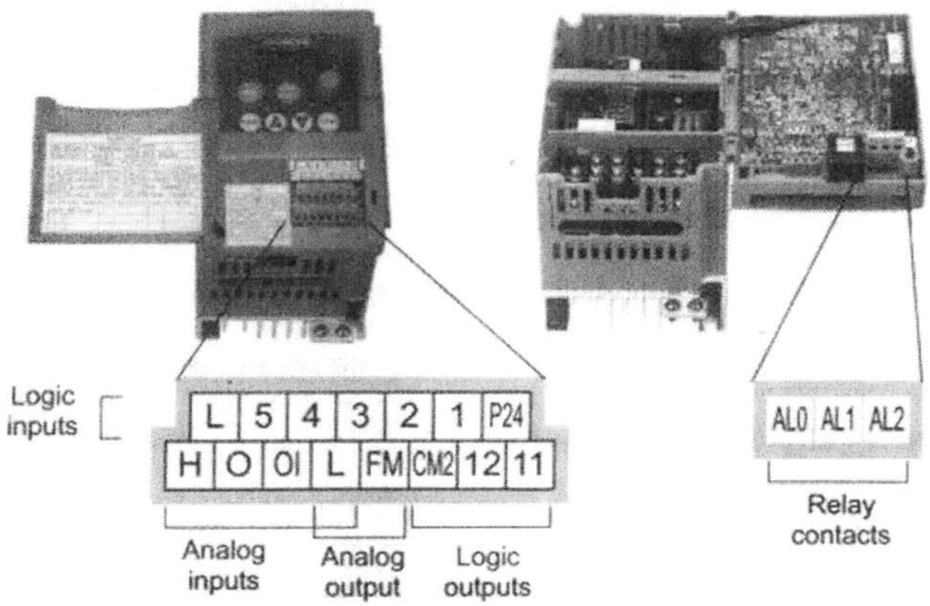

Figure 3-23 Diagram of wire terminals on the motor controller [48]

In order to turn the motor on and off via computer, wires needed to be connected to terminals P24 and 1. These wires were interfaced with the digital input/output terminals on the PCI-4351. Since terminal P24 is a +24 V source and the PCI 4351 has a +5 V source, the wires needed to be connected in series with a relay circuit. An external emergency button to turn off the motor was also hooked up in series with the relay circuit.

An analog current input signal to the motor controller was necessary for controlling the speed of the motor. A wire was connected to the OI terminal of the motor controller and the other end was connected to the positive analog output terminal (pin 15) in the PCI 6208A. The other wire was connected to the L terminal of the motor controller and the other end was connected to the negative (ground) terminal of the corresponding analog output terminal (pin 14) in the PCI 6208A.

In order to maintain flexibility with regard to potentially changing hardware, a switching function between sending a voltage or current analog output was used. Since the PCI 6208A sends out a current output, the current setting should always be on. But in the case of needing to switch to a card which sends voltage outputs, the option will be available. Wires were connected to the terminals P24 and 3 with a relay circuit in series because of the disparity in voltage supplies.

The relay circuit used for digital outputs is shown in Figure 3-24. An SPST reed relay with properties listed in Table 3-6 was used in the circuit. The transistor used is a 2N2222 NPN with properties listed in Table 3-7. Other constant variables were the +5 V power supply and the digital input signal. Since the PCI 4351 has a digital output low level logic maximum of 0.4 V and a minimum high logic level of 3.8 V with a maximum current of 8 mA, the only variable needed to be selected was the resistance into the base of the transistor. In order to determine the necessary resistance, a variable resistor was placed before the base of the transistor and 3.8 V was supplied to the input, then the resistance was turned down until it turns on an LED connected to the relay. Knowing this threshold resistance assisted in the selection of a resistor. Finally, a 1.8 kohm resistor proved to be an adequate design for switching.

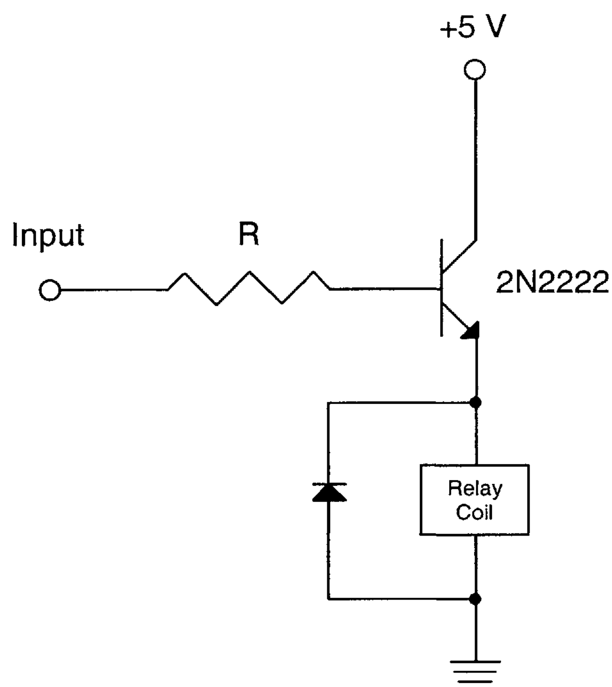

Figure 3-24 Relay circuit used to switch a +24V source to motor controller inputs

Table 3-6 Properties of the SPST reed relay

Properties	**Value**
Voltage Rating	5 VDC
Coil Resistance	250 ohms
Contact Rating	0.5 A at 125 VAC
Nominal Current	20 mA

Table 3-7 Properties of the 2N2222 type transistor

Properties	Value
Typical h	200
Max. Vce	30 V
Ic	800 mA
Dissipation	1.8 W

3.3.14.2. Heater Controller Wiring

There are three sets of wires that needed to be connected to the heater controller. The functions are:

1. Switching between two set point temperatures with a digital signal
2. Controlling the set point temperature with an analog current signal
3. Monitoring the fluid outlet temperature of the heater

A diagram of the heater controller wiring terminals is shown in Figure 3-25.

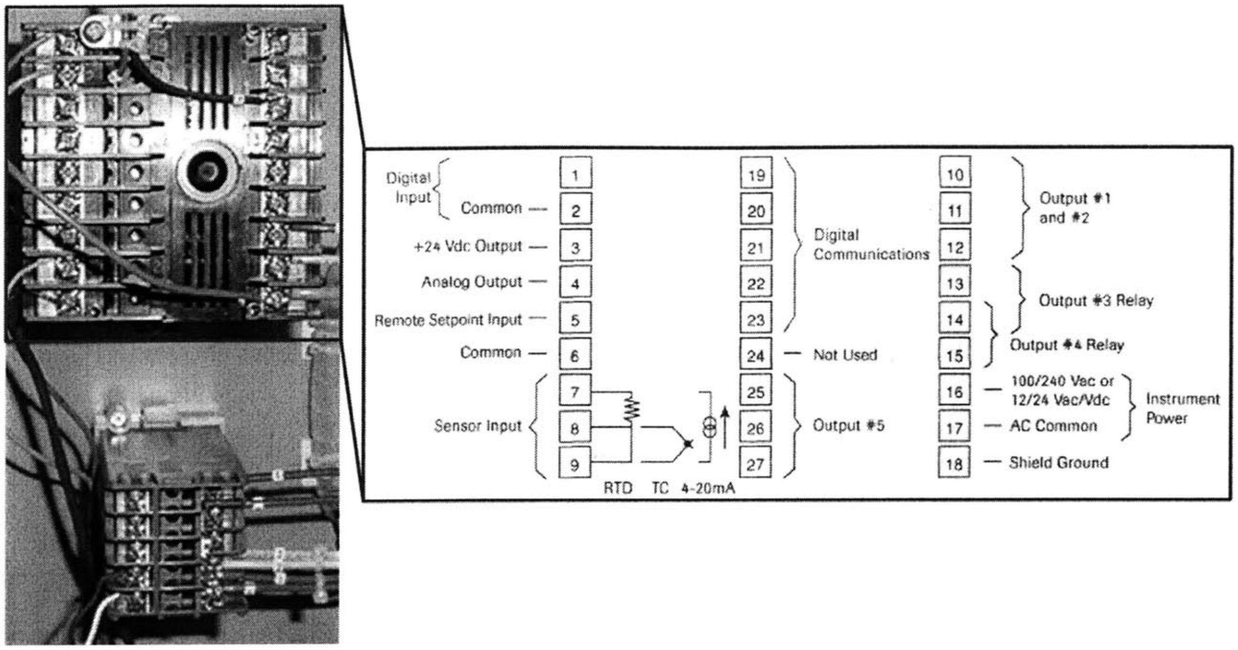

Figure 3-25 Wiring terminals of the heater controller [52]

The first set of wires was connected to terminals 1 and 2 and the other ends were connected to the top terminals of the emergency shutoff button. The wires were hooked up to the top terminals of the button.

In order to control the set point temperature of the heater via computer, wires were connected to terminals 5 and 6 of the heater controller. One end of a wire was connected to terminal 5 on the heater controller and the other end connected to pin 33 on the PCI 6208A, corresponding to a positive current output channel. The other wire was connected to terminal 6 on the heater controller and pin 32 on the PCI 6208A, which is the analog ground channel corresponding to pin 33.

A K-type thermocouple was used to measure the fluid outlet temperature of the heater. Since the particular thermocouple used has dual lead wires, a set was inputted to the PCI 4351 for computer monitoring and the other set was hooked up to terminals 8 and 9 on the heater controller. Since RF interference in the heater controller box causes a noisy signal, a shielded thermocouple attachment was necessary for stable measurements.

The thermocouple's positive lead should be attached to terminal 8, the negative lead to terminal 9, and the ground lead to terminal 18.

3.3.14.3. Heater Controller Over-temperature Wiring

The over-temperature controller protects the heater coils from exceeding a maximum temperature. A diagram of the over-temperature controller is shown in Figure 3-26.

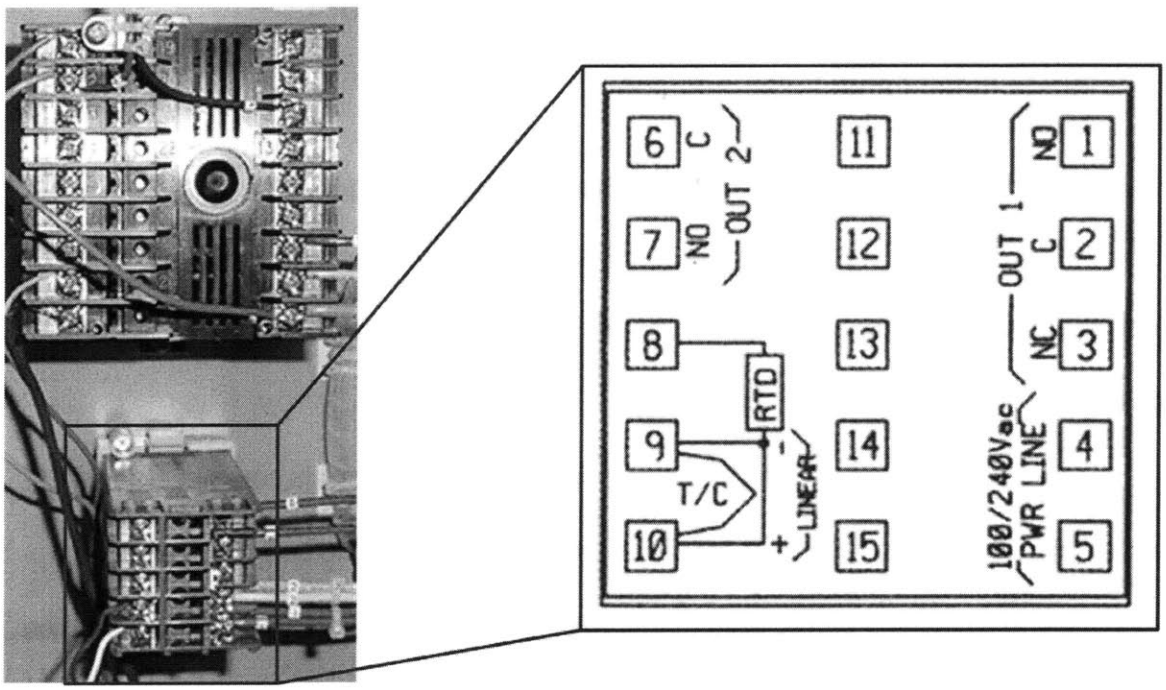

Figure 3-26 Over-temperature terminal diagram [53]

The only terminals used on this controller are 9 and 10. A J-type thermocouple was attached to a heating coil within the heater. The positive lead was wired to terminal 10 and the negative lead to terminal 9. This thermocouple is shielded, so RF interference does not effect the measurement.

3.3.14.4. Mixing Valve Positioner Wiring

The two mixing valve positioners control the position of the valve stem with a 4-20 mA current signal. The Valve1 (farthest from the wall) positioner was wired from its positive terminal to the PCI 6208A pin 18 and its negative terminal to the PCI 6208A pin 17. The Valve2 (closest to the wall) positioner was wired from its positive terminal to the PCI 6208A pin 36 and its negative terminal to the PCI 6208A pin 35.

3.3.14.5. Thermocouple Wiring

All of the thermocouples in the system were inputted to the PCI 4351 through the TC 2190. A photo of the thermocouple inputs on the TC 2190 is shown in Figure 3-27. Table 3-8 shows the temperature readings and their corresponding inputs channels.

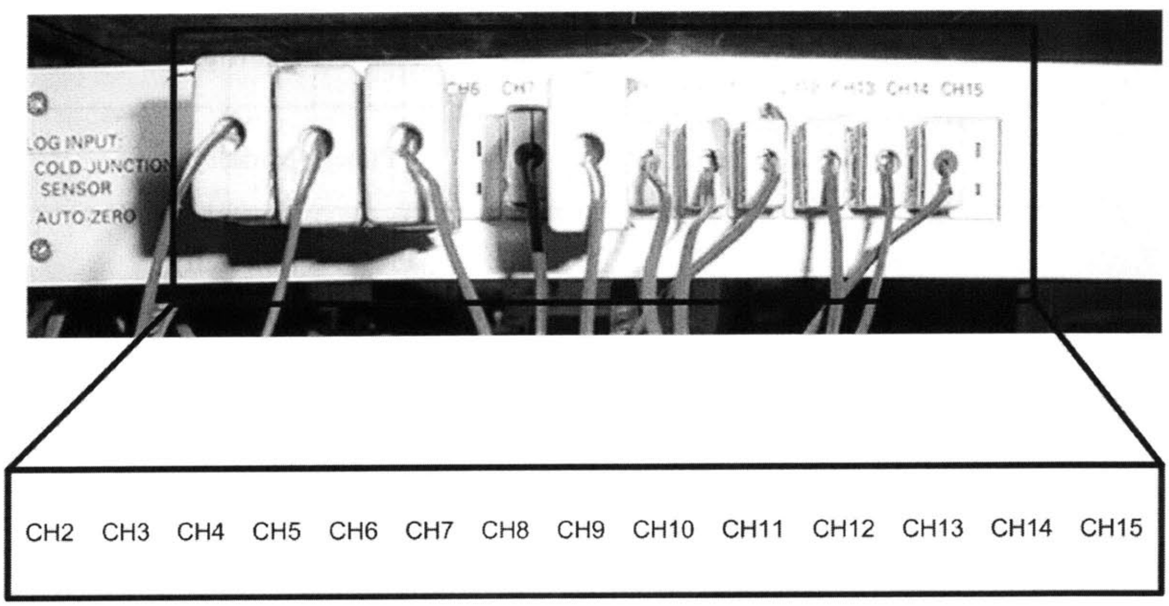

Figure 3-27 TC 2190 Thermocouple Inputs

Table 3-8 Description of the thermocouples interfaced with the TC 2190

Thermocouple Channel	Description
3	Outlet of the cold heat exchanger
4	Valve1 outlet
5	Valve2 outlet
7	Expansion Tank
8	Outlet of the hot heat exchanger
9	Platen (Front Right)
10	Platen (Back Right)
11	Platen (Middle)
12	Platen (Front Left)
13	Platen (Back Left)
14	Top Platen

3.3.14.6. Miscellaneous Wiring

Since there is a large distance between the machine frame and the computer, a 25 wire cable was used to cover the distance. A picture of the 25 pin connector and its numbering is shown in Figure 3-28. Wires were distributed from the 25 pin connector mounted on the machine frame to the components within the frame. A 25 pin connector was also mounted to the computer stand, with wires distributed to their respective components. A description of the wires connected to the 25 pins between the machine frame and computer stand is in Table 3-9. There are also a number of wires coming out of a circuit board located near the computer, which are also attached to a 25 pin connector. A description of the wire connections between the circuit board and other terminals is shown in Table 3-10.

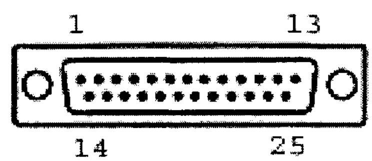

Figure 3-28 25 pin connector used to link wires from the machine to the computer

Table 3-9 Pin Identification for the interface between the machine frame and computer stand

25 Pin Port Number	Connection	Description
1	DIO Ground Pin in 4351	Expansion tank high level sensor ground connection
2	DIO Pin 1 in 4351	Expansion tank high level sensor digital input
3	DIO Ground Pin in 4351	Expansion tank low level sensor ground connection
4	DIO Pin 2 in 4351	Expansion tank low level sensor digital input
5	Pin 18 in 6208A	Analog positive current output (channel 0) to control valve 1 (closest to front of the machine)
6	Pin 17 in 6208A	Analog ground (channel 0) to control valve 1 (closest to front of the machine)
7	Pin 36 in 6208A	Analog positive current output (channel 1) to control valve 2 (near the wall)
8	Pin 35 in 6208A	Analog ground (channel 1) to control valve 2 (near the wall)
9	Direct connection to Relay 1 and 2	Connects to the motor controller terminal P24. When this connection is shorted through the motor controller terminal 1 it turns the motor on and off and when it's shorted through the motor controller terminal 3 it changes the accepted signal from voltage to current.
10	Direct connection to Relay 1	Connects to the motor controller terminal 1. When it is shorted with P24 it will be programmed to turn the motor on/off. The

		wiring is also routed to an emergency button so the motor can be turned off externally. The motor can also be turned on/off through the LabView program where it is hooked up to DIO Pin 3 in the 4351.
11	Direct connection to Relay 2	Connects to the motor controller terminal 3. When it is shorted with P24 it will be programmed to change the accepted analog signal from voltage to current. The wiring is routed to DIO Pin 4 in the 4351 so that control is through LabView.
12	Pin 14 in 6208A	Analog ground (channel 2) to motor controller terminal L
13	Pin 15 in 6208A	Analog positive current output (channel 2) to motor controller terminal OI
14	Hard wire to bottom of emergency button	This connection is to the heater controller terminal 1. This will be used to change the set point temperature, acting as an emergency shutoff.
15	Hard wire to bottom of emergency button	This connection is to the heater controller terminal 2. This will be used to change the set point temperature, acting as an emergency shutoff.
16	Pin 33 in 6208A	Analog positive current output (channel 3) to heater controller terminal 5
17	Pin 32 in 6208A	Analog ground (channel 3) to heater controller terminal 6

Table 3-10 Pin identification for the interface between the circuit board and other terminals

25 Pin Port Number	Connection	Description
1	Wire to the top of the button	Eventually connects to the motor controller terminal 1.
2	Pin 11 of main 25-pin connector	Connects to the motor controller terminal 3.
3	DIO 3	Digital output control for the motor controller terminal 1.
4	DIO 4	Digital output control for the motor controller terminal 3.
5	Pin 9 of main 25-pin connector	Connects to the motor controller terminal P24.
6	DIO +5 V	+5 V supplied by the 4351.
7	Pin 1 of main 25-pin connector	Ground connection for the expansion tank high level sensor.
8	Pin 3 of main 25-pin connector	Ground connection for the expansion tank low level sensor.
9	DIO Ground	Digital I/O ground supplied by the 4351.
10	Pin 2 of main 25-pin connector	High voltage side connection for the expansion tank high level sensor.
11	DIO 1	Digital input for the expansion tank high level sensor.

12	Pin 4 of main 25-pin connector	High voltage side connection for the expansion tank low level sensor.
13	DIO 2	Digital input for the expansion tank low level sensor.

3.3.15 System Frame/Support and Enclosure

Given the large dimensions of the major components and the safety risk posed by the motor-pump and the heater, an enclosure was needed. The requirements of the HME system frame and enclosure were to: (1) isolate the system from the rest of the laboratory for safety and appearance; and (2) provide support to components that will be positioned off the floor. A customizable framing product (Unistrut) was chosen to construct the frame of the enclosure and provide support to the piping, valves, cold heat exchanger, and expansion tank. Figure 3-29 shows the framing design.

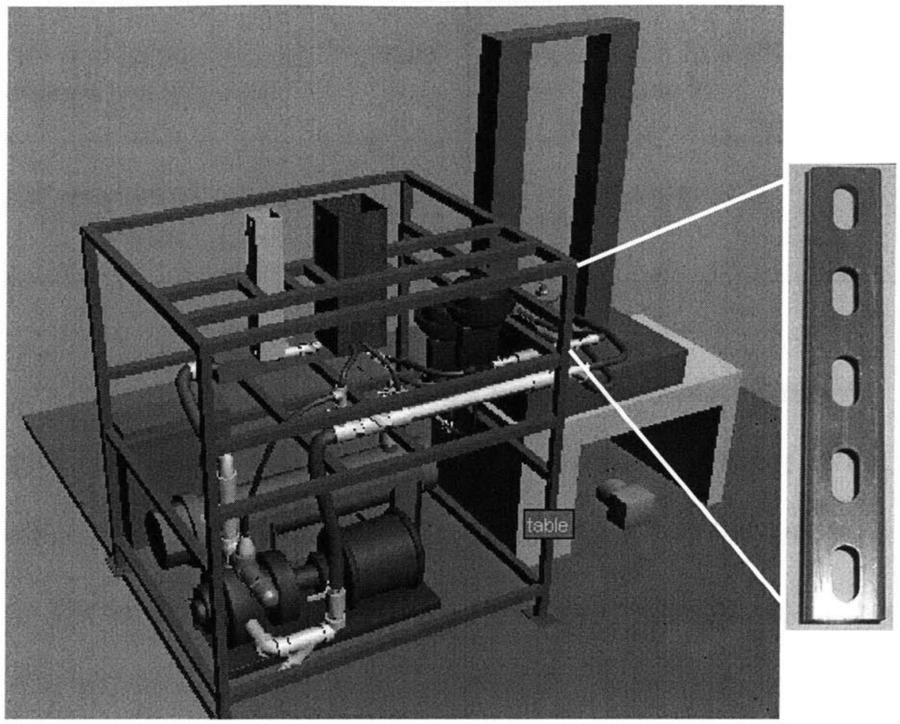

Figure 3-29 3D model showing approximate component locations and the Unistrut frame

An enclosure was affixed to the outside of this frame to protect the user from the motor-pump rotation and the chance of hot-oil leaks. This enclosure was made of aluminum sheet metal and plastic sheeting (see Figure 3-16). There are doors on each side to access the system for routine maintenance. Steel straps and pipe hangers were used to secure pipes, fittings, and the cold heat exchanger to the frame. The expansion tank and valves were directly bolted to the Unistrut frame.

3.3.16 Exhaust System

Vaporization of Paratherm MR at higher temperatures caused by leakage in the system creates an unsafe operating environment. In order to alleviate this situation a complete system enclosure and exhaust fan was required. A Kansas State University website provided an exhaust fan sizing equation for kitchens [54]. Using Equation 3-5 as a minimum CFM requirement for the fan should provide enough air movement to exhaust most of the smoke generated by the system. The dimensions of the system enclosure are 5' x 5.5' x 5.5' for a total volume of roughly 150 ft^3. Using Equation 3-5, the minimum air flow required for the exhaust fan is 30 CFM. At high temperatures the system produces more smoke than a conventional kitchen, so it makes sense to size the fan for a larger air volume. Therefore, a 10" exhaust fan with a 350 CFM capacity should be adequate for the system. A 10" flexible duct connects the fan with the main exhaust line in the building. This set-up has proven to eliminate the majority of the oil vapor expelled from the system.

$$Minimum\_CFM = Room\_Volume \times 0.2$$

Equation 3-5

3.3.17 Miscellaneous/Minor Component Selection and Methods

In addition to the major components cited above, several minor components were specified to complete the system. Some relevant methods, such as pipe cleaning and installation are also briefly mentioned.

3.3.17.1. Pipe and Fitting Selection

In selecting the pipes and fittings, three main issues had to be addressed: (1) material choice; (2) connection type; and (3) pipe dimensions. Given that Paratherm MR is not corrosive, carbon steel (black steel) pipe and ductile iron and cast iron fittings were chosen because of their wide availability and low cost. Typical hot-oil systems offer two choices for the selection of piping: (1) high temperature flexible hose, and (2) rigid pipe. Moreover, the three main options for piping connections are: (1) NPT threaded; (2) welded; and (3) flanged.

Though welded fittings are generally recommended for hot-oil applications, Multitherm (a manufacturer of thermal hot oils) suggests that threaded fittings that are back-welded or using thread sealant are also acceptable (see Appendix G.2). Moreover, Paratherm was contacted and informed of the pressure (100 psi) and temperature range (25°C -180°C) of the specified system, and they indicated a threaded option may be viable given the low pressure. Furthermore, the hot and cold heat exchangers, as well as the mixing valves, most isolation valves, Y-type strainers, and pressure relief valves are readily available with threaded connections. With the exception of the pump, which is available in both flanged and threaded connections, all other components are most commonly and cost effectively found with NPT threaded. Given the relatively low pressure of the system and the difficulty posed by welded fittings, NPT connections were specified.

Given the wide availability of threaded rigid carbon steel pipe, this is the main piping component. However, at certain locations in the system, there was difficulty (in terms of location and orientation) in using rigid pipe. Here high temperature flexible hose with threaded fitting were used to ease connection problems. The pipe dimensions were largely dictated by component sizes:

1. Pump: 2" NPT fittings
2. Hot heat exchanger: 2.5" NPT fittings
3. Cold heat exchanger: 1.0" NPT fittings
4. Mixing Valves: 0.5" NPT fittings
5. Platens: 1.25" NPT fittings

Based on these sizes, rigid pipe in the largest available diameter was used to minimize the system pressure drop. Each major component was separated by at least one flexible hose with a female union (for easy installation/placement and removal). Reducers, diffusers, Y-junctions, T-junctions and 45° and 90° fittings were used to route the piping.

3.3.17.2. Isolation Valves

Isolation of every major component of the fluid system was necessary. Therefore, ball valves will serve as isolation valves before and after the mixing valves, platens, heat exchangers, pump, and expansion tank. These valves can be manually closed off when major components need removal or maintenance. Ball valves work well because of their minimal pressure loss when fully opened. Some locations, such as the cold heat exchanger output, where pressure loss is high relative to the rest of the system have full-port valves, while reduced-port valves were used in other locations.

3.3.17.3. Y-Strainer

A strainer was necessary to catch debris in the system before it is permitted to enter the pump. A 2" carbon steel Y-strainer with a 1/32" perforated Type 304 stainless steel screen (approximately equivalent to a 20 mesh screen) was selected. According to the manufacturer, based on a flow rate of 40 GPM, the strainer can be expected to have a 2-3 psi pressure drop.

3.3.17.4. Pressure Relief Valve

Given the choice of a positive displacement pump, a pressure relief valve was needed to ensure the system does not over-pressurize and damage the pump. The pump itself has a built-in pressure relief valve that was set at 125 psi. However, given that the system is designed for 100 psi, a redundant pressure relief valve that has a blow-out pressure of <100 psi was needed. A 2" Cast Iron (30-100 psi) pressure relief was selected and installed directly downstream of the pump (set at 100 psi).

3.3.17.5. Component Layout

The last step before construction could begin was to determine a rough layout of the system. Figure 3-30 shows the conceptual layout of a single platen subcircuit.

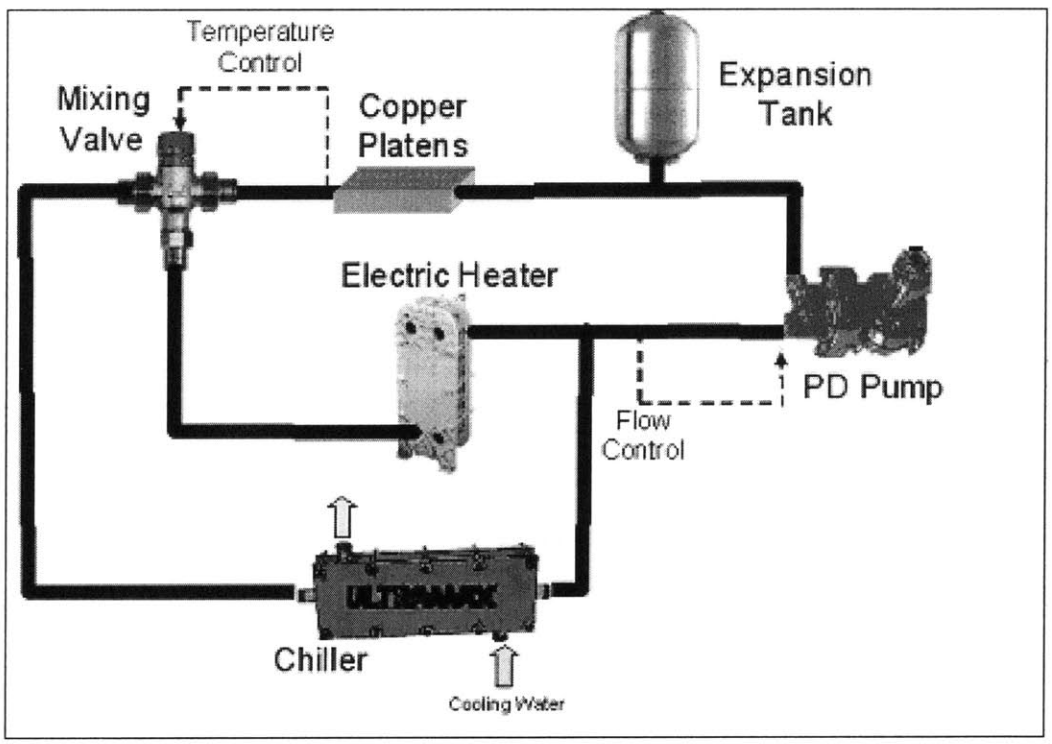

Figure 3-30 Schematic of a single platen subcircuit in the system

Based on this information, the physical dimensions of the major components, and rough dimensions of the minor components, a model was generated in 3D Studio Max to approximate the system layout prior to the purchasing of parts. Figure 3-31 shows this model. The placement of some items, such as the heater controller were changed during construction, however, the modeled layout is generally consistent with the actual system.

Reference the HME System Bill of Materials for a full listing of all system components (Appendix G.4).

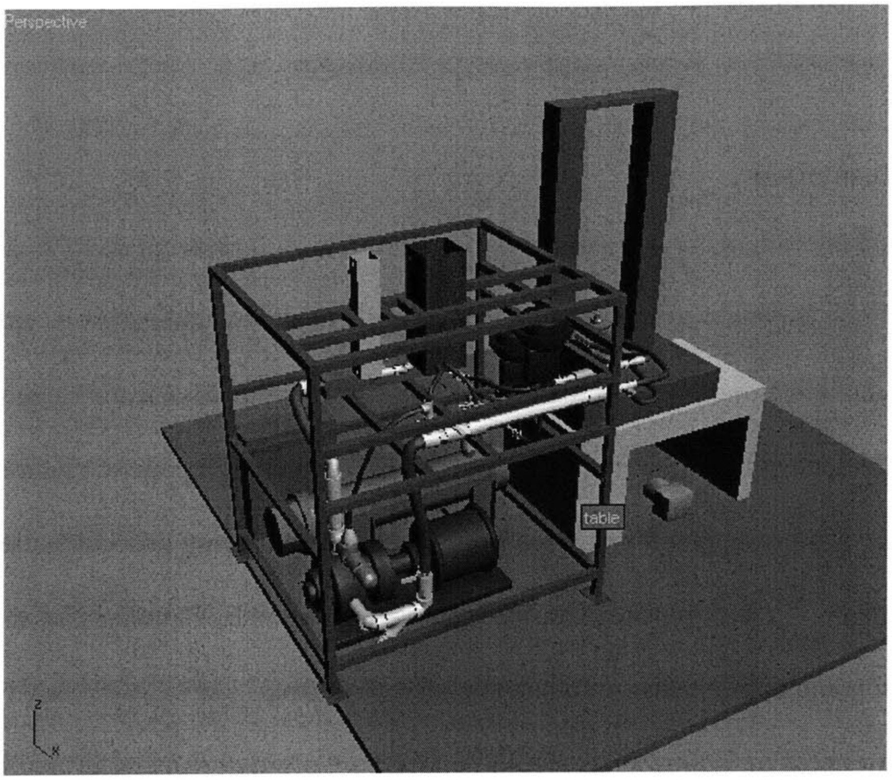

Figure 3-31 3D Studio Max model of the proposed system layout

3.3.17.6. Pipe Sealing

Loctite 567 was used to seal the NPT threaded connections. It is an anaerobic sealant that sets in contact with an active material in the absence of air. For locations where an inactive pipe material was used (all pipes except carbon steel) Loctite 7649 structural adhesive primer was used as an activator. Loctite was placed only on the male ends of pipe 1" and smaller and both on the male and female ends of pipes larger than 1" diameter. After the system was assembled, leakage ensued and several other thread sealants were applied (Loctite 5900, Duralco Epoxy, Jetlock#2, GE high temperature silicone caulk, Permatex No.2 sealant, Loctite 294, X-Pando pipe sealant, etc) at different locations in the system. No thread sealant either placed in the threads or around the perimeter of the pipe was able to stop leakage. Loctite 5900, however, was shown to significantly reduce leakage if applied in large amounts around the outside of the threaded connection (as seen at the platen-hose interface).

3.3.17.7. Insulation

There are two main alternatives for insulating hot-oil systems up to T=200°C: (1) fiberglass; and (2) closed cell foam-glass. Though fiberglass is inexpensive and commonly available, there is the tendency of hot-oil (that may leak from the system) to wick into the open cells of the fiberglass and oxidize, which will generate heat and may cause a fire. Therefore, given that threaded connections are being proposed, closed cell Foamglas insulation (a product of Corning) is recommended by Paratherm to insulate the system piping and components to reduce the chance of fire.

A thickness of 1.5 inches is recommended by Corning to ensure proper insulation for a T=200°C system. Jacketing material can either be aluminum (which will require securing the aluminum jacketing to the insulation with metal straps), or ASG (a type of high temperature fabric used to protect fiberglass insulation that is already attached to the Foamglas). Either option is acceptable, however, the ASG Foamglas will be easier to install and remove (simply slip fit the insulation over the pipe and secure with the adhesive tape provided on the insulation) then the aluminum (secure the aluminum over the pipe with metal straps). Foamglas can be purchased in standardized pipe lengths (0.5"-2.5" diameter and 1.5" -2" thickness) as well as specially shaped for other components such as valves. The material can be cut on-site with the use of a saw. Given leakage in the current system, no insulation has been purchased. Once the leakage has been resolved, Foamglas should be installed. In the case of a fire, a Class ABC Dry Chemical Fire Extinguisher is located next to the system.

3.3.17.8. Pipe Installation

The pipes were installed by 2-3 people starting from the pump outlet and proceeding toward the heat exchangers, mixing valves, platens, and back to the pump inlet. Certain subsections were pre-assembled in a vice to ease installation. Strap wrenches were found to be ineffective at properly tightening the connections. Rather, large pipe wrenches were used to torque down the fittings, unions, and hoses.

3.3.17.9. System Cleaning

Prior to construction, each component was cleaned in a mineral spirit bath and scrubbed with wire brushes to remove any oils, lacquers and dirt. This is to ensure that the system remains free of debris for good heat transfer performance and to avoid clogging the 1/8" channels in the platen.

CHAPTER

4 Modeling of HME II

4.1 Introduction

A significant portion of the thermal fluid system design was completed by Dirckx [29]. In order to understand the dynamics of the system, he created a thermal simulation in MATLAB. This initial simulation assisted in the selection of the hot heat exchanger. A summary of his model is described in Section 4.2.

4.2 Initial Thermal Model

The initial thermal fluid simulation included four major system components: platens, hot heat exchanger, cold heat exchanger, and mixing valves. The components were modeled independent of each other and the fluid flow rate and temperature is passed along the flow path. Since this was a discrete simulation, the fluid was simulated as packets of flow rate and temperature with its size dictated by the time step chosen. There were imposed time delays between the outlet of the platens and entrance to the heat exchangers and between the outlet of the heat exchangers and entrance to the platens. These delays caused oscillations in the model, but do not show up in the real system because the fluid is mixed, not discrete packets. A schematic of the information flow is shown in Figure 4-1. The platens were modeled as an insulated thermal mass with the only heat transfer from the Paratherm MR fluid convection. A shell-and-tube heat exchanger analysis modeled the hot heat exchanger, while the cold heat exchanger was modeled with curve fitted Manufacturer's data. The mixing valves were open loop and calculate the flows necessary to achieve a commanded temperature. Dirckx's thesis [29] provides for a more detailed explanation of the model.

After the construction of the HME II, a number of experiments were run to confirm the system performance. The model simulated a heating step from 40 to 150 °C at a system flow rate of 40 GPM to take under 100 seconds. However, experiments showed that this step could only be achieved in 860 seconds. This implied the initial model vastly overestimates the heating capacity of the system. Since a thorough understanding of the thermal fluid system dynamics was not only essential in the selection of components, but also helpful in designing a high performance control system, a more accurate model was developed.

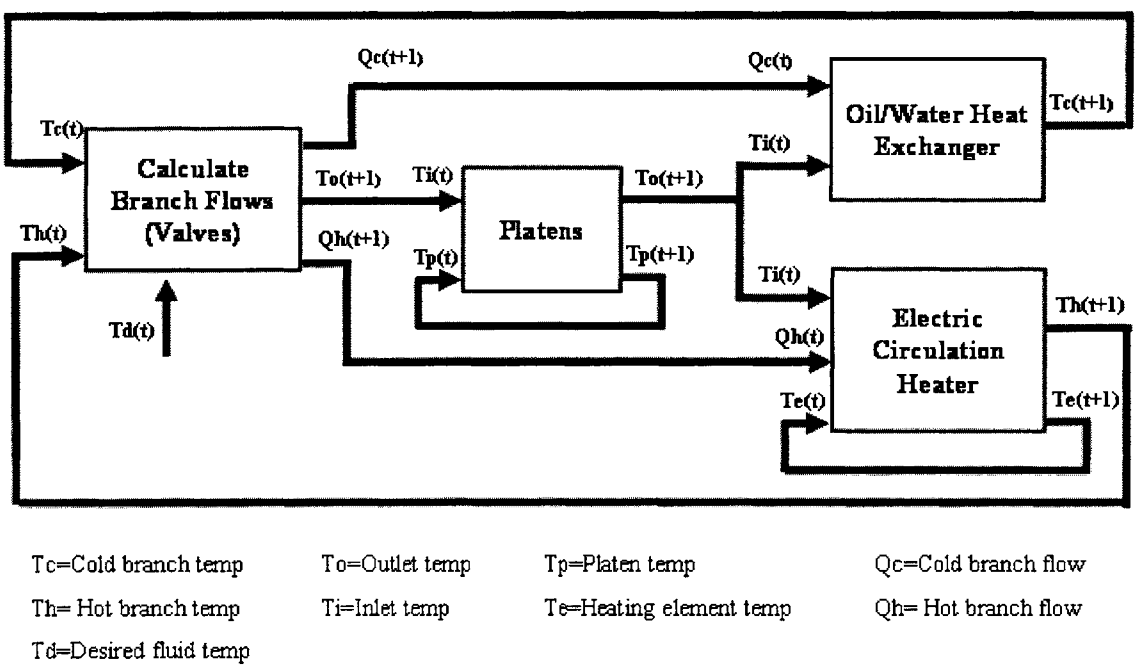

Figure 4-1 Information flow for the initial simulation [29]

4.3 Modifications to the Model

The initial model created by Dirckx overestimated the heating capacity of the system. After running a number of tests on the system, the data suggested that the cold and hot heat exchanger models needed to be redesigned. For the new system simulation, the base program was reused with the same flow and logic assumptions. However, major modifications to the hot heat exchanger and cold heat exchanger models were made. The platen and mixing valve models have no changes.

A flowchart of the simulation is shown in Figure 4-2. The simulation starts with an initialization of the constant parameters, such as the heater power, maximum heater temperature, time step, system flow rate, and delays. Then, a desired temperature profile is defined. The simulation proceeds to define the initial temperatures of the fluid out of each component in the model. Once these are set, the program enters a "for" loop with each iteration corresponding to a time step. In the "for" loop, temperature of the fluid and fluid flow rates are passed from component to component. The first component in the loop is the cold heat exchanger with the temperature of the fluid input defined by the temperature profile and initial flow rate half of the defined system flow rate. The temperature out of the cold heat exchanger will be an input to the mixing valve model. The next component in the loop is the hot heat exchanger with the temperature of the fluid input defined by the temperature profile and initial flow rate half of the defined system flow rate. Another variable monitored in the heater model is the temperature of its thermal mass. The temperature of the fluid out of the hot heat exchanger will be an input to the mixing valve model. Next, the simulation analyzes the platen model where the flow rate and temperature of the fluid input is defined in the initial conditions. The surface temperature of the platen is also monitored in this component model. A delay between the platens and the heat exchangers is imposed. The program then analyzes the mixing valve component model where the flows to the cold and hot heat exchangers are calculated. Finally, a delay between the mixing valves and platens are imposed. This sequence is repeated. Each of these major component models will be discussed in detail in the following sections.

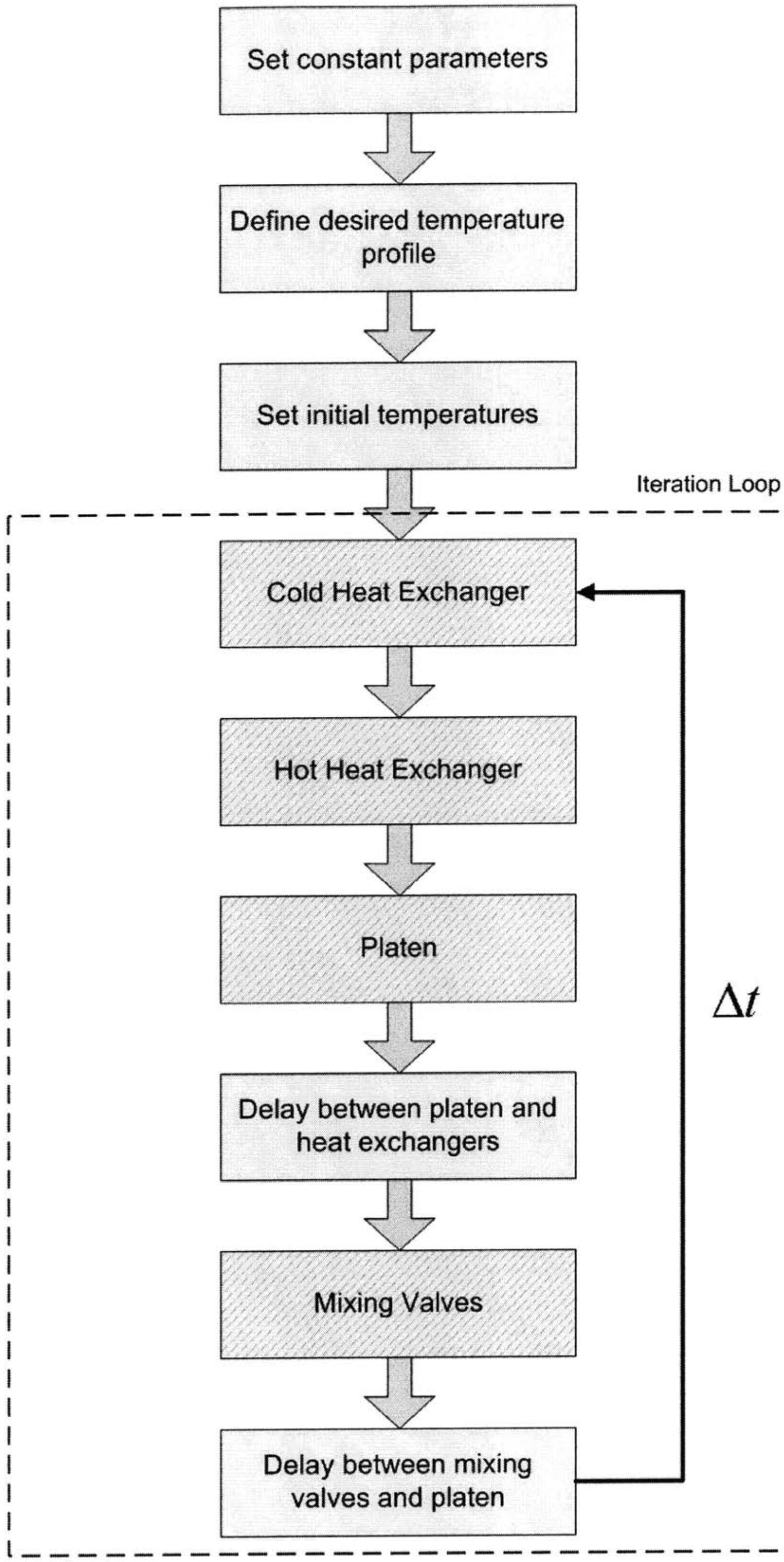

Figure 4-2 Flowchart of the simulation

4.3.1 Hot Heat Exchanger

As mentioned in Section 3.3.3, the hot heat exchanger is a 30 kW electric circulation heater from Vulcan. The initial heater model used a shell-and-tube heat exchanger analysis. This proved to overestimate the heating capacity, so instead a conservation of energy approach to model the heater dynamics was implemented. Assumptions behind the model include a mixed vessel that was perfectly insulated and the heater body was treated as a lumped thermal mass. A diagram of the heater with its defined control volume and energy flows is shown in Figure 4-3.

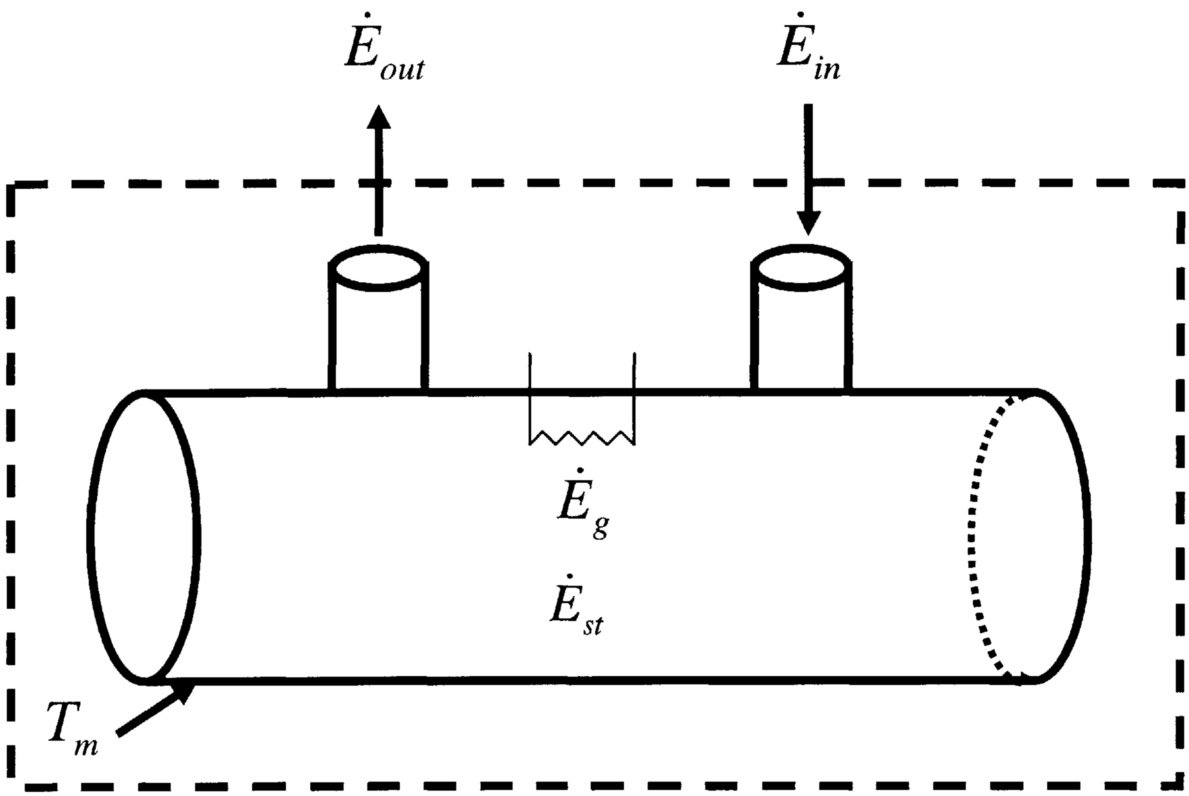

Figure 4-3 Diagram of the heater with energy flows and its defined control volume

Conservation of energy for this system is shown in Equation 4-1 [55]. The energy entering the system is from the fluid flowing into the heater. Equation 4-2 is the energy entering the system, where Q is the flow rate of fluid into the heater, ρ_i is the density of the fluid at the inlet temperature, c_{pi} is the specific heat of the fluid at the inlet temperature, and T_i is the temperature of the fluid at the inlet. The energy generated by the system is a perfect transfer of energy from the electric heating coils to the fluid shown in Equation 4-3. The energy out of the system is the thermal energy of fluid exiting the heat exchanger and the heat transfer between the fluid in the heat exchanger and the thermal mass of the heater body. Equation 4-4 describes the energy out of the system, where Q is the flow rate of fluid exiting the heater, ρ_o is the density of the fluid at the outlet temperature, c_{po} is the specific heat of the fluid at the outlet temperature, T_o is the temperature of the fluid at the outlet, h_{fm} is the heat transfer coefficient between the fluid in the heat exchanger and the thermal mass of the heat exchanger, A_{fm} is the area of heat transfer between the fluid and thermal mass in the heat exchanger, T_a is the average of the fluid inlet and outlet temperatures, and T_m is the temperature of the thermal mass. The last term in the conservation of energy equation is the energy storage term given by Equation 4-5. The terms are the following: ρ_a is the density of the average fluid temperature, c_{pa} is the specific heat of the average fluid temperature, V is the fluid volume within the heat exchanger, and T_a is the average fluid temperature. T_a is the average of the inlet and outlet temperatures with the derivative calculated using the previous time step value.

$$\dot{E}_{st} = \dot{E}_{in} + \dot{E}_g - \dot{E}_{out}$$

Equation 4-1

$$\dot{E}_{in} = Q\rho_i c_{pi} T_i$$

Equation 4-2

$$\dot{E}_g = 30\,\text{kW}$$

Equation 4-3

$$\dot{E}_{out} = Q\rho_o c_{po} T_o + h_{fm} A_{fm} (T_a - T_m)$$

Equation 4-4

$$\dot{E}_{st} = \rho_a c_{pa} V \frac{dT_a}{dt}$$

Equation 4-5

Another equation is used to calculate the temperature of the heater's thermal mass. This equation needs to be solved before calculating the outlet fluid temperature using the conservation of energy equation. The rate of change in temperature of the heater thermal mass is calculated using Equation 4-6, where h_{fm}, A_{fm}, T_a, and T_m have been described earlier and ρ_m is the density of the material of the thermal mass, c_{pm} is the specific heat of the thermal mass, and V_m is the volume of the thermal mass.

$$\frac{dT_m}{dt} = \frac{h_{fm} A_{fm} (T_a - T_m)}{\rho_m c_{pm} V_m}$$

Equation 4-6

The heater is assumed to be the carbon steel shell with a mass of 50 kg. The heat transfer coefficient is calculated the same way as Dirckx [29] where an effective diameter is calculated using Equation 4-7, where P_T is the heater coil pitch and OD_T is the diameter of the coils [56]. Once the effective diameter is known, the Nusselt number is calculated using Equation 4-7, where Re is the Reynolds number and Pr is the Prandtl number [57]. Once the D_e and Nu are known, the h_{fm} is calculated using Equation 4-9, where k_m is the thermal conductivity of the fluid inlet temperature. Equation 4-6 can then be solved by Euler integration. Plugging in T_m and manipulating the conservation of energy equation to isolate T_o, it can be solved in a straightforward manner. The complete MATLAB code for the heater can be found in Appendix E.3.

$$D_e = \frac{4\left(P_T^{\,2} - OD_T^{\,2}\pi/4\right)}{\pi OD_T}$$

Equation 4-7

$$Nu = 0.36\,\mathrm{Re}^{0.55}\,\mathrm{Pr}^{1/3}$$

Equation 4-8

$$h_{fm} = \frac{Nu \times k_m}{D_e}$$

Equation 4-9

4.3.2 Cold Heat Exchanger

The initial cold heat exchanger model utilized curve fitted manufacturer's data to predict the thermal response. Only a limited number of data points were provided, so the model tended to deviate from the actual performance. The modified model simulated the cold heat exchanger as a plate-and-frame heat exchanger. A diagram of the MaxChanger model MX-22 from Tranter PHE is shown in Figure 4-4. This heat exchanger has 40 stainless steel plates 24" long and 4" wide spaced 0.048" apart with Paratherm MR flowing in one direction and city water flowing in the opposite direction alternating between plates. The MX-22 was analyzed as a counter flow parallel heat exchanger using an effectiveness method under the following assumptions:

1. The heat exchanger is perfectly insulated.
2. Axial conduction is neglected.
3. Potential and kinetic energy changes are negligible.

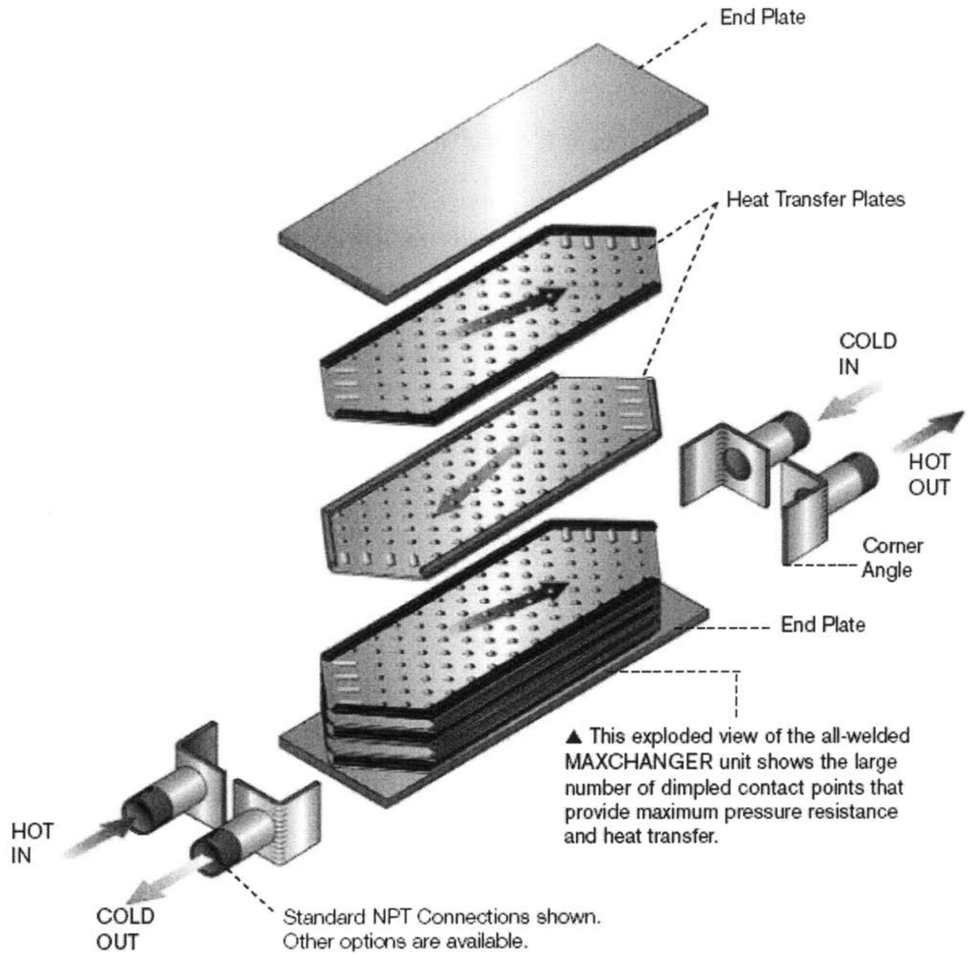

Figure 4-4 Schematic of the MaxChanger model MX-22 from Tranter PHE [58]

The first step necessary for this type of analysis is finding the heat transfer coefficients for the hot and cold sides. Since the entrance of the fluid channels is non-circular, a hydraulic diameter, D_h, is calculated. This is used to calculate the Reynolds number given by Equation 4-10, where *Vel* is the velocity of the fluid, ρ is the density of the fluid, and μ is the fluid viscosity. The Nusselt number is calculated using a single-phase 45° Chevron plate analysis shown in Equation 4-11 with the coefficients summarized in Table 4-1 [59]. The heat transfer coefficients can be found using Equation 4-12. This analysis is done for both the cold water flow and hot oil flow.

$$Re = \frac{Vel \times D_h \times \rho}{\mu}$$

Equation 4-10

$$Nu = C \times Re^n \times Pr^{1/3}$$

Equation 4-11

Table 4-1 Coefficients for varying Reynolds numbers with Chevron 45° plates

Reynolds Number	C	n
<10	0.718	0.349
10-100	0.400	0.598
>100	0.300	0.663

$$h = \frac{Nu \times k}{D_h}$$

Equation 4-12

Once the heat transfer coefficients for the two flows are calculated, an effectiveness method is used to find the outlet temperature of the Paratherm MR [60]. The rate of heat transfer is given by Equation 4-13, where C_{min} is the minimum capacity rate, $T_{h,i}$ is the hot fluid inlet temperature, $T_{c,i}$ is the cold fluid inlet temperature, and ε is the effectiveness. For a counter flow heat exchanger ε is calculated by using Equation 4-14. C^* is the capacitance ratio (Equation 4-15) and NTU is the number of transfer units (Equation 4-16), which indicates the size of the heat exchanger. Equation 4-16 has $\overline{U}$, which is the overall heat transfer coefficient and A_s is the total heat transfer surface area. Finally, the hot fluid outlet temperature is calculated using Equation 4-17.

$$q = C_{min}(T_{h,i} - T_{c,i})\varepsilon$$

Equation 4-13

$$\varepsilon = \frac{1-\exp[-NTU(1-C^*)]}{1-C^*\exp[-NTU(1-C^*)]}$$

Equation 4-14

$$C^* = \frac{C_{min}}{C_{max}}$$

Equation 4-15

$$NTU = \frac{\overline{U}A_s}{C_{min}}$$

Equation 4-16

$$T_{h,o} = -\frac{q}{C_h} + T_{h,i}$$

Equation 4-17

4.3.3 Platen

The platen model is the same as the one in the initial simulation created by Dirckx [29]. This model treats the copper platens as a lumped thermal mass and the only heat transfer is from the fluid to the surface area of the 18 1/8" diameter channels in each platen. In the model it is necessary to calculate the fluid temperature out of the platens, which involves finding the heat transfer coefficient. First, the Reynolds number for internal flow given in Equation 4-18 should indicate whether the flow is laminar (Re$\leq$ 2300) or turbulent (Re$\geq$ 2300), where *Vel* is the velocity of the fluid, *D* is the diameter of the channel, ρ is the density of the fluid, and μ is the dynamic viscosity of the fluid. The Prandtl number needs to be calculated using Equation 4-19, where c_p is the specific heat of the fluid, μ is the dynamic viscosity of the fluid, and *k* is the thermal conductivity of the fluid. Once these dimensionless numbers are found, the Nusselt number for flow in the laminar regime using a constant temperature approximation is 3.66 or for flow in the turbulent regime it can be calculated using Equation 4-20 (valid when 0.5<Pr<2000 and

3000<Re<5x10^6) [57]. The friction factor in Equation 4-20 can be calculated using Equation 4-21 assuming 3000<Re<5x10^6. Once these values are found, the heat transfer coefficient is calculated using Equation 4-22.

$$\mathrm{Re} = \frac{(Vel)D\rho}{\mu}$$

Equation 4-18

$$\Pr = \frac{c_p \mu}{k}$$

Equation 4-19

$$Nu_D = \frac{(f/8)(\mathrm{Re} - 1000)\Pr}{1 + 12.7(f/8)^{1/2}(\Pr^{2/3} - 1)}$$

Equation 4-20

$$f = (0.790 \ln \mathrm{Re} - 1.64)^{-2}$$

Equation 4-21

$$h = \frac{(N_u)k}{D}$$

Equation 4-22

The temperature of the fluid out of the platens can be calculated using Equation 4-23, where T_{ip} is the temperature of the fluid into the platen, T_s is the temperature of the channel surface, P is the perimeter of the channel, L is the length of the channel, $\dot{m}$ is the mass flow rate of the fluid, c_p is the specific heat of the fluid, and h is the heat transfer coefficient. Once the outlet temperature is found, the median temperature of the fluid can be estimated and the energy transferred from the fluid to the platen is calculated using Equation 4-24, where T_{median} is the estimated median temperature of the fluid in the platens, A is the contact surface area between the fluid and platen, and the other variables have been defined earlier.

$$T_{op} = (T_{ip} - T_s)e^{-\frac{PL}{\dot{m}c_p}h} + T_s$$

Equation 4-23

$$q = hA(T_{median} - T_s)$$

Equation 4-24

The rate of change of platen surface temperature can be calculated by dividing the energy transfer by the thermal mass of the platens. Euler integration is used to solve for the platen temperature after each time step. Not included in the model is heat loss to the environment and heat transfer to the surface area within the manifolds.

4.3.4 Mixing Valves

The mixing valve model is also the same as the one used in [29]. Conservation of mass and momentum is used to calculate the fluid flows for the hot and cold side for a commanded mixing valve outlet temperature and flow given in Equation 4-25 and Equation 4-26, respectively. The terms in these two equations are the following: Q is the flow rate, ρ is the fluid density, c_p is the fluid specific heat, and T is the fluid temperature, with the subscripts c referring to the cold side, h referring to the hot side, and p referring to the outlet platen side. The mixing valves are treated as linear. There is also an imposed finite amount of time it takes to move the mixing valve position, which is simulated in the model. If the desired valve position cannot be reached in the given time step, the outlet fluid temperature is calculated at that given position.

$$Q_h = \frac{Q_p \rho_p c_{pc}(T_p - T_c)}{\rho_h c_{ph}(T_h - T_c) + \rho_h c_{pc}(T_p - T_c)}$$

Equation 4-25

$$Q_c = \frac{Q_p \rho_p - Q_h \rho_h}{\rho_c}$$

Equation 4-26

4.4 Optimal Operating Conditions for each Phase of the Process Cycle

Using the model described in Section 4.3, a variety of simulations were run to predict the thermal response of the system. One of the goals of the HME II was to reduce the process cycle time and it has been documented that the limiting rate of this process cycle is the heating and cooling phases. Therefore, flow rate dependent simulations were run to determine the optimal operating conditions.

4.4.1 Flow Rate Dependencies

Three sets of temperature step responses were simulated under total system flow rate conditions of 10, 20, 30, and 40 GPM. The first simulation is shown in Figure 4-5, where the open loop platen temperature command was stepped from 55 to 120 °C and back down to 55 °C. This figure indicates that flow rate does not affect the time constant when commanding a platen temperature of 120 °C. A physical explanation for this effect is that there is enough hot fluid in the hot heat exchanger to get the platens up to 100 °C very quickly with the heater coils needing to heat up only a small amount of additional cold fluid from the cold side of the system. The simulation also suggests that a higher flow rate will cool down the platens at a faster rate. Since the cold heat exchanger does not have a large fluid storage capacity, cooling of the fluid only takes place within a small volume and is primarily driven by a temperature gradient rather than a constant heat flux. Therefore, running fluid through the cold heat exchanger at a faster rate should cool the system fluid faster.

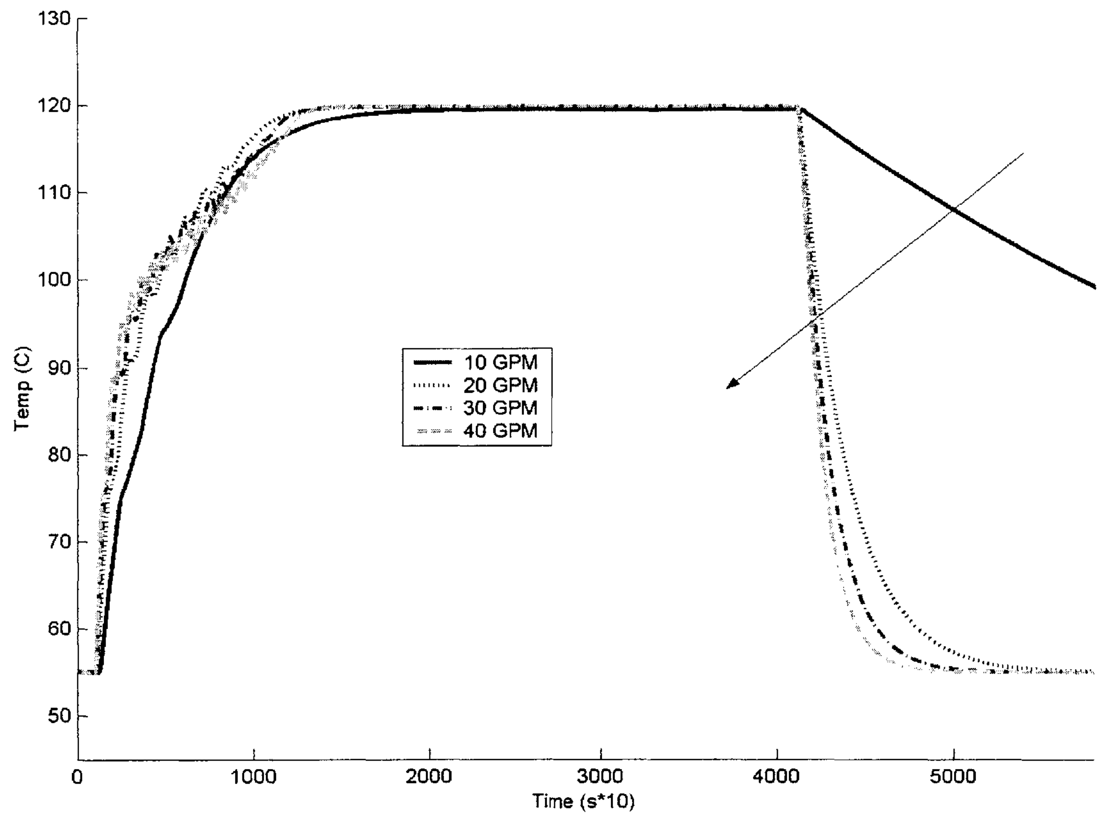

Figure 4-5 Simulated open loop platen step response between predetermined temperatures of 55 and 120 °C at varying flow rates (arrow points in the direction of increasing flow rate)

The second simulation shown in Figure 4-6 shows the open loop thermal step response for predetermined temperatures from 55 to 140 °C and back down to 55 °C. The most noticeable difference from the first simulation is the heating response. At the higher set point temperature there is not enough hot fluid stored in the hot heat exchanger to quickly get the platen temperature up to 140 °C. Around 100 °C, the hot supply diminishes and the system fluid relies on heat from the heater coils. The heater increases the fluid temperature quicker at the lower flow rates because the fluid spends a longer time in contact with the heater coils. It takes roughly 70 seconds longer for the platens to get to 140 °C at 40 GPM versus 10 GPM. The cooling response is the similar to the previous simulation for the same reasons stated before.

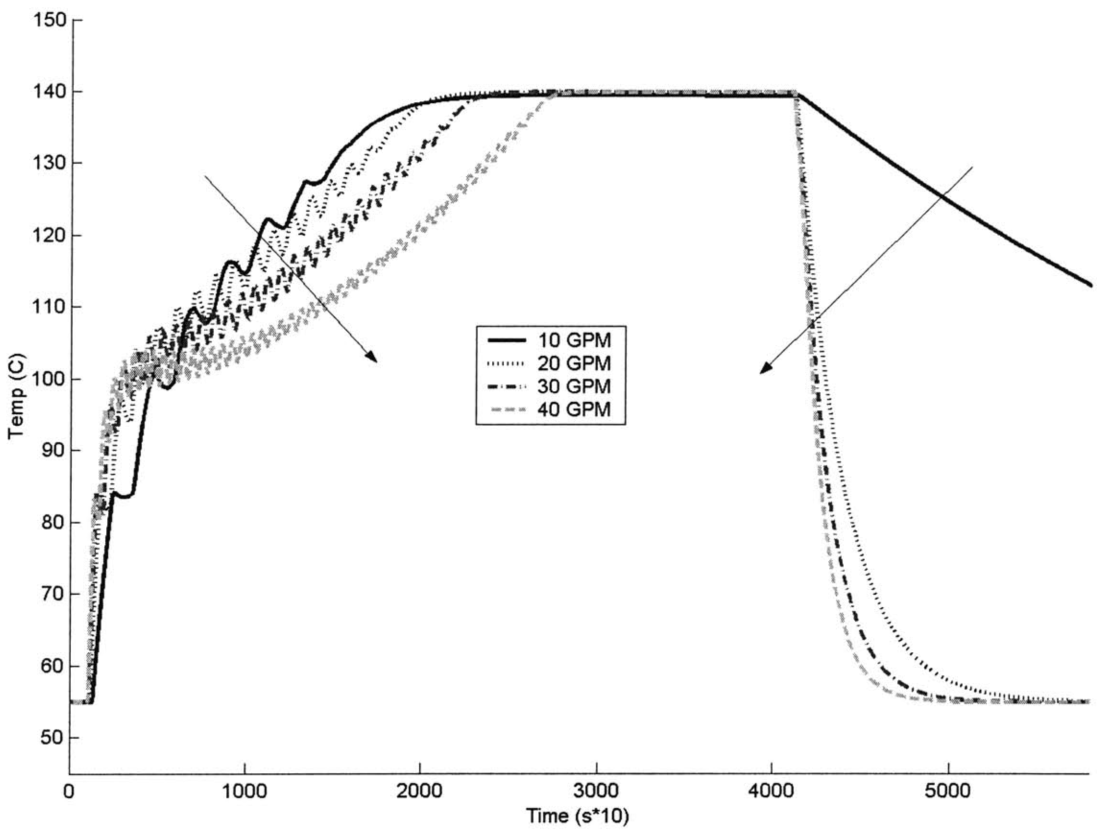

Figure 4-6 Simulated open loop platen step response between predetermined temperatures of 55 and 140 °C at varying flow rates (arrows points in the direction of increasing flow rate)

The third simulation shown in Figure 4-7 shows the open loop thermal platen step response for predetermined temperatures from 55 to 160 °C and back down to 55 °C. The slow heating response at the higher flow rates is exacerbated in this simulation. All of the simulations indicate that heating should occur at the lowest flow rate possible, while cooling should occur at the highest flow rate.

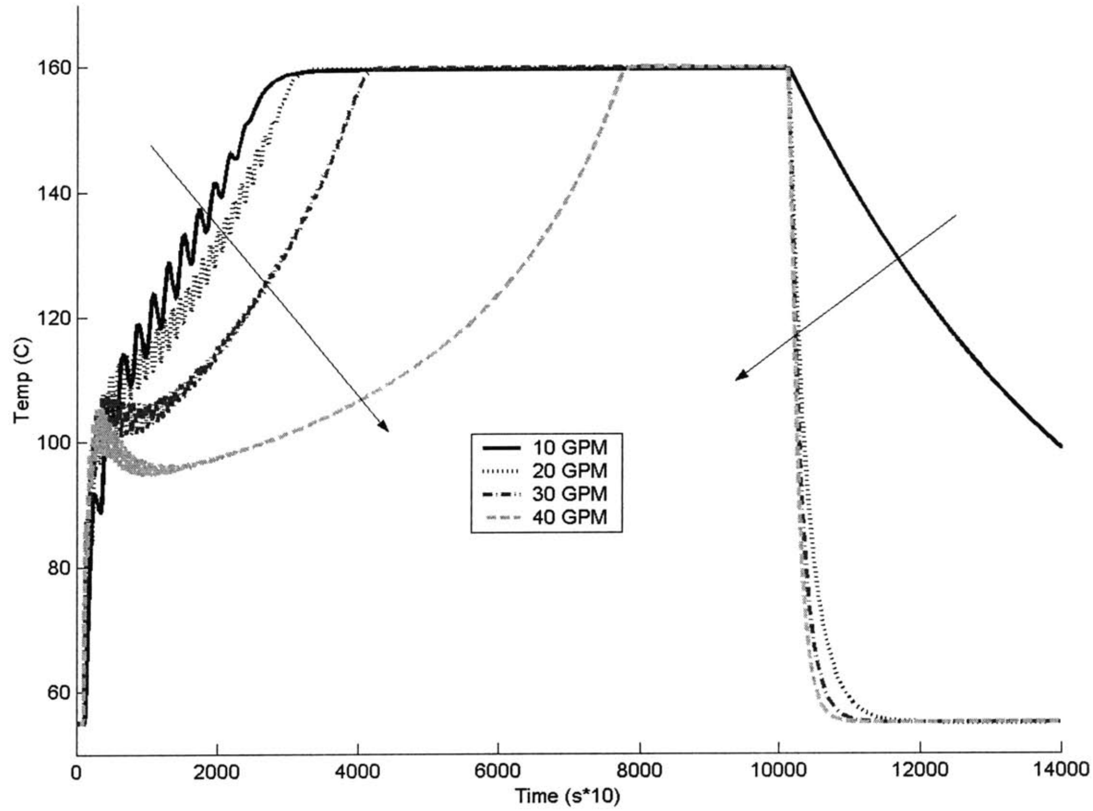

Figure 4-7 Simulated open loop platen step response between predetermined temperatures of 55 and 160 °C at varying flow rates (arrows points in the direction of increasing flow rate)

4.5 Empirical Data Verifying Optimized Conditions

The simulations in Section 4.4 indicate that a low flow rate will produce the fastest heating response and a high flow rate will produce the fastest cooling response. A number of tests were run to confirm these simulation results. Empirical data from these experiments are highlighted in the following sections.

4.5.1 Heating of the Platens at Various Flow Rates

The experimental results of an open loop heating response with the mixing valve switched from fully open on the cold side to fully open on the hot side at varying system flow rates is shown in Figure 4-8. The trend of faster heating at lower flow rates is consistent with the simulation. By just looking at the heating response dominated by the heater coils (i.e. between 200 and 400 seconds), the heating rate in this regime was calculated for the different flow rates (Figure 4-9). The heating rate appears to be linearly related to the flow rate during this portion of the heating cycle. The heating rate and temperature when the heater coils dominate the thermal response differ from the simulation. Possible explanations for these discrepancies will be discussed in Section 4.6.2.

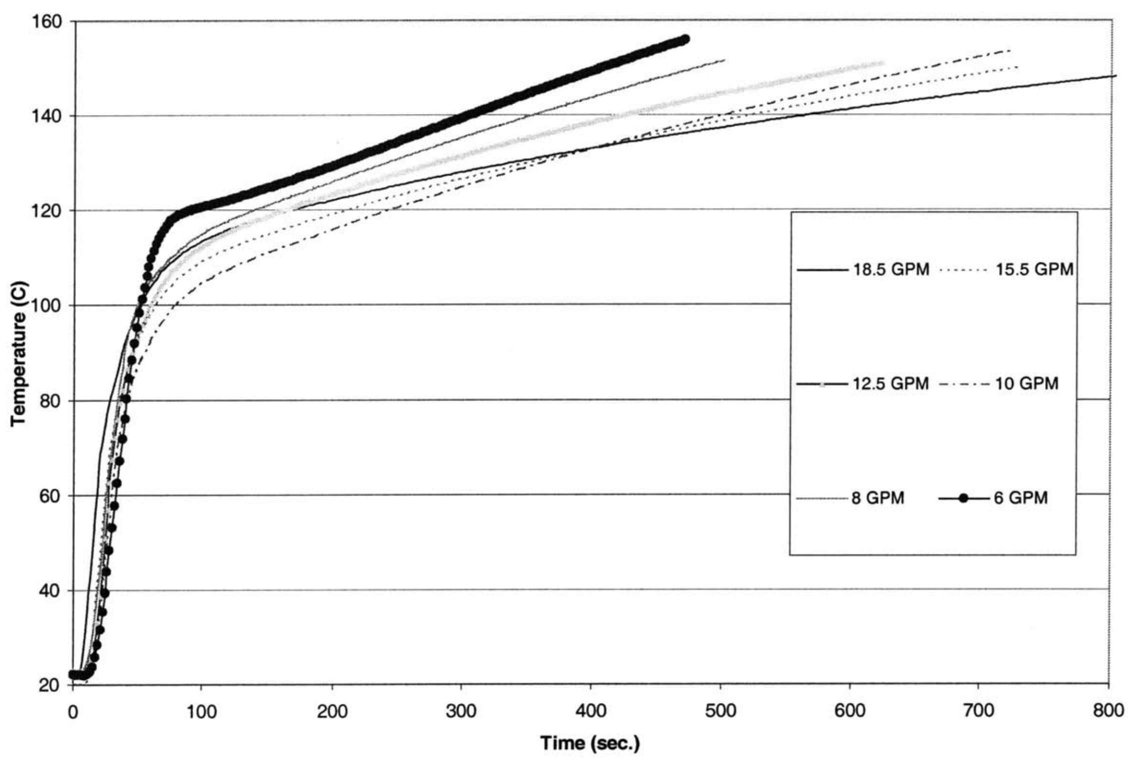

Figure 4-8 Open loop response from fully cold to fully hot of the average bottom platen temperature at varying bottom platen flow rates

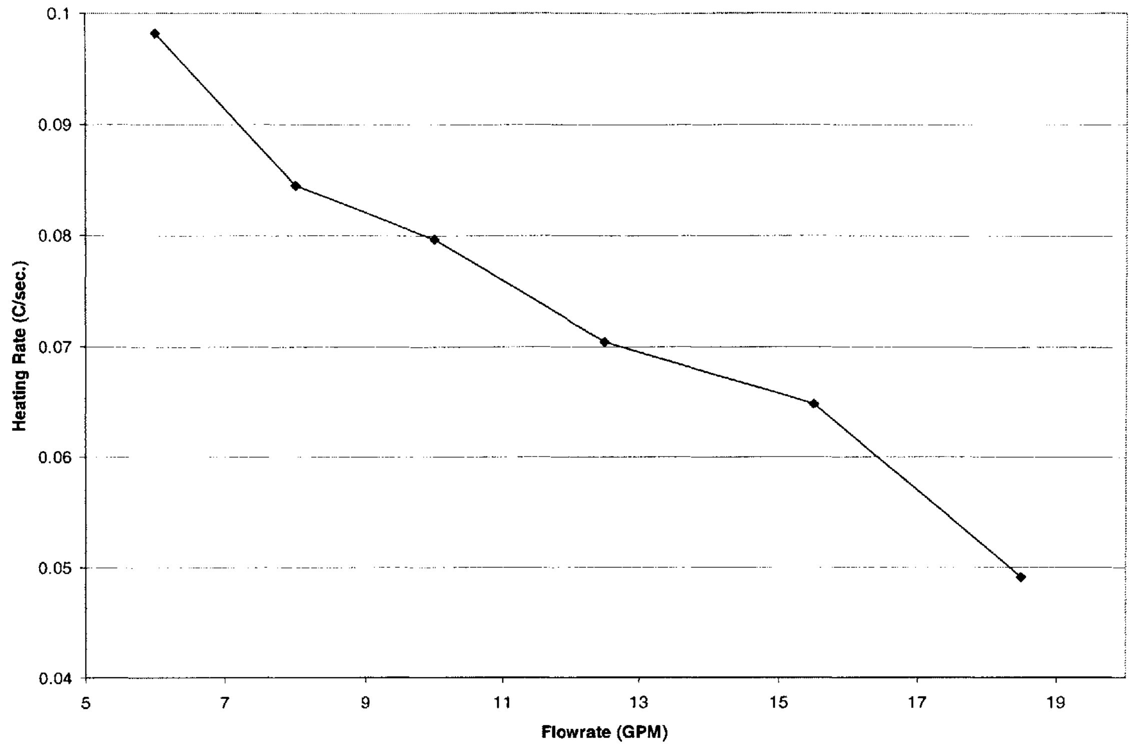

Figure 4-9 Heating rate of the bottom platen at varying flow rates during the heater dominated response

4.5.2 Cooling of the Platens at Various Flow Rates

The experimental results of the open loop response starting from an average bottom platen temperature at roughly 155 °C to fully open on the cold side at varying flow rates is shown in Figure 4-10. These results are consistent with the general trend of the simulations, where the higher flow rates correspond to a faster cooling rate. The only significant discrepancy with the experimental data and simulation is the cooling curve at 6 GPM flowing through the bottom platen. The simulation has the bottom platen temperature taking a very long time to cool down compared with the higher flow rates. This drastic change in cooling rate can be attributed to the fluid transition from turbulent to laminar flow through the cold heat exchanger. The actual system has a number of imperfections and characteristics including chevron plates which will keep the flow in the turbulent regime at the low flow rate.

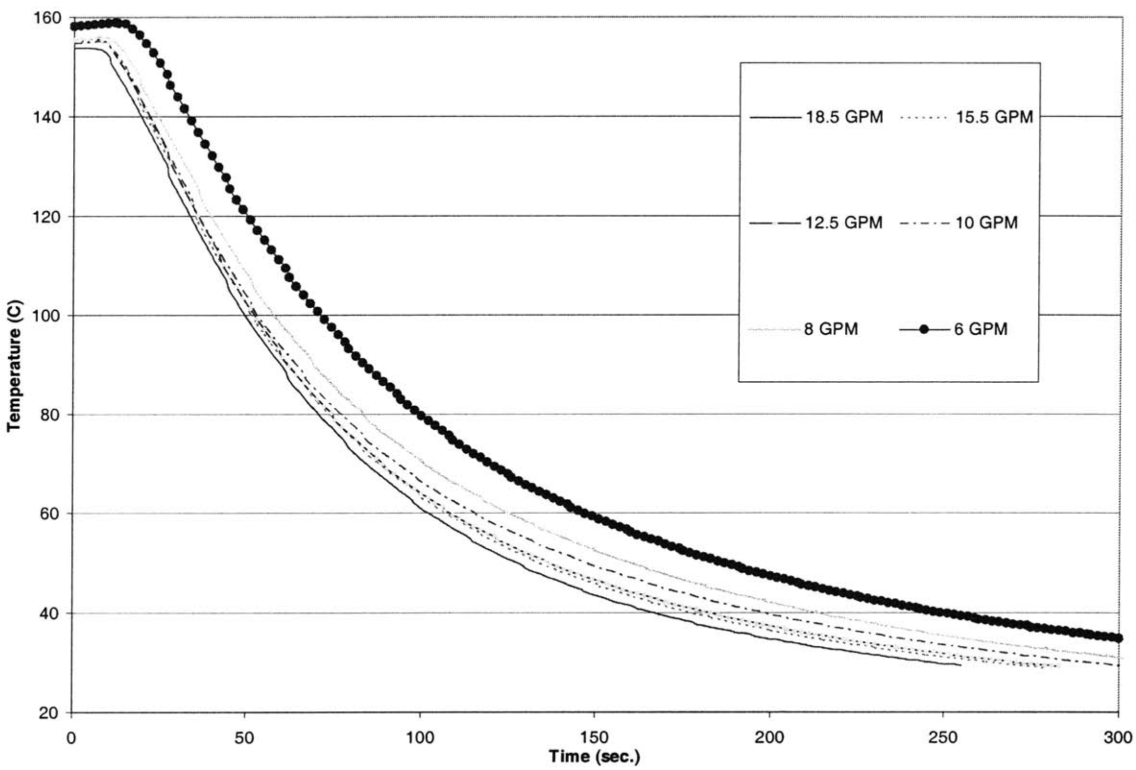

Figure 4-10 Temperature response of the average bottom platen temperature when cooled from roughly 155 °C to fully open cold

4.5.3 Low Flow Rate during De-Embossing

In order to reduce the embossing cycle time, it is necessary to reduce the system flow rate during heating and increase the system flow rate during cooling. However, these procedures have some caveats. Figure 4-11 shows a simulation of a typical embossing cycle with a commanded open loop embossing temperature of 120 °C and a commanded open loop de-embossing temperature of 55 °C at a platen flow rate of 6 GPM. The corresponding experimental data for these same processing conditions is shown in Figure 4-12. During the cooling phase in both the simulation and experiment, the hot heat exchanger fluid temperature recovers to its set point temperature, which in this case is 180 °C. Because a high flow rate is desired during cooling, the same embossing cycle is simulated and run experimentally at a platen flow rate of 18 GPM. The results are shown in Figure 4-13 and Figure 4-14. During cooling in both the simulation and experiment, the hot heat exchanger temperature recovers to its set point temperature during the initial transient, but once the mixing valves open the hot supply a little, the hot heat exchanger outlet temperature begins to decrease. This would be detrimental to the heating phase for the ensuing cycle. Therefore, it is recommended that during cooling, the flow rate is only increased when the mixing valves are fully opened on the cold side.

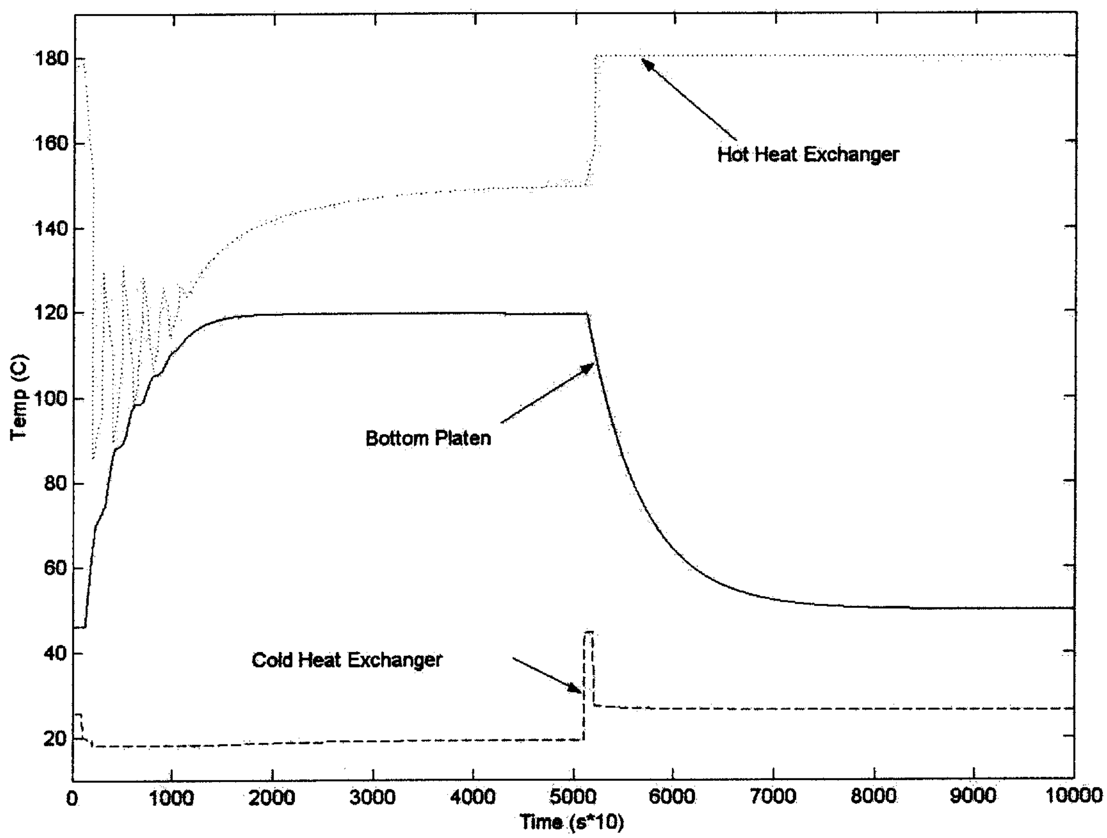

Figure 4-11 Simulation of an open loop step response with predetermined temperatures from 46 to 120 to 50 °C at a platen flow rate of 6 GPM

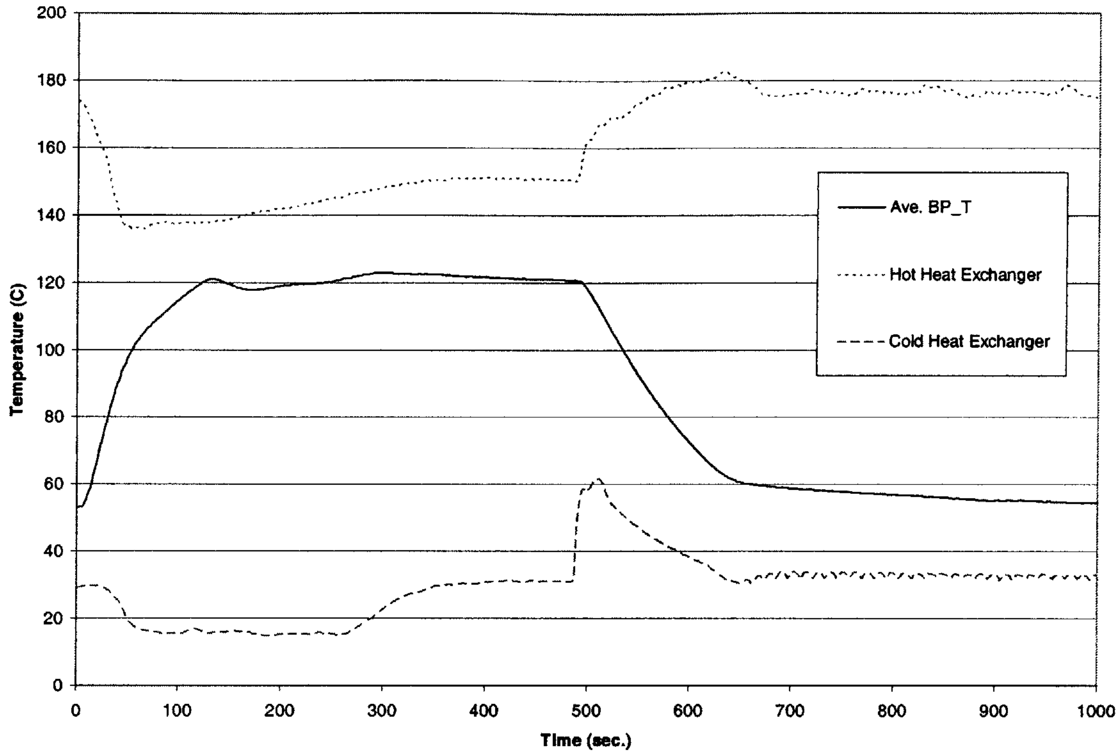

Figure 4-12 Experimental Data for a closed loop control step response from 55 to 120 to 55 °C at a platen flow rate of 6 GPM

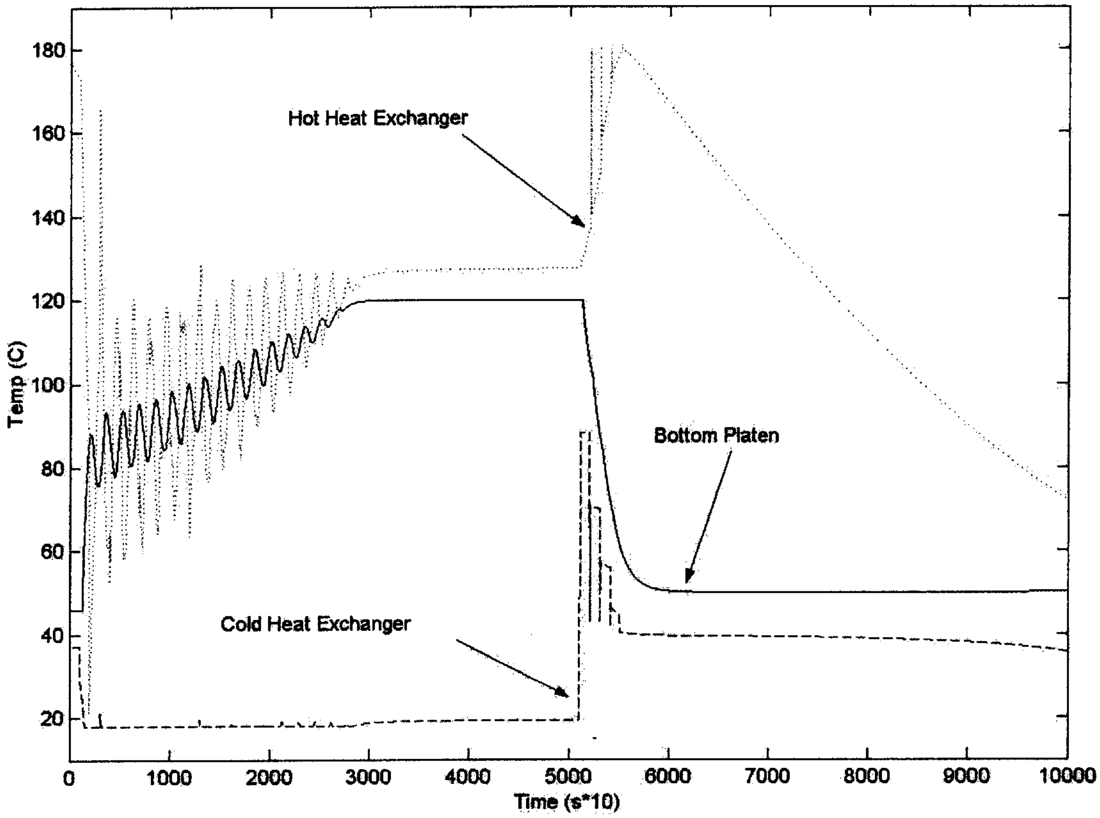

Figure 4-13 Simulation of an open loop step response with predetermined temperatures from 46 to 120 to 50 °C at a platen flow rate of 18 GPM

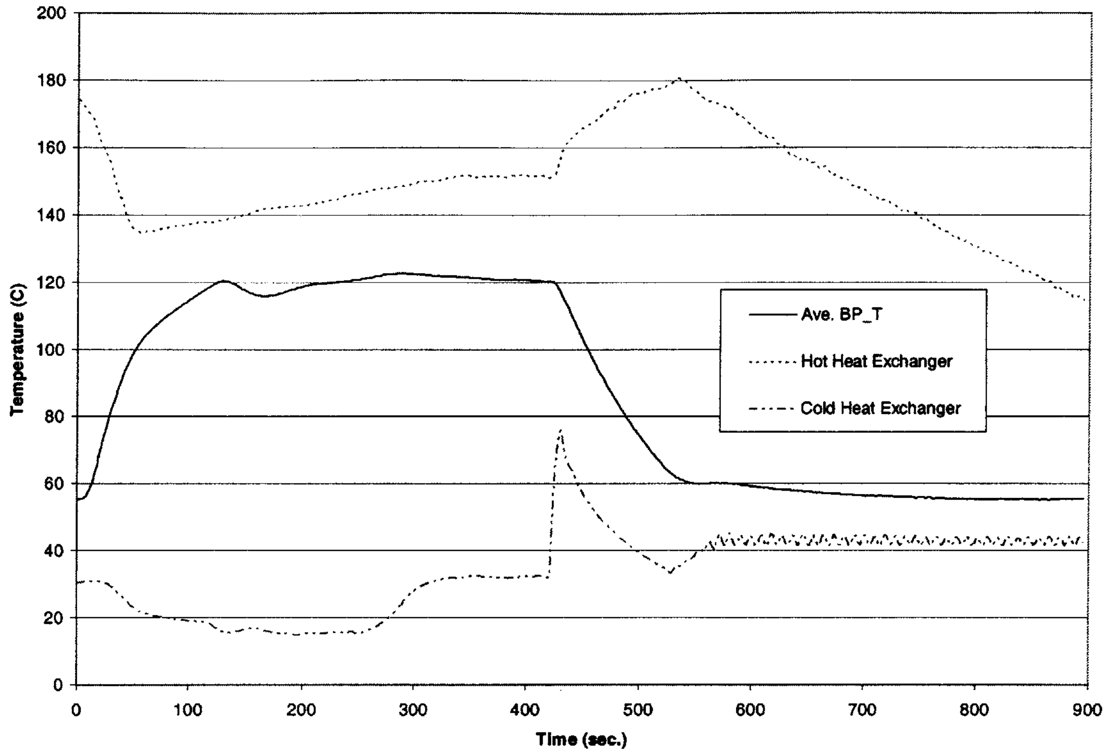

Figure 4-14 Experimental Data for a closed loop control step response from 55 to 120 to 55 °C at a platen flow rate of 18 GPM

4.6 Empirical Data vs. Theoretical Simulation

The model captures the general trends of flow rate dependent thermal responses at different conditions. This information served as a basis when designing the control system for fast cycle times. It is important to directly compare the simulation with empirical data to check the accuracy of the model. Possible sources of discrepancies between the model and experimental data are discussed in Section 4.6.2.

4.6.1 Various Test Conditions

The simulation was run at a number of processing conditions and compared with corresponding empirical data to check the accuracy of the model. Figure 4-15 compares the open loop simulation versus the closed loop experimental step response from 46 to 120 to 50 °C at a flow rate of 6 GPM per platen. The model is open loop, which accounts for the first-order response of the platen temperature. The experimental data on the other hand has closed loop platen temperature PI control on the heating side and closed loop valve fluid outlet temperature PI control on the cooling side. The controllers were not optimized, which is why the experimental data had some overshoot. Both of the heat exchanger temperature responses follow the general temperature transient. However, the simulation models the heat exchangers as having unusually quick responses during the transient periods. Another test condition is shown in Figure 4-16, to confirm the simulation's ability to accurately capture the thermal response at various processing conditions. This condition was for an open loop simulation versus closed loop experimental temperature step response from 50 to 140 to 50 °C at a flow rate of 6 GPM per platen. Again, the platen temperature response is modeled fairly well, and the same effects from the heat exchangers are observed. Therefore, the model can reliably be utilized as a tool for designing the system controls.

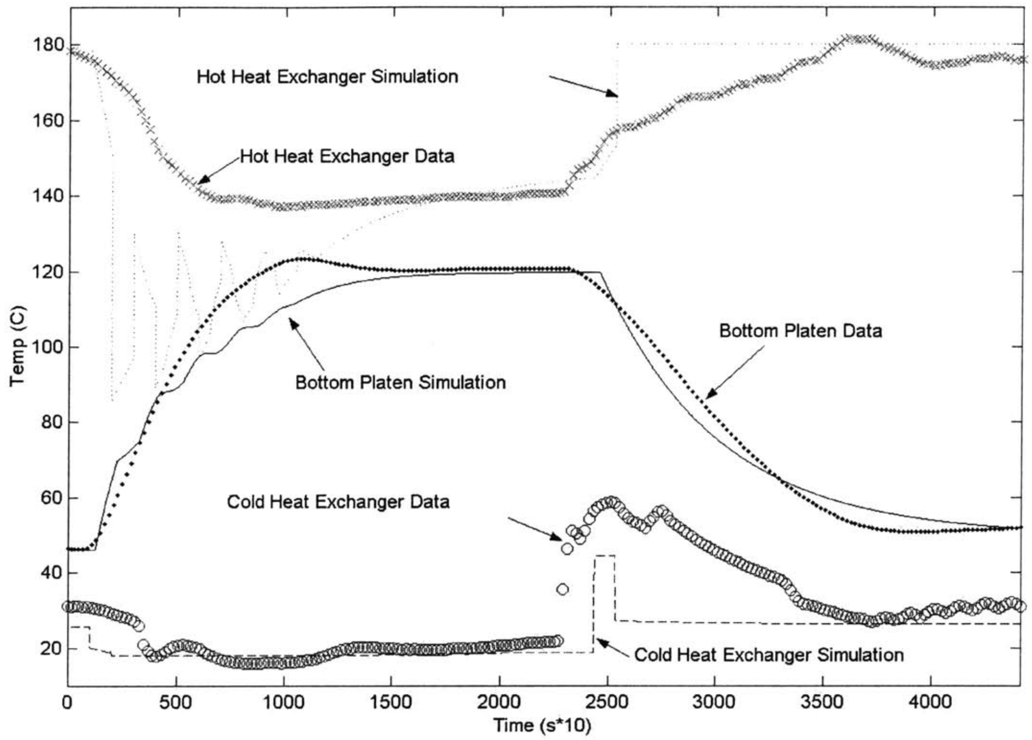

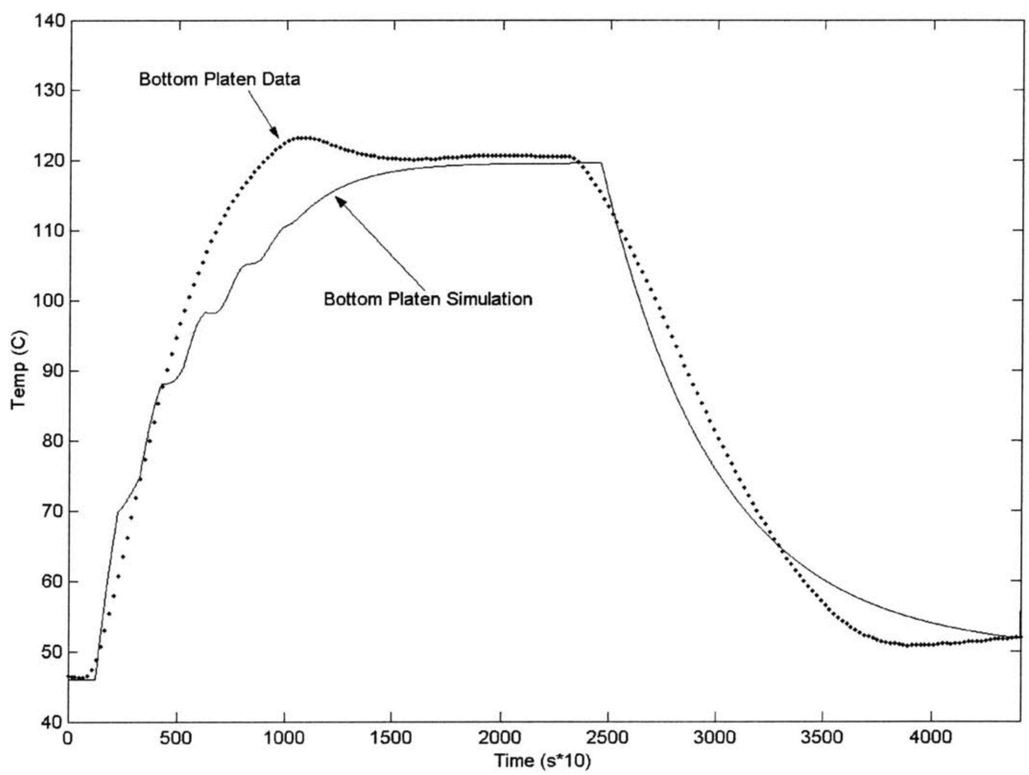

Figure 4-15 Simulated open loop and experimental closed loop control data for a step response from 46 to 120 to 50 °C at a flow rate of 6 GPM per platen

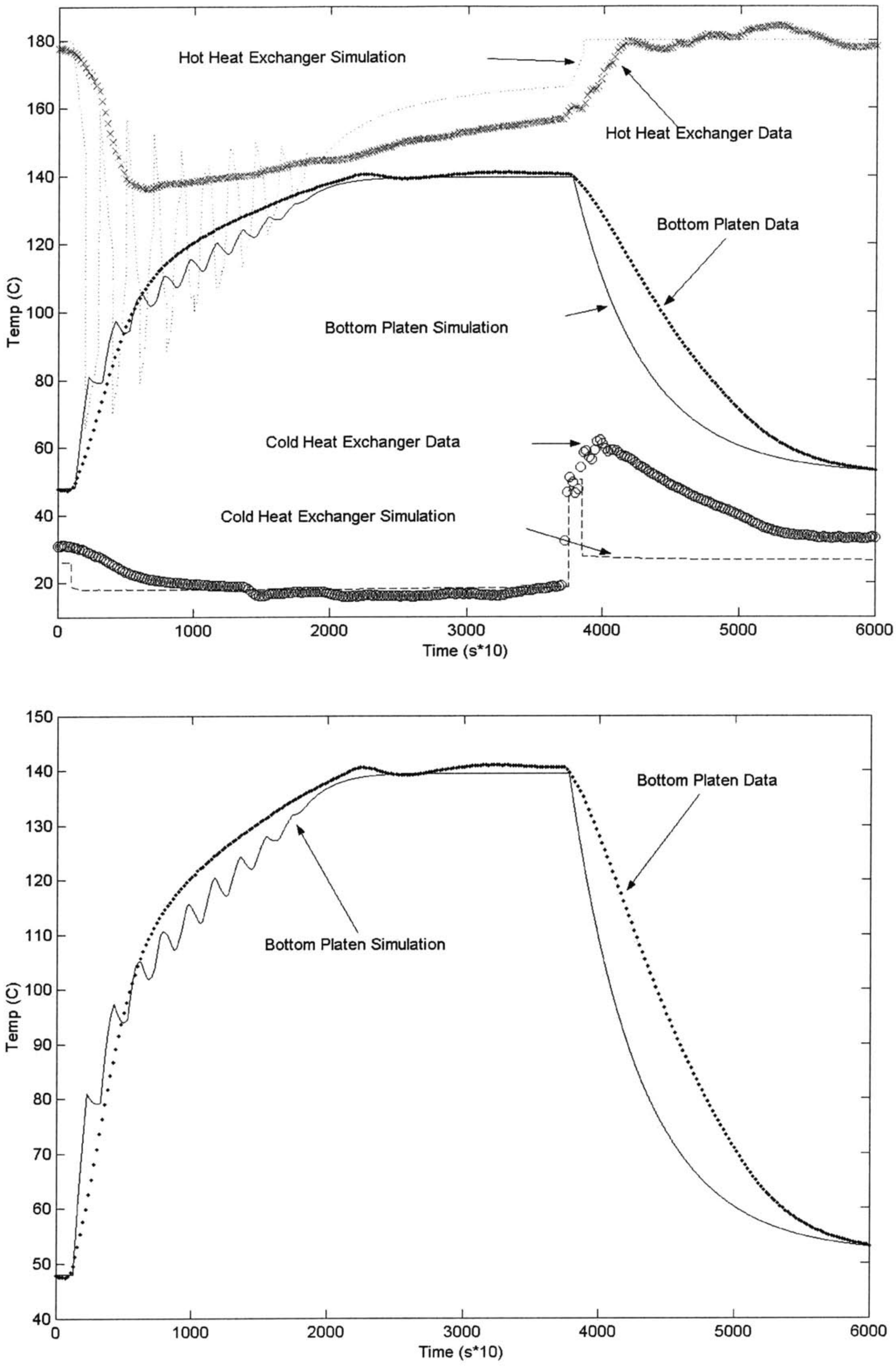

Figure 4-16 Simulated open loop and experimental closed loop data for a step response from 50 to 140 to 50 °C at a flow rate of 6 GPM per platen

4.6.2 Model Discrepancies

A number of effects were not modeled in the simulation and some have a larger effect than others. The following list of discrepancies is certainly not exhaustive but stands out to have a significant effect on the model.

4.6.2.1. Efficiency of Heater

The model assumed the electric heater to be 100% efficient in transferring all of its resistive energy into the working fluid. This assumption was valid to a certain degree, because electric circulation heaters are very efficient. However, since hot oil is used as the working fluid, fouling can occur at the heater coil fluid interface. This buildup over time can reduce the efficiency of the heater. Fouling resistances can be incorporated in the model using equations and constants described in most heat exchanger textbooks [61].

4.6.2.2. Closed-Loop Controllers

As mentioned before, the simulation assumed the mixing valves to be open loop and set to predetermined temperatures. Therefore, the thermal responses shown in the simulations are representative of the ideal first-order performance. The controllers used to obtain the experimental data work well, but do not match the controllers in the simulation. The PI controllers used in the experiments had some overshoot associated with the platen temperature response. As the controller is improved, the experimental data for the platen temperature should correspond better with the simulation.

4.6.2.3. Valve Characteristics

The simulation treats the mixing valves as linear, meaning the hot and cold flows are proportional to the mixing valve stem position. From a controls point of view, the mixing valve with a linear characteristic is the equivalent of a constant gain. However, a number of experiments confirmed that the valve characteristic associated with different flow rates was not linear. Steady state temperatures for set valves positions at system flow rates of 38 GPM and 12 GPM are shown in Figure 4-17 and Figure 4-18, respectively. The difference between the valve characteristics is apparent for different flow rates, with the lower flow rate condition having less of a non-linear response. From this steady state data, the valve gain was calculated by dividing the percent change in output by the percent change in valve position [62]. The resulting valve gains for system flow rates of 38 GPM and 12 GPM are shown in Figure 4-19 and Figure 4-20, respectively. In order to get close to a linear valve characteristic, it is ideal to operate at a low system flow rate. Incorporating these non-linear valve characteristics at different flow rates in the model could improve the accuracy of the simulation.

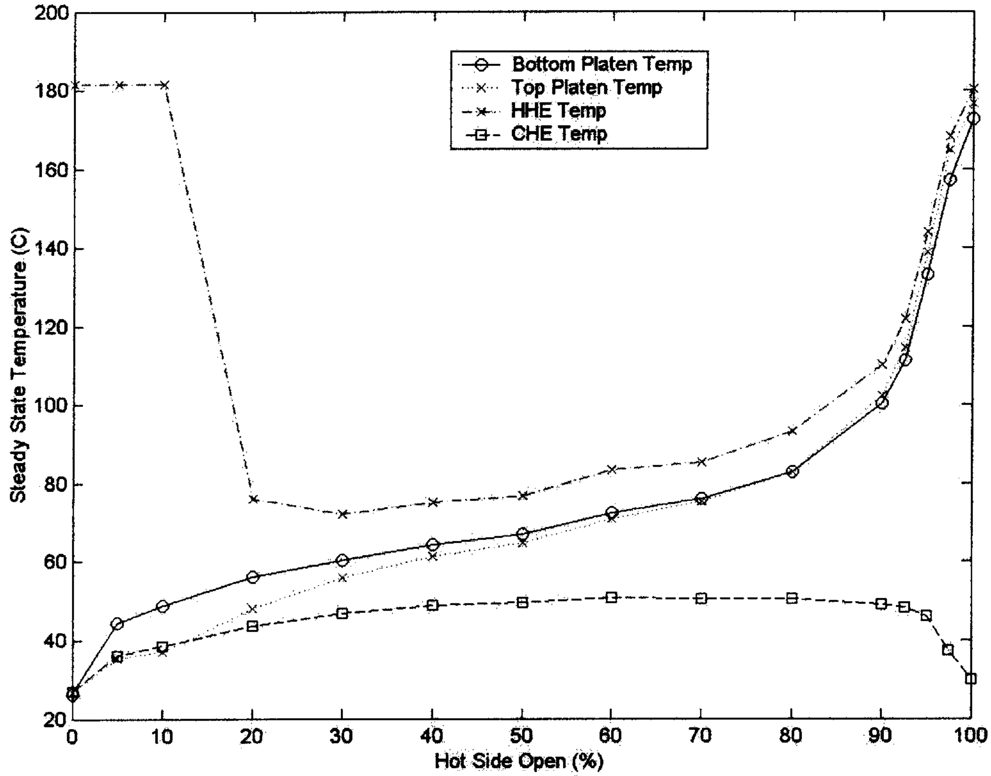

Figure 4-17 Steady state temperatures at certain valve positions at a total system flow rate of 38 GPM

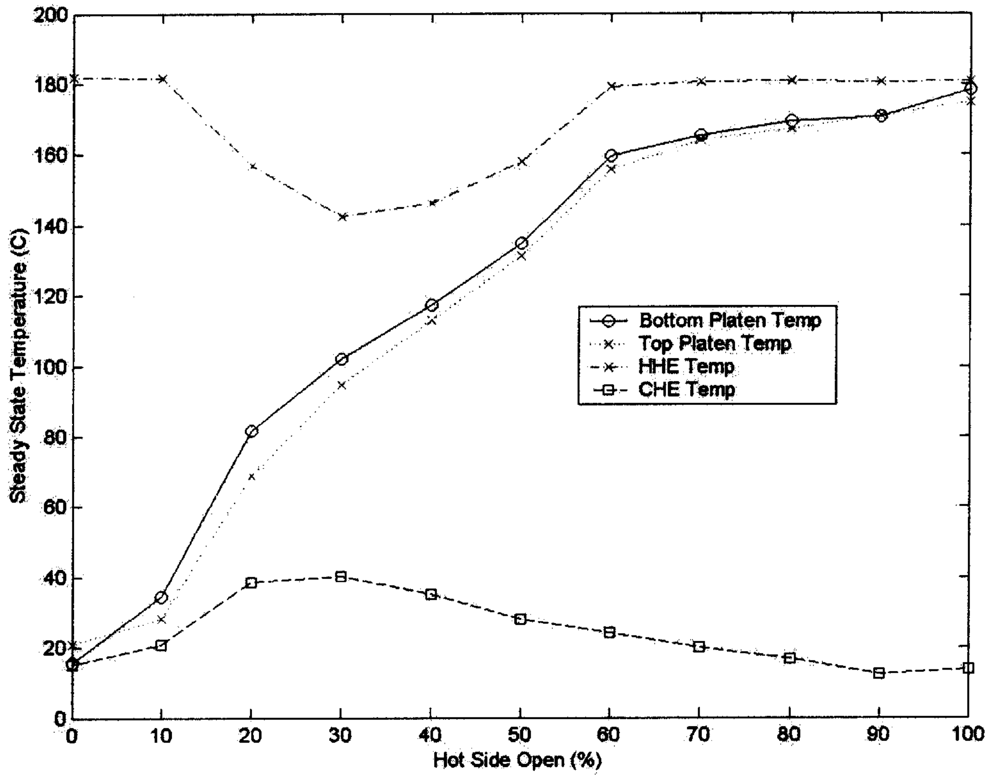

Figure 4-18 Steady state temperatures at certain valve positions at a total system flow rate of 12 GPM

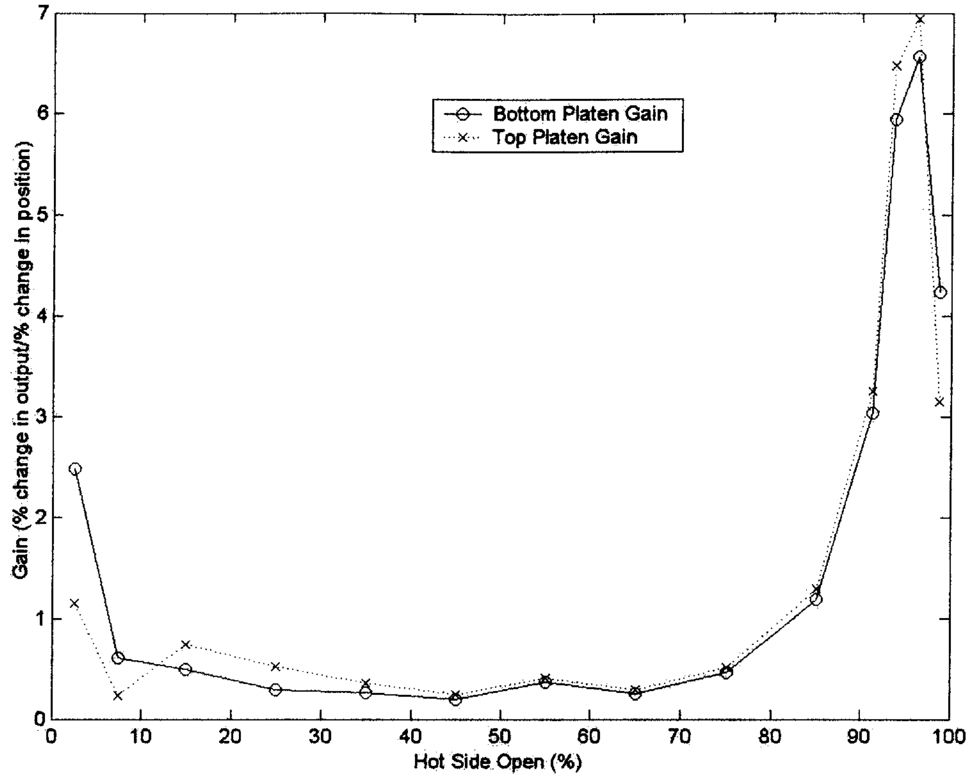

Figure 4-19 Valve gains for the platen temperature at a total system flow rate of 38 GPM

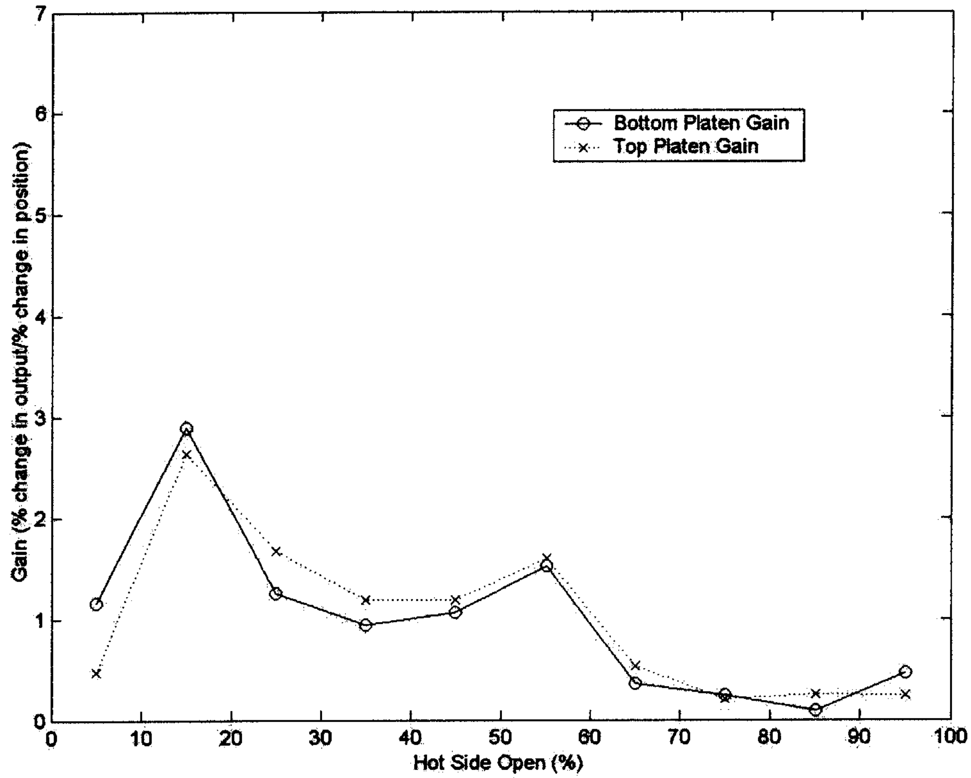

Figure 4-20 Valve gains for the platen temperature at a total system flow rate of 12 GPM

4.6.2.4. Location of Sensors

There are four pipe plug probe thermocouples monitoring the fluid temperature at different locations in the system. Depending on the sensor's radial location in the pipe, the temperature measurement will be different during transients. During rapid heat up cycles, the temperature of the fluid out of the mixing valves tends to be higher than the temperature of the fluid out of the hot heat exchanger. This is counter-intuitive because one would expect atmospheric heat loss and mixing of a little amount of cold fluid with the hot fluid. This effect is due to the fact that the sensor measuring the temperature at the hot heat exchanger is closer to the edge of the flow. The thermocouples measuring the temperature out of the mixing valves are in the middle of the flow. These effects are eliminated once the fluid flow is fully developed. This should have a negligible effect on the outcome of the experiment.

4.6.2.5. Pressure Differentials

The model assumed the same fluid flow through the top and bottom platens. Experimentally, this is not the case because there are differences in pressure for the top and bottom platens between the mixing valves and the heat exchangers. This is reflected in the difference between the top and bottom valve characteristics. Ideally, the valves should have a linear characteristic when the upstream pressure for the cold and hot supplies is the same (Figure 4-21).

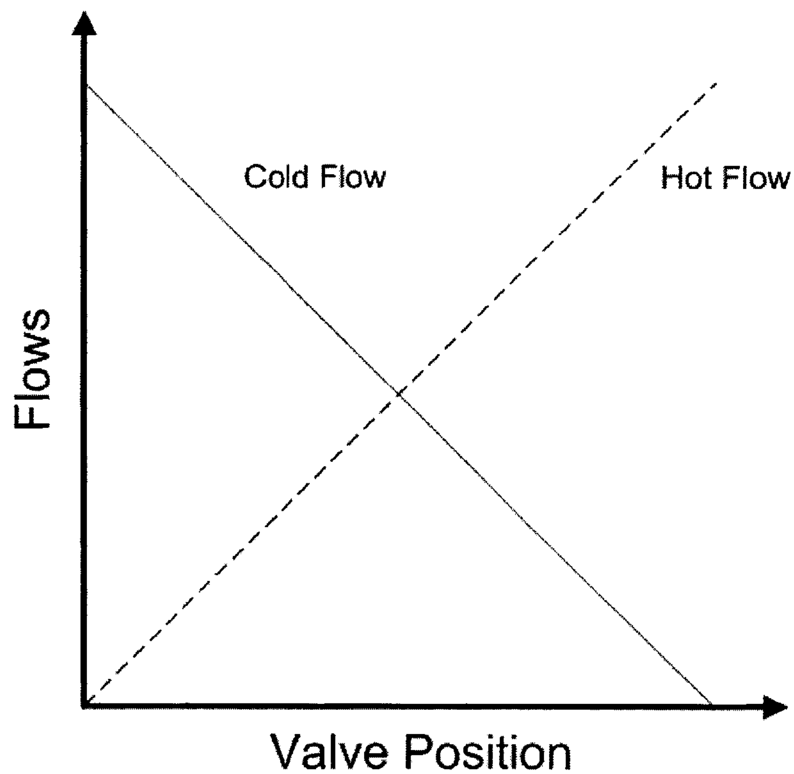

Figure 4-21 Linear valve characteristic curve

4.6.2.6. Losses due to Piping or Atmosphere

Atmospheric losses and modeling of the system pipes were not accounted for in the simulation. There is a large amount of surface area from the heater body and lengths of un-insulated pipe where heat loss to the environment can be significant. Experimental observation showed a decrease in roughly 4 °C from the temperature of the fluid out of the mixing valve to the corresponding platen temperature during steady state conditions. Part of this temperature loss could be attributed to convection to the environment. If atmospheric losses were accounted for in the model the response of the system would be slower during heating and faster during cooling.

A significant amount of pipes were not accounted for in the simulation. The thermal mass of all the pipes in the system are estimated at roughly 100 kg. This added mass would also slow down the system response if included in the simulation.

CHAPTER

5 Control of HME II

5.1 Goals of the HME II Control System

The control objectives for the HME II were the following: steady state error within ±1 °C, fastest possible heating and cooling rates, and being robust to a number of processing conditions. Hardware limitations and its effect on the control of the system are discussed in this chapter. In addition, discussions of the design of the control system in order to meet the objectives are covered in detail with confirmed experimental data.

5.2 Heater Limitations

When developing the control system, problems with the heater and mixing valves limited the flexibility of the design and performance. As mentioned in Section 4.5.1, the heater increases the temperature of the fluid quicker at lower flow rates, but even at a system flow rate of 12 GPM the heater can only increase the temperature of the fluid roughly 0.1 °C/second once the platen temperature is above 120 °C. This slow dynamic can limit the type of controller used and imposes a minimum heating rate for desired platen temperatures above 120 °C.

5.3 Mixing Valve Limitations

Since the control element in the thermal fluid system is the mixing valves, the performance of the system is entirely dependent on the quality of the mixing valve actuators. The main problem with the spring-diaphragm actuators used in our system is stiction. Stiction is defined as, "a property of an element such that its smooth movement in response to a varying input is preceded by a static part followed by a sudden abrupt jump called the slip jump. In a mechanical system, the slip jump originates due to static friction, which exceeds the dynamic friction during smooth movement [63]." A diagram of typical valve stiction behavior is shown in Figure 5-1. The valve starts from rest at point A and after the controller output overcomes the deadband (AB) and stickband (BC), the valve jumps to point D and continues to move. The valve may repeat the behavior just described between D and E if the velocity of the valve stem goes to zero [64]. One might consider using a linear electromechanical actuator.

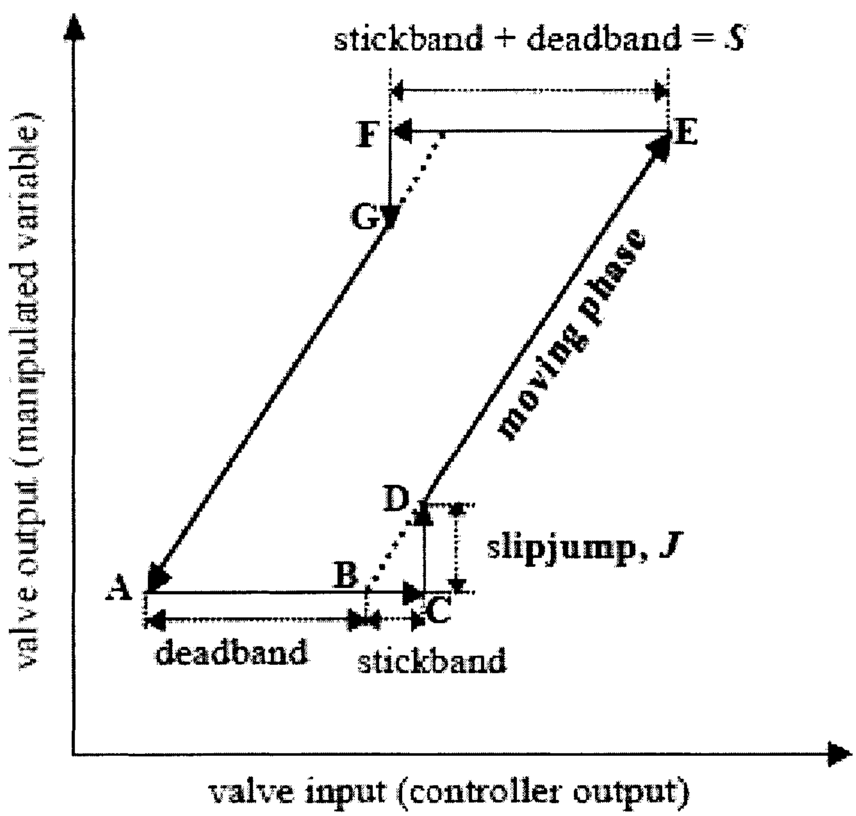

Figure 5-1 Typical response of a valve with stiction [64]

Initial experiments run under closed-loop control with a proportional controller provided evidence of valve stiction. Figure 5-2 shows the closed-loop platen temperature feedback response using a proportional controller with a gain of P=0.1 and system flow rate of 12 GPM. Linear control theory states that a system under strictly proportional control will settle to a steady state temperature with a constant error. However, the experimental data showed the temperature of the platens continuing to increase and never reaching a steady-state temperature. The hot and cold heat exchanger temperatures also increased, which would suggest that the mixing valve was not moving after a certain point and the mixture of fluid out of the valve was increasing in temperature solely due to the supply temperatures increasing.

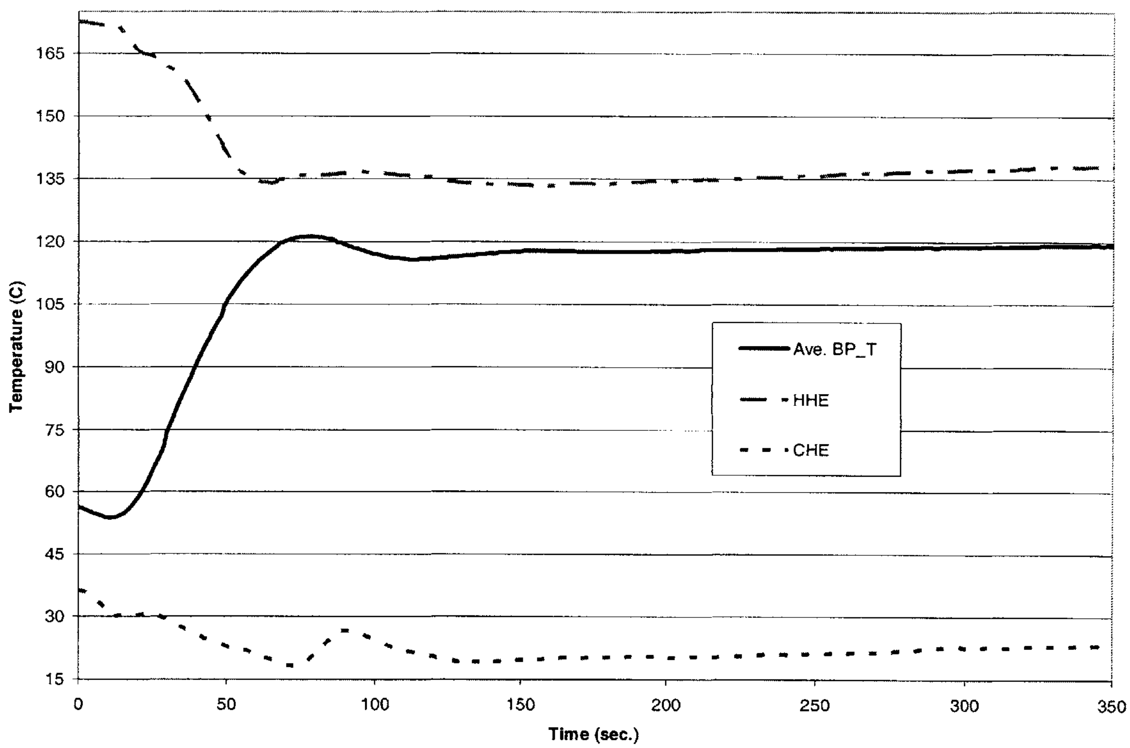

Figure 5-2 Closed-Loop platen temperature feedback response using a proportional controller with a gain of P=0.1 and system flow rate of 12 GPM

Valve stiction is a problem in the valve industry, where hundreds of spring-diaphragm actuators are needed to control complex mixing in processing plants. Numerous research papers have been published regarding this potentially expensive problem. A widely implemented control solution to this problem is using a PI controller [63,65]. This comes at no surprise since "over 90% of the process control systems are based on PID type controllers, which represent a basic standard as regards process tuning [66]." Therefore, a PI controller was implemented to control the mixing valve actuators.

5.4 Sampling Rate Limitations

Another hardware limitation which affected the design of the control system was the data acquisition sample rate. The PCI 4351 was used to acquire the thermocouple measurements and its specifications are described in Section 3.3.12. Its maximum sampling rate given the number of analog inputs it reads is roughly 1.5-2.0 seconds because of onboard signal conditioning. This is extremely slow from a controls perspective, but this PCI card provides the necessary temperature precision.

A case study was conducted to observe the effect of the sampling rate on the temperature response of the system. A Labjack data acquisition system [67] was used, which is capable of fast sampling, but is limited in precision and number of data acquisition channels. All of the tests were run with a single feedback signal from a thermocouple bonded between two pieces of PMMA in between the platens. The sampling rate does not significantly affect the response of the system when the controller has conservative gains (Figure 5-3). However, as the controller gains become more aggressive, a slow sampling rate struggles to keep the temperature stable (Figure 5-4). The sampling rate becomes even more of an issue when the feedback signal has a faster thermal response, such as the fluid out of the mixing valve. During the heating transient, the temperature of the fluid out of the valves can increase by 35 °C within 2 seconds. The sampling rate limitation of the PCI 4351 can be improved by switching to a PCI card with external signal conditioning. However, the control system was designed with this limitation.

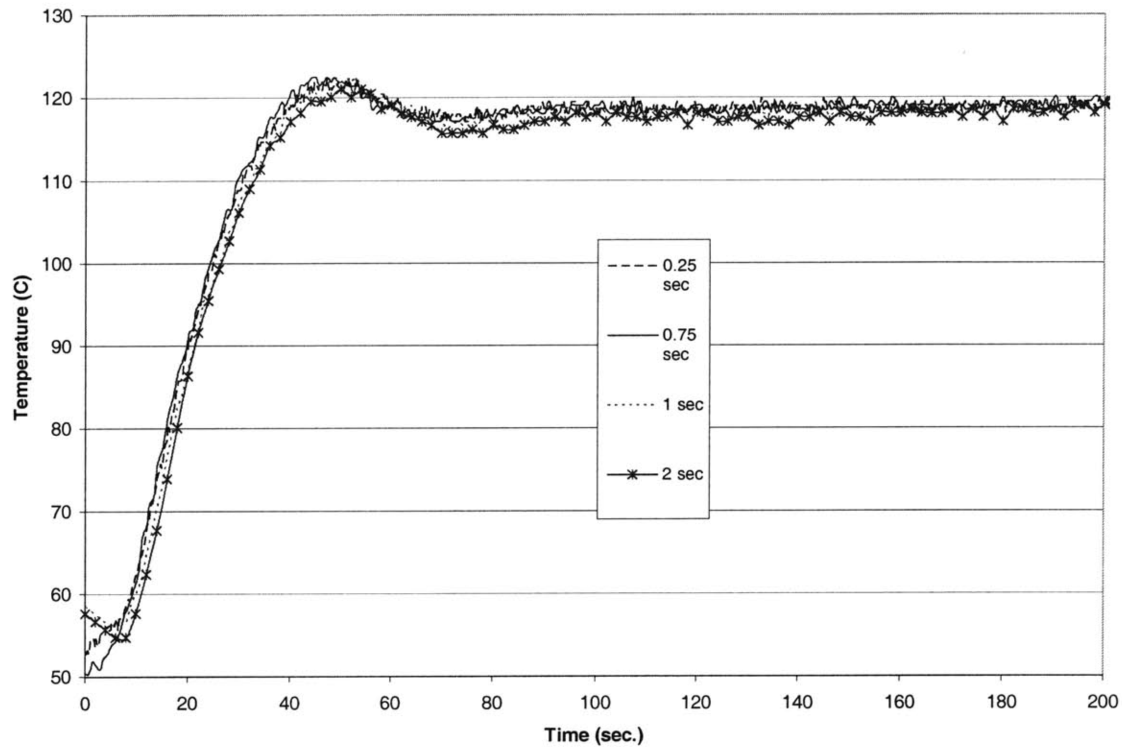

Figure 5-3 PMMA temperature response with closed-loop PMMA temperature feedback using a proportional controller with a gain of P=0.1, a desired set point temperature=120 °C, and a system flow rate of 12 GPM at varying sample rates

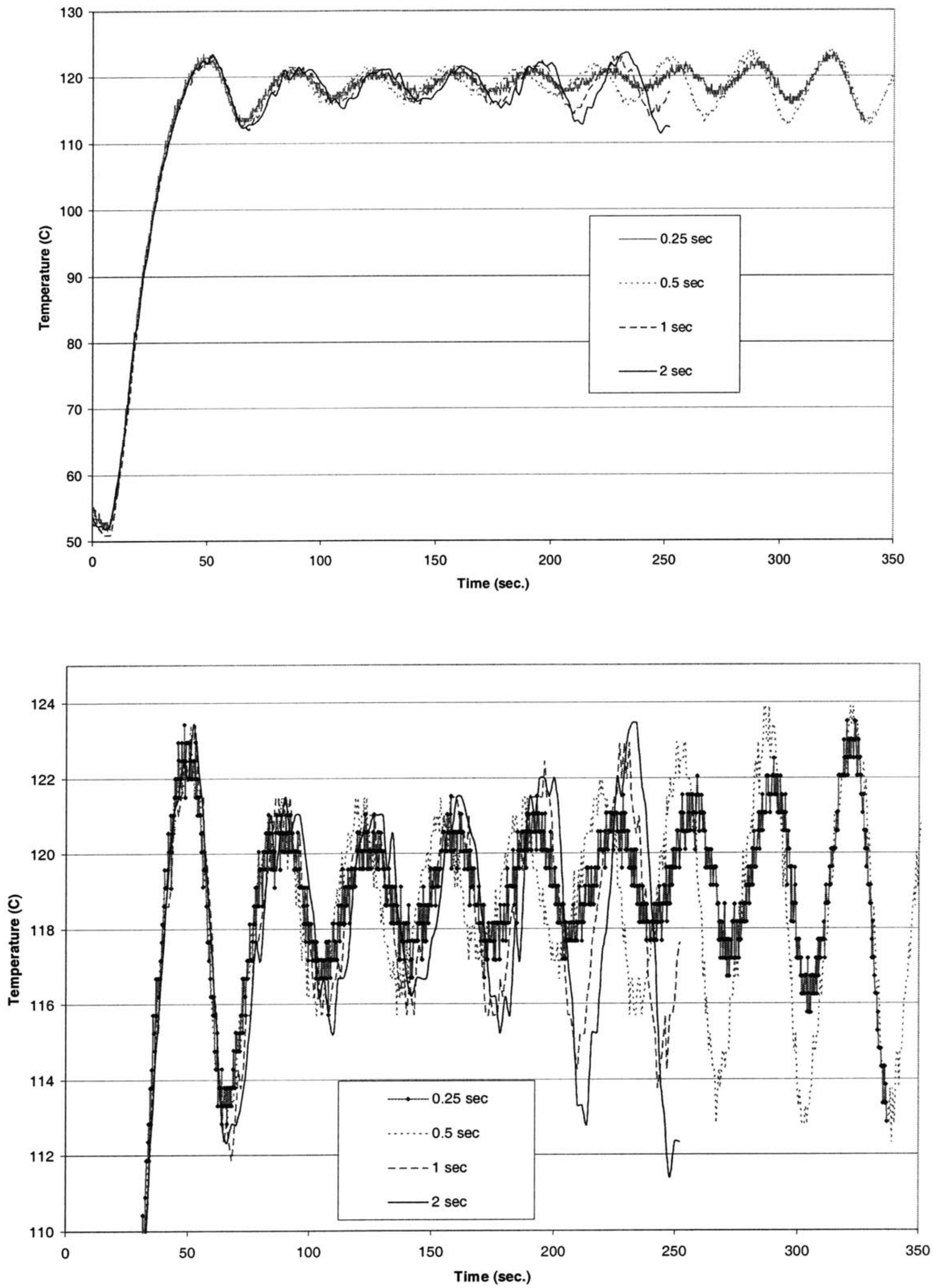

Figure 5-4 PMMA temperature response with closed-loop PMMA temperature feedback using a proportional controller with a gain of P=0.25, a desired set point temperature=120 °C, and a system flow rate of 12 GPM at varying sample rates (Bottom figure is a close-up of the top figure)

5.5 Initial Controller Design Study

Designing a linear controller typically involves creating a block diagram with the components and system dynamics modeled as transfer functions. Using this model, a root locus analysis can be implemented and additional poles and zeros can be placed in the frequency domain (s-plane) to achieve the desired performance. These additional poles and zeros will be the controller.

Simulink was used to design a controller for the HME II. A closed-loop block diagram schematic used for this analysis is shown in Figure 5-5. This diagram is valid because the error between the desired temperature and actual temperature is passed through the controller. The resulting output is sent to the mixing valves positioners as a 4-20 mA current signal. A change occurs in the valve position and the resulting fluid out of the valves should change the platen temperature.

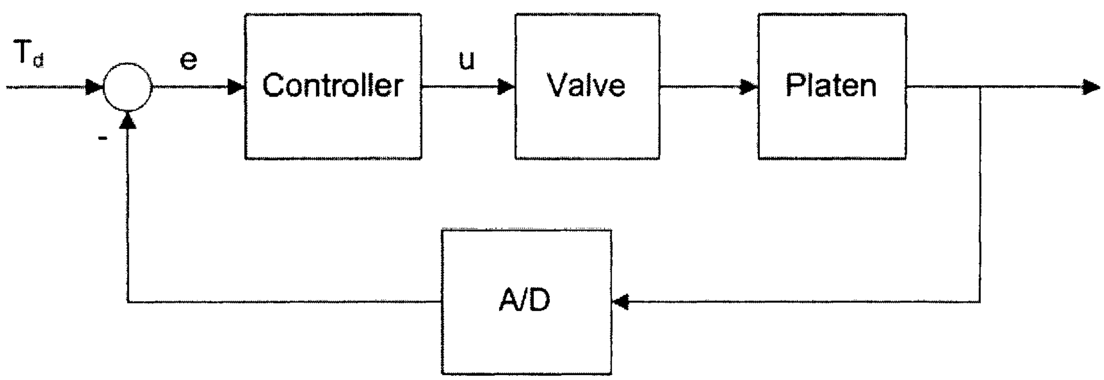

Figure 5-5 Block diagram of the HME II system with closed-loop platen temperature feedback

The valves needed to be modeled, so a transfer function was fit to an open loop step response for the fluid temperature out of the valves. This temperature response is shown in Figure 5-6. The shape of the curve is a 3^{rd} order system which can be decomposed into a lightly damped 2^{nd} order system plus a slow 1^{st} order system. Using the principle of superposition the open loop response of the valve can be summarized by

Equation 5-1 [68], where K is a constant for the 1st order system, τ is the time constant for the 1st order system, ξ is the damping ratio for the 2nd order system, and ω_n is the natural frequency for the 2nd order system. The constant ξ was found by using the overshoot method. Using ξ, the natural frequency, ω_n, was calculated by estimating the settling time. The time constant (τ) was estimated by superimposing a 1st order response on the 2nd order system to produce the curve in Figure 5-6. Finally, K is a scaling factor necessary to match the general shape of the response. The constant parameters were estimated from the curve in Figure 5-6 and are listed in Table 5-1.

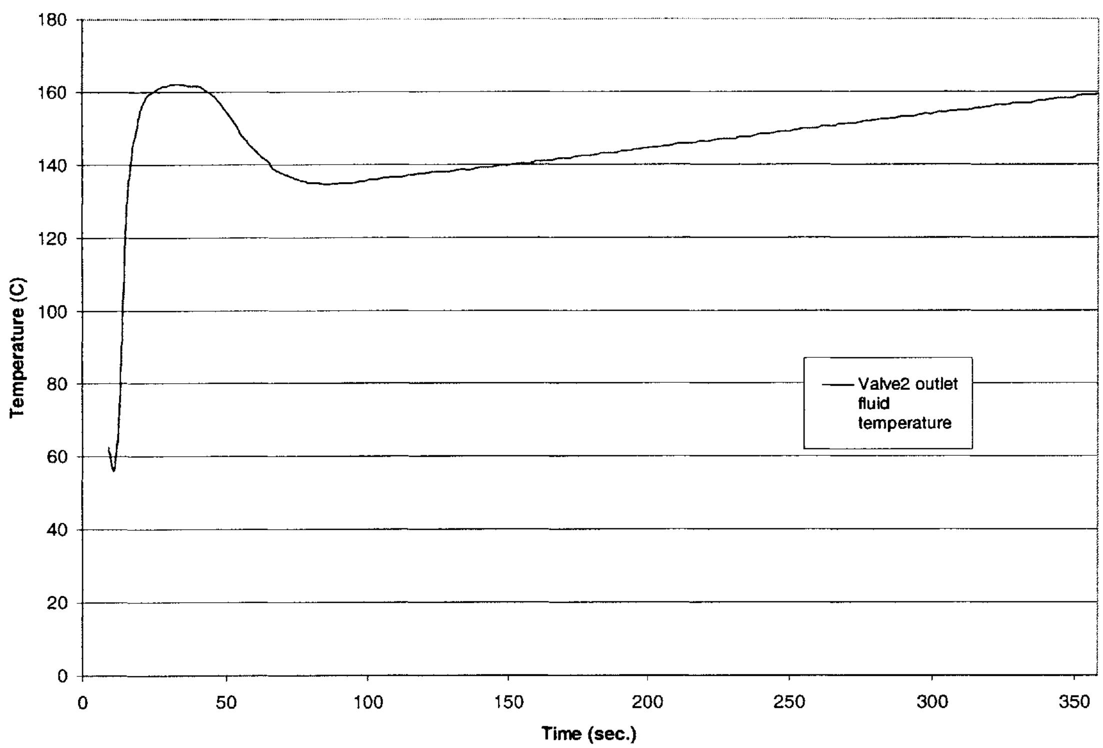

Figure 5-6 Open loop step response of the fluid temperature out of the mixing valve, corresponding to the bottom platen

$$\frac{Ks^2 + (2\xi\omega_n K + \omega_n^2)s + (\omega_n^2 + K\omega_n^2)}{s^3 + (2\xi\omega_n + \tau)s^2 + (\omega_n^2 + 2\xi\omega_n\tau)s + \tau\omega_n^2}$$

Equation 5-1

Table 5-1 Parameters for the third order system

Parameters	Value
ξ	0.4
ω_n	0.125
τ	0.01
K	0.005

The open loop block diagram transfer function of the valve fluid outlet temperature with correction factors for the real system is shown in Figure 5-7. When the values from Table 5-1 were inputted into the Simulink diagram, the simulation output compared with the data is shown in Figure 5-8. There was not a strong correlation between the simulation and actual data; however the simulation does capture the general shape of the response.

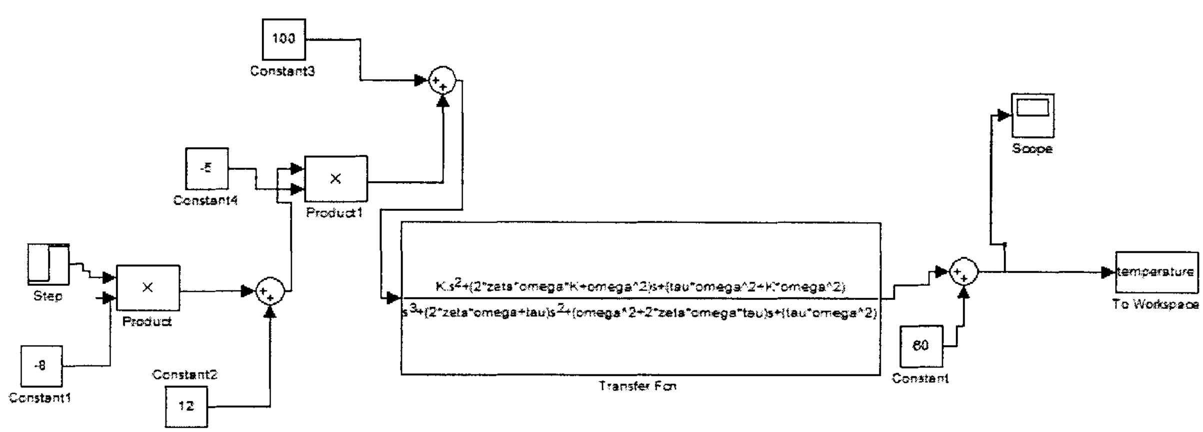

Figure 5-7 Simulink block diagram of the open loop response for the valve fluid outlet temperature with correction factors to compensate for the real system

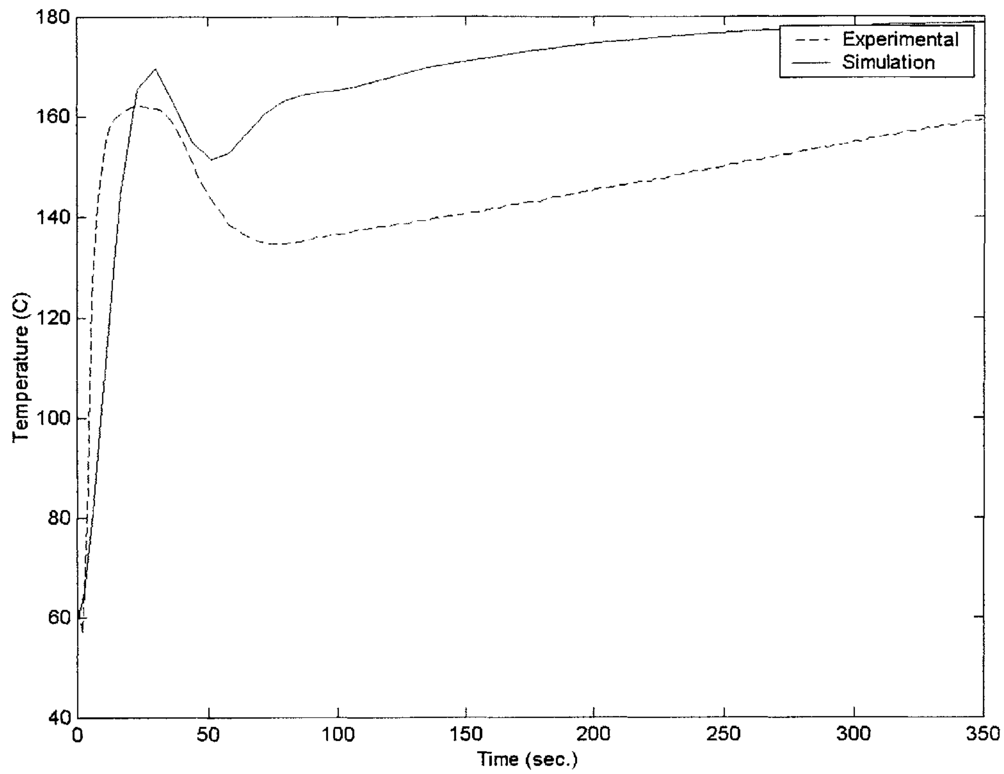

Figure 5-8 Open loop response of the valve fluid outlet temperature

The transfer function for the valve outlet fluid temperature, in addition to a 1st order response for the platen transfer function with a time constant of five seconds was used to complete the block diagram. Root locus analysis was implemented and appropriate poles and zeros were placed in the S-plane to get the desired response. However, the simulation provided responses that were not possible to achieve with the system. Therefore, it was safe to assume that linear theory would not be a viable technique to design a controller for the system. Discrepancies between the simulation and actual performance could be attributed to highly non-linear effects such as saturation and stiction in the valves. Another approach to designing a controller was needed and will be discussed in the following sections.

5.6 Controller Design for Heating

The objectives for the heating cycle were: fast as possible heating rates, steady state error within ±1 °C, and quick settling times for a target set point temperature of 120 °C. In order to address fast heating rates it had been confirmed that low system flow rates produce the fastest response. Therefore, a system flow rate of 12 GPM was chosen because it was low enough for faster heating, but fast enough so the pump motor did not overheat.

The second objective for the heating cycle was settling to a steady state temperature within ±1 °C. Since the system dynamics are highly non-linear, traditional linear control system design tools are ineffective. Section 5.3 mentions the problems with the mixing valve actuators and suggests using a PI controller. A PI controller was implemented with platen temperature feedback (Figure 5-2) and proved to be effective in getting to a set point temperature with minimal steady state error with properly tuned gains. However, this controller used throughout the whole heating cycle breaks down in performance when the desired set point temperature is above 120 °C. At a desired set point temperature above 120 °C, the mixing valves saturate for an extended period of time waiting for the heater to raise the system temperature to the set point level. During this time, the controller accumulates a large amount of error from the integrator term in the controller. This integrator windup led to a large overshoot and a long settling time.

In order to satisfy the third objective of the heating cycle, which was a fast settling time, a proportional controller was used in conjunction with the PI controller. The proportional controller is implemented whenever the mixing valves are saturated. Once the valves are no longer saturated, the controller will switch to PI control with the integrator term initial condition equal to zero. The proportional controller gain is large relative to the PI controller gains. A large proportional controller gain will get the temperature of the platens close to the desired set point. Once the controller is switched to PI control the smaller proportional gain provides for stability while the integrator term ensures minimum error.

5.7 Controller Design for Cooling

The objectives for the cooling cycle were fast cooling rates and maintaining a set point temperature within ±1 °C for a period of time long enough to de-emboss a part at a target set point temperature of 55 °C. In order to achieve the fastest cooling rate, a high flow rate is desired as mentioned in Section 4.5.2. A system flow rate of 38 GPM was used only when the valves were fully closed to the hot flow, to prevent the hot supply from cooling down. When the valves come out of saturation, the system flow rate was turned down to 12 GPM.

Temperature from the platens is the ideal feedback variable; however because of the high system gain at typical de-embossing temperatures, referred to in Section 4.6.2.3, in combination with the slow thermal response of the platens it is extremely difficult to maintain a steady temperature. An indirect way of controlling the temperature of the platens is to control the fluid temperature out of the mixing valve (Figure 5-9). The platens have a slow thermal response relative to the fluid so this response will be a filtered version of the fluid temperature response. Also, there will be a small temperature offset at steady state between the platen and valve.

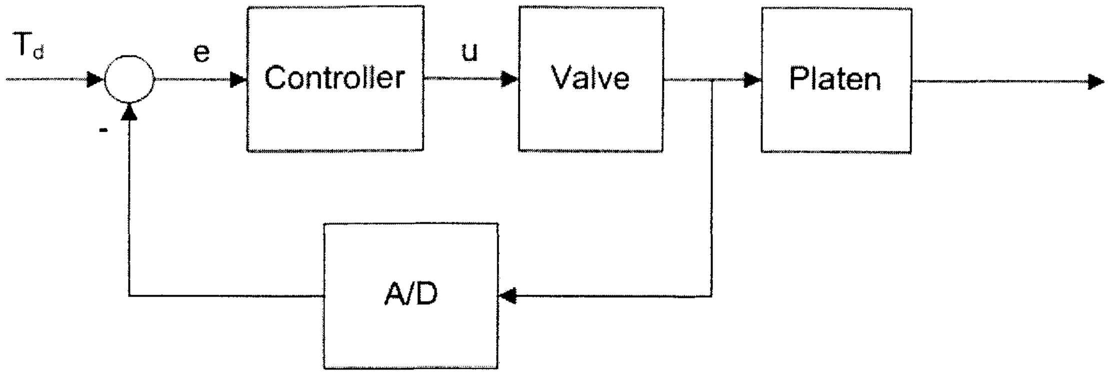

Figure 5-9 Block diagram of the HME II system with closed-loop valve outlet fluid temperature feedback

An example of the valve fluid outlet temperature feedback during cooling is shown in Figure 5-10. The PI controller was used to get the fluid temperature to the set point temperature. The behavior of the Valve2 outlet fluid temperature is highly oscillatory, which is unavoidable because of high loop gain, valve stiction, and a slow sampling rate. Referring back to Figure 4-18, a de-embossing set point temperature of 55 °C at a system flow rate of 12 GPM corresponds to a hot side valve percentage opening of 15%. Translating this valve position to a system gain on Figure 4-20 shows that the valve gain is the highest at this desired temperature. A physical explanation for the high gain is that when the system temperature is around 55 °C the cold fluid supply is near its limit making the valves nearly saturated. When the outlet temperature nears its set point, the valves will open the hot supply a little. The hot supply has 5 gallons of roughly 150 °C fluid, which mixes with the cold fluid increasing the temperature dramatically and causing the controller to overcompensate. This process repeats itself causing a limit cycle. The effective gain will actually be higher than the one stated in the Figure 4-20, because the feedback measurement is from the fluid temperature and not the platen.

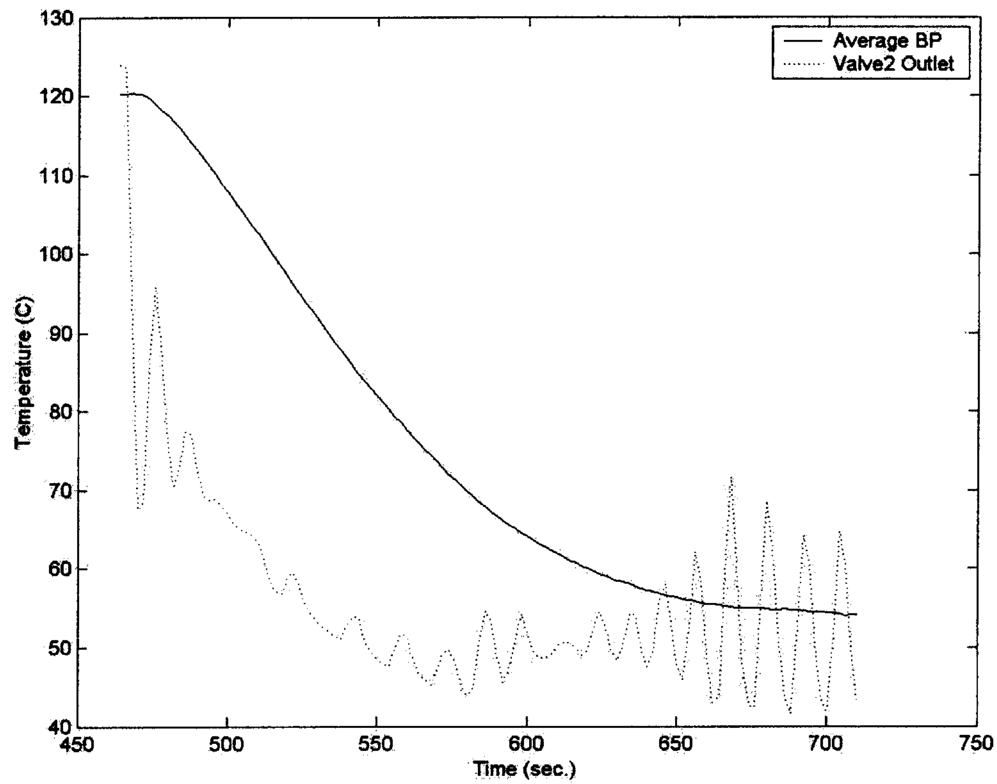

Figure 5-10 Cooling cycle with Valve2 fluid outlet temperature feedback to a set point of 55 °C and a system flow rate of 12 GPM (Switching PI control)

Given the high loop gain, one would think to just reduce the controller gain avoiding the high amplitude oscillations. However, because of the problems with valve stiction the controller gain has to be above a certain threshold. If the changes in current signal to the valves are too small to overcome static friction, the valve will not change positions at all.

Another reason the oscillations cannot be avoided is the slow sampling rate of the PCI 4351. As stated earlier, the fluid temperature can increase by 35 °C in only 2 seconds. If the sampling rate could be four times as fast, theoretically the fluid temperature should only change by roughly 9 °C per sample which is a lot more manageable. A faster sampling rate would reduce the amplitude of oscillation seen in

Figure 5-10. Despite the large amplitude of oscillation of the valve outlet temperature, the platen temperature follows a smooth temperature curve. Therefore, it is acceptable to control the valve outlet fluid temperature during the cooling cycle.

5.8 Optimal Variable Controller Gains

The justification for using certain flow rates and controllers for different phases of the process cycle was covered in the previous two sections (Section 5.6 and Section 5.7). The top and bottom platen and both valve outlet fluid temperatures were controlled independently of each other. The final controller design for heating and cooling is summarized in Table 5-2 and Table 5-3, respectively. Compensated set point temperatures were imposed for the cooling cycle to better match the temperature response for the top and bottom platens, which are shown in Table 5-4. The system flow rate is set to operate at 12 GPM during heating and cooling, with the exception of the case where both valves are saturated during cooling, the flow rate will be increased to 38 GPM. A representative heating and cooling response is shown in Figure 5-11. This section will discuss the selection of the specific controller gains for each phase of the process.

Table 5-2 Platen controller gains for different phases of the heating cycle

Heating Phase Controller Gains				
Condition	**Top Platen Controller**		**Bottom Platen Controller**	
Valve is saturated (Fully hot)	P=0.5	I=0	P=0.5	I=0
Valve is out of saturation	P=0.05	I=0.002	P=0.1	I=0.002

Table 5-3 Valve controller gains for different phases of the cooling cycle

Cooling Phase Controller Gains				
Condition	**Valve1 Controller**		**Valve2 Controller**	
When (Valve Temp-SP) > 15 °C	P=0.01	I=0.0005	P=0.01	I=0.0005
When (Valve Temp-SP) < 15 °C	P=0.02	I=0.001	P=0.015	I=0.001

Table 5-4 Valve compensated set points for different phases of the cooling cycle

Cooling Phase Compensated Set Point Temperatures		
Condition	**Valve1 compensated set point temperature**	**Valve2 compensated set point temperature**
When (Valve Temp-SP) > 15 °C	SP °C + 10 °C	SP °C - 8 °C
When (Valve Temp-SP) < 15 °C	SP °C	SP °C - 3 °C

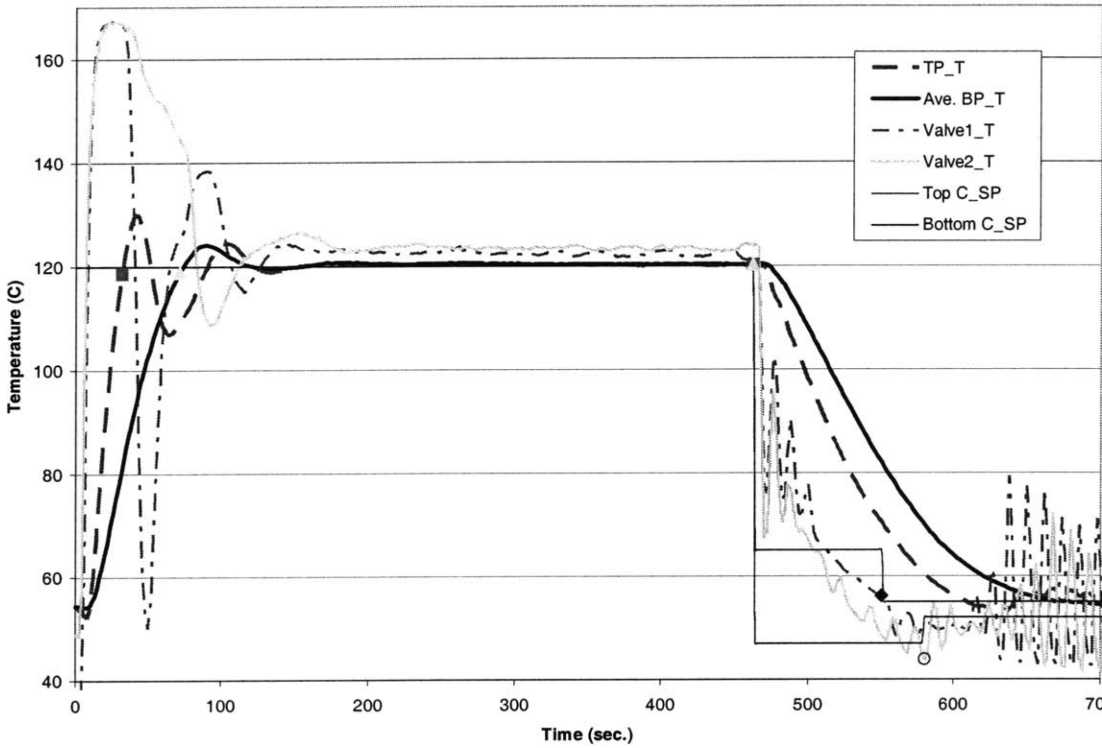

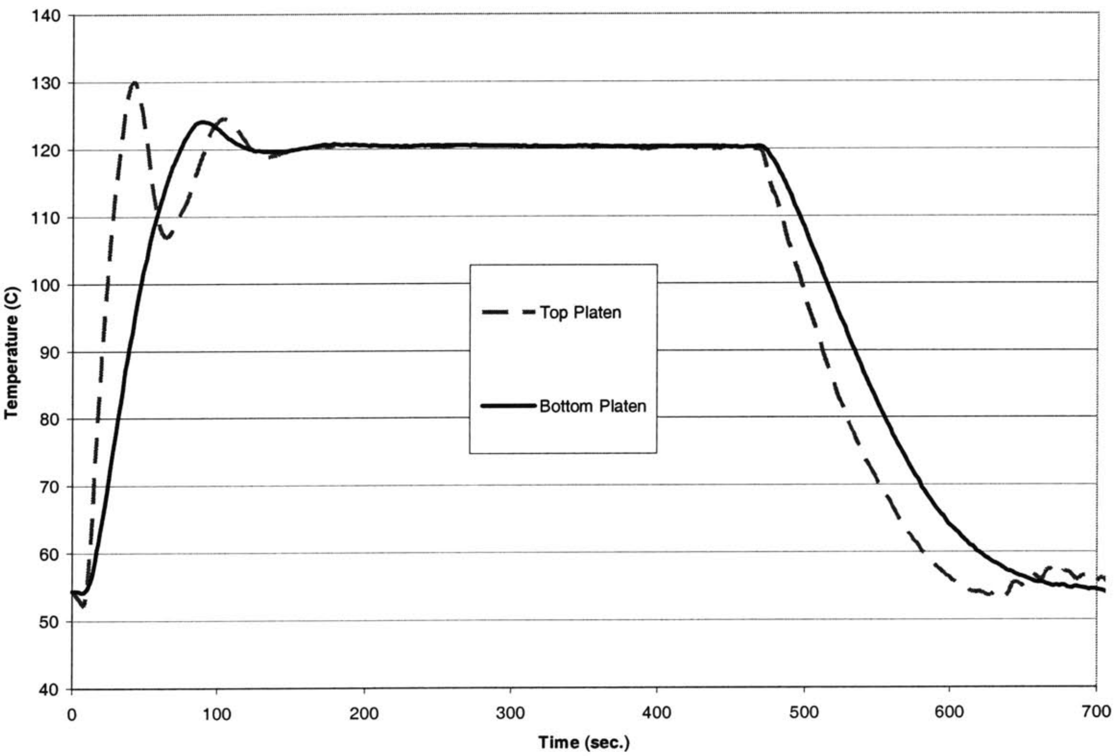

Figure 5-11 Heating and cooling response for a closed loop step test from 55 to 120 to 55 °C using the final control system (Bottom figure is the same as the top but with only the platen responses)

5.8.1 Selection of Heating Controller Gains

During the initial phase of the heating cycle, the controllers for both the top and bottom platens have high proportional gains. The proportional gain of P=0.5 was chosen because it gets the temperature close to the set point quickly with minimal overshoot. When the mixing valves are out of saturation, the reason for having the top platen proportional gain of P=0.05 and the bottom platen proportional gain of P=0.1 was that the top platen had a faster thermal response than the bottom platen as shown in Figure 5-11. The top platen having a faster response is because it has less thermal mass than the bottom platen. Therefore, the top platen takes longer to settle if it has the same gain as the bottom platen. An integrator gain of 0.002 was used in combination with the proportional gains for both the top and bottom platens to keep the steady state error near zero. A series of experiments with varying combinations of proportional and integrator gains were conducted and the selected gains showed the best performance in terms of settling the quickest and maintaining a steady state error within ± 1°C for a target set point temperature of 120 °C.

5.8.2 Selection of Cooling Controller Gains

Control of the valve outlet fluid temperature requires lower gains because of the inherently high system loop gain at de-embossing temperatures. The proportional and integral gains are initially kept low for the initial phase of cooling to avoid too much integrator windup. The PI gains are increased when the temperature gets close to the set point temperature to prevent valve stiction. Although the top platen has a faster response than the bottom platen, the proportional gain for the Valve1 is higher than Valve2 because it was found to be more prone to stiction.

Compensated set point temperatures were also included in the control system to match the cooling rate for the top and bottom platens. Since the top platen has a much faster response than the bottom platen, the top platen imposes a set point temperature higher than the desired set point temperature for the initial cooling phase. On the other hand, the bottom platen has an imposed set point temperature lower than the desired set point temperature to speed up the cooling rate. The exact compensation formulas were selected based on the response which best matched the top and bottom platen temperature cooling responses without sacrificing too much speed.

5.9 Empirical Data for the given Controller

Once the controller was built, a number of experiments were run to test its performance. A list of experiments and their testing conditions using the same controller are summarized in Table 5-5. Preliminary tests suggested that embossing PMMA at a temperature of 120 °C with sufficient force and de-embossing at 55 °C produced a fully replicated part [27]. Therefore, this processing condition was used to benchmark the performance of the controller. Figure 5-11 shows a profile of this processing condition (Run 2) and it shows a worst case overshoot of roughly 10% during heating, which is acceptable. The only stringent heating requirement was that the temperature settles to ± 1 °C of the set point temperature. During the cooling transient, the highest temperature differential between the top and bottom platens was only 13 °C, which was a drastic improvement over the approximately 50 °C temperature differential seen in the HME I. The system was able to heat the both of the platens to 120 ± 1 °C in 138 seconds and cool both of the platens to 55 ± 1 °C in 190 seconds. Therefore, given an embossing hold time of roughly 30 seconds the whole process cycle can be completed in 6 minutes. This is a significant improvement over the HME I with a reported heat time of approximately 15 minutes and cool time of approximately 5 minutes [29]. Granted, these times are quoted for higher embossing temperatures, but from a manufacturing standpoint as long as parts are fully replicated regardless of embossing temperature the fastest cycle time should be implemented.

Table 5-5 Description of test conditions for each run for the top and bottom platens using the same controller

Run Number	Location	Init. Temp. (°C)	Emboss Temp. (°C)	De-emboss Temp (°C)
1	Top	42	110	55
	Bottom	56.5	110	55
2	Top	54.5	120	55
	Bottom	54.4	120	55
3	Top	87.5	150	55
	Bottom	73.6	150	55
4	Top	50.8	170	55
	Bottom	53.5	170	55
5	Top	64.6	110	65
	Bottom	62.7	110	65
6	Top	56.8	120	65
	Bottom	60.1	120	65
7	Top	60.4	170	65
	Bottom	63.1	170	65
8	Top	75.6	110	77.5
	Bottom	74.2	110	75
9	Top	78.4	120	77.2
	Bottom	73.8	120	75
10	Top	65.6	170	77.1
	Bottom	63.3	170	75

The rest of the heating and cooling times for Runs 1-4 are shown in Figure 5-12 and Figure 5-13, respectively. The reported cooling times represent the first time the platens come within the stated temperature tolerance. Figure 5-12 suggests the controller is robust to different heating conditions. The top and bottom platens for each test settled to the set point temperature at approximately the same amount of time. As expected, the higher set point temperature took much longer to get to because of the slow heat exchanger dynamics. The reason for the 110 °C set point temperature heating taking longer than the 120 °C condition was because of more overshoot. Figure 5-13 shows that the cooling times for different starting temperatures do not change much. It also shows that the top platen responds a lot faster than the bottom platen.

Runs 8-10 suggest that the controller does not work effectively in getting the top platen down to a de-embossing set point temperature of 75 °C. The top platen gets within 3 °C of the set point temperature, which should only have a negligible effect to the final part. If this effect indeed has a significant effect on the output part, a conditional can be implemented in the control system to accommodate for this de-embossing temperature. Information regarding Runs 5-10 and thermal response graphs for the rest of the runs can be found in Appendix F.

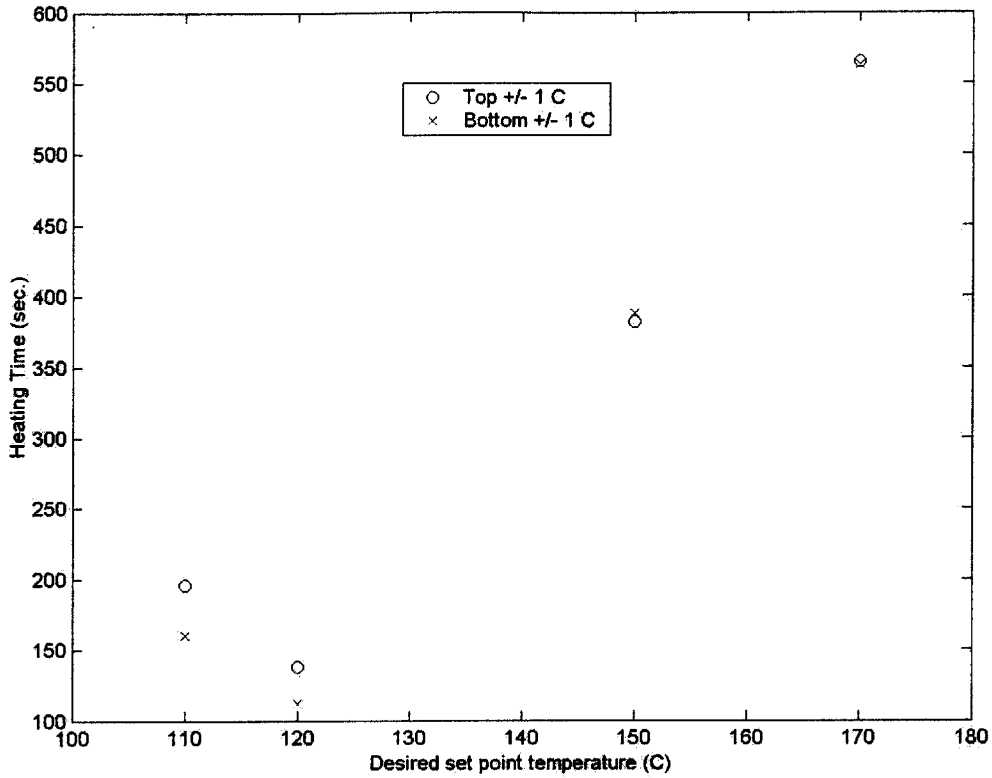

Figure 5-12 Heating times for Runs 1-4 described in Table 5-5

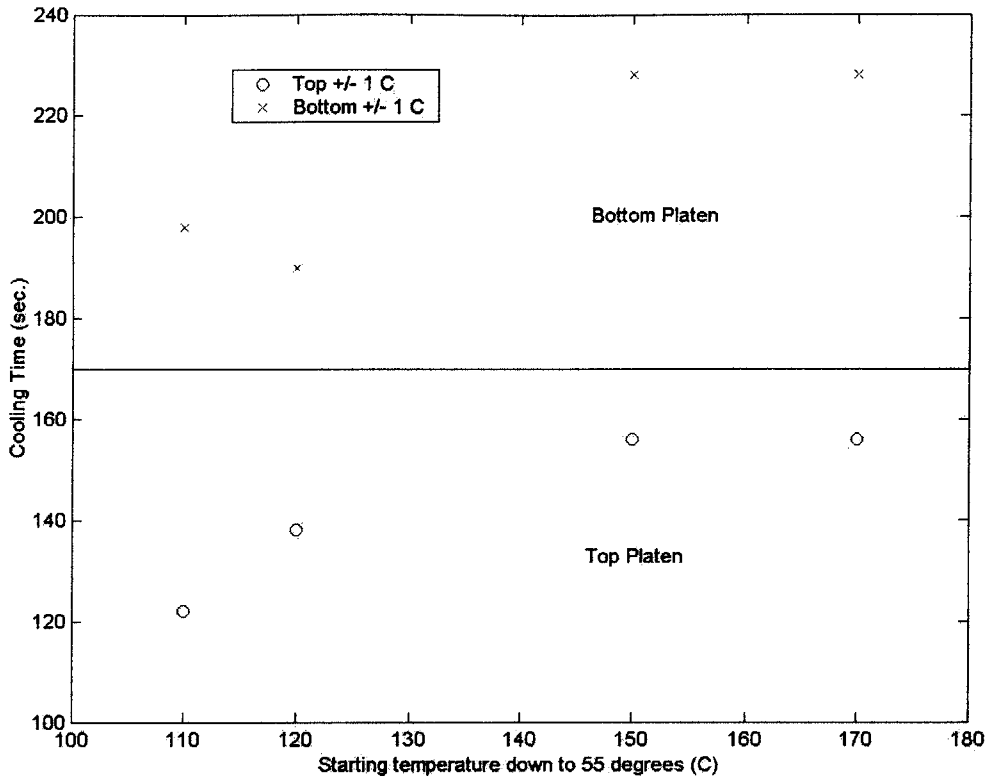

Figure 5-13 Cooling times for Runs 1-4 described in Table 5-5

Repeatability of the controller was also tested, since this is a significant issue in manufacturing. Figure 5-14 shows the thermal response of three cycles between 55 °C and 120 °C. The shape of the thermal response looks identical and repeatable for each cycle. Quantification of the repeatability is shown in Table 5-6, where the settling times to within ± 1 °C were calculated. The worse case was for the bottom platen during heating which had a settling time deviation of roughly 15%; however this deviation should have been much less because the first cycle had the bottom platen starting temperature 3 °C lower than the other two cycles. Overall, the controller developed for the process was repeatable to an acceptable degree.

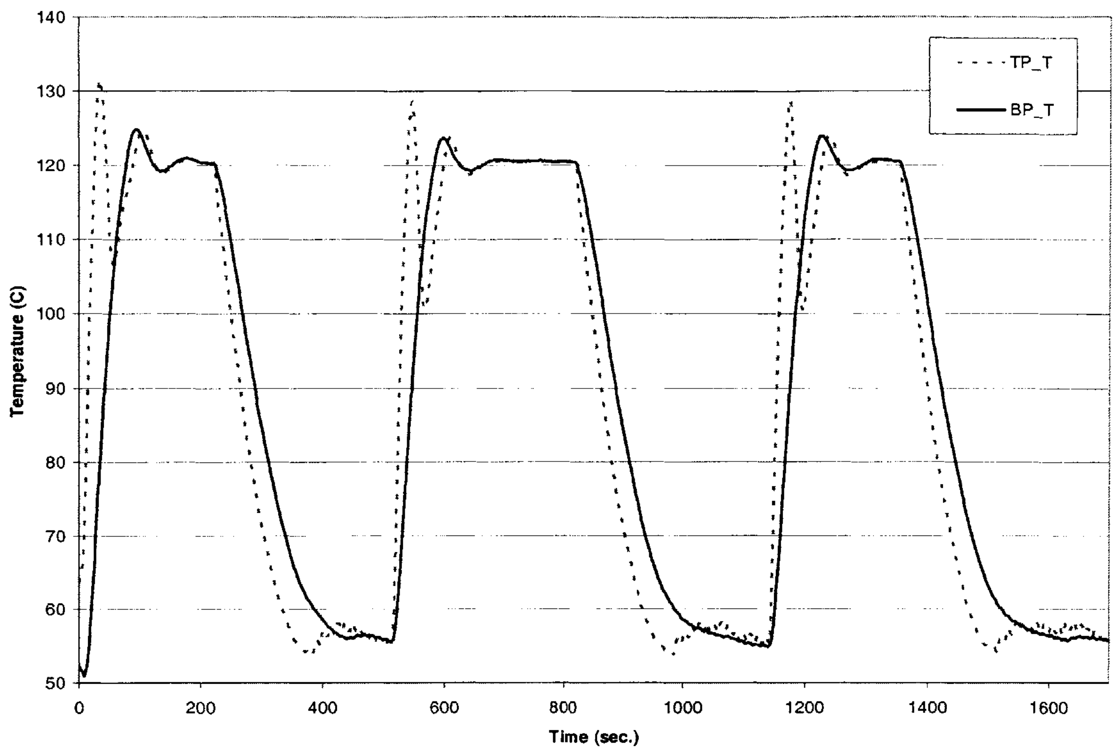

Figure 5-14 Three repeated cycles between 55 °C and 120 °C

Table 5-6 Settling times to within ±1 °C for the response shown in Figure 5-14

	1st cycle	**2nd cycle**	**3rd cycle**	**Mean**	**Std. Dev.**
Heating					
Top	117 s	138 s	140 s	132 s	13 s
Bottom	143 s	110 s	112 s	122 s	19 s
Cooling					
Top	138 s	138 s	142 s	139 s	2 s
Bottom	282 s	264 s	272 s	273 s	9 s

CHAPTER

6 Software Design for Automation of the HME II

6.1 Overview of the Software Platform

A graphical user interface (GUI) was developed in Labview 7.0 to automate the thermal cycle process. A screen capture of the user interface is shown in Figure 6-1. This program allows a user to input an embossing and de-embossing set point temperature and manually switch between cooling and heating. Real time monitoring of all the temperatures in the system are displayed in the two charts at the bottom of the screen. The program is split into six sections: motor controls, expansion tank fluid level monitoring, system controls, top platen controls and indicators, bottom platen controls and indicators, and temperature monitoring. These will be discussed in the following sections.

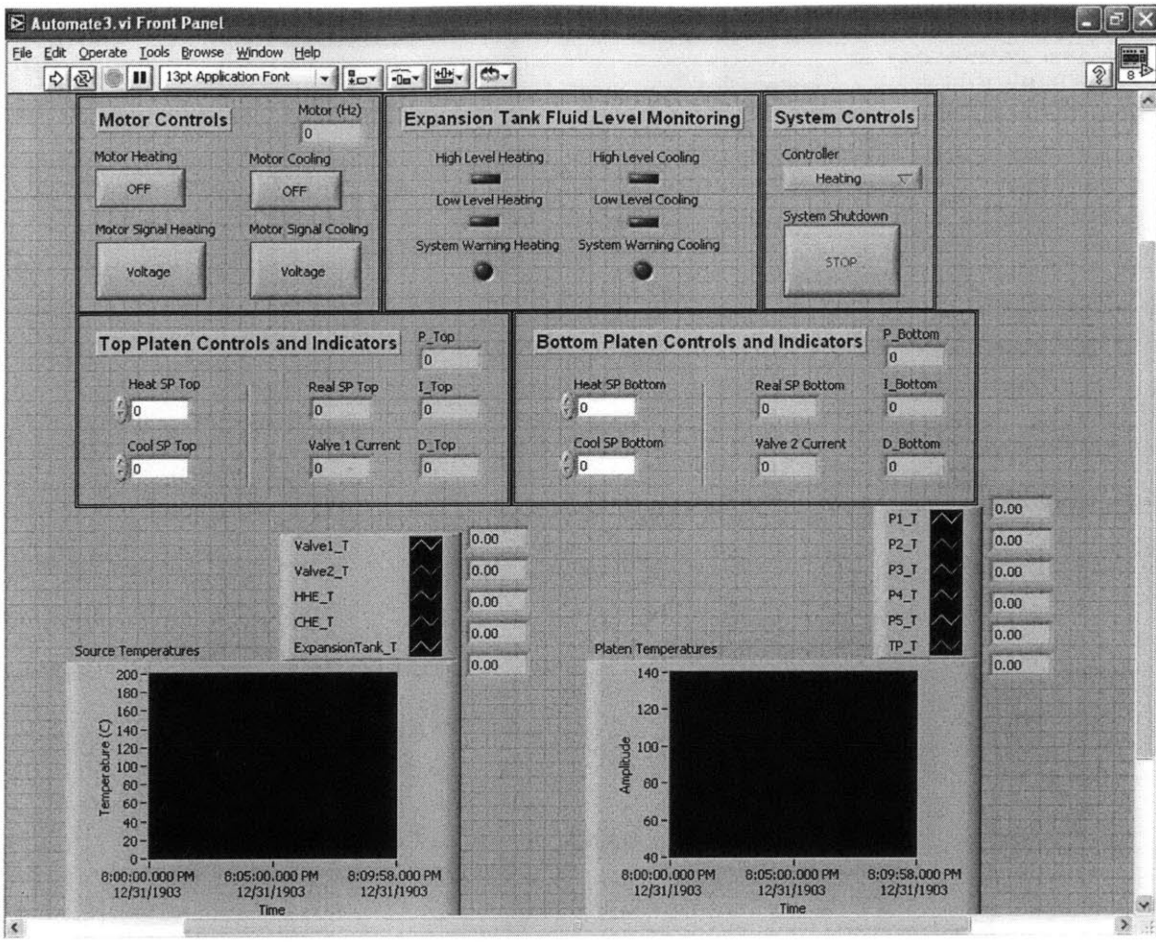

Figure 6-1 Labview graphical user interface for the thermal control system

6.1.1 Motor Controls

The motor control section allows the user to turn the motor on or off and change between sending a voltage or a current analog output (Figure 6-2). Since the PCI 6208A operates with an analog current output, the current setting should always be on. This section also monitors the frequency of the motor. The frequency of the motor is linearly related to speed which is theoretically linearly related to the system flow rate from the gear pump. However, empirical data has shown that this is inexact. Since the program is set-up to operate at a system flow rate of 12 GPM and 38 GPM, it was found experimentally that the motor should operate at ~12.5 Hz and ~50 Hz, respectively.

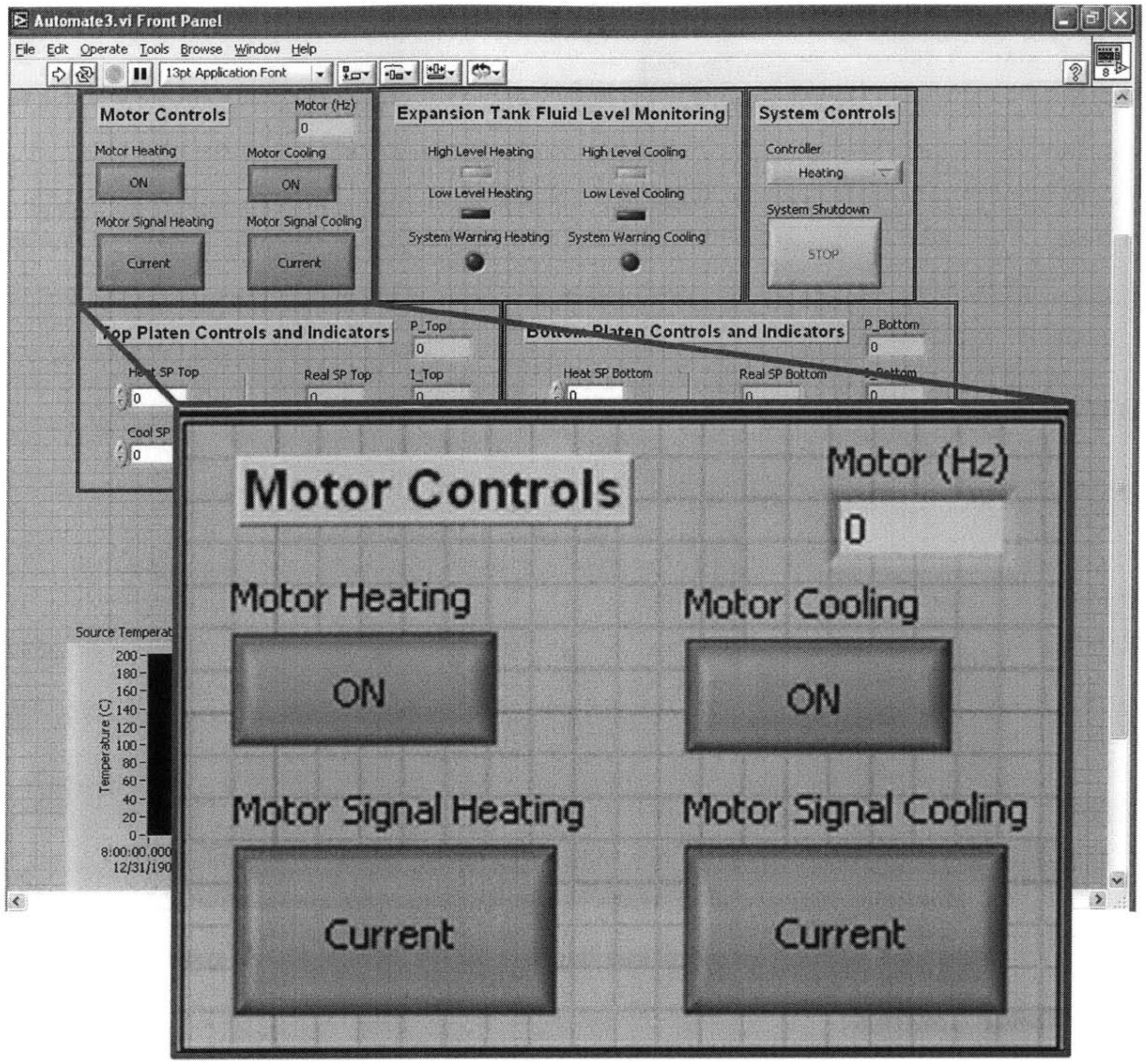

Figure 6-2 Motor controls labview interface

6.1.2 Expansion Tank Fluid Level Monitoring

Monitoring the fluid level in the expansion tank is a safety feature incorporated in the Labview interface (Figure 6-3). The fluid level should always be between the top and bottom level sensors. Therefore, during normal operation the high level sensor should be on and the low level sensor should be off. If either the high level sensor is off or the low level sensor is on, the system warning light will turn on indicating the system should be shut down.

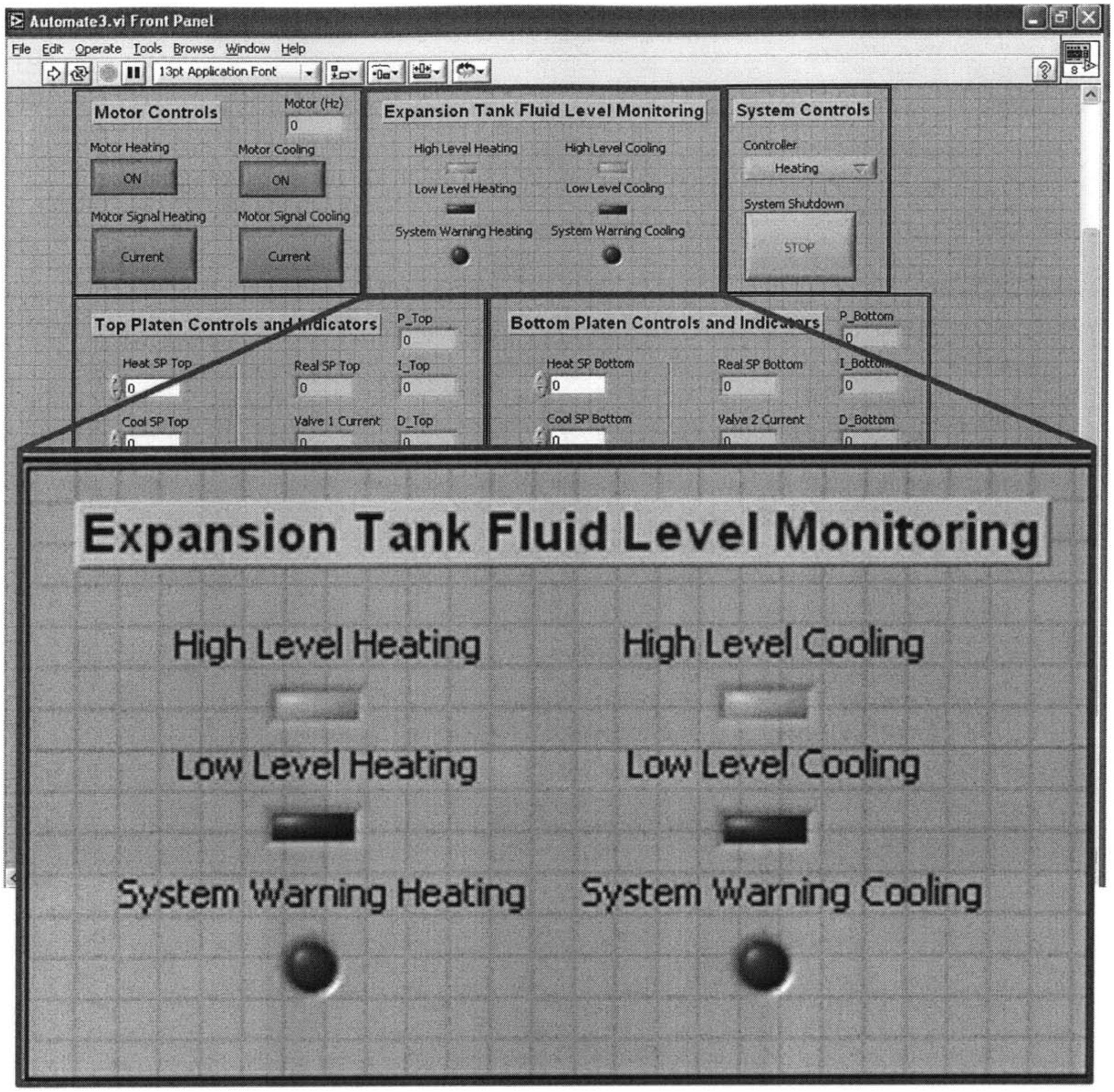

Figure 6-3 Expansion tank fluid level monitoring Labview interface

6.1.3 System Controls

The system controls section of the screen allows the user to switch the controller between heating and cooling. A program shutdown button is also necessary to turn off all data acquisition and data output to the valves. Turning off the program also stops the writing of data to a file. The stop button should always be used to shut down the program.

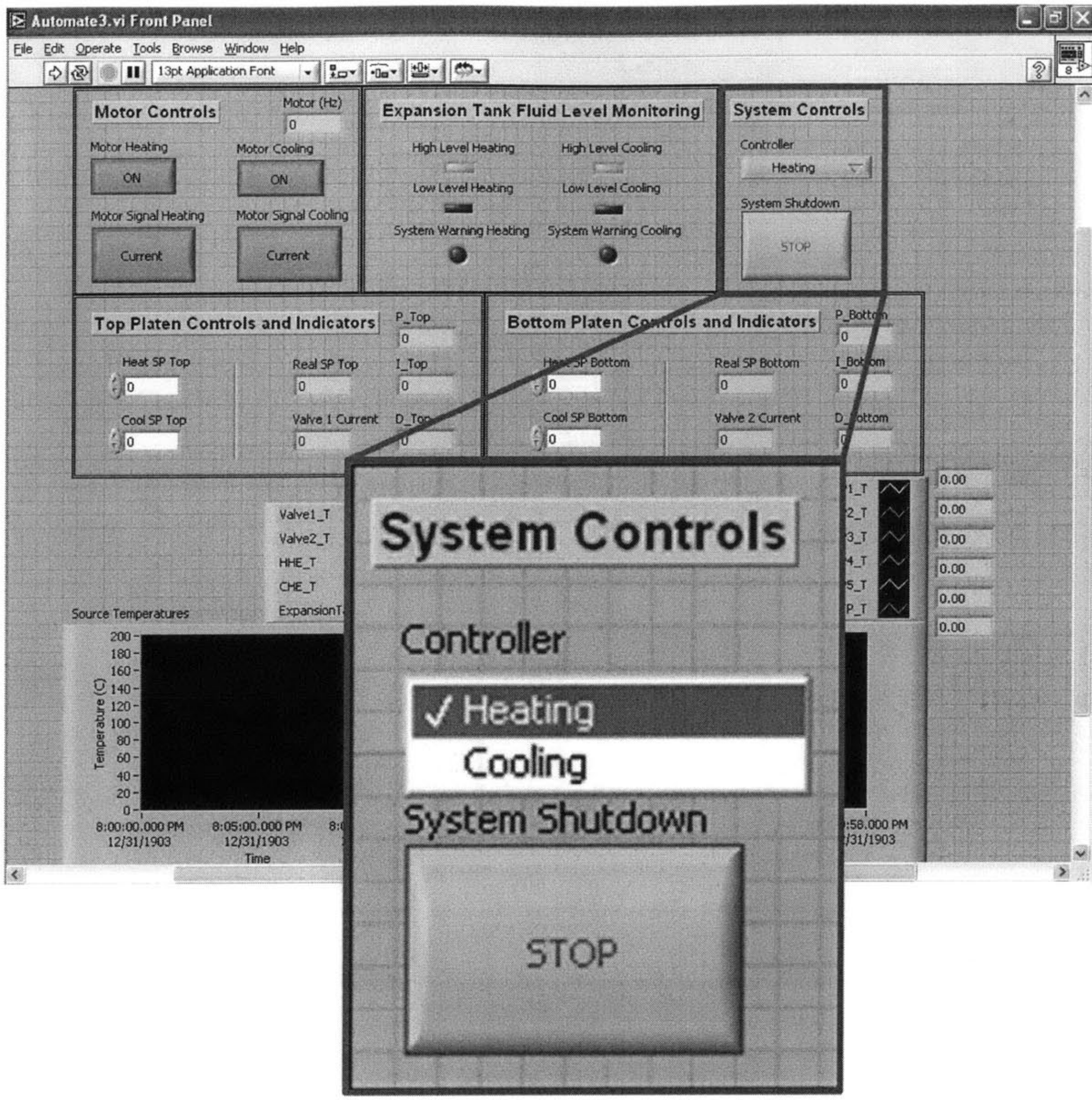

Figure 6-4 System controls Labview interface

6.1.4 Top and Bottom Platen Controls and Indicators

The top platen controls and indicators section includes two user inputs and five indicators (Figure 6-5). Two user inputs include the desired top platen embossing set point temperature and the de-embossing set point temperature. “Real SP Top” shows the compensated set point used in the control system. The “Valve 1 Current” displays the current in mA sent to the mixing valve positioners. Three indicators on the right side show the PID controller gains. The gains correspond to platen feedback during heating and valve fluid outlet feedback during cooling. Bottom platen controls and indicators are identical in terms of function and user inputs.

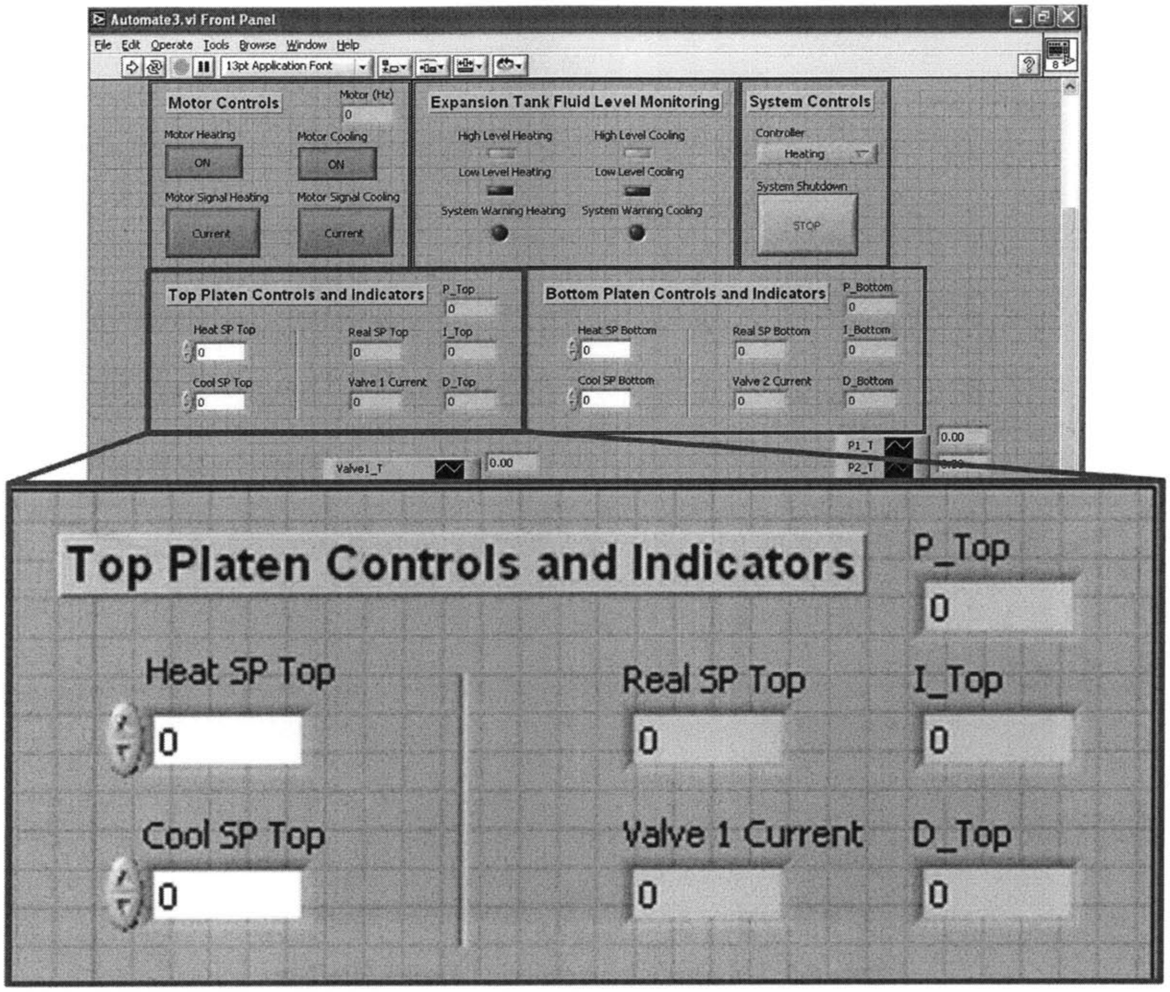

Figure 6-5 Top platen controls and indicators Labview interface

6.1.5 Temperature Monitoring

Temperature monitoring is vital to know when embossing and de-embossing temperatures are reached (Figure 6-6). The "source temperatures" (left) display monitors the temperature of the valve1 outlet fluid, valve2 outlet fluid, hot heat exchanger outlet fluid, cold heat exchanger outlet fluid, and expansion tank fluid. The "platen temperatures" (right) display monitors the temperature of five locations on the bottom platen, discussed in Section 3.3.13.1, and a single location on the top platen. Both of the displays only show ten minutes of temperature history and it is updated every two seconds.

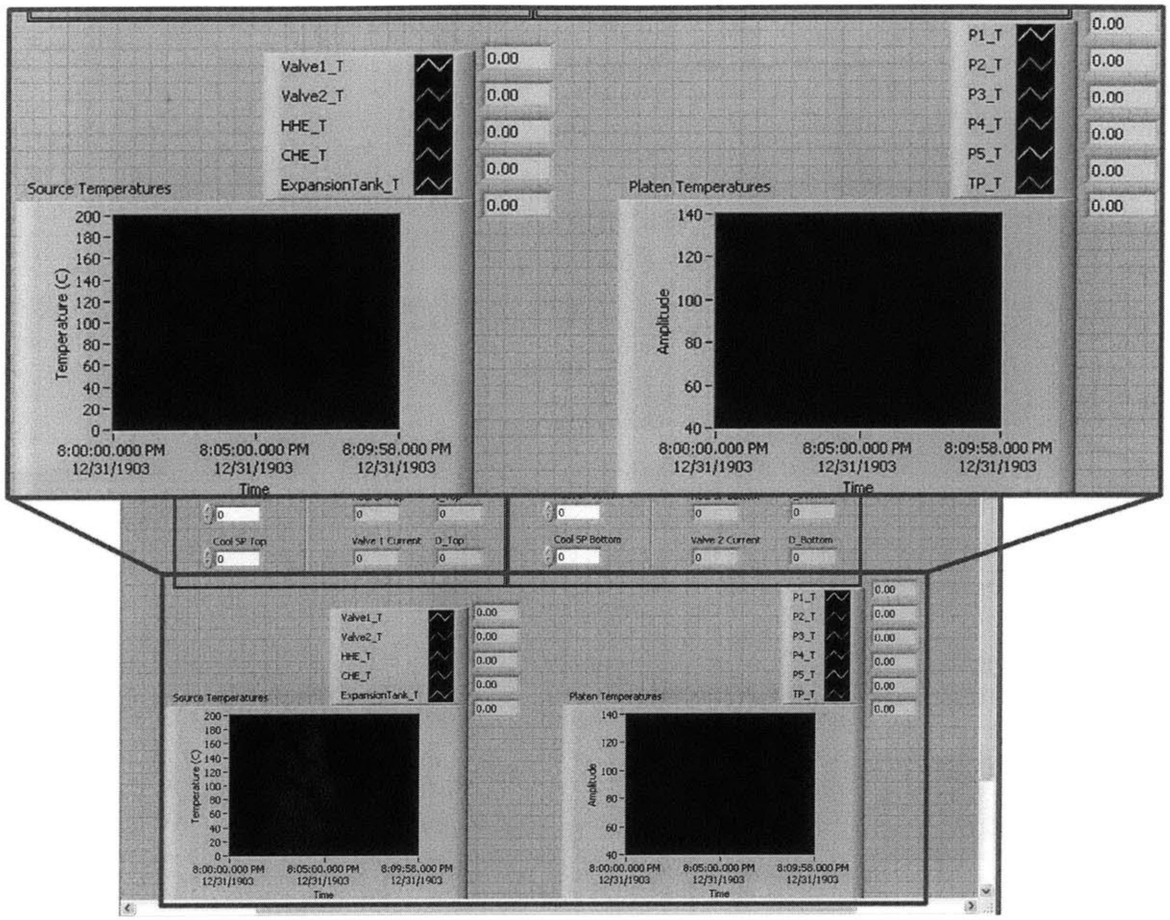

Figure 6-6 Temperature monitoring Labview interface

6.2 Program Function

6.2.1 General Functions

Once the program is started, it prompts the user to create a new file where the data will be written (Figure 6-7). Another function which occurs concurrently with creating and opening a new file is configuring the channels for analog inputs in the following order: Valve1_T, Valve2_T, HHE_T, CHE_T, P1_T, P2_T, P3_T, P4_T, P5_T, Expansion Tank_T, TP_T. These channels were initially configured in NI Measurement

& Automation Explorer as traditional virtual channels. After completing these operations, the program enters a while loop.

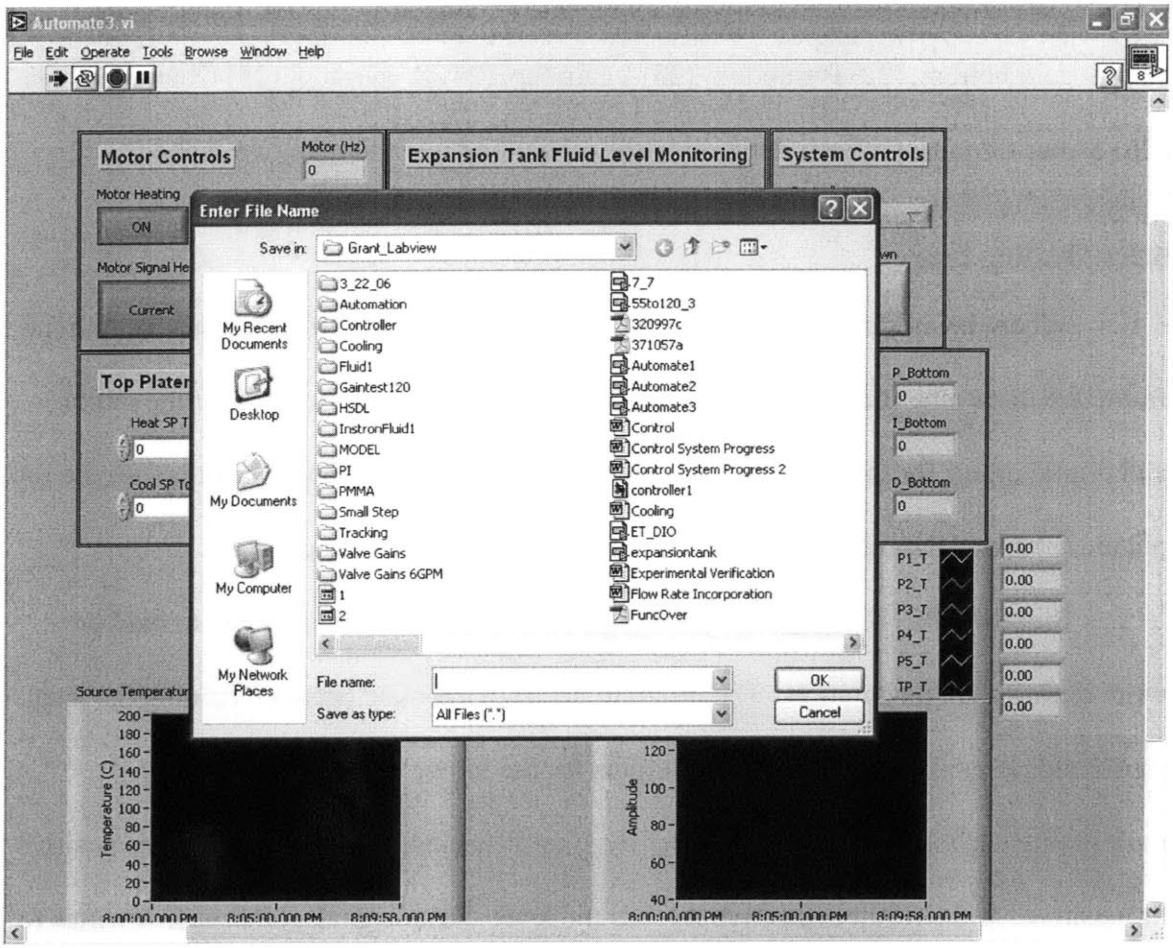

Figure 6-7 Picture of the prompt window which appears upon startup

Once in the while loop, the configured analog inputs are displayed on two charts and written to the opened file. A total list of signals are written to the opened file and are placed in this order: (1) Time stamp, (2) Valve1 outlet temperature, (3) Valve2 outlet temperature, (4) Hot heat exchanger outlet temperature, (5) Cold heat exchanger outlet temperature, (6) P1 (Front right bottom platen) temperature, (7) P2 (Back right bottom platen) temperature, (8) P3 (Middle bottom platen) temperature, (9) P4 (Front left bottom platen) temperature, (10) P5 (Back left bottom platen) temperature, (11) Expansion tank temperature, (12) Top platen temperature, (13) Minutes, (14) Seconds, (15) Valve1 current signal (mA), (16) Valve2 current signal (mA), (17) Compensated set point bottom platen, (18) Compensated set point top platen, (19) P gain bottom, (20) I gain bottom, (21) D gain bottom, (22) P gain top, (23) I gain top, (24) D gain top, (25) Controller type, (26) Motor frequency. Each iteration in the while loop is set to take two seconds.

6.2.2 Heating Logic

When the user chooses heating, the case structure frame "0" is active. Within the frame are three other case structures: (1) switch between digital outputs for the motor and digital inputs for the level sensors, (2) switch between different controllers for the top platen, (3) switch between different controllers for the bottom platen.

Since the PCI 4351 has only one digital I/O port it can choose only to read or write during a single iteration. The program needs to alternate between reading the level sensor signals and writing the digital outputs for the motor. This is achieved by multiplying each iteration frame number by -1 and checking to see if the result is positive or negative. If the result is positive it reads the level sensor signals, otherwise it writes to the motor digital outputs. Another manipulation within the frame scales the motor frequency to current, which is shown in Equation 6-1.

$$Current = Motor_{frequency} \times .26666 + 4$$

Equation 6-1

The other two case structures relate to switching controllers for the top and bottom platens. As mentioned in Section 0, two different controllers will be implemented depending on the mixing valve current signals. When the valve current is 4 mA, the controllers will be strictly proportional; otherwise the controller will be under PI control.

For the bottom platen, the feedback signal is the average of the five temperature measurements taken from the bottom platen. For the top platen, the feedback signal is a single temperature measurement from a drilled port in the side of the top spacer plate. Once these signals are acquired, the measurements are compared with their respective set point temperatures and go through a PID controller. The output signal is then manipulated with Equation 6-2 to convert it to current, which will be sent to the mixing valves.

$$Current = Output \times (-8) + 12$$

Equation 6-2

6.2.3 Cooling Logic

When the user chooses cooling, the case structure frame "1" is active. Within the frame are three other case structures: (1) switch between digital outputs for the motor and digital inputs for the level sensors, (2) switch between different controllers and compensated set point temperatures for the Valve1 outlet, (3) switch between different controllers and compensated set point temperatures for the Valve2 outlet.

The case structure with the digital I/O's is the same as the one described in the heating logic with an imbedded case for the motor output. The additional conditional determines whether to run the motor at a high flow rate or low flow rate. If the both the mixing valve currents are 20 mA, corresponding to fully open on the cold side, the motor frequency is set to 50 Hz (38 GPM). For all other conditions the motor frequency is set to 12.5 Hz (12 GPM).

The valve1 fluid outlet temperature feedback goes through the same manipulations as the platen feedback mentioned in the previous section. However, the conditional to switch between controllers is when the difference between the actual valve1 fluid temperature and set point temperature below 15 °C. Also, the compensated set point temperature is changed when the conditional is met. The valve2 fluid temperature feedback follows the same logic. A more detailed explanation of the selected set points and gains are covered in Section 5.8.

CHAPTER

7 Process Control for Fabrication of Micro-Fluidic Devices

7.1 Background on Process Control

In any manufacturing process a general understanding of the processing parameters and their effects on the output part is critical to reducing variation. Therefore, it is important to understand and try to reduce the natural variation of the machine being used to create parts. In-vivo measurements of the parts being created during the micro-embossing process is nearly impossible, therefore a way of determining if the part is in compliance off line is critical for process control.

7.2 Metrology Problems

Polymer micro- and nano-devices typically consist of simple geometries such as channels, vias, and gratings. These devices will typically operate as predicted based on the accuracy of a few critical dimensions. As mentioned in Section 1.3.2, laminar microfluid flow at certain aspect ratios for Newtonian fluids is governed by Hagan-Pouseille flow. This equation shows that fluid flow is sensitive to a critical dimension of the channel created. Therefore, being able to measure critical dimensions becomes important for process control for these devices.

7.3 Types of Measurement Tools

A number of metrology tools exist that rely on vastly different physics such as mechanical imaging, electron discharge, or optical imaging. These techniques vary in terms of highest possible resolution in the vertical and lateral directions. A number of different surface characterization tools are summarized in Table 7-1. MIT has a number of these metrology tools available for use and a few of the ones investigated will be discussed in the following sections.

Table 7-1 Analytical techniques for surface characterization and their limitations with regards to vertical and lateral resolution and the materials they can characterize [69]

Technique	Main information	Vertical resolution (depth probed, typical)	Lateral resolution (typical)	Types of solid specimen (typical)	Use (popularity)
Optical profiler and laser interferometry	3D and 2D imaging Morphology Profilometry Topographic mapping Film thickness Wear volume Scar and crater depth Defects	~0.1 nm	A few sub μm to a few tens of μm	All	Medium
Confocal microscopy	3D and 2D imaging Morphology Profilometry Topographic imaging Film thickness Wear volume Scar and crater depth Defects	Variable from a few nm to a few μm	Optical, 0.5 to 4 μm; SEM, 1 to 50 μm	Almost all	Medium
Optical scatterometry	Profilometry Topographic imaging/mapping Periodic structure Morphology Defects	≥0.1 nm	A few sub μm to a few tens of μm; ≥ laser wavelength λ/2 for topography	Almost all	Not common
Light microscopy (general)	Imaging Morphology Damages Defects	Variable	Variable	All	Extensive
Stylus profilometry	Profilometry Topographic tracing Film thickness Morphology Scar and crater depth Wear volume	0.5 nm	100 nm	Almost all; flat smooth films	Extensive
Scanning tunneling microscopy (STM)	Topographic imaging Compositional mapping Morphology Profilometry Film thickness Spectroscopy Structure Defects	<0.03 to 0.05 nm	Atomic	Conductors	Medium
Atomic force microscopy (AFM) or scanning force microscopy (SFM)	Topographic imaging Friction force mapping Morphology Profilometry Film thickness Wear volume Scar and crater depth Structure Defects	<0.03 to 0.05 nm	Atomic to 1 nm	All	Medium
Variable-angle spectroscopic ellipsometry (VASE)	Film thickness Microstructure Optical properties	Tens of nm to μm	Millimeter	Planar surface and interface	Medium
X-ray fluorescence (XRF)	Film thickness (1 to 10^4 nm) Element composition (qualitative mapping)	10 μm	10 to 150 μm	All but low-Z elements: H, He, and Li	Extensive

7.3.1 Scanning Electron Microscope

A scanning electron microscope (SEM) works by directing electrons through a lens on the sample. Once the electrons hit the sample, some are rejected and collected by detectors that form the image. This imaging technique requires that the sample be conductive, however the plastic devices of interest do not fall into this category. Therefore, an alternative imaging technique is the environmental scanning electron microscope (ESEM). The ESEM creates an environment within the vacuum chamber that allows for imaging of non-conductive materials. MIT has a Philips/FEI XL30 FEG-SEM with a resolution of 3.5 nm at 30 KV [70]. This technique captures high resolution images, but does not provide any quantitative information.

7.3.2 Atomic Force Microscope

An atomic force microscope (AFM) works by detecting the deflection of a cantilever tip scanning the material surface and comparing it to a desired deflection in a DC feedback amplifier. This serial imaging technique is particularly slow, but has a high resolution. A Quesant Q-Scope Model 250 AFM is available for use at MIT with a horizontal resolution of roughly 60 nm for a representative scanning range. This metrology technique is promising because it has a high resolution while providing quantitative data. However, it is cumbersome to take measurements, has a limited range (roughly 80 μm), and it has some problems with controller induced artifacts, such as overshoot.

7.3.3 Interferometer

An optical interferometer works by splitting light into two beams, one going to the internal reference surface and the other to the sample. Once the light is reflected off the sample, the beams recombine inside the interferometer and undergo constructive and destructive interference producing the light and dark fringe patterns. The interferometer available for use at MIT is a Zygo model 5000 series. Its vertical resolution is extremely high at 0.1 nm, but its horizontal resolution is limited to 0.45 μm. One of its advantages is that it can quickly capture an image and provide quantitative data.

7.4 Best Technique for Different Devices

A process variation study on the HME I was conducted by Ganesan [33] using a DRIE silicon tool and PMMA. A series of critical lateral features were measured with the Zygo model 5000 and a number of potential sources of variation were conjectured. However, a re-evaluation of the measurements done by the author and Thaker [32] revealed that process variation detected in the initial study was dominated by measurement uncertainty making the variation data inconclusive. A run chart for a particular feature's die-part difference replicated under the same processing conditions using the interferometer is shown in Figure 7-1. Another metrology method was investigated to conclusively detect process variation for these embossed parts.

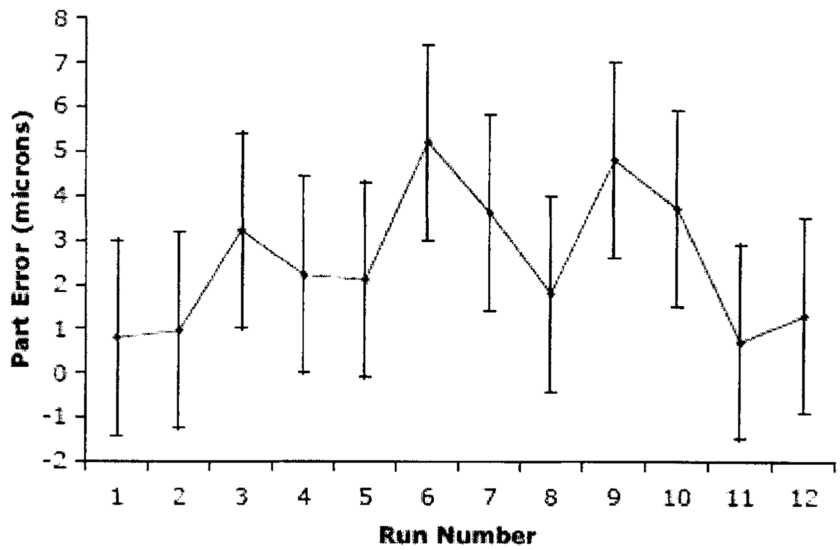

Figure 7-1 Run chart for a feature measured with the Zygo 5000 with measurement error bars [32]

The AFM described in Section 7.3.2, was used to characterize and detect process variation for the smaller features (~4 μm) created by Ganesan [33]. Its high resolution proved to be advantageous in terms of minimizing the measurement uncertainty and a 12 % process variation was detected. The run chart for the measured feature is shown in Figure 7-2. This shows that the AFM can be a viable metrology tool in detecting process variation at small feature scales.

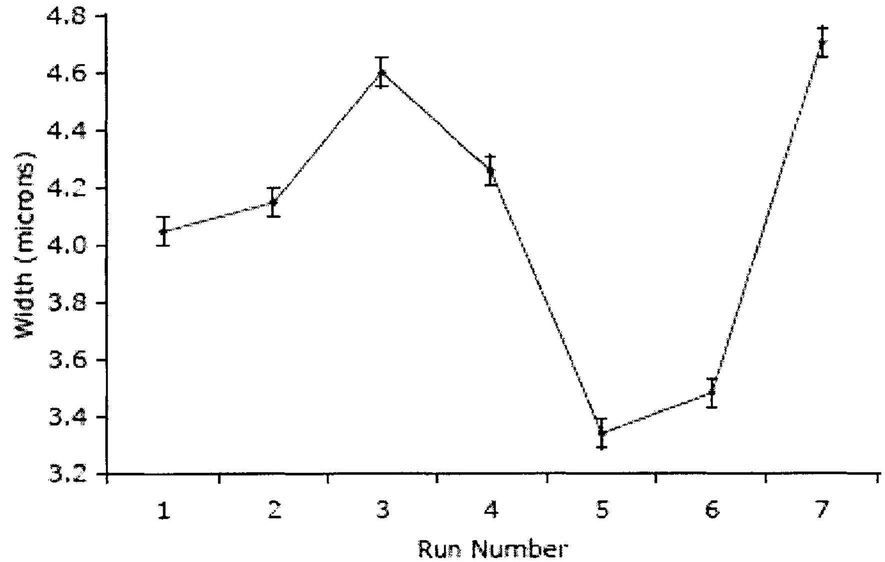

Figure 7-2 Run chart based on AFM measurements on a feature approximately 4 microns in width

Another viable metrology technique studied by Wang [27] was using the Zygo 5000 scans and processing the data using a protocol developed in MATLAB to extract depth measurements. This measurement proved to be reliable because of the extremely high vertical resolution of the interferometer. The advantage to using this technique is that it cuts down on processing time.

7.5 Tool Design for Process Control Study

Literature has shown that tools used for micro-embossing can be fabricated using, DRIE in silicon, LIGA, microEDM, SU-8 on silicon, electroforming, and CNC high precision milling [71,72,73,74,75]. Each has their advantages and disadvantage in terms of ease of fabrication and possible feature aspect ratios. Since our laboratory is interested in studying manufacturing aspects for micro-embossing, a tool was designed to study the effects of feature size, angle, spacing, uniformity, and fluid flow. A suitable technique for fabricating the tool is DRIE on silicon because of the availability of resources and its versatility in creating different depths with almost vertical sidewalls.

A 4" mask was co-designed by the author, Thaker, and Wang with the intention of creating tools using DRIE on silicon. H. Taylor, an SMA II student, fabricated the tools using the mask. A schematic of the tool layout is shown in Figure 7-3. The base set of features intended to evaluate different angles consist of a channel, circle, equilateral triangle, square, and hexagon. In order to study the effects of feature size, the widths of each base set are 300, 100, 30, 10, 3, and 1 μm. There are also three spacing schemes, where the spacing between feature sets is 10, 1 and 0.1 times the feature's width. This whole section is replicated 8 times across the wafer to evaluate the wafer scale uniformity. Various aspect ratios can also be studied by varying the etch depth from wafer to wafer. In addition to the base testing layout a number of different functional fluid channels and vias are included on the tool.

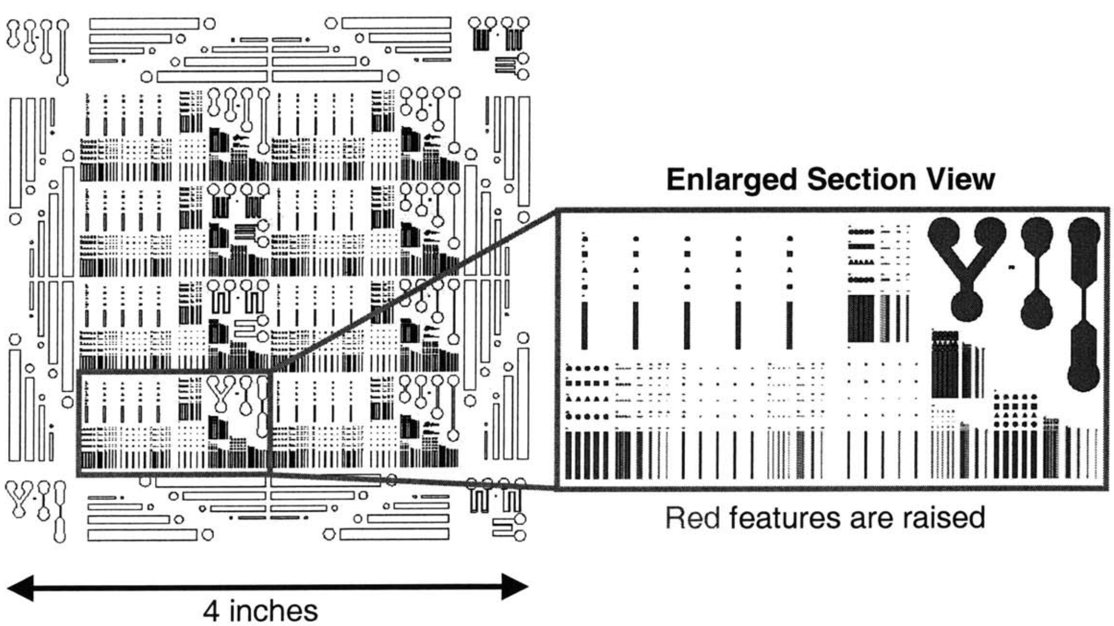

Figure 7-3 Tool design for 4" silicon wafer

7.6 Variability Study for HME II

Using an SU-8 tool with the pattern mentioned in Section 7.5, a series of PMMA fluid channel features were fabricated using the HME II. This test was conducted to quantify the natural process variation of the HME II. A PMMA work piece roughly 5 mm by 15 mm was embossed with a trough roughly 35 μm in depth, 800 μm wide, and 8000 μm long on the silicon wafer. The processing conditions were an embossing temperature of 120 °C, de-embossing temperature of 65 °C, and a force of 300 N. Twelve parts were fabricated under these conditions by the author and Thaker [76]. The depths were measured in the same area of the channel for each part using the algorithm developed by Wang [27]. The results are summarized in the run chart in Figure 7-4. Measurement uncertainty dominates, making the detection of any natural process variation for the HME II unfeasible. Therefore, one conclusion is that the parts are fully formed under the specified conditions and do not have any detectable depth variation.

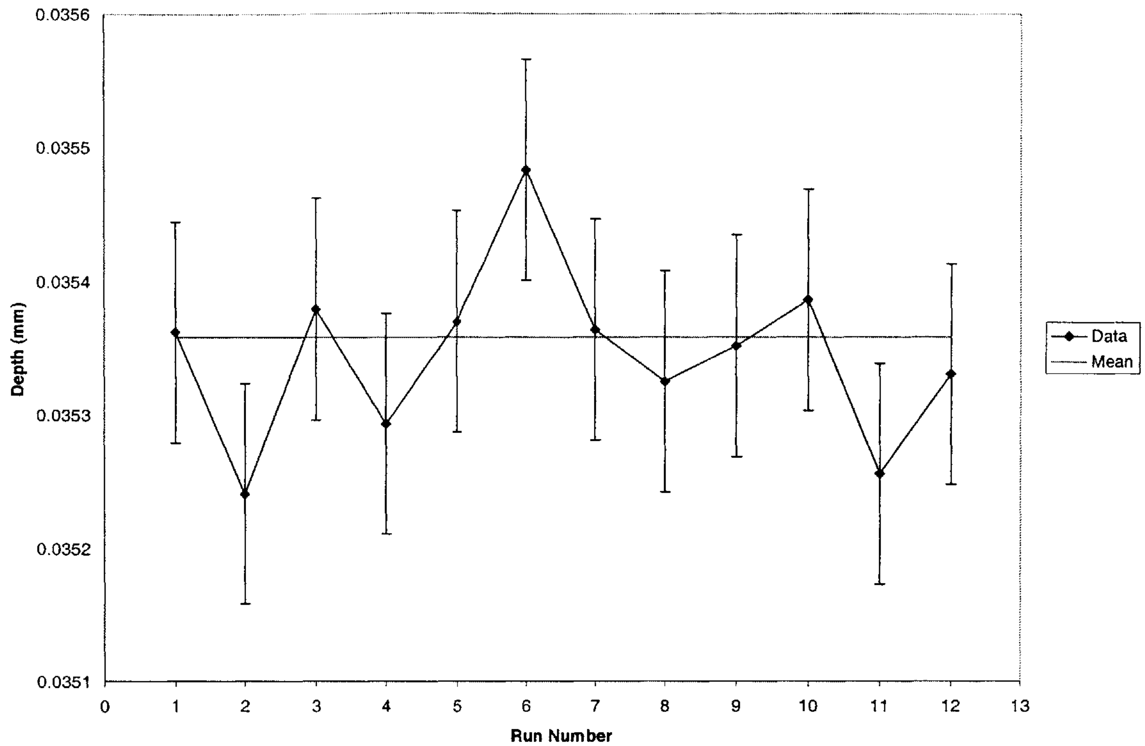

Figure 7-4 Run chart for part depth under identical processing conditions

CHAPTER

8 Conclusions and Future Work

8.1 Summary

A second generation hot micro-embossing machine (HME II) was designed and constructed by Dirckx [29], Shoji, and Thaker [76]. To fully understand the system dynamics and machine limitations the machine was modeled and characterized. This information was used to develop a temperature controller with the following capabilities: steady state error within ±1 °C, fast heating and cooling rates, and being robust to a number of processing conditions. Finally, a Labview GUI automated the temperature cycle while allowing users to manipulate relevant processing parameters.

8.1.1 Best Thermal Performance Curve

With the HME II a typical embossing thermal cycle from 55 °C to 120 °C was able to heat the both of the platens to 120 ± 1 °C in 138 seconds and cool both of the platens to 55 ± 1 °C in 190 seconds. Therefore, given an embossing hold time of roughly 30 seconds the whole process cycle can be completed in 6 minutes. This is a marked improvement over the 15 minute heating time and 5 minute cooling time achieved by the old system.

8.1.2 Software Capabilities

A Labview GUI automates the thermal process and provides the user with enough control over relevant processing parameters such as embossing and de-embossing set point temperatures. Further development and modifications to the controller can be easily implemented.

8.2 Improvements to the Controller

Various linear controllers were used for the system. This worked well for a number of processing conditions, but was not robust to operating condition changes. It has been tuned for a limited range of temperature changes and for a particular platen arrangement. Modifying the gains on the existing controller could make some slight improvements regarding overshoot and settling time of the temperature response. However, making the control system robust to the whole gamut of processing conditions and the ability to track an arbitrary waveform may require using an entirely different controller. A non-linear adaptive controller might improve the performance of the machine. Also, a multiple loop controller might improve the cooling performance, since it will be able to directly monitor the platen temperature instead of just the temperature of the fluid entering the platens.

8.3 Improvements to the Hardware

As mentioned in Section 5.3, there are problems with the mixing valves and its actuator. Stiction and deadband are problems that not only make controlling the valves difficult, but also increase the complexity of analyzing the system dynamics. A fast responding electromechanical actuator could alleviate a lot of control problems.

Another improvement to the hardware would be installing a data acquisition card with a faster sampling rate. This would make for easier control of the temperature, especially in combination with a quick responding valve actuator.

8.4 Improvements to the Software

Currently, the program is only set to accommodate a step input for heating and cooling. All modifications to the controller gains, compensated set point temperatures, and motor speeds can be set in the block diagram of the program. A simple modification can be made to include sine, square, triangle, sawtooth, and DC waveforms using the "Simulate Signal.vi" shown in Figure 8-1. The user should take caution when using this VI and be aware of the system sampling rate and limitations regarding the maximum heating and cooling rates. Preliminary tests show that the tracking ability of a PI controller is limited and waveforms should only be run at a very low frequency. If the user wants to define a ramp waveform a "Simulate Arbitrary Signal.vi" shown in Figure 8-2 should be used. Again, good judgment should used when defining a heating or cooling rate.

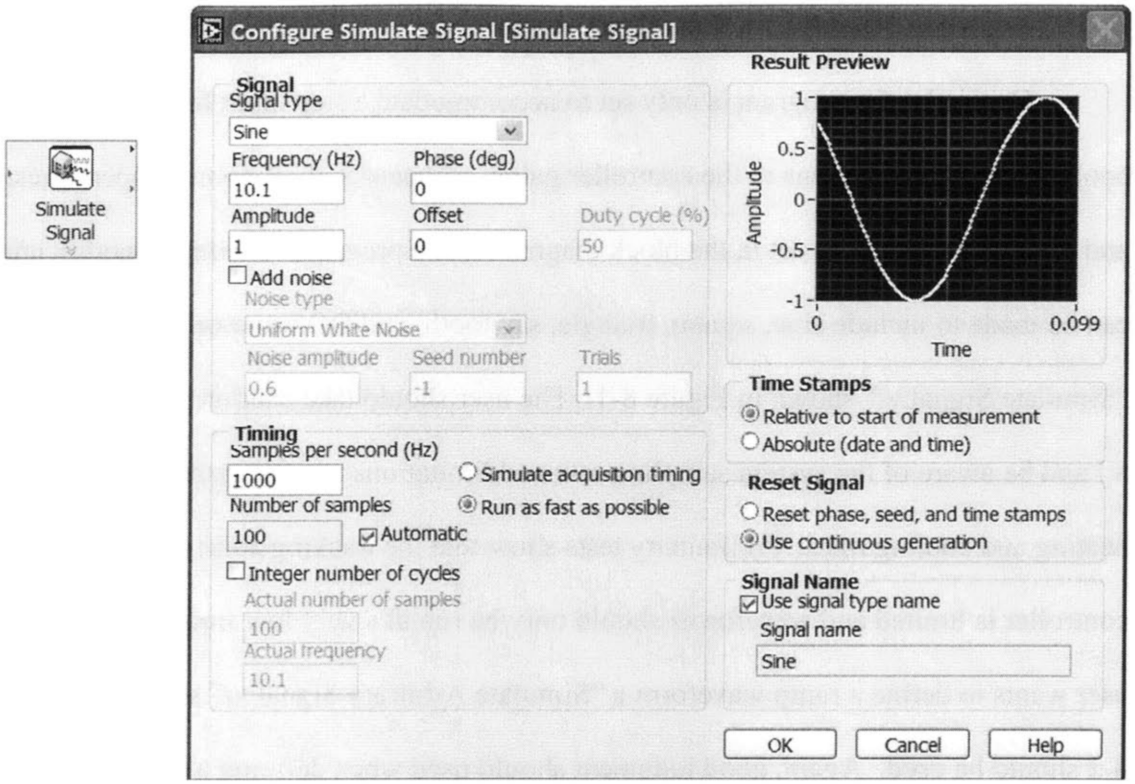

Figure 8-1 Simulate signal Labview VI

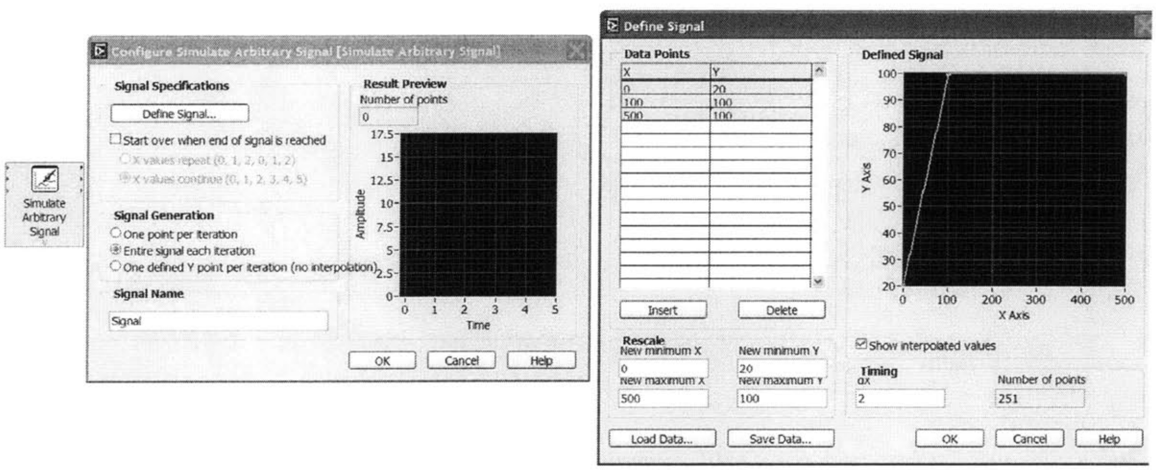

Figure 8-2 Simulate arbitrary signal Labview VI

Eventually, complete automation of the embossing process is desired. This would include the addition of Instron control, heater control, and safety shutdown. The Instron can be controlled in Labview with the appropriate drivers and it has most of the capabilities available in the Merlin software. Control of the heater should only involve programming of the data acquisition and setting up the digital I/O. All of the wiring for heater control is completed. Once the HME II is ready for production cycling the safety system should be programmed. This should only involve some simple logic to shut down the motor and heater when the level sensors engage.

8.5 Recommendations for HME III

For the future, a HME III should be designed and constructed. The HME II has some limitations stated in this thesis and an ideal hot micro-embossing system for manufacturing should be flexible in design and capabilities. The following sections outline possible areas of improvement, which may be addressed in the HME III.

8.5.1 Fully Welded System

If the decision is to stick with a hot oil thermal system, a fully welded system is necessary. Experience suggests that NPT fittings will leak when put through a number of thermal cycles no matter what type of thread sealant is used. Experiments have shown that heating is the rate limiting step in the thermal cycle, but its performance can be improved at lower flow rates. Lower system flow rates will allow for a smaller pump and smaller pipes to be installed. This will lower the thermal mass of the system and speed up the thermal response.

8.5.2 Vacuum Environment

Currently, all of the PMMA parts have been created in atmospheric conditions. Some of the parts created on the first generation system by Ganesan had air bubbles shown in Figure 8-3. A paper by Roos suggests that embossing polymers under a vacuum improves the large area uniformity of the part by eliminating any entrapped air

[77]. Since the goal of the HME II is to emboss a 4" PMMA wafer, a vacuum might be necessary to eliminate the air which may get trapped in that large area.

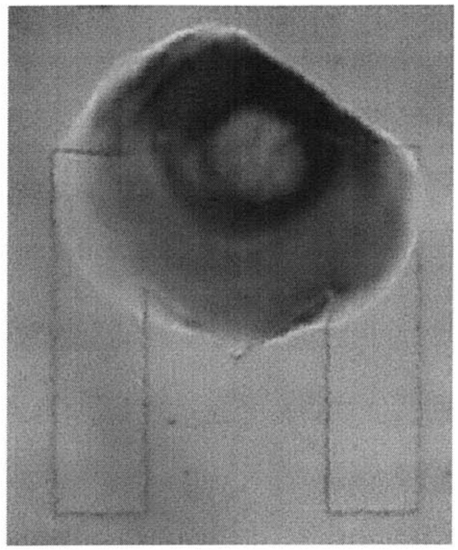

Figure 8-3 Bubble on a feature created in PMMA

8.5.3 Automatic De-Embossing and Loading of a Work Piece

The eventual goal of the machine is to have a fully automated process. Automatic temperature control has been achieved in Labview and coordinated force control can be integrated into the software. However, a subsystem to de-emboss the PMMA and reload a work piece has yet to be designed. Requirements for a work piece loader would include accurate displacement control for repeatable re-registration of the work piece. Quality force control is also necessary to ensure no damage is done to the plastic during handling. This last subsystem would complete the automation of the micro-embossing process.

Appendix

A Material Properties

A.1 Properties of OT-201

From the Omega product webpage:

http://www.omega.com/Temperature/pdf/OT-201.pdf

Typical Properties

Material	Silicone Grease
Continuous Temperature	200°C (392°F)
Cure	Not required
Adheres to Most*	Wets most Surfaces
Thermal conductivity (k) (BTU) (in)/(hr) (ft²) (°F)	Extremely High 16
Electrical Insulation Volume Resistivity ohm–cm	Very High 10^{14}

*M = Metal PA = Paper Products
C = Ceramic W = Wood
PL = Plastic

A.2 Properties of Paratherm MR

From the Paratherm product webpage:

http://www.paratherm.com/Paratherm-MR/MRtabdataSI.asp

Paratherm MR™

Tabular Data (SI Units) Rev. 1000

Temperature		Density		Viscosity		Specific Heat	Thermal Conductivity	Vapor Pressure	
°C	**°F**	**g/ml**	**kg/mþ**	**mmú/s**	**mPa-s**	**cal/(g-°C)**	**W/(m-K)**	**mm Hg**	**kPa**
-20	-4	0.8398	840	31.8	26.7	0.4962	0.1477		
-15	5	0.8358	836	24.8	20.7	0.4995	0.1473		
-10	14	0.8317	832	19.7	16.4	0.5027	0.1468		
-5	23	0.8277	828	15.9	13.2	0.5059	0.1464		

0	32	0.8237	824	13.1	10.8	0.5092	0.1459		
5	41	0.8197	820	10.9	8.96	0.5124	0.1455		
10	50	0.8156	816	9.2	7.54	0.5157	0.1451		
15	59	0.8116	812	7.90	6.41	0.5189	0.1446		
20	68	0.8076	808	6.83	5.51	0.5221	0.1442		
25	77	0.8036	804	5.96	4.79	0.5254	0.1438		
30	86	0.7996	800	5.24	4.19	0.5286	0.1433		
35	95	0.7955	796	4.65	3.70	0.5319	0.1429	0.01	
40	104	0.7915	792	4.15	3.29	0.5351	0.1425	0.01	
45	113	0.7875	787	3.73	2.94	0.5383	0.1420	0.01	
50	122	0.7835	783	3.38	2.65	0.5416	0.1416	0.01	
55	131	0.7794	779	3.07	2.39	0.5448	0.1412	0.02	
60	140	0.7754	775	2.81	2.18	0.5481	0.1407	0.03	
65	149	0.7714	771	2.58	1.99	0.5513	0.1403	0.04	0.01
70	158	0.7674	767	2.38	1.82	0.5545	0.1398	0.05	0.01
75	167	0.7634	763	2.20	1.68	0.5578	0.1394	0.06	0.01
80	176	0.7593	759	2.05	1.55	0.5610	0.1390	0.11	0.02
85	185	0.7553	755	1.91	1.44	0.5643	0.1385	0.17	0.02
90	194	0.7513	751	1.79	1.34	0.5675	0.1381	0.22	0.03
95	203	0.7473	747	1.68	1.25	0.5707	0.1377	0.27	0.04
100	212	0.7432	743	1.58	1.17	0.5740	0.1372	0.33	0.04
105	221	0.7392	739	1.49	1.10	0.5772	0.1368	0.53	0.07
110	230	0.7352	735	1.41	1.04	0.5805	0.1364	0.73	0.10
115	239	0.7312	731	1.34	0.977	0.5837	0.1359	0.92	0.12
120	248	0.7272	727	1.27	0.923	0.5869	0.1355	1.12	0.15
125	257	0.7231	723	1.21	0.874	0.5902	0.1351	1.32	0.18
130	266	0.7191	719	1.15	0.830	0.5934	0.1346	1.94	0.26
135	275	0.7151	715	1.10	0.789	0.5967	0.1342	2.56	0.34
140	284	0.7111	711	1.06	0.752	0.5999	0.1337	3.17	0.42
145	293	0.7070	707	1.01	0.717	0.6031	0.1333	3.79	0.51
150	302	0.7030	703	0.975	0.685	0.6064	0.1329	4.40	0.59
155	311	0.6990	699	0.938	0.656	0.6096	0.1324	5.33	0.71
160	320	0.6950	695	0.905	0.629	0.6129	0.1320	6.25	0.83
165	329	0.6910	691	0.873	0.603	0.6161	0.1316	7.17	0.96

170	338	0.6869	687	0.844	0.580	0.6193	0.1311	8.09	1.08
175	347	0.6829	683	0.817	0.558	0.6226	0.1307	9.01	1.20
180	356	0.6789	679	0.792	0.537	0.6258	0.1303	12.0	1.60
185	365	0.6749	675	0.768	0.518	0.6291	0.1298	14.9	1.99
190	374	0.6708	671	0.746	0.500	0.6323	0.1294	17.9	2.39
195	383	0.6668	667	0.735	0.484	0.6355	0.1289	20.9	2.78
200	392	0.6628	663	0.706	0.468	0.6388	0.1285	23.8	3.18
205	401	0.6588	659	0.688	0.453	0.6420	0.1281	30.5	4.06
210	410	0.6548	655	0.671	0.439	0.6453	0.1276	37.1	4.95
215	419	0.6507	651	0.654	0.426	0.6485	0.1272	43.8	5.84
220	428	0.6467	647	0.639	0.413	0.6517	0.1268	50.4	6.72
225	437	0.6427	643	0.625	0.402	0.6550	0.1263	57.1	7.61
230	446	0.6387	639	0.612	0.391	0.6582	0.1259	70.9	9.45
235	455	0.6347	635	0.599	0.380	0.6615	0.1255	84.8	11.3
240	464	0.6306	631	0.587	0.370	0.6647	0.1250	98.6	13.1
245	473	0.6266	627	0.575	0.361	0.6679	0.1246	112	15.0
250	482	0.6226	623	0.565	0.351	0.6712	0.1242	126	16.8
255	491	0.6186	619	0.554	0.343	0.6744	0.1237	153	20.4
260	500	0.6145	615	0.545	0.335	0.6776	0.1233	180	24.0
265	509	0.6105	611	0.535	0.327	0.6809	0.1228	207	27.6
270	518	0.6065	606	0.527	0.319	0.6841	0.1224	234	31.3
275	527	0.6025	602	0.518	0.312	0.6874	0.1220	261	34.9
280	536	0.5985	598	0.510	0.305	0.6906	0.1215	312	41.7
285	545	0.5944	594	0.503	0.299	0.6938	0.1211	363	48.5
290	554	0.5904	590	0.500	0.295	0.6972	0.1207	482	64.2
295	563	0.5863	586	0.496	0.291	0.7005	0.1202	600	80.0
300	572	0.5823	582	0.493	0.287	0.7038	0.1198	719	95.8
305	581	0.5782	578	0.490	0.283	0.7071	0.1194	837	111.6
310	590	0.5742	574	0.487	0.279	0.7104	0.1189	956	127.4
316	601	0.5701	570	0.483	0.276	0.7137	0.1185	1074	143.2

A.3 Properties of CC High Temperature Cement

From the Omega product webpage:

http://www.omega.com/Temperature/pdf/CC_CEMENT.pdf

Physical Properties†

Cement	OMEGABOND 600	OMEGABOND 700	CC High Temperature
Type of Cement (One or Two Part)	One Part	One Part	Two Part
Coefficient of thermal expansion, in/in/°F	2.6×10^{-6}	12.4×10^{-6}	4.6×10^{-6}
Color	Off White	White	Tan
Compressive strength, PSI	4500-5500	3500	3900
Density, lbs/ft³	160		141
Dielectric constant	3.0 - 4.0		5.0 to 7.0
Dielectric strength at 20°C (70°F), Volts/mil	76.0 to 101.0		25.0 to 51.0
Dielectric strength at 400°C (750°F), Volts/mil	25.0 to 38.0		12.5 to 25.0
Dielectric strength at 795°C (1475°F), Volts/mil	12.5 to 25.0		≤1.3
Maximum service temperature, °C (°F)	1426 (2600)	871 (1600)	843 (1550)
Modulus of rupture, PSI	450		
Tensile strength, PSI	250		425
Volume resistivity at 20°C (70°F), ohm-cm	10^{10}-10^{11}		10^{7}-10^{9}
Volume resistivity at 400°C (750°F), ohm-cm	10^{9}-10^{10}		10^{4}-10^{6}
Volume resistivity at 795°C (1475°F), ohm-cm	10^{8}-10^{9}		10^{2}-10^{3}
Flexural strength, PSI		435	
Absorption, %			10 - 12
Shrinkage, %			0.5
Thermal Conductivity, Btu-in/ft²-hr-°F	10 - 12	4.5 to 5.9	8
Mix Ratio	Mix 100 Parts powder with 13 parts water by weight.	Mix 75-80% powder with 20-25% water by weight.	Mix 3 parts powder to 1 part liquid by weight, or 2 parts filler to 1 part liquid by volume.
Curing Schedule	OMEGABOND 600® cures at room temperature by internal chemical action in 18-24 hours. Cure time can be accelerated by low temperature oven drying at 82°C (180°F). If the cement is to be exposed to elevated temperatures, cure for 18-24 hours at ambient temperature, then oven dry for 4 hours at 82°C (180°F) and for an additional 4 hours at 105°C (220°F). This helps to prevent spilling.	OMEGABOND 700® cures at room temperature with a chemical set action in 18-24 hours, Cure time can be accelerated by low temperature oven drying at 82°C (180°F). If the cement is to be exposed to elevated temperatures, cure for 18-24 hours at ambient temperature, then oven dry for 4 hours at 82°C (180°F) and for an additional 4 hours at 105°C (220°F). This helps to prevent spilling.	CC High Temperature Cement hardens with an internal chemical-setting action with an initial set in approximately 30 minutes. The final set is reached in 18 to 24 hours when cured at room temperature. If it is desired to accelerate the curing time, set the drying oven to 65°C (150°F) and the cement will cure in 4 hours. If the drying oven is set to 105°C (220°F), the cement will cure in 3 hours.
Distinguishing Characteristics and Applications	High dielectric strength. Used to pot nickel chromium resistance heating wire. Won't stick to smooth quartz.	Used on metals or other materials which have a high coefficient of thermal expansion. Excellent bonding characteristics.	Used to cement on and insulate thermocouples for surface temperature measurement.

†These physical properties were determined under laboratory conditions using applicable ASTM procedures. Actual field data may vary. Do not use physical properties data for specifications.

** Air Set Cements are also available See OMEGABOND® 300, OMEGABOND® 400 and OMEGABOND® 500. These cements set or cure through loss of moisture by evaporation. Atmospheric conditions therefore affect the drying rate. Air Set Cements are used mainly in the thin film applications (less than ¼" thickness.)*

*** Porous substrates may require dampening with Thinning Liquid before application of mixed cement. For OMEGABOND® 600 and OMEGABOND® 700 (one part cements), order OMEGABOND® Thinning Liquid, Model No. **OB-TL**, Price **$36** (8 fluid oz). For CC High Temperature Cement, use CC High Temperature Cement Liquid Binder to dampen porous substrates.*

A.4 Properties of Silicon

Information obtained from the Matweb website:

http://matweb.com/search/SpecificMaterial.asp?bassnum=AMESi00

Physical Properties	Metric	English	Comments
Density	2.329 g/cc	0.0841 lb/in³	
a Lattice Constant	5.43072 Å	5.43072 Å	
Molecular Weight	28.086 g/mol	28.086 g/mol	
Volume Compressibility, 10^-10 m²/N	0.306	0.306	
Mechanical Properties			
Knoop Microhardness	11270	11270	N/mm² Microhardness
Modulus of Elasticity	112.4 GPa	16300 ksi	
Compressive Yield Strength	120 MPa	17400 psi	
Bulk Modulus	98.74 GPa	14300 ksi	
Poisson's Ratio	0.28	0.28	
Shear Modulus	43.9 GPa	6370 ksi	Calculated
Electrical Properties			
Electrical Resistivity	0.01 ohm-cm	0.01 ohm-cm	
Magnetic Susceptibility	-3.90E-06	-3.90E-06	Atomic (cgs)

Critical Superconducting Temperature	6.7 - 7.1 K	6.7 - 7.1 K	6.7-7.1 K from 12.0-13.0 GPa pressure
Dielectric Constant	11.8	11.8	
Band Gap	1.107 eV	1.107 eV	
Electron Mobility, cm^2/V-s	1900	1900	
Hole Mobility, cm^2/V-s	500	500	
Thermal Properties			
Heat of Fusion	1800 J/g	774 BTU/lb	
CTE, linear 20°C	2.49 μm/m-°C	1.38 μin/in-°F	at 25°C
CTE, linear 250°C	3.61 μm/m-°C	2.01 μin/in-°F	at 227°C
CTE, linear 500°C	4.15 μm/m-°C	2.31 μin/in-°F	at 527°C
CTE, linear 1000°C	4.44 μm/m-°C	2.47 μin/in-°F	at 1027°C
Specific Heat Capacity	0.702 J/g-°C	0.168 BTU/lb-°F	
Specific Heat Capacity	0.794 J/g-°C	0.19 BTU/lb-°F	Gas

Thermal Conductivity	124 W/m-K	861 BTU-in/hr-ft²-°F	
Melting Point	1412 °C	2570 °F	
Boiling Point	3265 °C	5910 °F	
Heat of Formation	0 kJ/mol	0 kJ/mol	Crystal
Heat of Formation	450 kJ/mol	450 kJ/mol	Gas
Debye Temperature	372 °C	702 °F	
Optical Properties			
Refractive Index	3.49	3.49	at 589 nm
Reflection Coefficient, Visible (0-1)	0.3 - 0.7	0.3 - 0.7	varies irregularly with wavelength.
Descriptive Properties			
CAS Number	7440-21-3		
Crystal Structure	Cubic	Diamond Structure - Space Group Fd3m	

A.5 Properties of PMMA

Information obtained from the Matweb website:

http://matweb.com/search/SpecificMaterial.asp?bassnum=O1303

Physical Properties	Metric	English	Comments
Density	1.19 - 1.2 g/cc	0.043 - 0.0434 lb/in³	Average = 1.19 g/cc; Grade Count = 4
Water Absorption	0.13 - 0.35 %	0.13 - 0.35 %	Average = 0.22%; Grade Count = 4
Water Absorption at Saturation	1.1 %	1.1 %	Grade Count = 1
Mechanical Properties			
Hardness, Barcol	49	49	Grade Count = 1
Hardness, Rockwell M	90 - 94	90 - 94	Average = 92; Grade Count = 2
Tensile Strength, Ultimate	60 - 83 MPa	8700 - 12000 psi	Average = 73.2 MPa; Grade Count = 4
Tensile Strength, Yield	60 MPa	8700 psi	Grade Count = 1
Elongation at Break	4.2 - 5.5 %	4.2 - 5.5 %	Average = 4.8%; Grade Count = 4
Tensile Modulus	2.8 - 3 GPa	406 - 435 ksi	Average = 2.9 GPa; Grade Count = 2
Flexural Modulus	3 - 3.3 GPa	435 - 479 ksi	Average = 3.2 GPa; Grade Count = 2
Flexural Yield Strength	100 - 114 MPa	14500 - 16500 psi	Average = 110 MPa; Grade Count = 2
Compressive Yield Strength	100 - 124 MPa	14500 - 18000 psi	Average = 110 MPa; Grade Count=2
Izod Impact, Notched	0.22 - 0.25 J/cm	0.412 - 0.468 ft-lb/in	Average = 0.23 J/cm; Grade Count = 2
Electrical Properties			
Electrical Resistivity	1e+015 - 1.6e+016 ohm-cm	1e+015 - 1.6e+016 ohm-cm	Average = 9E+15 ohm-cm; Grade Count = 2
Surface Resistance	1.9e+015 ohm	1.9e+015 ohm	Grade Count = 1
Dielectric Constant	2.7 - 4	2.7 - 4	Average = 3.3; Grade Count = 2
Dielectric Constant, Low Frequency	3.5 - 4	3.5 - 4	Average = 3.8; Grade Count = 2

Dielectric Strength	17 kV/mm	432 kV/in	Grade Count = 2
Dissipation Factor	0.02 - 0.055	0.02 - 0.055	Average = 0.038; Grade Count = 2
Dissipation Factor, Low Frequency	0.055 - 0.06	0.055 - 0.06	Average = 0.057; Grade Count = 2
Thermal Properties			
CTE, linear 20°C	61 - 130 μm/m-°C	33.9 - 72.2 μin/in-°F	Average = 98.3 μm/m-°C; Grade Count=3
Specific Heat Capacity	1.5 J/g-°C	0.359 BTU/lb-°F	Grade Count = 3
Thermal Conductivity	0.19 - 0.25 W/m-K	1.32 - 1.74 BTU-in/hr-ft²-°F	Average = 0.2 W/m-K; Grade Count = 4
Maximum Service Temperature, Air	65 - 112 °C	149 - 234 °F	Average = 94.5°C; Grade Count = 4
Deflection Temperature at 1.8 MPa (264 psi)	99 - 112 °C	210 - 234 °F	Average = 100°C; Grade Count=4
Vicat Softening Point	110 °C	230 °F	Grade Count = 1
Minimum Service Temperature, Air	-40 °C	-40 °F	Grade Count = 1
Glass Temperature	100 °C	212 °F	Grade Count = 1
Optical Properties			
Refractive Index	1.49	1.49	Grade Count = 1
Haze	0.6 - 1 %	0.6 - 1 %	Average = 0.77%; Grade Count = 3
Transmission, Visible	92 %	92 %	Grade Count = 3
Processing Properties			
Processing Temperature	180 °C	356 °F	Grade Count = 1

B Component Specifications

B.1 Hot Heat Exchanger by Vulcan

These specifications are provided by Vulcan.

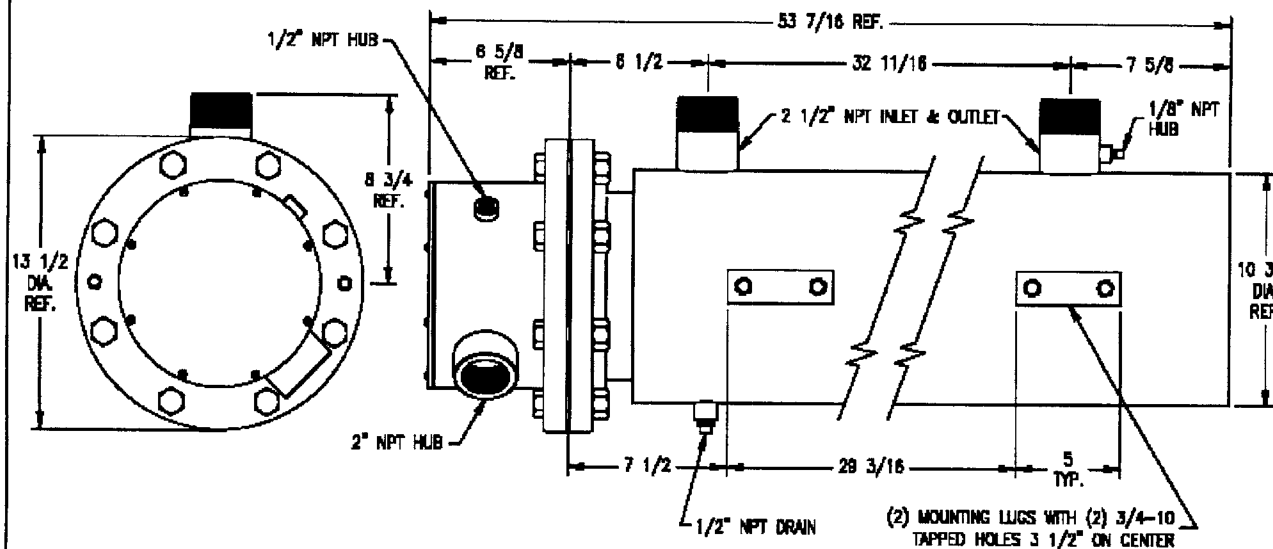

DESIGN SPECIFICATIONS:
8"-150# CIRCULATION HEATER – BOLTED FLANGE CONSTRUCTION

1. CARBON STEEL FLANGES AND SHELL ASSEMBLY
2. (18)-.475 DIAMETER INCOLOY ELEMENTS.
3. MOISTURE RESISTANT TERMINAL HOUSING
4. (2) 2 1/2" NPT EXTERNALLY THREADED INLET/OUTLET CONNECTIONS
5. (8) BOLTS & NUTS (3/4-10) EQUALLY SPACED ON A 11 3/4" D.B.C.
6. SHELL BODY WRAPPED WITH 1" FIBERGLASS INSULATION AND SECURED WITH HEAVY GAGE OUTER JACKET
7. HEAVY DUTY MOUNTING LUGS (WITH TAPPED HOLES) WELDED TO SHELL BODY
8. (1) 1/2" NPT DRAIN PLUG
9. HOUSING INCLUDES AN OVER-TEMP TYPE "J" THERMOCOUPLE
10. HYDROSTATIC TEST AT 225 PSI (MIN)

THIS IS THE MASTER DOCUMENT IF IN RED

-1	30,000	480	3PHΔ
P/N	WATTS	VOLTS	PHASE

REV.	SYM.	DESCRIPTION	DATE	REVISED BY
REVISIONS				

EXCEPT WHERE OTHERWISE STATED DIMENSIONS ARE IN INCHES. FOR TOLERANCES ON FINISHED DIMENSIONS SEE STD. TOLERANCE PROCEDURE

8"-150# CIRCULATION HEATER
MASSACHUSETTS INSTITUTE OF TECHNOLOGY

DN BY T.VERWEY | DATE 02-24-05 | CH BY | PAGE 1 OF 1
SCALE 1 : 6 | FOR USE ON | SIZE A | DWG NO. P8/4100/8 | REV.

Vulcan ELECTRIC COMPANY
PORTER, MAINE 04068

THIS IS A C.A.D. DRAWING. ALL CHANGES TO DRAWING MUST BE DONE ON C.A.D.

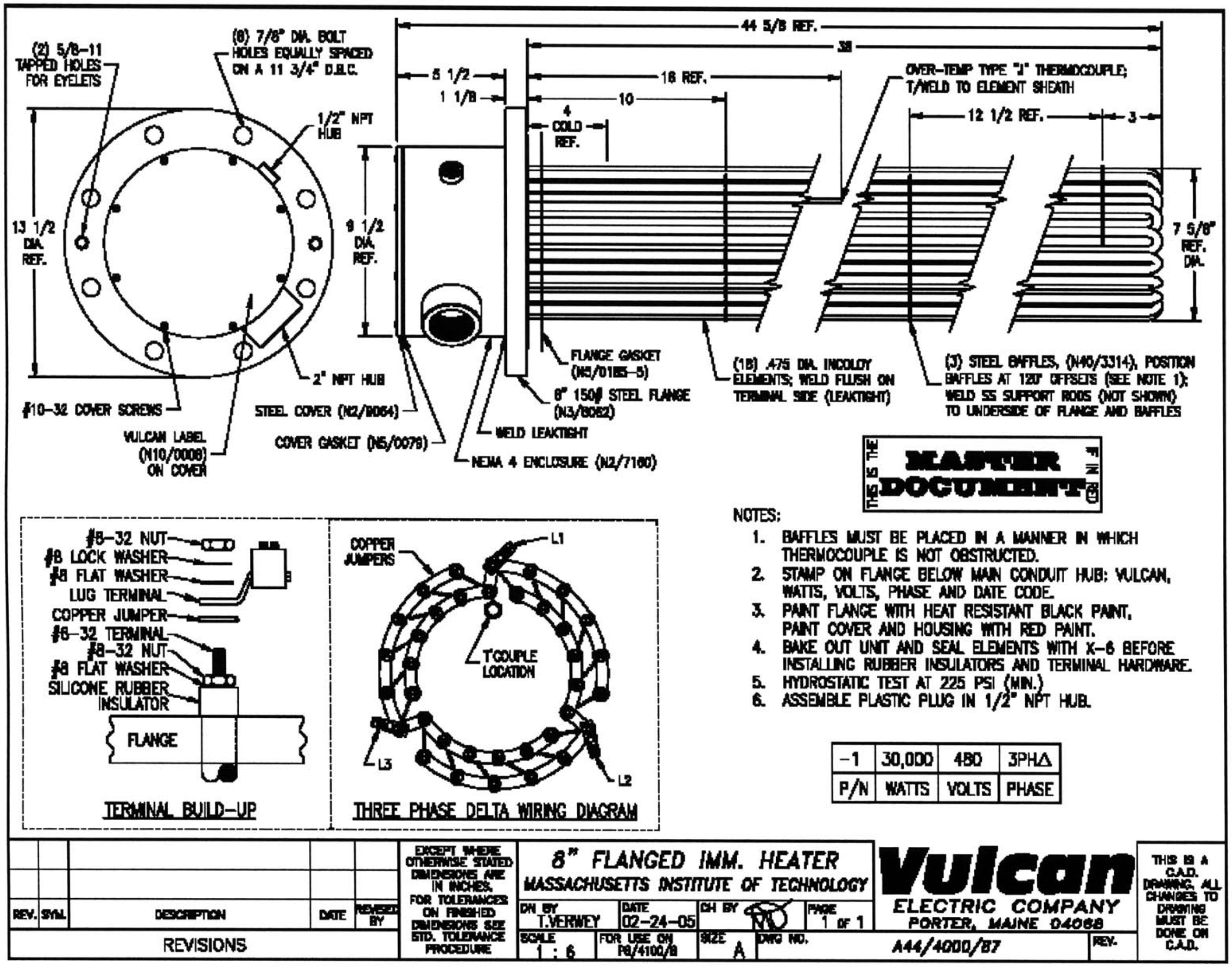
(2) 5/8-11 TAPPED HOLES FOR EYELETS
(8) 7/8" DIA. BOLT HOLES EQUALLY SPACED ON A 11 3/4" D.B.C.
1/2" NPT HUB
13 1/2 DIA. REF.
9 1/2 DIA. REF.
2" NPT HUB
#10-32 COVER SCREWS
VULCAN LABEL (N10/0008) ON COVER
STEEL COVER (N2/8064)
COVER GASKET (N5/0079)
44 5/8 REF.
38
5 1/2
1 1/8
16 REF.
10
4 COLD REF.
OVER-TEMP TYPE "J" THERMOCOUPLE; T/WELD TO ELEMENT SHEATH
12 1/2 REF.
3
7 5/8" REF. DIA.
FLANGE GASKET (N5/0185-5)
8" 150# STEEL FLANGE (N3/8062)
WELD LEAKTIGHT
NEMA 4 ENCLOSURE (N2/7160)
(18) .475 DIA. INCOLOY ELEMENTS; WELD FLUSH ON TERMINAL SIDE (LEAKTIGHT)
(3) STEEL BAFFLES, (N40/3314), POSITION BAFFLES AT 120° OFFSETS (SEE NOTE 1); WELD SS SUPPORT RODS (NOT SHOWN) TO UNDERSIDE OF FLANGE AND BAFFLES
THIS IS THE MASTER DOCUMENT
#8-32 NUT
#8 LOCK WASHER
#8 FLAT WASHER
LUG TERMINAL
COPPER JUMPER
#8-32 TERMINAL
#8-32 NUT
#8 FLAT WASHER
SILICONE RUBBER INSULATOR
FLANGE
TERMINAL BUILD-UP
COPPER JUMPERS
L1
L2
L3
T'COUPLE LOCATION
THREE PHASE DELTA WIRING DIAGRAM
NOTES:
1. BAFFLES MUST BE PLACED IN A MANNER IN WHICH THERMOCOUPLE IS NOT OBSTRUCTED.
2. STAMP ON FLANGE BELOW MAIN CONDUIT HUB: VULCAN, WATTS, VOLTS, PHASE AND DATE CODE.
3. PAINT FLANGE WITH HEAT RESISTANT BLACK PAINT, PAINT COVER AND HOUSING WITH RED PAINT.
4. BAKE OUT UNIT AND SEAL ELEMENTS WITH X-6 BEFORE INSTALLING RUBBER INSULATORS AND TERMINAL HARDWARE.
5. HYDROSTATIC TEST AT 225 PSI (MIN.)
6. ASSEMBLE PLASTIC PLUG IN 1/2" NPT HUB.
-1 | 30,000 | 480 | 3PHΔ
P/N | WATTS | VOLTS | PHASE
REV. | SYM. | DESCRIPTION | DATE | REVISED BY
REVISIONS
EXCEPT WHERE OTHERWISE STATED DIMENSIONS ARE IN INCHES. FOR TOLERANCES ON FINISHED DIMENSIONS SEE STD. TOLERANCE PROCEDURE
8" FLANGED IMM. HEATER
MASSACHUSETTS INSTITUTE OF TECHNOLOGY
DN BY T.VERWEY
DATE 02-24-05
CH BY
PAGE 1 OF 1
SCALE 1 : 6
FOR USE ON P8/4100/8
SIZE A
DWG NO. A44/4000/87
REV.
Vulcan
ELECTRIC COMPANY
PORTER, MAINE 04068
THIS IS A C.A.D. DRAWING. ALL CHANGES TO DRAWING MUST BE DONE ON C.A.D.

B.2 Plate and Frame Cold Heat Exchanger by Tranter

Drawing provided by Tranter PHE [58].

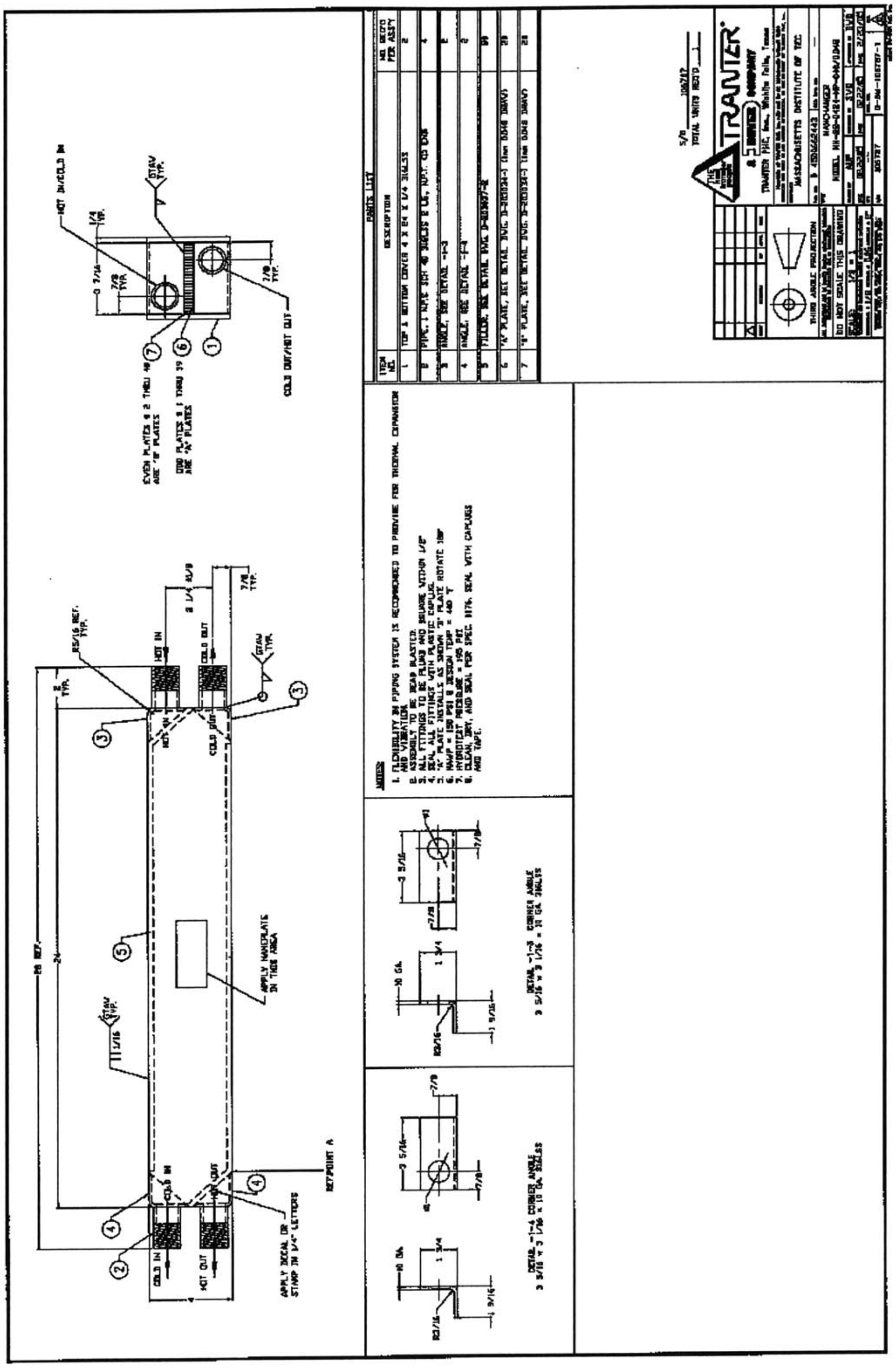

B.3 Mixing Valve Whole Assembly Specifications

From the Warren Controls Webpage:
http://www.warrencontrols.com/html/pdf/2800ProductSpec.pdf

Component 2820		Dimension (IN) by Valve Size (IN)		
Variable		1/2, 3/4, 1	1-1/4 & 1-1/2	2
A	250THD	4-7/8	5-3/4	6-1/2
	300THD	5	6-1/8	6-1/2
B	250THD	2-3/4	3-1/4	3-5/8
	300THD	3	3-1/2	3-7/8
C	DL49 Direct*	15-1/4	15-7/8	16-1/8
	DL49 Reverse	14-5/8	15-1/4	15-1/2
	DL84 Direct*	19-1/4	19-7/8	20-1/8
	DL84 or 84XR Reverse	18-5/8	19-1/4	19-1/2
H	DL49	1-3/4	2-3/8	2-3/4
(W/760)	DL84 or 84XR	3-5/8	4-1/4	4-1/2
Item		**Weight (LB) by Valve Size (IN)**		
Variable		1/2, 3/4, 1	1-1/4 & 1-1/2	2
	250THD	8-1/2	14-1/2	18-1/2
	300THD	8	15-1/2	19

Component 2830		Dimension (IN) by Valve Size (IN)		
Variable		1/2, 3/4, 1	1-1/4 & 1-1/2	2
A	250THD	4-7/8	5-3/4	6-1/2
	300THD	5	6-1/8	6-1/2
B	250THD	2-3/4	3-3/4	4
	300THD	2-3/4	3-3/8	3-3/4
C	DL49 Direct*	15-1/4	15-7/8	16-1/8
	DL84 or 84XR Direct*	N/A	19-7/8	20-1/8
H	DL49	1-3/4	2-3/8	2-3/4
(W/760)	DL84 or 84XR	N/A	4-1/4	4-1/2
Item		**Weight (LB) by Valve Size (IN)**		
Variable		1/2, 3/4, 1	1-1/4 & 1-1/2	2
	250THD	9	15-1/2	20
	300THD	8	15	18-1/2

Component 2832		Dimension (IN) by Valve Size (IN)		
Variable		1	1-1/2	2
A	250THD	4-7/8	5-3/4	6-1/2
	300THD	5	6-1/8	6-1/2
B	250THD	3-1/2	3-3/4	4
	300THD	2-3/4	3-3/8	3-3/4
C	DL49 Direct*	15-1/4	15-7/8	16-1/8
	DL84 Direct*	19-1/4	19-7/8	20-1/8
H	DL49	1-3/4	2-3/8	2-3/4
(W/760)	DL84	3-5/8	4-1/4	4-1/2
Item		**Weight (LB) by Valve Size (IN)**		
Variable		1	1-1/2	2
	250THD	9	16-1/2	21
	300THD	8	15	18-1/2

* Includes 1-3/8 inch for air fitting
H = Centerline of pipe to bottom of positioner
CF = Consult factory
N/A = Not Available

Allow 4-7/8 inch clearance above actuator for removal.

Actual shipping weights may vary.

Consult factory for drawings, weights, and dimensions of configurations not shown.

Face to face dimensions conform to historical Warren Controls standard and are NOT ANSI/ISA compatible.

Actuator	Weight (LB)
DL49	24-1/2
DL84 84XR	48-1/2

Positioner	Weight (LB)
760	10

Dimension (IN)		
D	DL49	11
	DL84 or 84XR	13-7/8
Radius	DL49	7-7/8
(W/760)	DL84 or 84XR	8-1/8

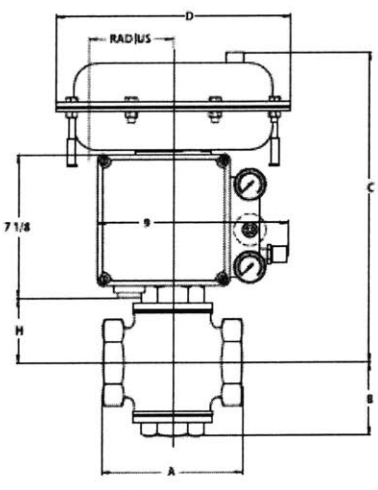

2-WAY or 3-Way
w/DL49 & 760 Positioner

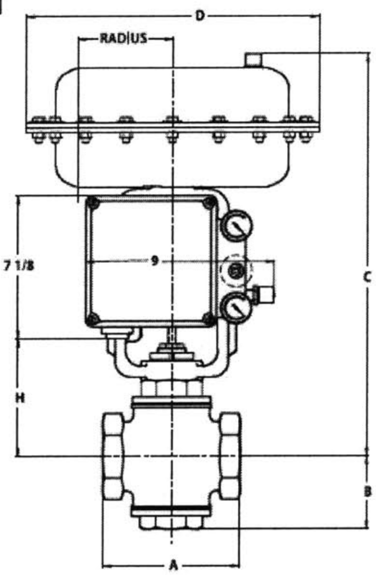

2-WAY or 3-Way
w/DL84 or 84XR & 760 Positioner

RADIUS is from centerline of actuator to outside edge of positioner.

Positioner Removal Clearance
Allow 3-1/4 inch beyond 760 for cover removal/service.

B.4 Valve Positioner Series 760E

From the Siemens Webpage:
http://www.sea.siemens.com/instrbu/docs/pdf/sd760r4.pdf

	760P Pneumatic Positioner	**Common ***	**760E Electro/Pneumatic Positioner**
Temperature Range		-40 to 85°C	
Ingress		NEMA 4X, IP65	
Connections		Pneumatic - 1/4" NPT Gauge - 1/8" NPT Electrical - 3/4" NPT, - M25 (optional) Exhaust - 1/4" NPT	
Finish		Epoxy/Polyester powder coat	
Output Configuration		Single or double acting	
Action		Direct or reverse	
Supply Pressure		150 psig max.	
Air Consumption	0.5 scfm (typical)		0.6 scfm (typical)
Flow Capacity Standard Spool		9 scfm (Cv = 0.3)	
Flow Capacity High Flow Spool		18 scfm (Cv = 0.6) Supply (1/2 pressure gain of std.)	
Flow Capacity Lo Flow Spool		9 scfm (Cv = 0.3) Supply	
Input Signal	3-15 psig, 3-27 psig	Up to 50% Split range	4-20 mA
Feedback Signal		90 degree rotary standard 1/2" to 6" rectilinear optional	
Feedback Configuration		Cam characterization	
Pressure Gain		160 %/% @ 60 psig supply std. (800 psi/psi)	
Span		Adjustable -60 to +25% of normal span	
Zero		Adjustable -10 to +60% of normal span	
Linearity (Independent)	0.5% of normal span (typical)		0.75% of normal span (typical)
Hysteresis	0.75% of normal span (typical)		1.0% of normal span (typical)
Deadband		Less than 0.25% of span	
Repeatability		Within 0.5% valve travel	
Supply Pressure Effect		Less than 0.2% valve travel for a 5 psig change in supply pressure	

B.5 Roper 3711 Positive Displacement Pump

From Roper Pumps 3600 Series Manual

SERIES: 3611, 3711, 4611, 4711
GRAPH 1
THEORETICAL GPM

ACTUAL DELIVERY IN GPM [l/min] = GRAPH 1 - GRAPH 2

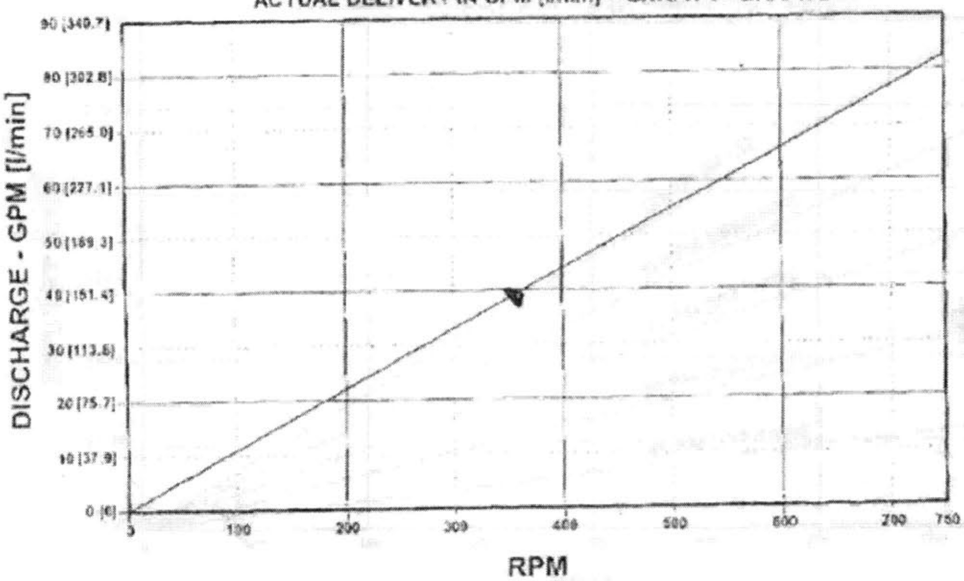

SERIES: 3611, 4611, 3711, 4711
GRAPH 3
INPUT HORSEPOWER

TOTAL INPUT HORSEPOWER [kW] = GRAPH 3 + GRAPH 4

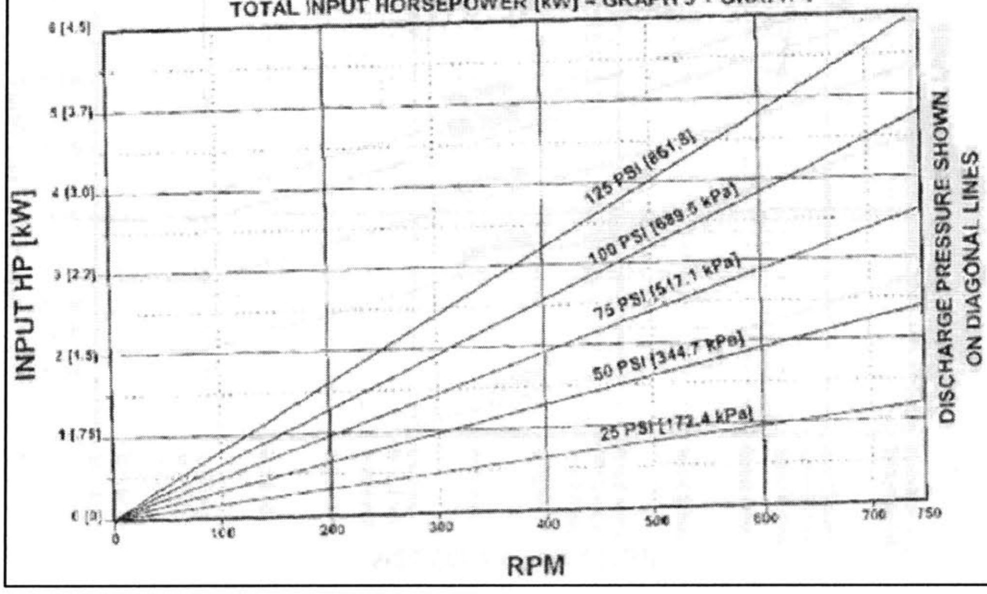

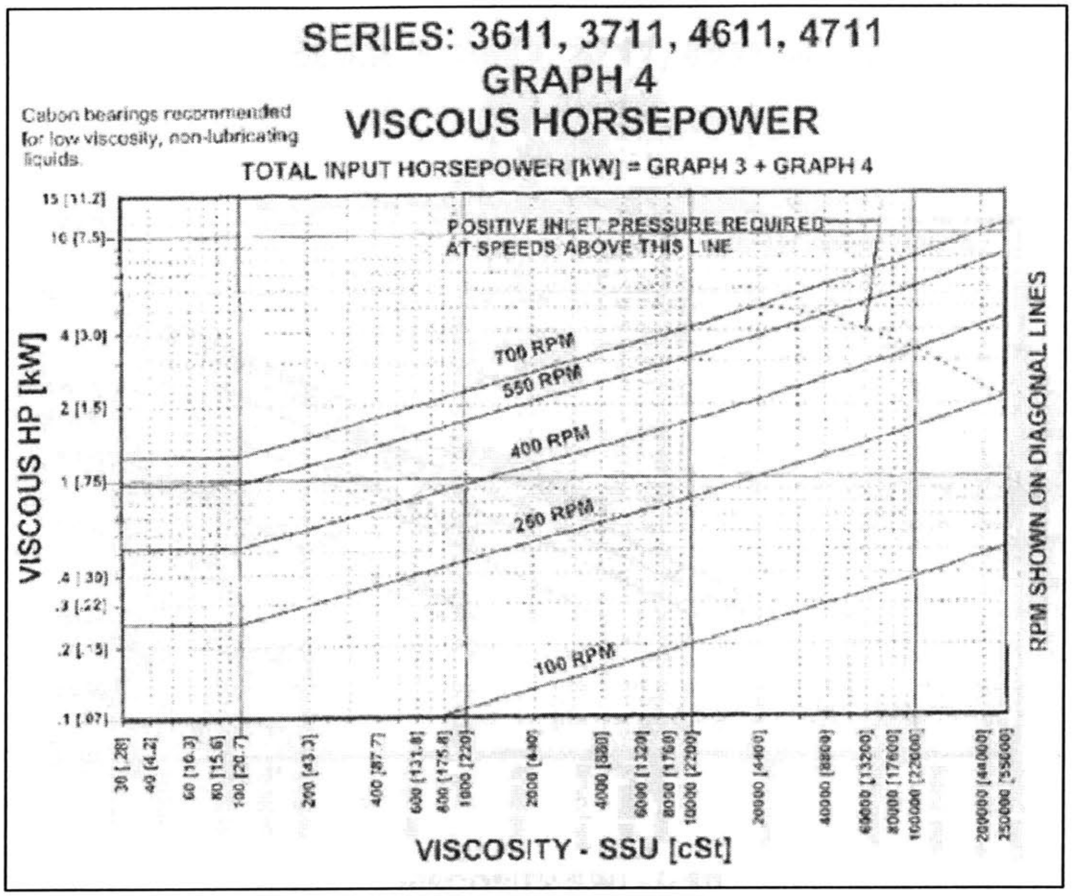
SERIES: 3611, 3711, 4611, 4711
GRAPH 4
VISCOUS HORSEPOWER
Cabon bearings recommended for low viscosity, non-lubricating liquids.
TOTAL INPUT HORSEPOWER [kW] = GRAPH 3 + GRAPH 4
POSITIVE INLET PRESSURE REQUIRED AT SPEEDS ABOVE THIS LINE
700 RPM
550 RPM
400 RPM
250 RPM
100 RPM
VISCOUS HP [kW]
RPM SHOWN ON DIAGONAL LINES
VISCOSITY - SSU [cSt]

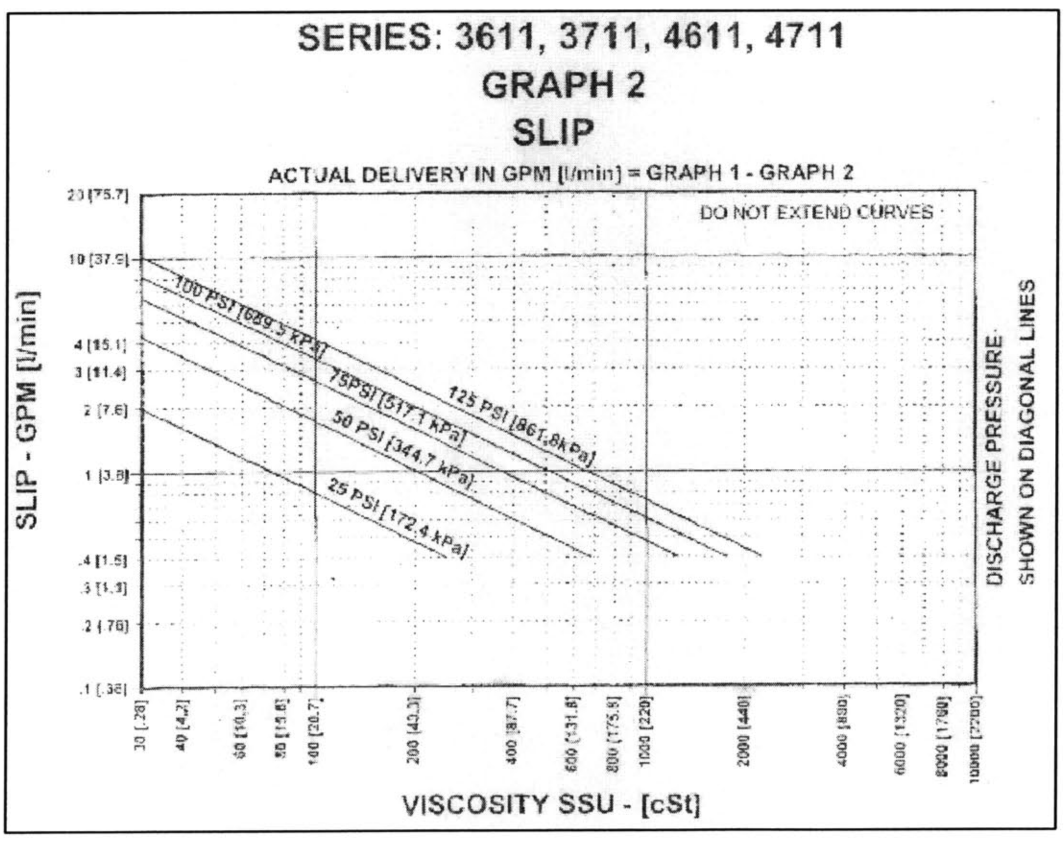
SERIES: 3611, 3711, 4611, 4711
GRAPH 2
SLIP
ACTUAL DELIVERY IN GPM [l/min] = GRAPH 1 - GRAPH 2
DO NOT EXTEND CURVES
100 PSI [689.5 kPa]
125 PSI [861.8 kPa]
75PSI [517.1 kPa]
50 PSI [344.7 kPa]
25 PSI [172.4 kPa]
SLIP - GPM [l/min]
DISCHARGE PRESSURE
SHOWN ON DIAGONAL LINES
VISCOSITY SSU - [cSt]

C Fluid Flow Model MATLAB Code

C.1 Main File

This is the most up-to-date fluid flow model for the system. It includes the following components: mixing valves, platens, hot heat exchanger, cold heat exchanger, pipes, pipe fittings, y-strainer, flow meters, and pump.

```
global t
global interval
global finalt
global PumpPressure

interval=1000;
finalt=40;
count=1;
len=linspace(0,finalt,interval);
Z=zeros(size(len));

%initialize vectors for mixing valve 1
Pout1o=Z;Qout1o=Z;Tout1o=Z;percent1o=Z;
%initialize vectors for mixing valve 2
Pout2o=Z;Qout2o=Z;Tout2o=Z;percent2o=Z;

%initialize vectors for platen2 output 1
Pout11ao=Z;Qout11ao=Z;Tout11ao=Z;Tsout11ao=Z;
%initialize vectors for platen2 output 2
Pout11bo=Z;Qout11bo=Z;Tout11bo=Z;Tsout11bo=Z;

%initialize vectors for other pipeTcombine1 output 1
Pout15o=Z;Qout15o=Z;Tout15o=Z;

%initialize vectors for pump1 output
Pout25o=Z;Qout25o=Z;Tout25o=Z;Pdiffo=Z;

%initialize vectors for PipeTSeparate1 output
Pout27ao=Z;Qout27ao=Z;Tout27ao=Z;Pout27bo=Z;Qout27bo=Z;Tout27bo=Z;

%initialize vectors for coldhex_new output
Pout30bo=Z;Qout30bo=Z;Tout30bo=Z;

%initialize vectors for hotwatt output
Pout30ao=Z;Qout30ao=Z;Tout30ao=Z;
```

```
%initialize vectors for PipeTSeparate2 output
Pout37a1o=Z;Qout37a1o=Z;Tout37a1o=Z;Pout37a2o=Z;Qout37a2o=Z;Tout37a2o=Z;
%initialize vectors for PipeTSeparate2c output
Pout34b1o=Z;Qout34b1o=Z;Tout34b1o=Z;Pout34b2o=Z;Qout34b2o=Z;Tout34b2o=Z;

%User defined parameters
Q=0.0025236; %Volumetric flow rate defined at Temperature=T
PumpPressure=5e5; %Initial Condition on the pump output pressure
Tdesired=170; %Temperature desired into Platen 1
Tdesired2=170; %Temperature desired into Platen 2
T=25; %Temperature at which the volumetric flow rate Q is defined
Tsinitial=25; %Initial temperature of the platens

for t=1:length(len)
   t=t-1;
   if t==0

%MIXING VALVE SECTION-----------------------------------------------------------------------
--------%
%Setting Initial conditions for the mixing valve 1
   Th1=180; Ti1=Tdesired; Tc1=25; percent1=0;
   %Setting the inital condition for the flow rate through platen 1 as half the mass flow
rate into
   %the system
   [rho,mu,cp,k]=props(T);
   [rho1,mu1,cp1,k1]=props(Ti1);
   Qi1=(Q*rho)/rho1/2;
   [Qh1,Qc1]=tempratios(Ti1,Qi1,Th1,Tc1);
   Ph1=0;
   Pc1=0;
%Executing the mixing valve 1
   [Pout1,Qout1,Tout1,percent1] =
valve_mixing(Qi1,Ti1,Ph1,Qh1,Th1,Pc1,Qc1,Tc1,percent1);

%Setting Initial conditions for the mixing valve 2
   Th2=180; Ti2=Tdesired2; Tc2=25; percent2=0;
   %Setting the inital condition for the flow rate through platen 1 as half the mass flow
rate into
   %the system
   [rho,mu,cp,k]=props(T);
   [rho2,mu2,cp2,k2]=props(Ti2);
   Qi2=(Q*rho)/rho2/2;
   [Qh2,Qc2]=tempratios(Ti2,Qi2,Th2,Tc2);
   Ph2=0;
   Pc2=0;
%Executing the mixing valve 2
```

```
  [Pout2,Qout2,Tout2,percent2] =
valve_mixing(Qi2,Ti2,Ph2,Qh2,Th2,Pc2,Qc2,Tc2,percent2);

%Executing the Pipe1 file after mixing valve 1 (User can define the diameter and length
of the pipe)
  [Pout3a,Qout3a,Tout3a] = Pipe1(Pout1, Qout1, Tout1, 0.3125, 0.5);

%Executing the fittings file after mixing valve 1 for an expansion in area
  [Pout4a,Qout4a,Tout4a] = fittings(Pout3a, Qout3a, Tout3a,11,0.5,1);

%Executing the flowmeter file after the expansion in area
  [Pout5a,Qout5a,Tout5a] = flowmeter(Pout4a,Qout4a,Tout4a);

%Executing the fittings file after mixing valve 1 for a reduction in area
  [Pout6a,Qout6a,Tout6a] = fittings(Pout5a,Qout5a,Tout5a,1,1,0.75);

%Executing the Pipe1 file after mixing valve 1 (User can define the diameter and length
of the pipe)
  [Pout7a,Qout7a,Tout7a] = Pipe1(Pout6a,Qout6a,Tout6a, 0.375,0.75);

%Executing the fittings file after mixing valve 1 for an expansion in area
  [Pout8a,Qout8a,Tout8a] = fittings(Pout7a,Qout7a,Tout7a,11,0.75,1.25);

%Executing the fittings file after mixing valve 1 for  a 90 degree turn
  [Pout9a,Qout9a,Tout9a] = fittings(Pout8a,Qout8a,Tout8a,2,1.25,1.25);

%Executing the Pipe1 file after mixing valve 1 (User can define the diameter and length
of the pipe)
  [Pout10a,Qout10a,Tout10a] = Pipe1(Pout9a,Qout9a,Tout9a,2,1.25);

%Executing the Pipe1 file after mixing valve 2 (User can define the diameter and length
of the pipe)
  [Pout3b,Qout3b,Tout3b] = Pipe1(Pout2, Qout2, Tout2, 0.3125, 0.5);

%Executing the fittings file after mixing valve 2 for an expansion in area
  [Pout4b,Qout4b,Tout4b] = fittings(Pout3b, Qout3b, Tout3b,11,0.5,1);

%Executing the flowmeter file after the expansion in area
  [Pout5b,Qout5b,Tout5b] = flowmeter(Pout4b,Qout4b,Tout4b);

%Executing the fittings file after mixing valve 21 for a reduction in area
  [Pout6b,Qout6b,Tout6b] = fittings(Pout5b,Qout5b,Tout5b,1,1,0.75);

%Executing the Pipe1 file after mixing valve 2 (User can define the diameter and length
of the pipe)
  [Pout7b,Qout7b,Tout7b] = Pipe1(Pout6b,Qout6b,Tout6b, 0.375,0.75);
```

```
%Executing the fittings file after mixing valve 2 for an expansion in area
   [Pout8b,Qout8b,Tout8b] = fittings(Pout7b,Qout7b,Tout7b,11,0.75,1.25);

%Executing the fittings file after mixing valve 2 for  a 90 degree turn
   [Pout9b,Qout9b,Tout9b] = fittings(Pout8b,Qout8b,Tout8b,2,1.25,1.25);

%Executing the Pipe1 file after mixing valve 2 (User can define the diameter and length
of the pipe)
   [Pout10b,Qout10b,Tout10b] = Pipe1(Pout9b,Qout9b,Tout9b,2,1.25);
%-------------------------------------------------------------------------------------------%



%PLATEN SECTION------------------------------------------------------------------------------
----%
%Executing the Platen 1 (User can define the initial platen temperature)
%(Assumption: same for both platens)
   [Pout11a,Qout11a,Tout11a,Tsout11a] = platen2(Pout10a,Qout10a,Tout10a, Tsinitial);

%Executing the Platen 2 (User can define the initial platen temperature)
%(Assumption: same for both platens)
   [Pout11b,Qout11b,Tout11b,Tsout11b] = platen2(Pout10b,Qout10b,Tout10b, Tsinitial);

%Executing the Pipe1 file after the Platen 1 (User can define the diameter and length of
the pipe)
   [Pout12a,Qout12a,Tout12a] = Pipe1(Pout11a,Qout11a,Tout11a, 2.66, 1.25);

%Executing the fittings file after the Platen 1 for a Long Radius 90 degree elbow
   [Pout13a,Qout13a,Tout13a] = fittings(Pout12a,Qout12a,Tout12a,3,1.25,1.25);

%Executing the fittings file after the Platen 1 for a reduction in area
   [Pout14a,Qout14a,Tout14a] = fittings(Pout13a,Qout13a,Tout13a,1,1.25,1);

%Executing the fittings file after the Platen 1 for a 45 degree elbow
   [Pout15a,Qout15a,Tout15a] = fittings(Pout14a,Qout14a,Tout14a,4,1,1);

%Executing the Pipe1 file after the Platen 2 (User can define the diameter and length of
the pipe)
   [Pout12b,Qout12b,Tout12b] = Pipe1(Pout11b,Qout11b,Tout11b, 2.66, 1.25);

%Executing the fittings file after the Platen 2 for a Long Radius 90 degree elbow
   [Pout13b,Qout13b,Tout13b] = fittings(Pout12b,Qout12b,Tout12b,3,1.25,1.25);

%Executing the fittings file after the Platen 2 for a reduction in area
```

```
   [Pout14b,Qout14b,Tout14b] = fittings(Pout13b,Qout13b,Tout13b,1,1.25,1);

%Executing the fittings file after the Platen 2 for a 45 degree elbow
   [Pout15b,Qout15b,Tout15b] = fittings(Pout14b,Qout14b,Tout14b,4,1,1);
%--------------------------------------------------------------------------------------------------%



%PIPETCOMBINE1 SECTION-----------------------------------------------------------------
---------%
%Executing the PipeTCombine1 bringing the two pipes together after the platens
%(User can define the diameter entering the PipeTCombine1)
   [Pout15,Qout15,Tout15] = PipeTCombine1(Pout15a,Qout15a,Tout15a,
Pout15b,Qout15b,Tout15b, 1);

%Executing the Pipe1 file after the PipeTCombine1 bringing the two pipes together after
the platens
%(User can define the diameter and length of the pipe)
   [Pout16,Qout16,Tout16] = Pipe1(Pout15,Qout15,Tout15,0.5,1);

%Executing the fittings file for an expansion in area
   [Pout17,Qout17,Tout17] = fittings(Pout16,Qout16,Tout16,11,1,2);

%Executing the Pipe1 file after the PipeTCombine1 bringing the two pipes together after
the platens
%(User can define the diameter and length of the pipe)
   [Pout18,Qout18,Tout18] = Pipe1(Pout17,Qout17,Tout17,5.5,2);

%Executing the fittings file after for a 90 degree elbow
   [Pout19,Qout19,Tout19] = fittings(Pout18,Qout18,Tout18,2,2,2);

%Executing the Pipe1 file after the PipeTCombine1 bringing the two pipes together after
the platens
%(User can define the diameter and length of the pipe)
   [Pout20,Qout20,Tout20] = Pipe1(Pout19,Qout19,Tout19,0.5,2);

%Executing the fittings file after for a 90 degree elbow
   [Pout21,Qout21,Tout21] = fittings(Pout20,Qout20,Tout20,2,2,2);
%--------------------------------------------------------------------------------------------------%



%Y-STRAINER SECTION---------------------------------------------------------------------
------%
%Executing the ystrain file after the pipe
   [Pout22,Qout22,Tout22] = ystrain(Pout21,Qout21,Tout21);
```

```
%Executing the fittings file after for a 90 degree elbow
   [Pout23,Qout23,Tout23] = fittings(Pout22,Qout22,Tout22,2,2,2);

%Executing the Pipe1 file
%(User can define the diameter and length of the pipe)
   [Pout24,Qout24,Tout24] = Pipe1(Pout23,Qout23,Tout23,0.7,2);
%-----------------------------------------------------------------------------------------------%


%PUMP SECTION-----------------------------------------------------------------------------------
---%
%Executing the Pump (User can define the flowrate desired at T=25C)
   [Pout25,Qout25,Tout25,Pdiff] = Pump1(Pout24,Qout24,Tout24);

%Executing the Pipe1 file after the Pump (User can define the diameter and length of the
pipe)
   [Pout26,Qout26,Tout26] = Pipe1(Pout25,Qout25,Tout25,1.7,2);

%Executing the fittings file after for a 90 degree elbow
   [Pout27,Qout27,Tout27] = fittings(Pout26,Qout26,Tout26,2,2,2);
%-----------------------------------------------------------------------------------------------%


%PIPETSEPARATE1 FILE----------------------------------------------------------------------------
------%
%Executing the PipeTSeparate1 (User can define the diameter entering the
PipeTSeparate1)
   [Pout27a,Qout27a,Tout27a,Pout27b,Qout27b,Tout27b] =
PipeTSeparate1(Pout27,Qout27,Tout27,Qh1,Th1,Qh2,Th2,2);

%Executing the Hot Pipe1 file after the PipeTSeparate1 (User can define the diameter
and length of the pipe)
   [Pout28a,Qout28a,Tout28a] = Pipe1(Pout27a,Qout27a,Tout27a,2,2);

%Executing the fittings file after the Hot Pipe1 file for an expansion in area
   [Pout29a,Qout29a,Tout29a] = fittings(Pout28a,Qout28a,Tout28a,11,2,2.5);

%Executing the Cold Pipe1 file after the PipeTSeparate1 (User can define the diameter
and length of the pipe)
   [Pout28b,Qout28b,Tout28b] = Pipe1(Pout27b,Qout27b,Tout27b,2,2);

%Executing the fittings file after the Cold Pipe1 file for a reduction in area
   [Pout29b,Qout29b,Tout29b] = fittings(Pout28b,Qout28b,Tout28b,1,2,1);
%-----------------------------------------------------------------------------------------------%
```

%HOT AND COLD HEAT EXCHANGER FILES---
--------------------%

```
%Executing the cold heat exchanger
   [Pout30b,Qout30b,Tout30b] = coldhex_new(Pout29b,Qout29b,Tout29b);

%Executing the hot heat exchanger
   [Pout30a,Qout30a,Tout30a] = hotwatt(Pout29a,Qout29a,Tout29a);

%Executing the fittings file after the Hot Pipe1 file for a reduction in area
   [Pout31a,Qout31a,Tout31a] = fittings(Pout30a,Qout30a,Tout30a,1,2.5,2);

%Executing the Pipe1 file hot heat exchanger (User can define the diameter and length of
the pipe)
   [Pout32a,Qout32a,Tout32a] = Pipe1(Pout31a,Qout31a,Tout31a,0.75,2);

%Executing the fittings file after the Hot Pipe1 file for a 90 degree elbow
   [Pout33a,Qout33a,Tout33a] = fittings(Pout32a,Qout32a,Tout32a,2,2,2);

%Executing the fittings file after the Hot Pipe1 file for a 45 degree elbow
   [Pout37a,Qout37a,Tout37a] = fittings(Pout33a,Qout33a,Tout33a,4,2,2);

%Executing the fittings file after the Cold Pipe1 file for a 90 degree elbow
   [Pout31b,Qout31b,Tout31b] = fittings(Pout30b,Qout30b,Tout30b,2,1,1);

%Executing the fittings file after the Cold Pipe1 file for a reduction in area
   [Pout32b,Qout32b,Tout32b] = fittings(Pout31b,Qout31b,Tout31b,1,1,0.75);

%Executing the Pipe1 file cold heat exchanger (User can define the diameter and length
of the pipe)
   [Pout33b,Qout33b,Tout33b] = Pipe1(Pout32b,Qout32b,Tout32b,0.6,0.75);

%Executing the fittings file after the Cold Pipe1 file for an expansion in area
   [Pout34b,Qout34b,Tout34b] = fittings(Pout33b,Qout33b,Tout33b,11,0.75,1);

%Executing the fittings file after the Cold Pipe1 file for a 45 degree elbow
   [Pout35b,Qout35b,Tout35b] = fittings(Pout34b,Qout34b,Tout34b,4,1,1);
%------------------------------------------------------------------------------------%


%PIPETSEPARATE2--------------------------------------------------------------%
%Executing the PipeTSeparate2 Hot (User can define the diameter entering the
PipeTSeparate2)
%(User can define the diameter entering the PipeTSeparate2)
```

```
   [Pout37a1,Qout37a1,Tout37a1,Pout37a2,Qout37a2,Tout37a2] =
PipeTSeparate2(Pout37a,Qout37a,Tout37a,Qh1,Qh2,2);

%Executing the PipeTSeparate2 Cold (User can define the diameter entering the
PipeTSeparate2)
%(User can define the diameter entering the PipeTSeparate2)
   [Pout34b1,Qout34b1,Tout34b1,Pout34b2,Qout34b2,Tout34b2] =
PipeTSeparate2(Pout35b,Qout35b,Tout35b,Qc1,Qc2,1);

%Executing the Pipe1 file before mixing valve 1 hot (User can define the diameter and
length of the pipe)
   [Pout38a1,Qout38a1,Tout38a1] = Pipe1(Pout37a1,Qout37a1,Tout37a1,1,2);

%Executing the Pipe1 file before mixing valve 2 hot (User can define the diameter and
length of the pipe)
   [Pout38a2,Qout38a2,Tout38a2] = Pipe1(Pout37a2,Qout37a2,Tout37a2,1,2);

%Executing the fittings file after the Hot Pipe1 file for a reduction in area
   [Pout39a1,Qout39a1,Tout39a1] = fittings(Pout38a1,Qout38a1,Tout38a1,1,2,0.5);

%Executing the fittings file after the Hot Pipe2 file for a reduction in area
   [Pout39a2,Qout39a2,Tout39a2] = fittings(Pout38a2,Qout38a2,Tout38a2,1,2,0.5);

%Executing the Pipe1 file before mixing valve 1 cold (User can define the diameter and
length of the pipe)
   [Pout35b1,Qout35b1,Tout35b1] = Pipe1(Pout34b1,Qout34b1,Tout34b1,1,1);

%Executing the Pipe1 file before mixing valve 2 cold (User can define the diameter and
length of the pipe)
   [Pout35b2,Qout35b2,Tout35b2] = Pipe1(Pout34b2,Qout34b2,Tout34b2,1,1);

%Executing the fittings file after the Cold Pipe1 file for a reduction in area
   [Pout36b1,Qout36b1,Tout36b1] = fittings(Pout35b1,Qout35b1,Tout35b1,1,1,0.5);

%Executing the fittings file after the Cold Pipe2 file for a reduction in area
   [Pout36b2,Qout36b2,Tout36b2] = fittings(Pout35b2,Qout35b2,Tout35b2,1,1,0.5);
%---------------------------------------------------------------------------------------------%

else

%MIXING VALVE SECTION------------------------------------------------------------------
--------%

%Setting desired conditions for the mixing valve 1
   percent1=percent1;
%Executing the mixing valve 1
```

```
  [Pout1,Qout1,Tout1,percent1] =
valve_mixing(Qi1,Ti1,Pout39a1,Qout39a1,Tout39a1,Pout36b1,Qout36b1,Tout36b1,perc
ent1);

%Setting desired conditions for the mixing valve 2
  percent2=percent2;
%Executing the mixing valve 2
  [Pout2,Qout2,Tout2,percent2] =
valve_mixing(Qi2,Ti2,Pout39a2,Qout39a2,Tout39a2,Pout36b2,Qout36b2,Tout36b2,perc
ent2);

%Executing the Pipe1 file after mixing valve 1 (User can define the diameter and length
of the pipe)
  [Pout3a,Qout3a,Tout3a] = Pipe1(Pout1, Qout1, Tout1, 0.3125, 0.5);

%Executing the fittings file after mixing valve 1 for an expansion in area
  [Pout4a,Qout4a,Tout4a] = fittings(Pout3a, Qout3a, Tout3a,11,0.5,1);

%Executing the flowmeter file after the expansion in area
  [Pout5a,Qout5a,Tout5a] = flowmeter(Pout4a,Qout4a,Tout4a);

%Executing the fittings file after mixing valve 1 for a reduction in area
  [Pout6a,Qout6a,Tout6a] = fittings(Pout5a,Qout5a,Tout5a,1,1,0.75);

%Executing the Pipe1 file after mixing valve 1 (User can define the diameter and length
of the pipe)
  [Pout7a,Qout7a,Tout7a] = Pipe1(Pout6a,Qout6a,Tout6a, 0.375,0.75);

%Executing the fittings file after mixing valve 1 for an expansion in area
  [Pout8a,Qout8a,Tout8a] = fittings(Pout7a,Qout7a,Tout7a,11,0.75,1.25);

%Executing the fittings file after mixing valve 1 for  a 90 degree turn
  [Pout9a,Qout9a,Tout9a] = fittings(Pout8a,Qout8a,Tout8a,2,1.25,1.25);

%Executing the Pipe1 file after mixing valve 1 (User can define the diameter and length
of the pipe)
  [Pout10a,Qout10a,Tout10a] = Pipe1(Pout9a,Qout9a,Tout9a,2,1.25);

%Executing the Pipe1 file after mixing valve 2 (User can define the diameter and length
of the pipe)
  [Pout3b,Qout3b,Tout3b] = Pipe1(Pout2, Qout2, Tout2, 0.3125, 0.5);

%Executing the fittings file after mixing valve 2 for an expansion in area
  [Pout4b,Qout4b,Tout4b] = fittings(Pout3b, Qout3b, Tout3b,11,0.5,1);

%Executing the flowmeter file after the expansion in area
```

```
  [Pout5b,Qout5b,Tout5b] = flowmeter(Pout4b,Qout4b,Tout4b);

%Executing the fittings file after mixing valve 21 for a reduction in area
  [Pout6b,Qout6b,Tout6b] = fittings(Pout5b,Qout5b,Tout5b,1,1,0.75);

%Executing the Pipe1 file after mixing valve 2 (User can define the diameter and length
of the pipe)
  [Pout7b,Qout7b,Tout7b] = Pipe1(Pout6b,Qout6b,Tout6b, 0.375,0.75);

%Executing the fittings file after mixing valve 2 for an expansion in area
  [Pout8b,Qout8b,Tout8b] = fittings(Pout7b,Qout7b,Tout7b,11,0.75,1.25);

%Executing the fittings file after mixing valve 2 for  a 90 degree turn
  [Pout9b,Qout9b,Tout9b] = fittings(Pout8b,Qout8b,Tout8b,2,1.25,1.25);

%Executing the Pipe1 file after mixing valve 2 (User can define the diameter and length
of the pipe)
  [Pout10b,Qout10b,Tout10b] = Pipe1(Pout9b,Qout9b,Tout9b,2,1.25);
%-----------------------------------------------------------------------------------------------%



%PLATEN SECTION--------------------------------------------------------------------------
----%
%Executing the Platen 1 (User can define the initial platen temperature)
%(Assumption: same for both platens)
  [Pout11a,Qout11a,Tout11a,Tsout11a] = platen2(Pout10a,Qout10a,Tout10a, Tsinitial);

%Executing the Platen 2 (User can define the initial platen temperature)
%(Assumption: same for both platens)
  [Pout11b,Qout11b,Tout11b,Tsout11b] = platen2(Pout10b,Qout10b,Tout10b, Tsinitial);

%Executing the Pipe1 file after the Platen 1 (User can define the diameter and length of
the pipe)
  [Pout12a,Qout12a,Tout12a] = Pipe1(Pout11a,Qout11a,Tout11a, 2.66, 1.25);

%Executing the fittings file after the Platen 1 for a Long Radius 90 degree elbow
  [Pout13a,Qout13a,Tout13a] = fittings(Pout12a,Qout12a,Tout12a,3,1.25,1.25);

%Executing the fittings file after the Platen 1 for a reduction in area
  [Pout14a,Qout14a,Tout14a] = fittings(Pout13a,Qout13a,Tout13a,1,1.25,1);

%Executing the fittings file after the Platen 1 for a 45 degree elbow
  [Pout15a,Qout15a,Tout15a] = fittings(Pout14a,Qout14a,Tout14a,4,1,1);
```

```
%Executing the Pipe1 file after the Platen 2 (User can define the diameter and length of
the pipe)
   [Pout12b,Qout12b,Tout12b] = Pipe1(Pout11b,Qout11b,Tout11b, 2.66, 1.25);

%Executing the fittings file after the Platen 2 for a Long Radius 90 degree elbow
   [Pout13b,Qout13b,Tout13b] = fittings(Pout12b,Qout12b,Tout12b,3,1.25,1.25);

%Executing the fittings file after the Platen 2 for a reduction in area
   [Pout14b,Qout14b,Tout14b] = fittings(Pout13b,Qout13b,Tout13b,1,1.25,1);

%Executing the fittings file after the Platen 2 for a 45 degree elbow
   [Pout15b,Qout15b,Tout15b] = fittings(Pout14b,Qout14b,Tout14b,4,1,1);
%------------------------------------------------------------------------------------------%


%PIPETCOMBINE1 SECTION-----------------------------------------------------------------
---------%
%Executing the PipeTCombine1 bringing the two pipes together after the platens
%(User can define the diameter entering the PipeTCombine1)
   [Pout15,Qout15,Tout15] = PipeTCombine1(Pout15a,Qout15a,Tout15a,
Pout15b,Qout15b,Tout15b, 1);

%Executing the Pipe1 file after the PipeTCombine1 bringing the two pipes together after
the platens
%(User can define the diameter and length of the pipe)
   [Pout16,Qout16,Tout16] = Pipe1(Pout15,Qout15,Tout15,0.5,1);

%Executing the fittings file for an expansion in area
   [Pout17,Qout17,Tout17] = fittings(Pout16,Qout16,Tout16,11,1,2);

%Executing the Pipe1 file after the PipeTCombine1 bringing the two pipes together after
the platens
%(User can define the diameter and length of the pipe)
   [Pout18,Qout18,Tout18] = Pipe1(Pout17,Qout17,Tout17,5.5,2);

%Executing the fittings file after for a 90 degree elbow
   [Pout19,Qout19,Tout19] = fittings(Pout18,Qout18,Tout18,2,2,2);

%Executing the Pipe1 file after the PipeTCombine1 bringing the two pipes together after
the platens
%(User can define the diameter and length of the pipe)
   [Pout20,Qout20,Tout20] = Pipe1(Pout19,Qout19,Tout19,0.5,2);

%Executing the fittings file after for a 90 degree elbow
   [Pout21,Qout21,Tout21] = fittings(Pout20,Qout20,Tout20,2,2,2);
```

```
%-----------------------------------------------------------------------------------------------------%


%Y-STRAINER SECTION--------------------------------------------------------------------------------
------%
%Executing the ystrain file after the pipe
  [Pout22,Qout22,Tout22] = ystrain(Pout21,Qout21,Tout21);

%Executing the fittings file after for a 90 degree elbow
  [Pout23,Qout23,Tout23] = fittings(Pout22,Qout22,Tout22,2,2,2);

%Executing the Pipe1 file
%(User can define the diameter and length of the pipe)
  [Pout24,Qout24,Tout24] = Pipe1(Pout23,Qout23,Tout23,0.7,2);
%-----------------------------------------------------------------------------------------------------%


%PUMP SECTION----------------------------------------------------------------------------------------
---%
%Executing the Pump (User can define the flowrate desired at T=25C)
  [Pout25,Qout25,Tout25,Pdiff] = Pump1(Pout24,Qout24,Tout24);

%Executing the Pipe1 file after the Pump (User can define the diameter and length of the
pipe)
  [Pout26,Qout26,Tout26] = Pipe1(Pout25,Qout25,Tout25,1.7,2);

%Executing the fittings file after for a 90 degree elbow
  [Pout27,Qout27,Tout27] = fittings(Pout26,Qout26,Tout26,2,2,2);
%-----------------------------------------------------------------------------------------------------%

%PIPETSEPARATE1 FILE-------------------------------------------------------------------------------
------%
%Executing the PipeTSeparate1 (User can define the diameter entering the
PipeTSeparate1)
  [Pout27a,Qout27a,Tout27a,Pout27b,Qout27b,Tout27b] =
PipeTSeparate1(Pout27,Qout27,Tout27,Qh1,Th1,Qh2,Th2,2);

%Executing the Hot Pipe1 file after the PipeTSeparate1 (User can define the diameter
and length of the pipe)
  [Pout28a,Qout28a,Tout28a] = Pipe1(Pout27a,Qout27a,Tout27a,2,2);

%Executing the fittings file after the Hot Pipe1 file for an expansion in area
  [Pout29a,Qout29a,Tout29a] = fittings(Pout28a,Qout28a,Tout28a,11,2,2.5);
```

%Executing the Cold Pipe1 file after the PipeTSeparate1 (User can define the diameter and length of the pipe)
[Pout28b,Qout28b,Tout28b] = Pipe1(Pout27b,Qout27b,Tout27b,2,2);

%Executing the fittings file after the Cold Pipe1 file for a reduction in area
[Pout29b,Qout29b,Tout29b] = fittings(Pout28b,Qout28b,Tout28b,1,2,1);
%---%

%HOT AND COLD HEAT EXCHANGER FILES--
---------------------%
%Executing the cold heat exchanger
[Pout30b,Qout30b,Tout30b] = coldhex_new(Pout29b,Qout29b,Tout29b);

%Executing the hot heat exchanger
[Pout30a,Qout30a,Tout30a] = hotwatt(Pout29a,Qout29a,Tout29a);

%Executing the fittings file after the Hot Pipe1 file for a reduction in area
[Pout31a,Qout31a,Tout31a] = fittings(Pout30a,Qout30a,Tout30a,1,2.5,2);

%Executing the Pipe1 file hot heat exchanger (User can define the diameter and length of the pipe)
[Pout32a,Qout32a,Tout32a] = Pipe1(Pout31a,Qout31a,Tout31a,0.75,2);

%Executing the fittings file after the Hot Pipe1 file for a 90 degree elbow
[Pout33a,Qout33a,Tout33a] = fittings(Pout32a,Qout32a,Tout32a,2,2,2);

%Executing the fittings file after the Hot Pipe1 file for a 45 degree elbow
[Pout37a,Qout37a,Tout37a] = fittings(Pout33a,Qout33a,Tout33a,4,2,2);

%Executing the fittings file after the Cold Pipe1 file for a 90 degree elbow
[Pout31b,Qout31b,Tout31b] = fittings(Pout30b,Qout30b,Tout30b,2,1,1);

%Executing the fittings file after the Cold Pipe1 file for a reduction in area
[Pout32b,Qout32b,Tout32b] = fittings(Pout31b,Qout31b,Tout31b,1,1,0.75);

%Executing the Pipe1 file cold heat exchanger (User can define the diameter and length of the pipe)
[Pout33b,Qout33b,Tout33b] = Pipe1(Pout32b,Qout32b,Tout32b,0.6,0.75);

%Executing the fittings file after the Cold Pipe1 file for an expansion in area
[Pout34b,Qout34b,Tout34b] = fittings(Pout33b,Qout33b,Tout33b,11,0.75,1);

%Executing the fittings file after the Cold Pipe1 file for a 45 degree elbow
[Pout35b,Qout35b,Tout35b] = fittings(Pout34b,Qout34b,Tout34b,4,1,1);
%---%

```
%PIPETSEPARATE2----------------------------------------------------------------%
%Executing the PipeTSeparate2 Hot (User can define the diameter entering the
PipeTSeparate2)
%(User can define the diameter entering the PipeTSeparate2)
   [Pout37a1,Qout37a1,Tout37a1,Pout37a2,Qout37a2,Tout37a2] =
PipeTSeparate2(Pout37a,Qout37a,Tout37a,Qh1,Qh2,2);

%Executing the PipeTSeparate2 Cold (User can define the diameter entering the
PipeTSeparate2)
%(User can define the diameter entering the PipeTSeparate2)
   [Pout34b1,Qout34b1,Tout34b1,Pout34b2,Qout34b2,Tout34b2] =
PipeTSeparate2(Pout35b,Qout35b,Tout35b,Qc1,Qc2,1);

%Executing the Pipe1 file before mixing valve 1 hot (User can define the diameter and
length of the pipe)
   [Pout38a1,Qout38a1,Tout38a1] = Pipe1(Pout37a1,Qout37a1,Tout37a1,1,2);

%Executing the Pipe1 file before mixing valve 2 hot (User can define the diameter and
length of the pipe)
   [Pout38a2,Qout38a2,Tout38a2] = Pipe1(Pout37a2,Qout37a2,Tout37a2,1,2);

%Executing the fittings file after the Hot Pipe1 file for a reduction in area
   [Pout39a1,Qout39a1,Tout39a1] = fittings(Pout38a1,Qout38a1,Tout38a1,1,2,0.5);

%Executing the fittings file after the Hot Pipe2 file for a reduction in area
   [Pout39a2,Qout39a2,Tout39a2] = fittings(Pout38a2,Qout38a2,Tout38a2,1,2,0.5);

%Executing the Pipe1 file before mixing valve 1 cold (User can define the diameter and
length of the pipe)
   [Pout35b1,Qout35b1,Tout35b1] = Pipe1(Pout34b1,Qout34b1,Tout34b1,1,1);

%Executing the Pipe1 file before mixing valve 2 cold (User can define the diameter and
length of the pipe)
   [Pout35b2,Qout35b2,Tout35b2] = Pipe1(Pout34b2,Qout34b2,Tout34b2,1,1);

%Executing the fittings file after the Cold Pipe1 file for a reduction in area
   [Pout36b1,Qout36b1,Tout36b1] = fittings(Pout35b1,Qout35b1,Tout35b1,1,1,0.5);

%Executing the fittings file after the Cold Pipe2 file for a reduction in area
   [Pout36b2,Qout36b2,Tout36b2] = fittings(Pout35b2,Qout35b2,Tout35b2,1,1,0.5);
%-----------------------------------------------------------------------------------------------%

end
```

```
%vectors for mixing valve output 1
Pout1o(count)=Pout1; Qout1o(count)=Qout1; Tout1o(count)=Tout1;
percent1o(count)=percent1;

%vectors for mixing valve output 1
Pout2o(count)=Pout2; Qout2o(count)=Qout2; Tout2o(count)=Tout2;
percent2o(count)=percent2;

%vectors for platen2 output 1
Pout11ao(count)=Pout11a; Qout11ao(count)=Qout11a; Tout11ao(count)=Tout11a;
Tsout11ao(count)=Tsout11a;
%vectors for platen2 output 2
Pout11bo(count)=Pout11b; Qout11bo(count)=Qout11b; Tout11bo(count)=Tout11b;
Tsout11bo(count)=Tsout11b;

%vectors for other pipeTcombine1 output
Pout15o(count)=Pout15; Qout15o(count)=Qout15; Tout15o(count)=Tout15;

%vectors for pump1 output
Pout25o(count)=Pout25; Qout25o(count)=Qout25; Tout25o(count)=Tout25;
Pdiffo(count)=Pdiff;

%vectors for PipeTSeparate1 output
Pout27ao(count)=Pout27a; Qout27ao(count)=Qout27a; Tout27ao(count)=Tout27a;
Pout27bo(count)=Pout27b; Qout27bo(count)=Qout27b; Tout27bo(count)=Tout27b;

%vectors for coldhex_new output
Pout30bo(count)=Pout30b; Qout30bo(count)=Qout30b; Tout30bo(count)=Tout30b;
%vectors for hotwatt output
Pout30ao(count)=Pout30a; Qout30ao(count)=Qout30a; Tout30ao(count)=Tout30a;

%vectors for PipeTSeparate2 output
Pout37a1o(count)=Pout37a1; Tout37a1o(count)=Tout37a1; Pout37a2o(count)=Pout37a2;
Qout37a2o(count)=Qout37a2; Tout37a2o(count)=Tout37a2;
Qout37a1o(count)=Qout37a1;
%vectors for PipeTSeparate2c output
Pout34b1o(count)=Pout34b1; Qout34b1o(count)=Qout34b1;
Tout34b1o(count)=Tout34b1; Pout34b2o(count)=Pout34b2;
Qout34b2o(count)=Qout34b2; Tout34b2o(count)=Tout34b2;

count=count+1;
end
```

```
figure(1)
title('Mixing Valve 1');
set(1,'Name','Mixing Valve 2');
subplot(4,1,1);plot(len,Pout1o);title('Mixing Valve Output 1');ylabel('Pressure
(Pa)');subplot(4,1,2);plot(len,Qout1o);ylabel('Flowrate (m^3/s)');
subplot(4,1,3);plot(len,Tout1o);ylabel('Temperature
(C)');subplot(4,1,4);plot(len,percent1o);ylabel('Valve Position (%)');

figure(2);
title('Mixing Valve 2');
set(2,'Name','Mixing Valve 2');
subplot(4,1,1);plot(len,Pout2o);title('Mixing Valve Output 2');ylabel('Pressure
(Pa)');subplot(4,1,2);plot(len,Qout2o);ylabel('Flowrate (m^3/s)');
subplot(4,1,3);plot(len,Tout2o);ylabel('Temperature
(C)');subplot(4,1,4);plot(len,percent2o);ylabel('Valve Position (%)');

figure(3)
title('Platen Output 1');
set(3,'Name','Platen Output 1');
subplot(4,1,1);plot(len,Pout11ao);title('Platen Output');ylabel('Pressure
(Pa)');subplot(4,1,2);plot(len,Qout11ao);ylabel('Flowrate (m^3/s)');
subplot(4,1,3);plot(len,Tout11ao);ylabel('Temperature
(C)');subplot(4,1,4);plot(len,Tsout11ao);ylabel('Platen Temperature (C)');


figure(4)
title('Platen Output 2');
set(4,'Name','Platen Output 2');
subplot(4,1,1);plot(len,Pout11bo);title('Platen Output');ylabel('Pressure
(Pa)');subplot(4,1,2);plot(len,Qout11bo);ylabel('Flowrate (m^3/s)');
subplot(4,1,3);plot(len,Tout11bo);ylabel('Temperature
(C)');subplot(4,1,4);plot(len,Tsout11bo);ylabel('Platen Temperature (C)');

figure(5)
title('Combining Fluid From Both Platens');
set(5,'Name','Combining Fluid From Both Platens');
subplot(3,1,1);plot(len,Pout15o);title('Combining fluid from both
platens');ylabel('Pressure (Pa)');subplot(3,1,2);plot(len,Qout15o);ylabel('Flowrate
(m^3/s)');
subplot(3,1,3);plot(len,Tout15o);ylabel('Temperature (C)');

figure(6)
title('Pump Output');
set(6,'Name','Pump Output');
subplot(4,1,1);plot(len,Pout25o);title('Pump Output');ylabel('Pressure
(Pa)');subplot(4,1,2);plot(len,Qout25o);ylabel('Flowrate (m^3/s)');
```

```
subplot(4,1,3);plot(len,Tout25o);ylabel('Temperature
(C)');subplot(4,1,4);plot(len,Pdiffo);ylabel('Pressure Head in whole system (Pa)');

figure(7)
title('Fluid Separation After The Pump');
set(7,'Name','Fluid Separation After The Pump');
subplot(6,1,1);plot(len,Pout27ao);title('Fluid separation after the
pump');ylabel('Pressure_Hot
(Pa)');subplot(6,1,2);plot(len,Qout27ao);ylabel('Flowrate_Hot (m^3/s)');
subplot(6,1,3);plot(len,Tout27ao);ylabel('Temperature_Hot
(C)');subplot(6,1,4);plot(len,Pout27bo);ylabel('Pressure_Cold (Pa)');
subplot(6,1,5);plot(len,Qout27bo);ylabel('Flowrate_Cold
(m^3/s)');subplot(6,1,6);plot(len,Tout27bo);ylabel('Temperature_Cold (C)');

figure(8)
title('Cold Heat Exchanger Output');
set(8,'Name','Cold Heat Exchanger Output');
subplot(3,1,1);plot(len,Pout30bo);title('Cold Heat Exchanger Output');ylabel('Pressure
(Pa)');subplot(3,1,2);plot(len,Qout30bo);ylabel('Flowrate (m^3/s)');
subplot(3,1,3);plot(len,Tout30bo);ylabel('Temperature (C)');

figure(9)
title('Hot Heat Exchanger Output');
set(9,'Name','Hot Heat Exchanger Output');
subplot(3,1,1);plot(len,Pout30ao);title('Hot Heat Exchanger Output');ylabel('Pressure
(Pa)');subplot(3,1,2);plot(len,Qout30ao);ylabel('Flowrate (m^3/s)');
subplot(3,1,3);plot(len,Tout30ao);ylabel('Temperature (C)');

figure(10)
title('Separate Hot Fluid');
set(10,'Name','Separate Cold Fluid');
subplot(6,1,1);plot(len,Pout37a1o);title('Separate Hot Fluid');ylabel('Pressure1
(Pa)');subplot(6,1,2);plot(len,Qout37a1o);ylabel('Flowrate2 (m^3/s)');
subplot(6,1,3);plot(len,Tout37a1o);ylabel('Temperature1
(C)');subplot(6,1,4);plot(len,Pout37a2o);ylabel('Pressure2 (Pa)');
subplot(6,1,5);plot(len,Qout37a2o);ylabel('Flowrate2
(m^3/s)');subplot(6,1,6);plot(len,Tout37a2o);ylabel('Temperature2 (C)');

figure(11)
title('Separate Cold Fluid');
set(11,'Name','Separate Cold Fluid');
subplot(6,1,1);plot(len,Pout34b1o);title('Separate Cold Fluid');ylabel('Pressure1
(Pa)');subplot(6,1,2);plot(len,Qout34b1o);ylabel('Flowrate1 (m^3/s)');
subplot(6,1,3);plot(len,Tout34b1o);ylabel('Temperature1
(C)');subplot(6,1,4);plot(len,Pout34b2o);ylabel('Pressure2 (Pa)');
```

```
subplot(6,1,5);plot(len,Qout34b2o);ylabel('Flowrate2
(m^3/s)');subplot(6,1,6);plot(len,Tout34b2o);ylabel('Temperature2 (C)');
```

C.2 Paratherm Fluid Properties

This function obtains the properties of Paratherm MR given a certain fluid temperature.

```
function [rho,mu,cp,k]=props(T)
%Sets porperties of Paratherm MR at given Temp in deg C for T: 0<=T<=250
rho=-.80441*T+823.69;
mu=.001*(1.0945E-12*T^6 - 9.6662E-10*T^5 + 3.4202E-07*T^4 - 6.2338E-05*T^3 +
6.3028E-03*T^2 - 3.5758E-01*T + 1.0649E+01);
cp=2.713*T+2131.8;
k=-8.714e-5*T+.14594;
```

C.3 Calculates the Hot and Cold Flows

This function calculates the hot and cold flow rates given a specified mixed outlet flow.

```
function [Qh,Qc]=tempratios(Tp,Qp,Th,Tc)
%Calculates flowrates of hot and cold sides to produce
%desired temperature and flow, accounting for changes in props
%Qp=flowrate through platen Tp=temp of fluid to platen
%Get properties
[rhoc,muc,cpc,kc]=props(Tc);
[rhoh,muh,cph,kh]=props(Th);
[rhop,mup,cpp,kp]=props(Tp);
%Calculate flowrates
Qh=(Qp*rhop*(cpc*Tc-cpp*Tp))/(rhoh*(cpc*Tc-cph*Th));
Qc=(Qp*rhop-Qh*rhoh)/rhoc;
tempratios=[Qh,Qc];
```

C.4 Mixing Valve

This file does not assume a pressure drop across the mixing valve.

```
function [Pout,Qout,Tout,percent] = valve_mixing(Qi,Ti,Ph,Qh,Th,Pc,Qc,Tc,percent);
global t
if t==0
   [rhoc,muc,cpc,kc]=props(Tc);
   [rhoh,muh,cph,kh]=props(Th);
   Qout=Qi;
   Tout=Ti;
   [rhoi,mui,cpi,ki]=props(Ti);
   Qout=Qout/6.31667e-5;
   CV=1000;
   deltaP=(rhoi/1000)/((CV/Qout)^2);
```

```
    deltaP=deltaP*6894.75729;
    Po=min(Ph,Pc);
    Pout=Po-deltaP;
    Qout=Qout*6.31667e-5;
    percent=((rhoh*Qh)/(rhoi*Qi))*100;

% %The valve position established from the initial conditions will be used to calculate
the pressure output
% %for the proceeding time steps
else
    [rhoc,muc,cpc,kc]=props(Tc);
    [rhoh,muh,cph,kh]=props(Th);
    Qout=Qi;
    Tout=Ti;
    [rhoi,mui,cpi,ki]=props(Ti);
    Qout=Qout/6.31667e-5;
    CV=1000;
    deltaP=(rhoi/1000)/((CV/Qout)^2);
    deltaP=deltaP*6894.75729;
    Po=min(Ph,Pc);
    Pout=Po-deltaP;
    Qout=Qout*6.31667e-5;
    percent=((rhoh*Qh)/(rhoi*Qi))*100;

end
```

C.5 Straight Pipe

This function calculates the pressure drop across a straight pipe.

```
function [Po,Qo,To] = Pipe1(Pin,Qin,Tm,length,diameterin)
global t

%User Defined Parameters
D=diameterin*.0254;
L=(length*12)*.0254;

[rho,mu,cp,k]=props(Tm);

%Flow
V=Qin/((pi*D^2)/4);
mdot=Qin*rho;

%Dimensionless quantities
Re=V*D*rho/mu;
Pr=cp*mu/k;
if Re<2300
```

```
  f=64/Re;
  Nu=3.66;
else
  f=(.790*log(Re)-1.64)^-2;
  Nu=((f/8)*(Re-1000)*Pr)/(1+12.7*(f/8)^.5*(Pr^(2/3)-1));
end

%Heat transfer
h=Nu*k/D;

%Find pressure drop
Pdrop=f*(L/D)*V^2*(rho/2);

%Assign block output
Po=Pin-Pdrop;
Qo=Qin;
To=Tm;
```

C.6 Pipe Fittings

This file is called upon to calculate the pressure drops across a variety of pipe fittings, including 90° elbows, 45° elbows, tees, and ball valves.

```
function [Po,Qo,To] = fittings(Pin,Qin,Tm,type,diameterin,diameterout)

Areain=pi*(diameterin/12/2)^2;
Areaout=pi*(diameterout/12/2)^2;
AreaRatio=Areaout/Areain;
switch type
case 1
  %Pipe is being reduced from diameter_in to diameter_out
  [Kl]=loss(AreaRatio);
case 2
  %Regular elbow 90 degrees, threaded
  Kl=1.5;
case 3
  %Long radius 90 degrees, threaded
  Kl=0.7;
case 4
  %Regular 45 degrees, threaded
  Kl=0.4;
case 5
  %180 degree bend, threaded
  Kl=1.5;
case 6
  %tees line flow, threaded
  Kl=0.9;
```

```
case 7
   %branch flow, threaded
   Kl=2.0;
case 8
   %ball valve, fully open
   Kl=0.05;
case 9
   %ball valve, 1/3 closed
   Kl=5.5;
case 10
   %ball valve, 2/3 closed
   Kl=210;
case 11
   %Pipe is being expanded from diameter_in to diameter_out
   Kl=(1-(1/AreaRatio))^2;
otherwise
   error(['Unhandled type = ',num2str(Kl)]);
end

g=32.2;                        %gravity in ft/sec^2
Q1=Qin*264.172*60;             %convert flowrate to gal/min
Q=Q1*(1/60)*(.13368);          %convert flowrate to ft^3/sec
V=Q/min(Areain,Areaout);       %velocity of the outlet (ft/s)
HL=Kl*(V^2)/(2*g);             %calculates the headloss
[rho,mu,cp,k]=props(Tm);       %gets density of the fluid at given temperature
rhoe=rho*2.2*(1/35.31467);     %convert density SI to english
Pressuredrop=HL*rhoe*(.006944444); %Calculate the Pressure drop in Psi
Pdrop=Pressuredrop*6894.75729;  %converts psi to Pa
Po=Pin-Pdrop;
To=Tm;
Qo=Qin;
```

C.7 Flow Meter

This file calculates the pressure drop across the flow meter. The information is found off flow meter data sheets.

```
function [Po,Qo,To] = flowmeter(Pin,Qin,Tm)
Qo=Qin;
To=Tm;
Po=Pin-8*6894.75729 ; %A little overestimate on the pressure drop across a 1"
flowmeter
```

C.8 Platen Model

This file is provided by Matthew Dirckx.

```
function [Pout,Qout,Tout,Tsnew] = platen2(Pin, Q, Tm, Ts)
global t
global interval
global finalt

[rho,mu,cp,k]=props(Tm);
D=.003175;
L=.132588;
%Flow
V=Q/(18*pi/4*D^2);
mdot=Q*rho;
%Dimensionless quantities
Re=V*D*rho/mu;
Pr=cp*mu/k;
if Re<2300
   f=64/Re;
   Nu=3.66;
else
  f=(.790*log(Re)-1.64)^-2;
  Nu=((f/8)*(Re-1000)*Pr)/(1+12.7*(f/8)^.5*(Pr^(2/3)-1));
end
%Heat transfer
h=Nu*k/D;

Tout=(Tm-Ts)*exp(-h*(pi*D*L)/(cp*mdot))+Ts;
[rhoo,muo,cpo,ko]=props(Tout);
Qout=(Q*rho)/rhoo;

%Find pressure drop
Qi=Q/18;
vi=Qi/(((1/8)*2.54)/100)^2;
Tm;
a=[0.0079916644363O8;-15.694208783140260;-
1.866667973048096;297.997934215463720;92.787840163674872;1309.0375406340274
00;906.132950733087450;3178.791014591897200;5954.364606136258800];
Pdrop=(a(1)*Tm^4)+(a(2)*vi^4)+(a(3)*Tm^3)+(a(4)*vi^3)+(a(5)*Tm^2)+(a(6)*vi^2)+(
a(7)*Tm)+(a(8)*vi)+a(9);
% Pdrop= 0.9274400765*Tm^2 + 1371.8412623064*vi^2 -471.6624180105*Tm+
2223.5061065699*vi +30874.9913112640

%Pdrop=f*L/D*V^2*rho/2;
Pout=Pin-Pdrop;

%Platen convective area
ConvA=L*pi*D*18;
```

```
%Power gain/loss from the fluid to the platens (W)
Q=h*ConvA*(Tm-Ts);
TMp=1000;

%Rate of change of Ts (degrees C/sec)
dTs=Q/TMp;

Tsnew=Ts+dTs*((finalt-1)/(interval-1));
```

C.9 Combining Flows

This file calculates the result of two flows combining into one.

```
function [Po,Qo,To] = PipeTCombine1(Ph, Qh, Th, Pc, Qc, Tc, diameterin)
global t

[rhoh,muh,cph,kh]=props(Th);
[rhoc,muc,cpc,kc]=props(Tc);

%User Defined Parameters
Di=diameterin*.0254;

%Assigns the output temperatures (same as the input)
rhoo=((rhoc*Qc)/(rhoc*Qc+rhoh*Qh))*rhoc+((rhoh*Qh)/(rhoc*Qc+rhoh*Qh))*rhoh;
cpo=((rhoc*Qc)/(rhoc*Qc+rhoh*Qh))*cpc+((rhoh*Qh)/(rhoc*Qc+rhoh*Qh))*cph;
Qo=(Qh*rhoh+Qc*rhoc)/rhoo;
To=(rhoc*Qc*cpc*Tc+rhoh*Qh*cph*Th)/(rhoh*Qh*cph+rhoc*Qc*cpc);
Po=min(Ph,Pc);
```

C.10 Y-Strainer

This file calculates the pressure drop across a 2" Y-strainer.

```
function [Po,Qo,To] = ystrain(Pin,Qin,Tm)
Qo=Qin;
To=Tm;
Po=Pin-2*6894.75729 ;  %A little overestimate on the pressure drop across a 2" Y-
strainer
```

C.11 Positive Displacement Pump

```
function [Pi,Qi,Tfi,Pdiff] = Pump1(P, Q, Tf)
global t
global PumpPressure
```

```
%Pump performance curve is a function of the selected Speed, ImpDiameter, and
Temperature

%The flow rate is set by the user
Qi=Q;

%The initial pressure out of the
%The temperature of the flui pump is set to 0, so that the negative of the output pressure
of the sytem is
%the total system pressure required for the particular flow rate set by the user.

if t==0
Pi=PumpPressure;
else
   Pi=PumpPressure-P;
end
PumpPressure=Pi;

%Fluid into the pump is set as the temperature of the fluid coming into the expansion
%tank (modeled the same as the temperature leaving the platens as there is assumed to be
no heat loss after
%the fluid exits the platens)
Tfi=Tf;
Pdiff=Pi-P;
```

C.12 Separation of Flows 1

This file calculates the separation of fluid flows after the pump outlet.

```
function [Ph,Qh,Tfh,Pc,Qc,Tfc] = PipeTSeparate1(Pin, Q, Tm, Qh1, Tfh1, Qh2, Tfh2,
diameterin)

global t
[rho,mu,cp,k]=props(Tm);

%User Defined Parameters
Di=diameterin*.0254;

%Assigns the output temperatures (same as the input)
Tfh=Tm;
Tfc=Tm;

[rhoh2,muh2,cph2,kh2]=props(Tfh2);
[rhoh1,muh1,cph1,kh1]=props(Tfh1);
Qh=((rhoh2*Qh2)+(rhoh1*Qh1))/rho;
Qc=Q-Qh;
Ph=Pin;
```

```
Pc=Pin;
```

C.13 Cold Heat Exchanger

This file uses information obtained from Maxchanger, the manufacturer of the cold heat exchanger.

```
function [Pout,Qout,Tout] = coldhex_new(Pin, Qin, Tin)
global t
%Pdrop and Tout from functions fitted to data provided by maxchanger
Pdrop=1.6481E10*Qin^2-2.2281E6*Qin;
Tout=-6.3296E-5*Tin^3+1.1668E-2*Tin^2-7.7929E-3*Tin+20.744;
[rhoi,mui,cpi,ki]=props(Tin);
[rhoo,muo,cpo,ko]=props(Tout);
Qout=Qin*rhoi/rhoo;
Pout=Pin-Pdrop;
```

C.14 Hot Heat Exchanger

```
function [Pout,Qout,Tout]=hotwatt(Pin,Qin,Tin)
watt=14400;
[rho,mu,cp,k]=props(Tin);
Tout=(watt/(Qin*rho*cp)+Tin);

[rhoi,mui,cpi,ki]=props(Tin);
[rhoo,muo,cpo,ko]=props(Tout);
Qout=Qin*rhoi/rhoo;

%Added as a place holder until the actual pressure behavior of the hot heat exchanger can
be established
Pdrop=1.6481E10*Qin^2-2.2281E6*Qin;
Pout=Pin-Pdrop;
Pout=Pin;
```

C.15 Separation of Flows 2

This file separates the fluid flows after the hot and cold heat exchangers.

```
function [P1,Q1,Tf1,P2,Q2,Tf2] = PipeTSeparate2(Pin, Q, Tm, Qin1, Qin2, diameterin)
global t

[rho,mu,cp,k]=props(Tm);

%User Defined Parameters
Di=diameterin*.0254;
```

```
%Assigns the output temperatures (same as the input)
Tf1=Tm;
Tf2=Tm;
%Calculates the flow rate into the two lines going into either the hot or cold valve
   Q1=Qin1;
   Q2=Qin2;

P1=Pin;
P2=Pin;
```

D Operation and Use Manual

D.1 Standard Use of the System

The following protocol is used to create a PMMA part using a silicon wafer tool. The most up-to-date software file automatically controls the temperature control system, but not the force subsystem.

Pretest Instructions

1. Make sure the air supply to the mixing valve positioners is set to roughly 27 psi.
2. Five ball valves are closed when the machine is not running to mitigate leakage of the Paratherm MR. Open the ball valves after the two mixing valve outlets, one at the outlet of both platens, the return to the pump inlet, and the pump outlet.
3. Check the fluid level in the cold trap tank and make sure it's around the room temperature level mark.
4. Hook up the water hose from the cold heat exchanger to the faucet and make sure the other end is going straight down the drain. If the waste doesn't go straight down the drain, the sink will overflow. Turn on the cold water to its maximum flow rate (5 GPM).
5. Turn on the exhaust fan to expel any vaporized Paratherm within the machine enclosure.
6. Turn on the heater controller, but do not increase the set point temperature above room temperature.

7. Open the LabView program called "Automate3.vi," in the Grant_Labview folder on the desktop.
8. Make sure within the "Motor Controls" panel that the "Motor Heating" and "Motor Cooling" buttons are "ON." Also, the "Motor Signal Heating" and "Motor Signal Cooling" buttons should both read "Current."
9. Open the Instron software and set the Instron to manual control.
10. Open the Merlin software and set the desired force profile needed to create the part. Maintain the end force for a long time (~15 minutes) to ensure the Instron holds the force for a sufficient amount of cooling time.
11. For the top platen, input the embossing set point temperature in "Heat SP Top" and the de-embossing set point temperature in "Cool SP Top."
12. For the bottom platen, input the embossing set point temperature in "Heat SP Bottom" and the de-embossing set point temperature in "Cool SP Bottom."
13. Make sure the controller setting in the program is set to Heating.
14. Place a 4" wafer size piece of acrylic on the bottom spacer plate and a 4" aluminum machined wafer on the acrylic. The purpose of the acrylic is to compensate for the misalignment of the platens.

Test Instructions

1. Run the program, save the file to some user defined directory and increase the set point temperature on the heater controller to 180 °C.
2. Monitor the temperature of the platens on the chart on the right side of the screen.

3. Once the temperature of both platens is near the embossing set point temperature (± 5°C), register the PMMA sample on the desired feature of the tool. (Note: Using PMMA too large in area may cause problems with de-embossing).
4. Quickly bring the top platen in close contact with the PMMA so it can heat up from both sides. This also prevents the PMMA from curling.
5. Wait approximately three minutes to ensure the PMMA reaches its equilibrium temperature.
6. Once the three minutes are up, switch over to the Merlin program and start the force/displacement profile. Also, record the timestamp on the LabView program when the Merlin program is started. This will allow for coordination of data during analysis.
7. When the force reaches its set point, monitor the displacement.
8. When the speed of the crosshead reaches a threshold of 1 μm/3 sec., go back to the LabView program and switch the controller to Cooling.
9. Monitor the temperature of both platens on the chart on the right side of the screen.
10. When the temperature reaches the cooling set point, stop the Instron from applying a force and manually disengage the top platen from the work piece.
11. De-emboss the PMMA from the tool. Practice has shown that using a razor while delicately handling the silicon wafer ensures the lowest probability of the tool breaking.
12. Once the PMMA is off the tool, the cycle can be repeated.

Posttest Instructions

1. Run the program called "55to120_3.vi," in the folder located in >>Desktop>>Grant_Labview>>DOE using Cooling control and keep the cooling set point around 50 °C.
2. Turn up the motor speed to 49 Hz to increase cooling.
3. Turn down the set point of the heater controller to 10 °C.
4. Monitor the temperature of all components in the system.
5. When the temperature of all components is below 50 °C, stop the motor in the program and then the LabView program can be stopped.
6. Turn off the power to the heater controller.
7. Turn off the water to the cold heat exchanger.
8. Turn off the exhaust fan.
9. Close the ball valves after the two mixing valve outlets, one at the outlet of both platens, the return to the pump inlet, and the pump outlet.

D.2 Operation of Controllers

D.2.1 Motor Controller Operation

The motor controller comes with a number of different options. Figure D-1 describes some parameters that may want to be configured at some point. The only two function codes which need to be changed when switching from manual to computer control are A_01 and A_02.

Func. Code	Name/SRW Display	Description	Run Mode Edit	Setting
A_01	Frequency source setting F-SET-SELECT TRM	Three options; select codes: 00...Keypad potentiometer 01...Control Terminal 02...Function F01 setting	X	01
A_02	Run command source setting F/R SELECT TRM	Two options; select codes: 01...Control Terminal 02...Run key on keypad, or digital operator	X	01
A_11	O-L input active range start frequency IN EXS 000.0Hz	The output frequency corresponding to the analog input range starting point	X	0
A_12	O-L input active range end frequency IN EXS 000.0Hz	The output frequency corresponding to the analog input range ending point	X	60
A_13	O-L input active range start voltage IN EX%S 000%	The starting point (offset) for the active analog input range	X	0
A_14	O-L input active range end voltage	The ending point (offset) for the active analog input range	X	100

	IN EX%E 100%			
A_15	O-L input start frequency enable IN LEVEL 0Hz	Two options; select codes: 00...Use offset (A_11 value) 01...Use 0 Hz	X	01
C_01	Terminal [1] function IN-TM 1 FW	Select function for terminal [1] 15 options	X	00 FW
C_03	Terminal [3] function IN-TM 3 AT	Select function for terminal [3] 15 options	X	16 AT
C_11	Terminal [1] active state IN-TM O/C-1 NO	Select logic convention, two option codes: 00...normally open [NO] 01...normally closed [NC]	X	00
C_13	Terminal [3] active state IN-TM O/C-3 NO	Select logic convention, two option codes: 00...normally open [NO] 01...normally closed [NC]	X	00

Figure D-1 Modified Programmable Drive Parameters

D.2.2 Motor Controller Notes

1. Make sure all of the inverter vents are opened before operation to prevent overheating.

2. Speed in RPM = (Frequency x 120)/# of poles.
3. The potentiometer and control terminal cannot be used at the same time. There is no override option.
4. There is an option of setting up to three jump frequencies with bounds. Since there are known resonant frequencies of the system, we can eliminate the motor from staying those frequencies.

D.2.3 Heater Controller Operation

It has been found that computer control of the heater is not necessary for normal operation of the machine. None of the features have been implemented, but the wiring is setup. The following paragraphs describe the procedures for gaining computer control of the heater controller.

The heater controller has different security levels, which gives access to certain menus. The security code is entered on the control PAGE Ctrl, at the MENU Loch. To access and enter the Security Code, press and hold RESET for more than 3 seconds to enter Setup mode. Security Lock is the first menu that will appear.

In order to gain computer control of the heater, switch #4 on the bottom of the controller needs to be down. Enable the remote set point by entering MENU rSP on the Ctrl PAGE and select ON. To scale the input signal, go to the ScAl PAGE, MENUs rSPL (remote set point low) and rSPH (remote set point high). Enter the sensor span low and high ranges. For example, for a 100 to 500 °F range, 4 mA would equal 100 °F, and 20 mA would equal 500 °F.

In order to utilize the digital input function, the rSP should be selected in the Ctrl PAGE. When the function is selected, the controller uses the Local Setpoint (Ctrl PAGE, SP) when the digital input switch is open. The remote set point is used when the switch is closed. The remote set point must be enabled (Ctrl PAGE, rSP=on) for this function to operate. The AUX indicator is ON when the remote set point is selected and OFF when the local set point is selected.

D.3 Troubleshooting the System

A number of problems occur on occasion when running the machine and the following sections should describe some problems that have been encountered. This list is not exhaustive, so consult the appendix or component manuals if the problem is not stated in one of the following sections.

D.3.1 Instron Instability

Problem: The Instron makes a grinding noise when it is in force control. It may also stop.

Solution: Tune the PID gains using the Instron software. Different materials being embossed change the effective stiffness of the system dynamics. Therefore, try to place a material of comparable stiffness you want to emboss with when tuning the PID gains.

D.3.2 Leakage near Platens

Problem: Paratherm Leaks at the interface between the hoses and platens.

Solution: Clean off the Paratherm from the surface of the interface as much as possible. Apply Loctite 6900 generously around the area of interest and try to get it to flow in most of the cracks. Let the Loctite cure at room temperature for at least 48 hours before running the machine again.

D.3.3 Possible Valve Closure

Problem: The pump makes an unusual sound and the temperatures being recorded in LabView do not reflect what should happen.

Solution: These clues typically indicate that a ball valve is closed. Sometimes the steps for operating the machine are not followed closely and a ball valve remains closed preventing normal operating flow. Check the flow meters to see if the flow is consistent with the motor setting.

D.3.4 Water is not Turned On

Problem: The temperature of the cold heat exchanger outlet remains at the same temperature as other components in the system.

Solution: It is not uncommon to forget to turn on the water to cool the cold heat exchanger. If the cold heat exchanger fluid outlet temperature is the same as other components within the system, or the system does not cool down when commanded to, it is a good indication that the water is not turned on. If this is the case, take caution when turning on the water because it can vaporize and burn you.

D.4 Draining the HME System

Maintenance, repair, or other factors may require the system to be drained of Paratherm MR fluid. The steps below outline the general procedures that should be followed to drain the system. Most fluid in the system will be removed with this technique; however, some fluid will remain in the lines leading to the platen due to the lower relative height.

1. Ensure power is off to all the major powered components of the system (heater, pump and exhaust fan). Turn off power at both the controllers and the junction boxes found on the ceiling (by pulling the boxes open).
2. Remove the aluminum panel on the front of the system (see Figure D-2) to access the bottom right side of the heater body. Note: The right side aluminum panel is a door which can simply be opened to access the heaters right side.

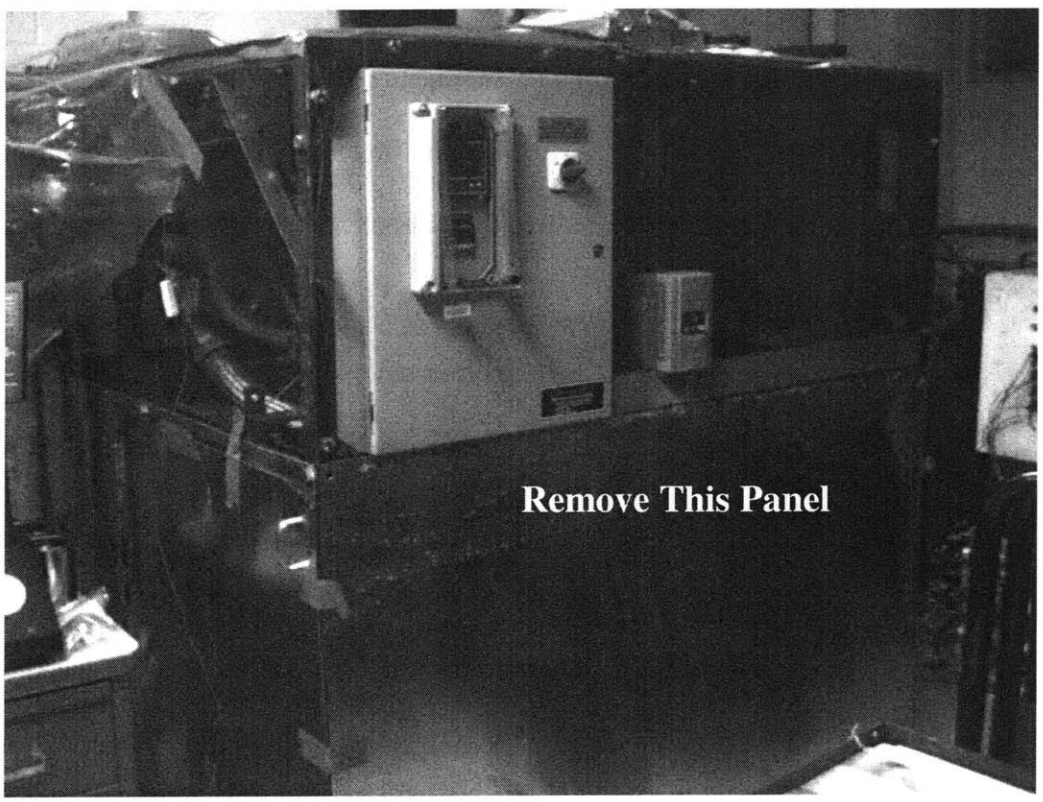

Figure D-2 Picture indicating panel to be removed from the system prior to draining

3. Set the mixing valve positions to half cold using the LabView Control program.
4. Ensure all valves in the system (including those near the expansion tank) are open.

5. Obtain: (1) two large buckets that can be easily placed and removed from under the heater body directly under the opening nut which allows the heater to be drained; and (2) two pairs of gloves resistant to organic liquids. Wear gloves and complete all subsequent steps with the help of two people if possible.

6. Place the first bucket underneath the heater opening nut and slowly open the nut until a steady and manageable flow of fluid drains from the system. If flow out of the heater is too high to manage, close a valve in the system to reduce the pressure head on the fluid exiting the heater (will reduce the flow rate). Once the flow rate has sufficiently subsided again, open the system valve that was closed to ensure the entire system is drained.

7. Switch out one bucket for the other quickly as they are filled and pour the Paratherm MR from the buckets back in the storage containers with the use of the mesh-funnel.

8. Repeat Step 6 until all the Paratherm MR is removed from the system. Note: as more fluid is removed from the system, the pressure head on the fluid remaining in the system is lower and the opening nut will have to be opened further to maintain a steady flow, until the opening nut can be removed completely to allow the last remaining amounts of Paratherm MR to drain from the system.

9. Once flow of fluid out of the heater ceases, power should be restored to the pump and it should be operated at an extremely low flow rate (on

the order of 1-2 GPM) for only a few minutes. This is to ensure no fluid remains backed-up in the system behind the pump.

10. Once all flow from the heater ceases, turn off the pump and cut its power.

11. Place Teflon tape around the opening nut and tighten the drain in the heater.

12. Clean all spilled Paratherm MR.

13. Replace the front aluminum panel that was removed to access the heater.

Note: The next time the system is drained a 1/8" ball valve and stop plug should be installed at the heater drain. A hose can then be connected to make it easier to drain the system in the future.

D.5 Re-filling the HME System

After the system has been drained and necessary maintenance, repair or other actions have been taken, the system has to be re-filled with Paratherm MR. The steps below outline the general procedures that should be followed to re-fill the system.

1. Ensure power is off to the heater and exhaust fan. Turn off power at both the controller and the heater junction box found on the ceiling (by pulling the box open).

2. Ensure all valves in the system (including those near the expansion tank) are open.

3. Ensure the fluid circuit is closed and no openings are present (missing sensors or pipe sections).

4. Begin pouring the Paratherm MR directly from the buckets to the cold baffle of the expansion tank until the tank is nearly full.

5. Wait for the level of the fluid in the system to go down and repeat Step 4 until the fluid level appears to have stabilized.

6. Turn on the pump and initially operate at 1-2 GPM. The fluid level should start going down. Repeat Step 4. Continue gradually increasing the flow rate of the pump (up to and not exceeding 39GPM) while adding fluid to the system until the fluid level in the expansion tank no longer changes. Note: monitor the noise from the pump. If excessive noise is emitting from the pump, reduce the pump flow rate or turn the pump if necessary and wait until the more fluid has time to work its way into the system. This may be a sign of pump cavitation.

7. Turn the pump off and close the valve connecting the expansion tank outlet to the pump inlet (normal operating position).

D.6 Switching out the Load Cell (1KN-50KN)

1. Place a compliant material between the top and bottom platen assemblies. Bring the two assemblies together until the top assembly is resting on the complaint material.

2. Remove the clevis pin holding the top assembly to the load cell. Use a small rubber headed hammer if necessary.

3. Disengage the top crosshead (the top assembly, now disconnected from the load cell, should remain resting on the bottom assembly).

4. Remove the three screws holding in the load cell and disconnect the communications cable between the load cell and the Instron frame.

5. Store the load cell.

6. Place the new load cell in the opening in the top crosshead and secure with the same three screws.

7. Connect the cable from the load cell to the Instron frame.

8. Open the Load Cell Calibration Protocol in the Instron software on the PC and calibrate the load cell.

9. Unscrew the top anvil from the top assembly and replace with the appropriate anvil for the new load cell.

10. Bring the top crosshead down until the pin in the top anvil enters the opening on the load cell and the holes for the clevis pin are aligned.

11. With the help of two people, one person should adjust the alignment of the top assembly while the other forces the clevis pin through the pin in the anvil and the load cell. Once the pin has been inserted, the securing device should be installed.

12. The top cross head can now be raised and the top assembly and top anvil should be secured. The compliant gasket layer can now be removed and tests can be carried out.

D.7 Changing the Platen Subsystem

1. The four screws securing the bottom steel plate to the Instron frame should be removed (this will allow the entire bottom platen assembly to move freely).

2. Place a compliant material between the top and bottom platen assemblies. Bring the two assemblies together until the top assembly is resting on the complaint material.

3. Remove the clevis pin holding the top assembly to the load cell. Use a small rubber headed hammer if necessary.

4. Disengage the top crosshead (the top assembly, now disconnected from the load cell, should remain resting on the bottom assembly).

5. Both the top and bottom assemblies are now free to move. Two people should move the entire table holding the Instron frame until the top and bottom assemblies can be moved out toward the back left of the Instron base (away from the load cell axis as shown in Figure D-3). This will allow the first generation system to be mounted in the Instron frame while still allowing the second generation system to rest on the Instron base and remain connected to the thermal-oil heat transfer system loop.

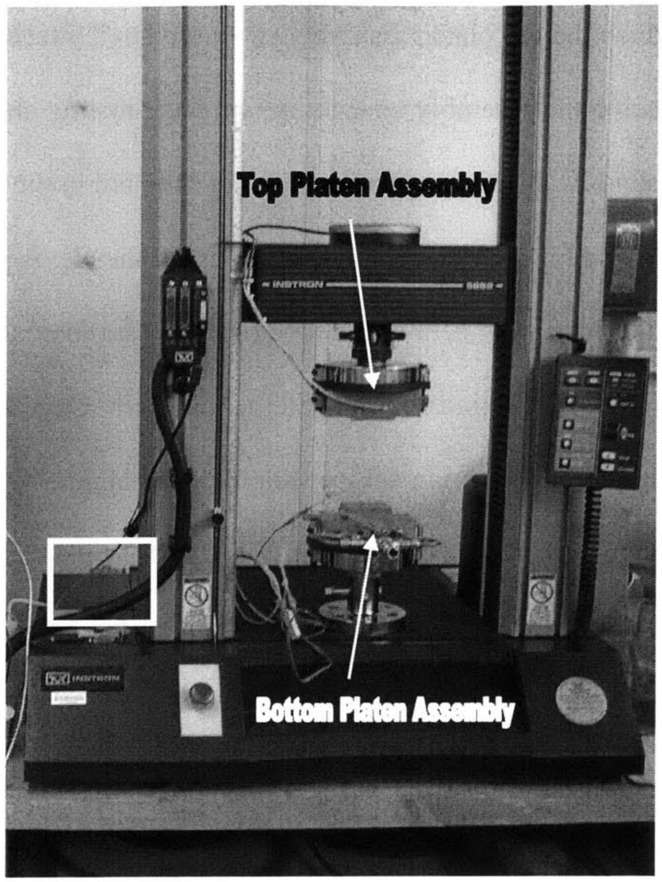

Figure D-3 Top and bottom platen assemblies for the first generation HME system and the location the second generation HME system should rest when not in use

6. Replace the centering ring on the Instron base where the bottom assembly rested.

7. Mount the bottom anvil and the first generation system bottom platen assembly.

8. Change out the load cell if required (see instructions 4-8 in Section D.6 for more details).

9. If using the same load cell, remove the top anvil still connected to the second generation system and mount it to the first generation system top platen assembly. If using a new load cell, mount the new load cells anvil to the first generation system top platen assembly.

10. Attach the top platen assembly (with top anvil attached) to the load by placing the assembly on a compliant layer resting on the bottom assembly and moving the Instron until the pin in the top anvil enters the opening on the load cell and the holes for the clevis pin are aligned.

11. Adjust the alignment of the top assembly and force the clevis pin through the pin in the anvil and the load cell. Once the pin has been inserted, the securing device should be installed.

12. The top cross head can now be raised and the top assembly and top anvil should be secured. The compliant gasket layer can now be removed and tests can be carried out.

E Thermal Fluid Model MATLAB Code

E.1 Main File

```
%Dynamic simulation for platens and heat exchangers.
%Td=command temp
%Tin=input temp to HXs Tc=output temp of CHX Th=output temp of HHX
      Tt=temp of HHX coil
%Tvo=output temp of control valve Tpi=input temp to platen Tpo=output
      temp of platen
%Tmax=max temp of coil
%Qp=flow thru platen Qc=flow thru cold branch Qh=flor thru hot branch
disp('go');
%Set up model
flag=4; watt=30E3; Tmax=190;
Qp=.00072; %System flow rate
dt=.1; %Time step size in seconds
delayv=round(2.5/dt); delayp=round(7.34/dt); %delayv=delay from valve
      to platen, delayp=from platen to HEXs
VPspeed=100;
%set up command temp profile
len=round(1000/dt); %len steps long
initial=53; %init temp
level1=170; t1=round(10/dt); %first command
level2=53; t2=t1+round(633/dt); %second command
settle=10/dt;
%generate command temp profile
    for i=1:(t1-1)
        Td(i)=initial;
    end
    for i=t1:(t2-1)
        Td(i)=level1;
    end
    for i=t2:len
        Td(i)=level2;
    end
    comgen=Td;
%Generate time variable for plotting
    for i=1:len
        Time(i)=i/dt;
    end
%Initial conditions
Th(1)=initial+127; Tc(1)=initial-21; Ts(1)=initial; Tt(1)=initial;
      TM(1)=initial;
Tin(1:1+delayp)=initial;
Tpi(1:1+delayv)=initial;
Qc(1)=Qp/2; Qh(1)=Qp/2;
VP(1)=0.5;
%break
%Program loop
for t=1:len

    %Find output of cold HX
```

```
    [Qout,Tc(t+1)] = cold2(Qc(t), Tin(t),dt);
    %Find output of hot HX
      [Qo,Th(t+1),TM(t+1)]=heater4(Qh(t),Tin(t+1),Tin(t),Th(t),TM(t),wa
      tt,dt);
    %Find outlet temp and new Current temp for platen
    [Qout,Tpo(t+1),Ts(t+1)] = platen(Qp, Tpi(t), Ts(t),dt);
    %Pipe delay between platen and HX
    Tin(t+1+delayp)=Tpo(t+1);
    %Find new flows
    %[Qh(t+1),Qc(t+1),Tvo(t+1)]=tempratios2(Td(t),Qp,Th(t),Tc(t));
      [Qh(t+1),Qc(t+1),Tvo(t+1),VP(t+1)]=valve_dyn(Td(t),Qp,Th(t),Tc(t)
      ,VP(t),dt,VPspeed);
    %Pipe delay between valve and platen
    Tpi(t+1+delayv)=Tvo(t+1);

end
%Generate Plot
figure(1)
plot(Ts,'-k')
hold on
plot(Tc,'--b')
plot(Th,':r')
hold off
set(gca,'XLim',[t1-settle,len],'YLim',[0,Tmax+10]);
Xlabel('Time (s*10)'); Ylabel('Temp (C)'); Title('Dynamic thermal
      response');
disp('Done');
```

E.2 Cold Heat Exchanger File

```
function [Qo,Tho]=cold2(Q,Thi,dt);
if Q<=0
    Q=3.15e-7;
end
Wp=4*(25.4/1000);                       %Width of a plate
Lp=24*(25.4/1000);                      %Length of a plate
Tp=0.05*(25.4/1000);                    %Thickness of a plate
Wc=0.048*(25.4/1000);                   %Width of a channel
Hc=Wp;                                  %Height of a channel
Lc=Lp;                                  %Length of a channel
TSA=22*(12*25.4/1000)*(12*25.4/1000);   %Total surface area of plates
Ac=Wc*Hc;                               %Cross-sectional area of the
      channel
P=2*Wc+2*Hc;                            %Wetted perimeter of the
      channel
Dh=(4*Ac)/P;                            %Hydraulic diameter of the
      channel
ks=16.3;                                %Thermal conductivity of 316
      Stainless Steel

%Analysis of Hot side Paratherm MR
[rhohi,muhi,cphi,khi]=props(Thi);       %Finds the fluid properties of
      the Paratherm MR hot inlet
```

```
Vp=Q/(21*Ac);                              %Velocity of Paratherm through
      a channel
mdothi=Q*rhohi;                            %Mass flow rate of Paratherm
Rep=(Vp*Dh*rhohi)/muhi;                    %Reynolds number for Paratherm
Prp=cphi*muhi/khi;                         %Prandtl number for Paratherm

%Using a chevron angle of 45 degrees
if Rep<10
    C=0.718;
    n=.349;
elseif Rep<100
    C=.4;
    n=.598;
else
    C=.3;
    n=.663;
end
Nuh=C*(Rep^n)*Prp^(1/3);

%Analysis of Cold city water
Tci=18;                                    %Temperature of the inlet city
      water (C)
Qw=6*.000063;
rhoci=1001;
muci=1080/10e6;
cpci=4184;
kci=598/10e3;
mdotci=Qw*rhoci;                           %Mass flow rate of city water
Vw=Qw/(20*Wc*Hc);                          %Velocity of water through a
      channel
Rew=(Vw*Dh*rhoci)/muci;                    %Reynolds number for water
Prw=cpci*muci/kci;                         %Prandtl number for water
                             %Flow in laminar regime
if Rew<10
    C=0.718;
    n=.349;
elseif Rew<100
    C=.4;
    n=.598;
else
    C=.3;
    n=.663;
end
%Effectiveness Heat Exchanger Analysis
Nuc=C*(Rew^n)*Prw^(1/3);
Ch=mdothi*cphi;
Cc=mdotci*cpci;
Cmin=min(Ch,Cc);
Cmax=max(Ch,Cc);
Cstar=Cmin/Cmax;
qmax=Cmin*(Thi-Tci);
Hh=Nuh*khi/Dh;
Hc=Nuc*kci/Dh;
U=1/(1/Hh+1/Hc+Tp/ks);
NTU=(U*TSA)/Cmin;
Eff=(1-exp(-NTU*(1-Cstar)))/(1-Cstar*exp(-NTU*(1-Cstar)));
q=qmax*Eff;
```

```
Tco=q/Cc+Tci;
dTo=-q/Ch;
Tho=dTo+Thi;
[rhoho,muho,cpho,kho]=props(Tho);
Qo=Q*rhohi/rhoho;
```

E.3 Hot Heat Exchanger File

```
function [Qo,To,TMo]=heater4(Qi,Ti,Tilast,Tolast,TM,watt,dt);
MassM=50;                               %Mass of the Heater + Coils
cpM=470;
Tm=Ti;                                  %(Tin+180)/2;
[rhom,mum,cpm,km]=props(Tm);
%HEX characteristics
L=38*.0254;                             %Length of shell
Nb=1;
B=L/Nb; N=36;                           %Baffle length, Number of tubes
ODt=.475*.0254;
C=.145*.0254;                           %Separation of tubes
Ds=8*.0254;                             %Diameter of shell
Pt=ODt+C;                               %Tube pitch
De=4*Pt^2/(pi*ODt)-ODt;                 %Effective HT area
As=Ds*C*B/Pt;                           %Characteristic flow area of shell
%Fluid correlations
Vs=Qi/As;                               %Fluid velocity
Re=Vs*De*rhom/mum;                      %Reynolds number
Pr=cpm*mum/km;                          %Prandtl number
Nu=.36*Re^.55*Pr^(1/3);                 %Nusselt number
h=Nu*km/De;

Ao=L*pi*ODt*N;
      %Convective area of tubes
V=pi*(4*.0254)^2*(46*.0254)-36*(pi*((.475/2)*.0254)^2*(38*.0254));
      %Volume of Fluid
[rhoi,mui,cpi,ki]=props(Ti);
[rhoil,muil,cpil,kil]=props(Tilast);
[rhool,muol,cpol,kol]=props(Tolast);
Ta=(Ti+Tolast)/2;
[rhoa,mua,cpa,ka]=props(Ta);
dTM=(h*(Ao+pi*Ds)*(Ta-TM))/(MassM*cpM);
TMo=dTM*dt+TM;
A=Qi*rhoi*cpi*Ti+watt+(rhoa*cpa*V/2)*(-Ti+Tilast+Tolast)/dt-
      h*(Ao+pi*Ds)*(Ta-TM);
To=A/(Qi*cpol*rhool+rhoa*cpa*V/2/dt);
if To>180
    To=180;
end
[rhoo,muo,cpo,ko]=props(To);
Qo=Qi*rhoi/rhoo;
```

E.4 Platen File

```
function [Qout,Tout,Tsnew] = platen(Q, Tin, Ts,dt);
```

```
[rhoi,mui,cpi,ki]=props(Tin);                           %Gets Paratherm MR
      fluid properties at inlet temperature
D=.003175;                                              %Diameter of
      channels in platen (m)
L=.132588;                                              %Length of the
      platen (m)
V=Q/(36*pi/4*D^2);                                      %Calculates the
      velocity of the fluid through a single channel
mdoti=Q*rhoi/36;                                        %Mass flow rate of
      fluid through a single channel
Re=(V*D*rhoi)/mui;                                      %Calculates the
      Reynolds number
Pr=(cpi*mui)/ki;                                        %Calculates the
      Prandtl number
if Re<2300                                              %Flow in laminar
      regime
    f=64/Re;
    Nu=3.66;
else                                                    %Flow in turbulent
      regime
    f=(.79*log(Re)-1.64)^-2;
    Nu=((f/8)*(Re-1000)*Pr)/(1+12.7*(f/8)^.5*(Pr^(2/3)-1));
end
h=(Nu*ki)/D;
Tout=(Tin-Ts)*exp(-h*(pi*D*L)/(cpi*mdoti))+Ts;          %Finds the outlet
      fluid temperature
[rhoo,muo,cpo,ko]=props(Tout);
Tmedian=(Tout+Tin)/2;
[rhom,mum,cpm,km]=props(Tmedian);
AreaP=L*pi*D*36;                                        %Calculates the
      internal platen surface area
q=h*AreaP*(Tmedian-Ts);                                 %Heat transfer from
      fluid to the copper
MassTherm=3446;                                         %Thermal mass of
      the platen including manifolds
dPt=q/MassTherm;                                        %Calculates the
      increase in platen surface temperature
Tsnew=Ts+dPt*dt;                                        %Updates the new
      platen surface temperature
Qout=Q*rhoi/rhoo;
```

E.5 Mixing Valve File

```
function [Qh,Qc,To,VPnew]=valve_dyn(Tp,Qp,Th,Tc,VP,dt,VPspeed)
%dynamic valve
if Th==0
    Th=180;
end
if Tc==0
    Tc=18;
end
[rhoc,muc,cpc,kc]=props(Tc);
[rhoh,muh,cph,kh]=props(Th);
[rhop,mup,cpp,kp]=props(Tp);
%Calculate flowrates
```

```
Qh=(Qp*rhop*cpc*(Tp-Tc))/(rhoh*cph*(Th-Tp)+rhoh*cpc*(Tp-Tc));
Qc=(Qp*rhop-Qh*rhoh)/rhoc;
low=1E-12;
if Qh<low
    Qh=low;
elseif Qh>Qp
    Qh=Qp;
end
if Qc<low
    Qc=low;
elseif Qc>Qp
    Qc=Qp;
end
Qtm=(Qh*rhoh+Qc*rhoc)/rhop;

VPd=Qh/Qp;
if abs(VPd-VP)<VPspeed
    VPnew=VPd;
else
    VPnew=VP+sign(VPd-VP)*VPspeed;
end
Qh=VPnew*Qp;
Qc=Qp-Qh;
To=((Qh*rhoh*cph*Th)+(Qc*rhoc*cpc*Tc))/(Qtm*rhop*cpp);
if To>Th
    To=Th;
elseif To<Tc
    To=Tc;
end
valve_dyn=[Qh,Qc,To,VPnew];
```

F Experimental Data

All of the experiment data in this Appendix section refers to tests explained in Section 5.9.

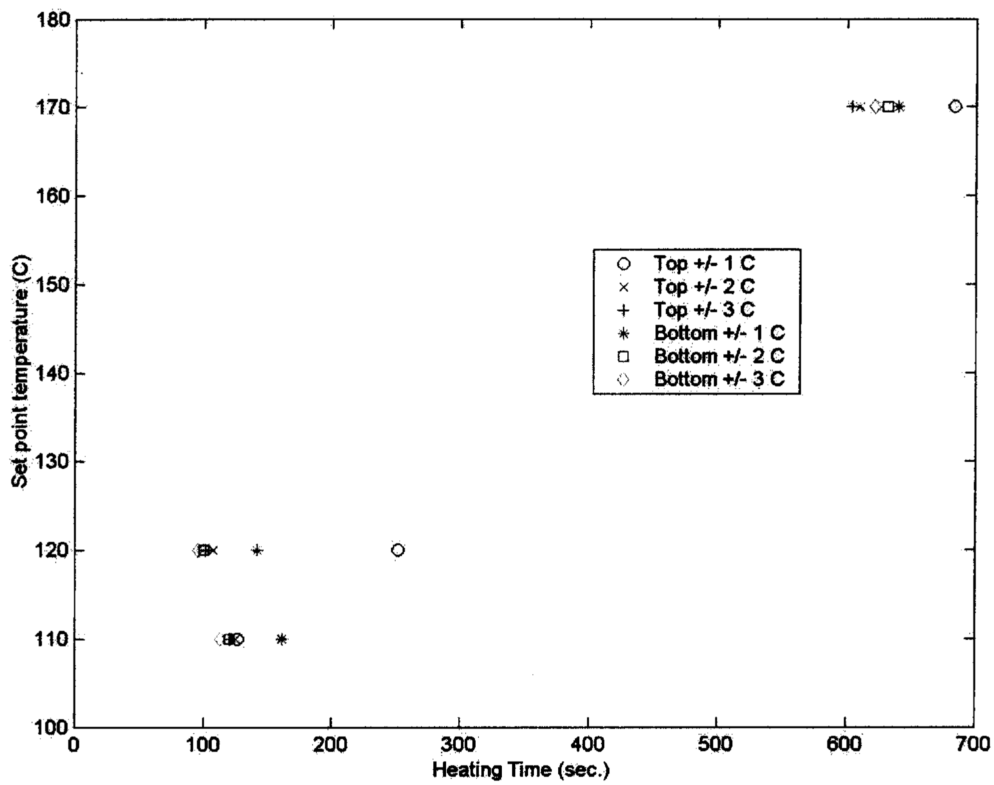

Figure F-1 Heating times for Runs 5-7

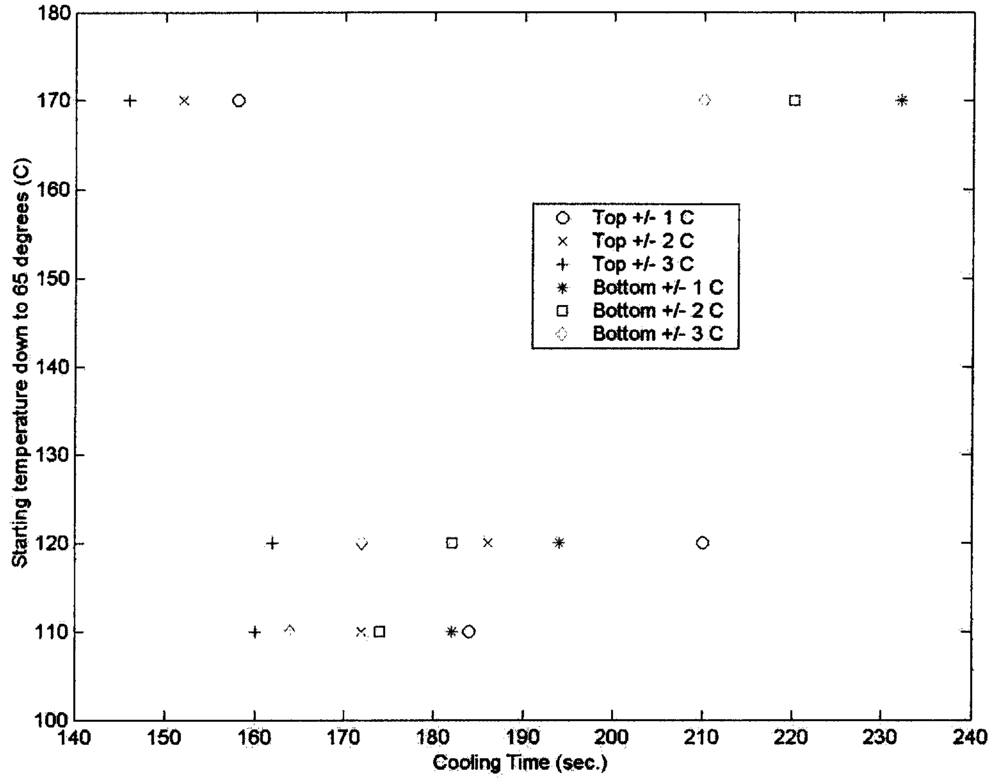

Figure F-2 Cooling times for Runs 5-7

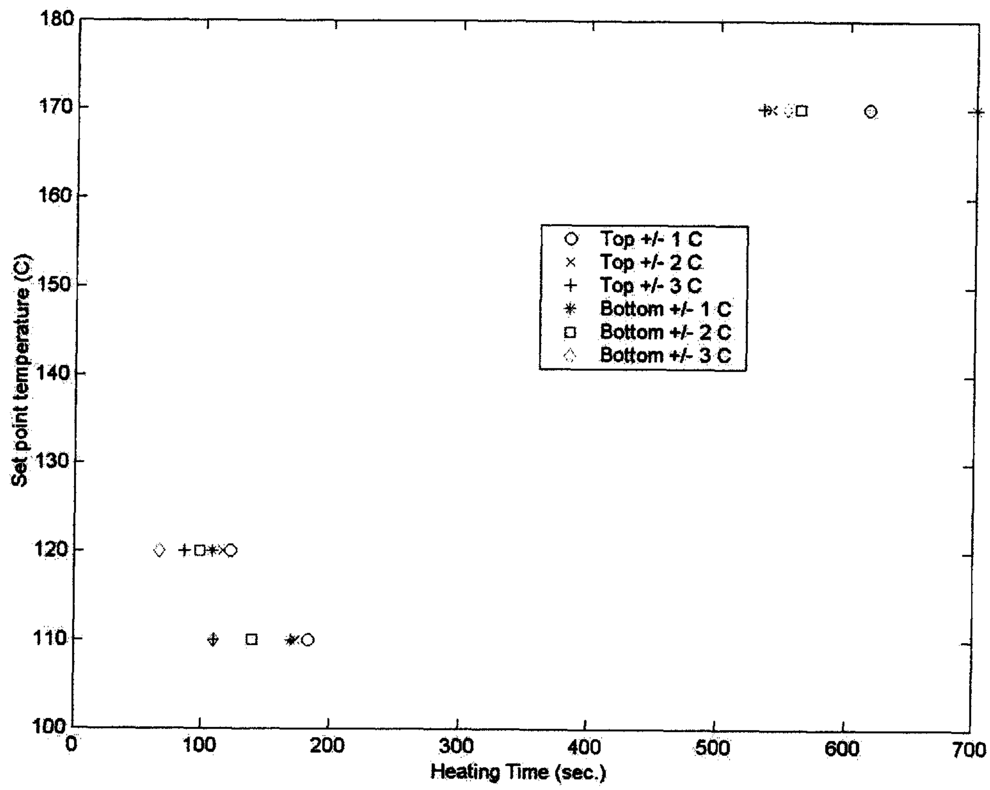

Figure F-3 Heating times for Runs 8-10

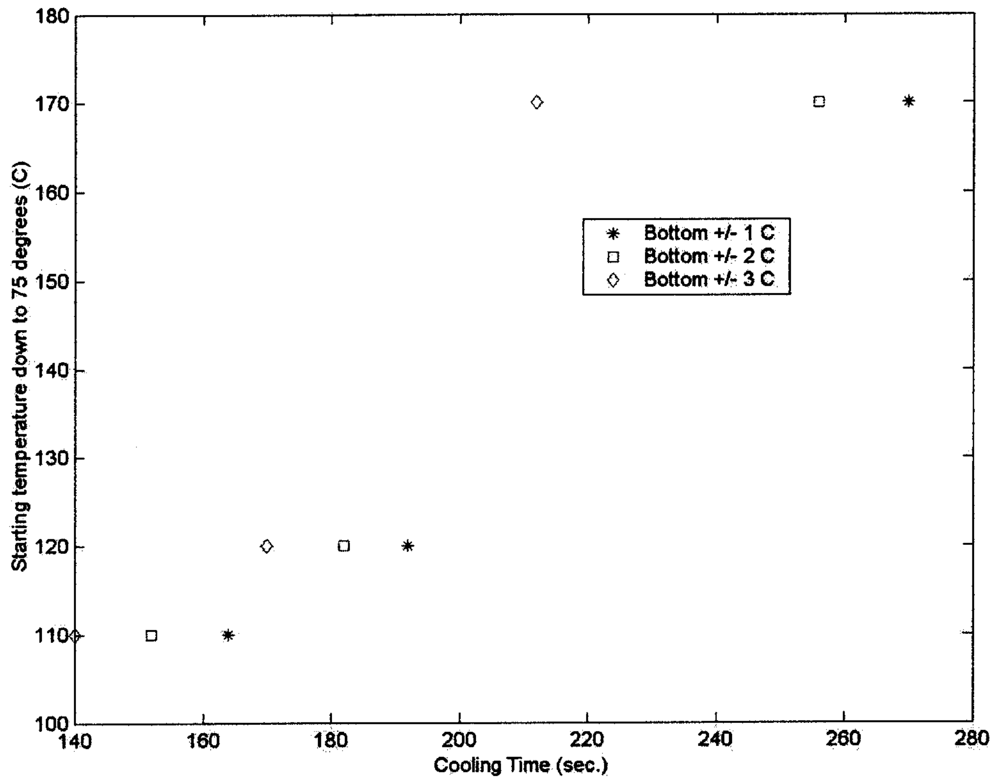

F-4 Cooling times for Runs 8-10

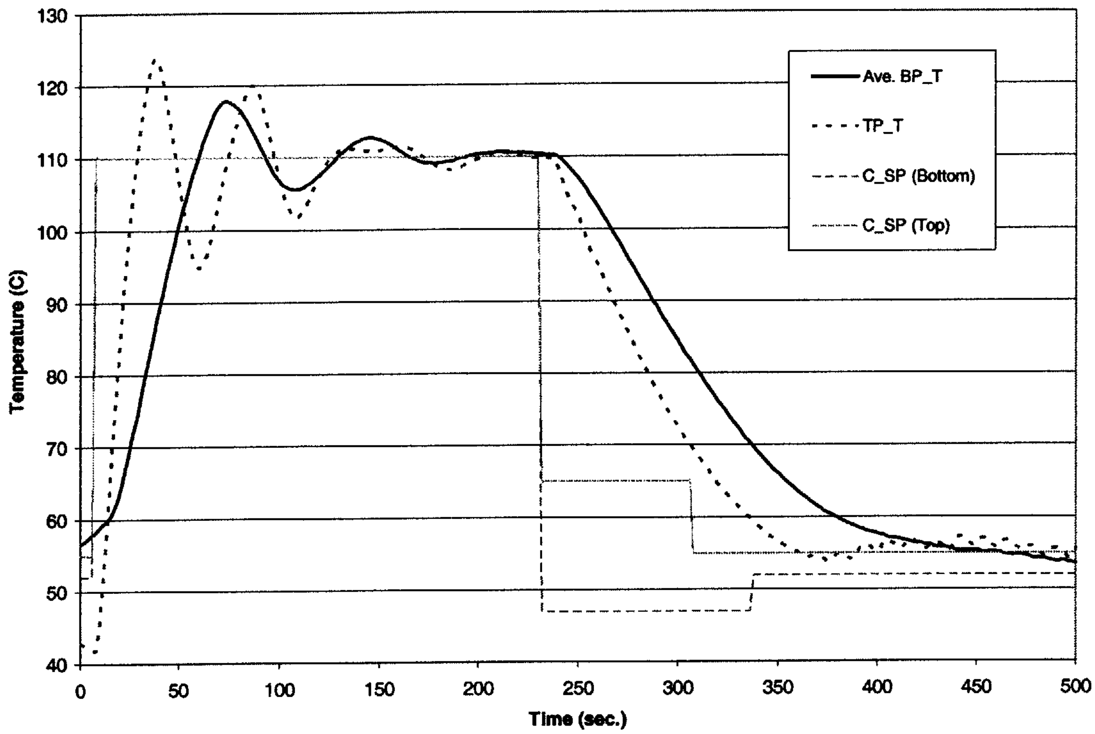

Figure F-5 Thermal Response for Run 1

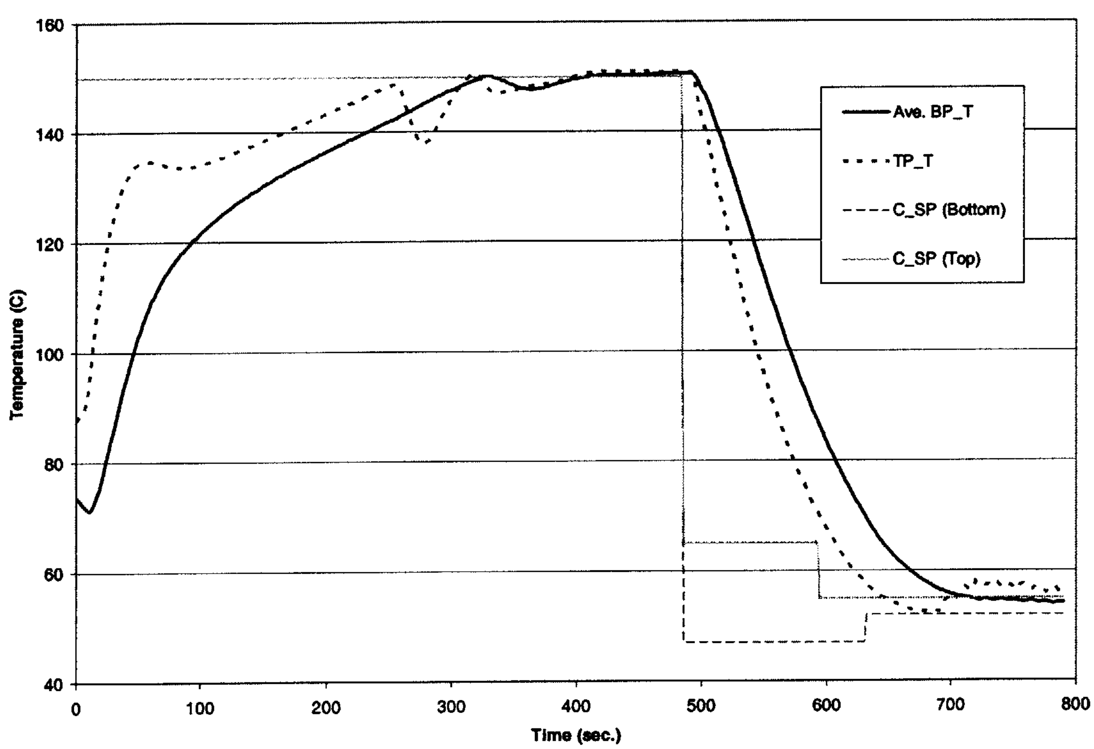

Figure F-6 Thermal Response for Run 3

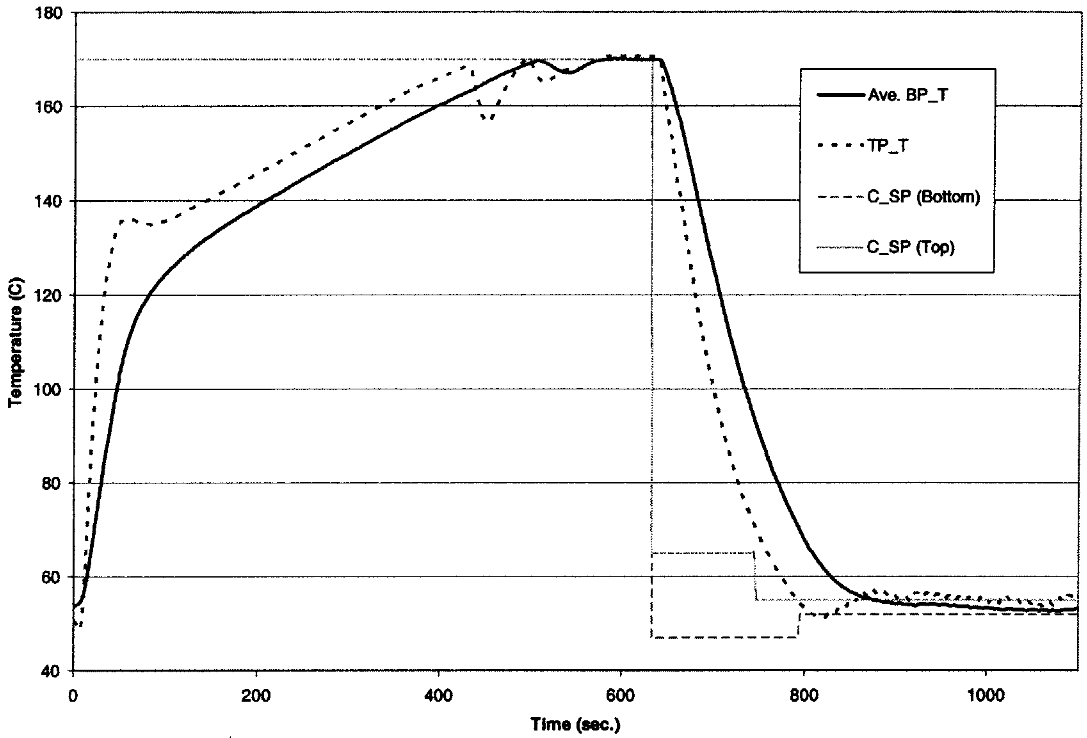

Figure F-7 Thermal Response for Run 4

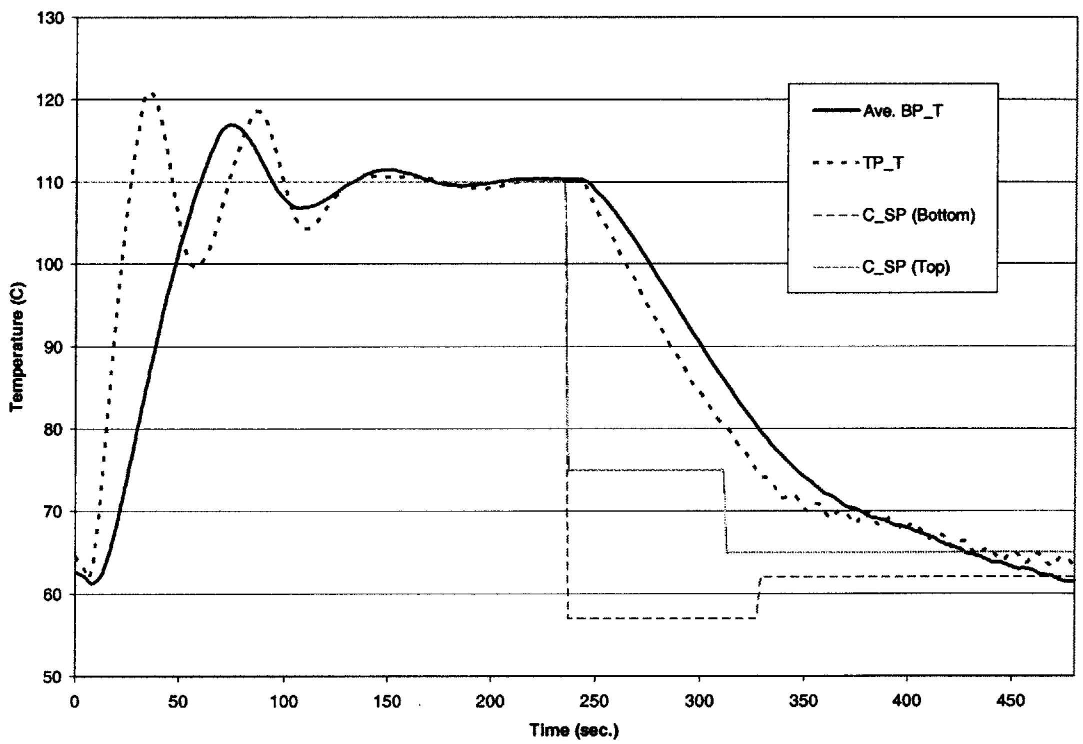

Figure F-8 Thermal Response for Run 5

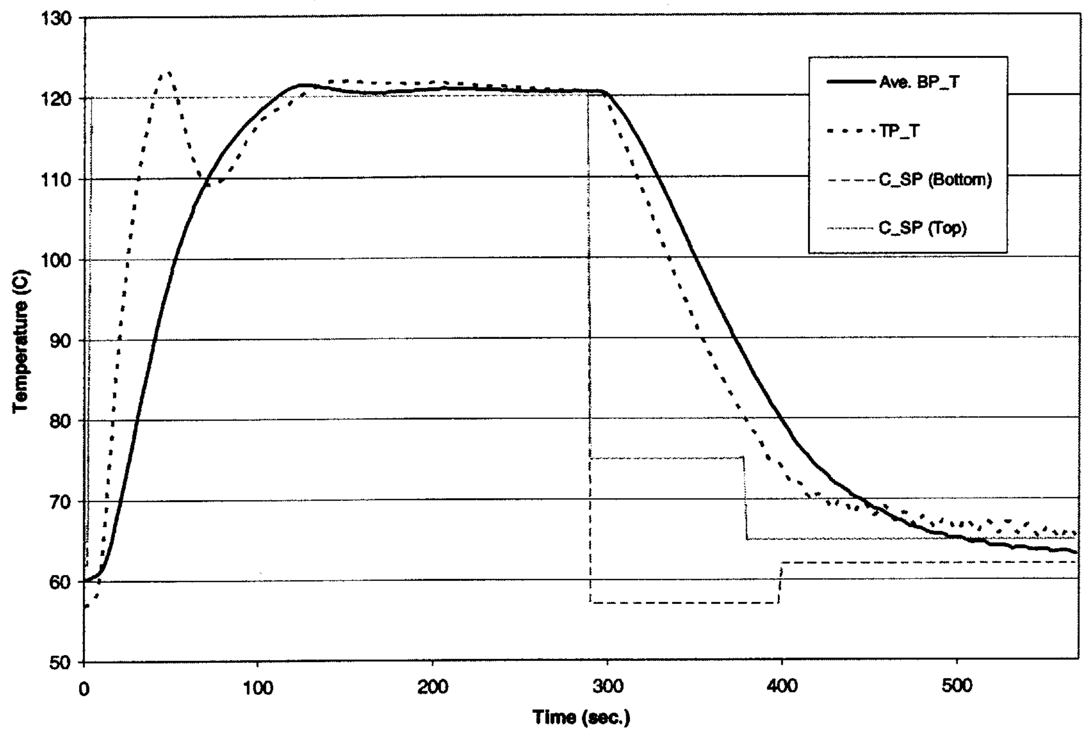

Figure F-9 Thermal Response for Run 6

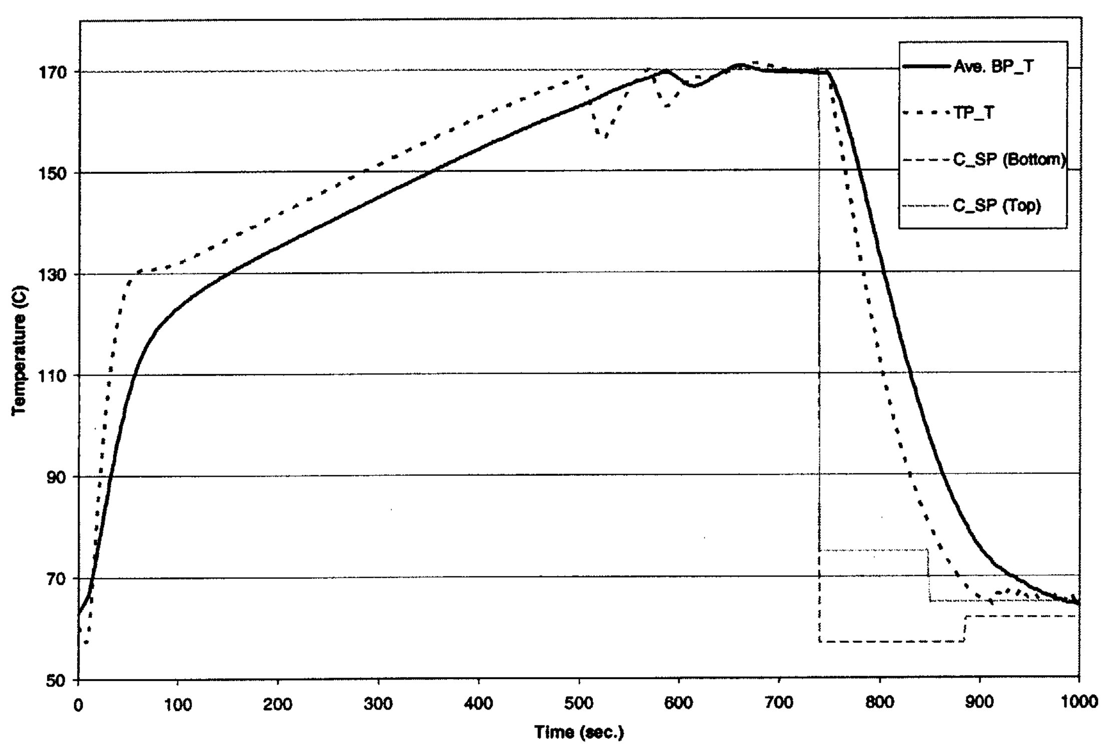

Figure F-10 Thermal Response for Run 7

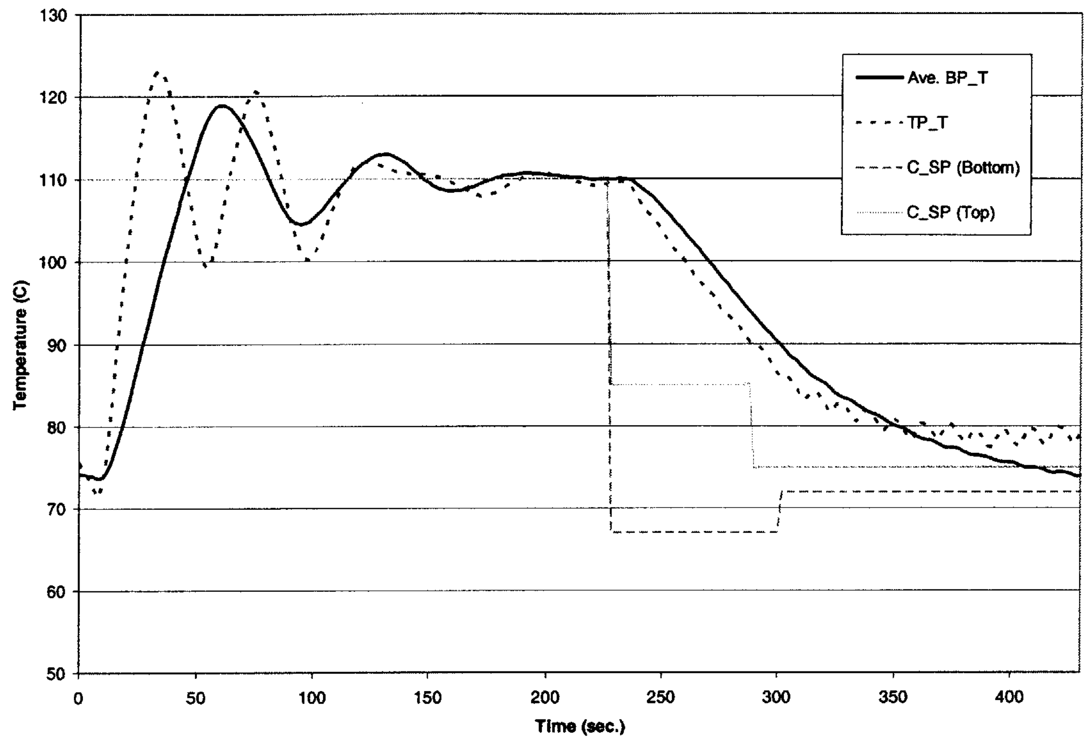

Figure F-11 Thermal Response for Run 8

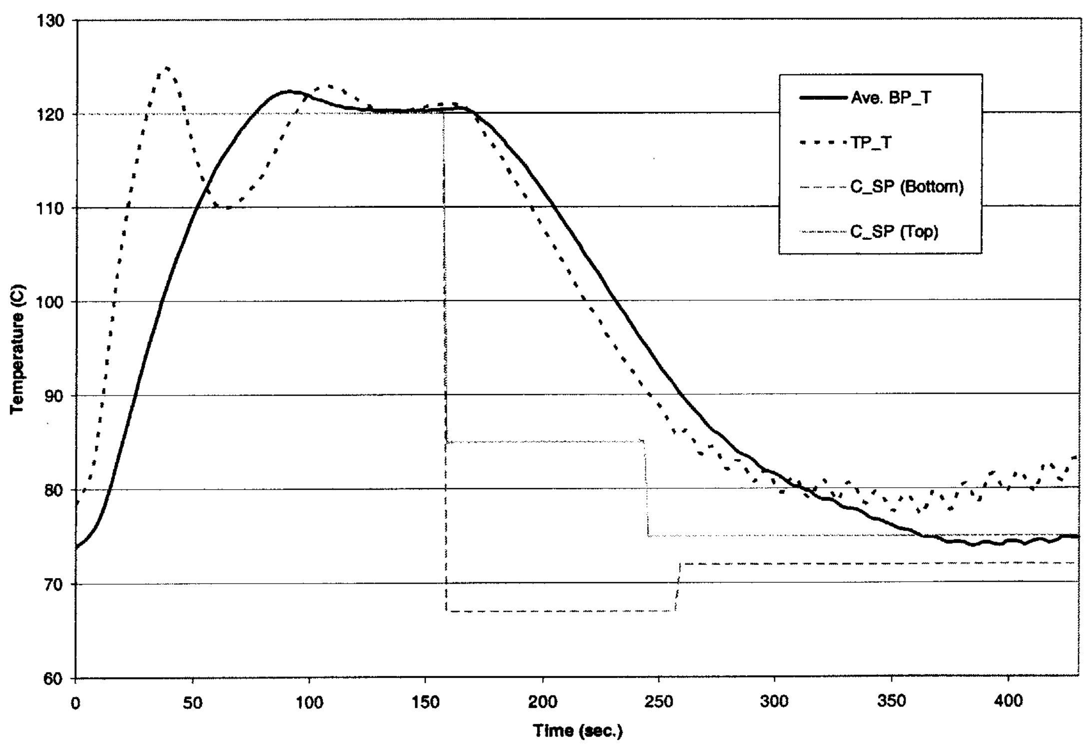

Figure F-12 Thermal Response for Run 9

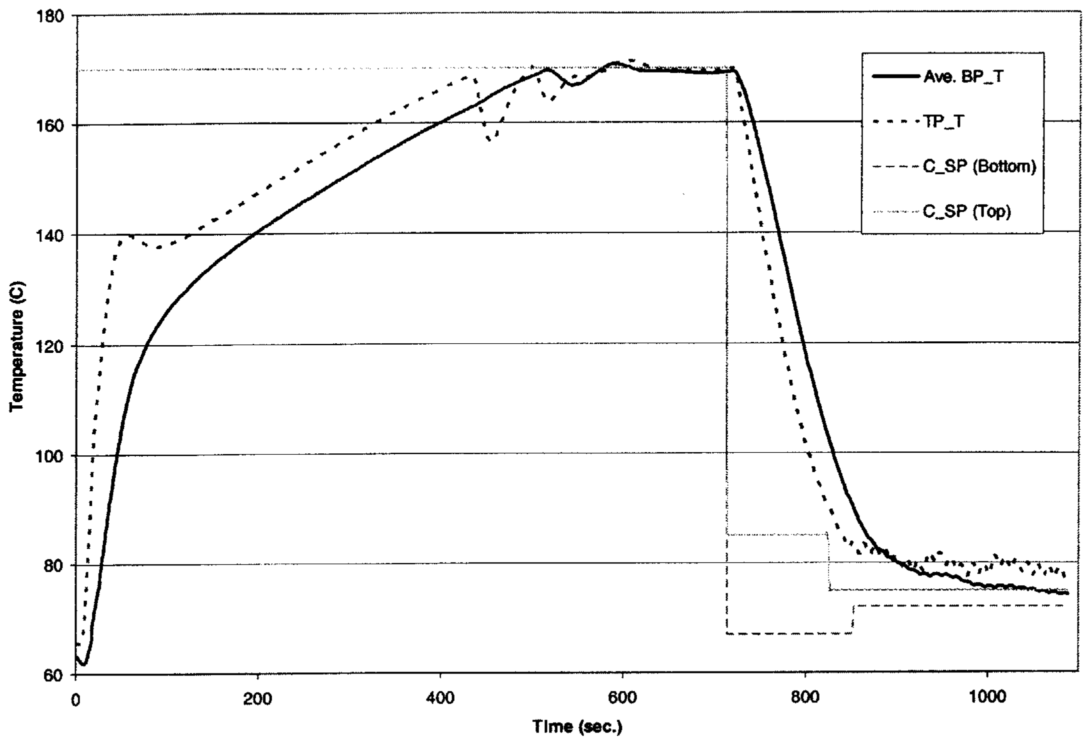

Figure F-13 Thermal Response for Run 10

G Miscellaneous

G.1 Expansion Tank Sizing

```
%System Volume estimate
manifolds=(pi/4)*1.5^2*7*4;
platens=(pi/4)*0.125^2*4.625*18*2;
coldhx=0.5*24*4*4;
hothx=(pi/4)*8^2*33-36*(pi/4)*(.475)^2*33;
pipe=pi*(.622/2)^2*110.496+pi*(.824/2)^2*9+pi*(1.049/2)^2*6+pi*(1.38/2)^2*111.84+
pi*(2.067/2)^2*148.8;
valves=2*pi*(1/2)^2*8;
pump=(1/4)/.004329;
system=manifolds+platens+coldhx+hothx+pipe+valves+pump;
expansion=system*(807.6-680)/(0.75*680-.25*807.6);
system=expansion+system;
system=system*.004329;
thermcoef=(150-30)*0.0007822;
exptank=thermcoef*system*2;
```

G.2 Paratherm System Guide

From Paratherm's technical data website:

http://www.paratherm.com/reg_eng.asp?target=/_techsheets/tech018.asp

Paratherm Corporation
Heat Transfer Fluids

Rev. 500

Recommended Hot Oil System Components

In designing and constructing a thermal oil system, attention must be paid to the selection of appropriate components. If care is not taken, poor operation, system failure and fires can result.

Pipe

Welded and flanged throughout. Specify schedule 40-ASTM-A-106 Grade B seamless carbon steel tubing. We strongly recommend the use of materials and methods to minimize entry of weld spatter and slag into the pipe, and to assure strong and leak-free welds. Pipe should be free of mill scale, welding flux, quench oils and lacquers.

Flanges/Fittings

Must be rated for 600°F (316°C) service. For optimum service we recommend 300 lb. forged steel, 1/16" raised face, schedule 40 bore (ASTM-A-181).

Studs/Nuts

Continuous threaded, alloy steel (ASTM-A-193, Grade B7), with heavy hex nuts (ASTM-A-194, Grade 2H).

Gaskets/Packings

Flange gaskets: Spiral-wound type (Flexitallic™, Garlock Flexseal™, or equal).

Valve stem packing: Rings of die-formed graphite foil (Grafoil™, Palfoil™ or equal).

Pump packing: End (non-extrusion) rings of braided carbon yarn (Palmetto™#1585, Garlock™ 498 or equal), center (sealing) rings of die-formed graphite (Grafoil™, Palfoil™ or equal).

Elastomeric O-Rings/Seals

For service to 400°F (204°C): Fluoroelastomer (Viton™, Fluorel™ or equal).

For higher temperature service, specify perfluoroelastomer rubber:
- To 450°F (232°C): Chemraz™ or equal.
- To 480°F (249°C): Zalak™ or equal.
- To 600°F (316°C): Kalrez™ or equal.

Insulation[2]

2" thick 900°F (482°C) rated cellular glass (Pittsburgh-Corning Foamglas™ or equal). Heat loss value not to exceed 80 BTU/ft.

Valves

300 lb cast or forged steel, or nodular (ductile) iron[3] rated for 600°F (316°C) continuous service minimum, with steel or stainless steel trim (Lunkenheimer™ 1110-W1 or equal; Worcester™ 4446XM or equal ball valves—specify for thermal oil application). For optimum service, bellows valves may be considered (ARI™ or equal).

NOTE: Install valves stem sideward.[2]

Pumps

Centrifugal: Cast carbon steel, carbon/tungsten carbide metal bellows mechanical seals (Dean Brothers™ R-400 or equal); magnetic drive—Sundstrand™ (Kontro), Dickow™ or equal, 'canned' (Sunstrand or equal). Positive displacement: Alloy steel, (Viking™ or equal). Flexible connections at inlet and outlet should be used.

Pressure Gauges/ Thermometers

Ratings to 100 psi, 650°F (343°C). Temperature range of 300°F to 600°F; thermometers should be calibrated to provide accurate readings in this range.

Expansion Joints

We suggest you provide for an expansion growth of 6" per 100 ft, minimum. Both loops and joint expansion devices are acceptable. Either must be high-temperature rated and must be considered part of the piping system.

Strainers

While many systems are supplied with 60 mesh mechanical screens (casings of forged or cast steel), we generally recommend 20 mesh

(cont'd. on reverse side)

1 Due to the expansion and contraction of components in the typical thermal oil system and the low viscosity, high lubricity and low surface tension of heat transfer fluids, threaded joints and compression fittings will often leak regardless of the type of sealant employed. We suggest that you back (seal) weld all threaded connections.

2 Hot organic heat transfer fluid permitted to wick through porous insulation will oxidize and decompose at system temperatures. This oxidation process creates extra heat. Confined within the insulation, the heat has little chance of escaping. Temperatures within the insulation can rise dramatically and in some cases will exceed the autoignition temperature of the heat transfer fluid. With the entry of fresh air, there is a hazard of fire (spontaneous combustion.)

Repair all leaks, and replace oil-soaked insulation immediately. Mount all valve stems facing sideward, and leave potential leak points uninsulated.

3 Ductile iron only. We do not recommend the use of cast iron in thermal oil systems.

1050 Colwell Road • Conshohocken, PA 19428 • 610-941-4900 • 800-222-3611 • FAX 610-941-9191

Recommended Hot Oil System Components

for 1/4" to 3" pipe, and .045" perforations for 4" diameter pipe and above.

NOTE: Once the construction debris is sufficiently removed from the system, some heater manufacturers remove the baskets entirely to assure no reduction in flow.

Sealants[1]

Customers report satisfactory service with Loctite™ PST to 400°F, and Fel Pro™ HPS Sealer to 600°F and Jet Lube™ TFW to 500°F. For permanent installations, satisfactory service has been reported with X-pando™.

Flow Protection

Most systems utilize a pressure differential switch to provide a method of shutting the system down when fluid flows drop below set limits. Another method used by some manufacturers is to provide *flow switches* which control flows independently through each branch of the heater.

Some systems are equipped with flowmeters in addition to the pressure differential switches. While this is an acceptable "belt and suspenders" technique, if the heat transfer fluid deteriorates, flowmeters can provide false readings.

These false readings can result from significant changes in the fluid's physical characteristics that occur with thermal degradation and normal aging.

Notes:

- Contractors must apply all national and local codes for thermal applications.
- Thermal heater room must be provided with a 2-hour fire rated enclosure.
- Full pump capacity must be maintained at all times when heater is in operation.

[redacted]

Questions? We'd like to hear from you. Call toll-free, 800-222-3611, or fax or e-mail us, [redacted] or visit our website, **www.paratherm.com.**

Rev. 500

G.3 Multitherm System Guide

From Multitherm's system design website:

http://www.multitherm.com/system-design.html

Thermal Fluid System Design

Piping:
Welded installations are recommended:

- Up through 1 1/2" - ASTM 106 Grade B Schedule 40 seamless carbon steel pipe.
- 2" through 24" - ASTM A 53 Type S Grade B Schedule 40 seamless carbon steel pipe.
- Mill scale and protective coatings should be removed prior to installation.
- Use of backing rings at pipe to pipe welds is recommended (Robvon or equal).

Threaded installations:

- Up through 1" - ASTM A 106 Grade B Schedule 80 seamless carbon steel pipe.
- 1" to 2" - ASTM A 106 Grade B Schedule 40 seamless carbon steel pipe.
- Greater than 2" - ASTM A 53 Type S Grade B Schedule 40 seamless carbon steel pipe
- Back weld all connections or use thread sealant (Felpro HPS, Copalite, X-PANDO or equal).

Flanges:
300 lb. forged steel; welded neck: 1/16" raised face, Schedule 40 bore, ASTM A 181. Use of backing rings at pipe-to flange welds in recommended.

Gaskets:
Spiral wound graphite filled (Grafoil, Flexitallic or equal) or expended/filled PTFE (Goretex, Gylon or equal).

Studs:
Alloy steel continuous threaded, ASTM A 193, Grade B7 or higher.

Nuts:
Heavy hex nuts, ASTM A 194, Grade 2H or higher.

Insulation:
Calcium silicate or fiberglass rated to 850°F is acceptable where potential for leaks is minimal. Closed cell foamed glass (Pittsburgh Corning or Equal) is recommended within several feet of flanges, valves, pipe taps or any potential leak point.

Note: Flanges should be left uninsulated to facilitate the detection of leaks. If flanges must be insulated after startup, closed cell formed glass is recommended.

Valves:
Cast or forged carbon steel; socket weld or flanged (300 lb.). Graphite or expanded/filled PTFE valve stem packing or bellows seal recommended.

Isolation Valves: Ball valves recommended (Orbit or equal)

Control Valves: Globe valves recommended

Note: Install valve stems pointing downwards to allow leaking fluid to drain away from insulation.

Pumps:
Positive Displacement: Alloy steel; gear-within-a-gear (Viking or equal) or sliding vane (Blackmer or equal).

Centrifugal: Ductile or cast iron wetted parts (Sihi, Dean brothers, Goulds, ITT, MP Pumps, or equal)

Mechanical Seals: Bellow type; carbon vs silicon/tungsten carbide seal faces recommended for low particulate loading; tungsten carbide vs. silicon carbide seal faces recommended for high particulate loading (BW/IP, A W Chesteron, John Crane, Durametallic, or equal)

Canned Motor: (Crane Chempump, Sundyne or equal)

Magnetic Drive: **(Caster, Dickow, Kontro or equal).**

G.4 HME System Bill of Materials

SECOND GENERATION HME SYSTEM BOM			
Part Description	**Cost**	**#**	**Total**
Roper 3711 Positive Displacement Pump & Motor (3 phase: 230-460V)	$2,784.00	1	$2,784.00
Hitachi L100-040HFU Motor Starter	$400.00	1	$400.00
Paxton 2830 3-way mixing valve 1/2" stainless steel body with linear trim	$858.00	2	$1,716.00
Paxton DL49 Actuator (49 sq. in.)	$374.00	2	$748.00
76E Moore 760 Electro-Pneumatic	$962.00	2	$1,924.00
Kinney-Tuthill KVO-5 Rotary Vane Pump (1 phase: 115 V)	$923.00	1	$923.00
Welded Stainless Steel Plate & Frame HX	$4,500.00	1	$4,500.00
Electric circulation heater	$3,000.00	1	$3,000.00
Chromalox SCR Power Controller with Process and High Limit Controller	$2,900.00	1	$2,900.00
5 Gallons of Paratherm MR	$210.00	5	$1,050.00
Copper			
Steel			
Insulation			
Gun drilling			
Brazing			

Welding of Expansion Tank fittings			
Electrical work done by facilities to wire the PD Pump and Hot Heat Exchanger	$1,800.00	1	$1,800.00
Anvil for the Instron	$1,000.00	1	$1,000.00
1 KN Load Cell for the Instron	$5,000.00	1	$5,000.00
2" Carbon Steel Y-strainer	$159.24	1	$159.24
2" Cast Iron (30-100 psi) Pressure Relief Valve	$330.73	1	$330.73
Loctite PST 567 (250 ml) Manufacturer #56765	$52.55	3	$157.65
Compressed Air Regulator With Pressure Gauge 1/2" Pipe Size, 5 To 60 PSI Range	$51.57	1	$51.57
Carbon Steel Hose With Galvanized Steel Braid W/Steel Male X Fem Fittings, 24" L, 1/2" ID, 300 PSI	$31.00	1	$31.00
Extra-Flex PTFE Hose With SS Wire Braid Znc-Pltd Rigid Male Fittings, 36" L, 1-1/4" ID, 1000PSI	$145.11	4	$580.44
Carbon Steel Hose With Galvanized Steel Braid W/Steel Male X Fem Fittings, 12" L, 1/2" ID, 300 PSI	$24.64	2	$49.28
Type 321 SS Hose With Type 304 SS Braid W/Male X Female Fittings, 18" L, 2" ID, 300 PSI (Same as 54905K54)	$147.73	1	$147.73
Carbon Steel Hose With Galvanized Steel Braid W/Steel Male X Female Fittings, 18" L, 1" ID, 300 PSI (Same as 56155K85)	$43.53	1	$43.53
Carbon Steel Hose With Galvanized Steel Braid W/Stl Male X Female Fittings, 12" L, 1" ID, 300 PSI (Same as 56155K85)	$39.93	1	$39.93
Carbon Steel Hose With Galvanized Steel Braid W/Stl Male X Fem Fittings, 24" L, 2" ID, 300 PSI (Same as 56155K68)	$74.83	3	$224.49
Carbon Steel Hose With Galvanized Steel Braid W/Stl Male X Fem Fittings, 36" L, 2" ID, 300 PSI	$88.99	1	$88.99
Black Welded Steel Pipe - Schedule 40 2" Pipe X 24" L, Threaded Ends, 1-1/16" Thread Length	$17.42	1	$17.42
Black Malleable Iron Pipe Fitting - 150 PSI 2" X 1/2" Pipe Size, Reducing Coupling	$7.77	3	$23.31
Black Malleable Iron Pipe Fitting - 150 PSI 1" Pipe Size, Lateral	$8.68	2	$17.36
Black Malleable Iron Pipe Fitting - 150 PSI 2" Pipe Size, Lateral	$31.73	2	$63.46
Black Malleable Iron Pipe Fitting - 150 PSI 3/4" X 1/4" X 3/4" Pipe Size, Reducing Tee	$2.74	3	$8.22
Black Malleable Iron Pipe Fitting - 150 PSI 2" X 1/2" X 2" Pipe Size, Reducing Tee	$10.60	2	$21.20
Black Welded Steel Pipe Nipple-Schedule 40 2" Pipe X 2-1/2" L, Threaded Ends, 1-1/16" L Thread	2.29	16	$36.64
Black Welded Steel Pipe Nipple-Schedule 40 1/2" Pipe X 1-1/2" L, Threaded Ends, 25/32" L Thread	$0.55	16	$8.80
Black Welded Steel Pipe Nipple-Schedule 40 3/4" Pipe X 1-1/2" L, Threaded Ends, 25/32" L Thread	$0.68	5	$3.40
Black Welded Steel Pipe Nipple-Schedule 40 1" Pipe X 2" Length, Threaded Ends, 1" Thread Length	$1.02	10	$10.20
Black Welded Steel Pipe Nipple-Schedule 40 2" Pipe X 4" Length, Threaded Ends, 1-1/16" L Thread	$2.76	2	$5.52
Black Welded Steel Pipe Nipple-Schedule 40 2" Pipe X 6" Length, Threaded Ends, 1-1/16" L Thread	$3.73	1	$3.73

Blk Forged Stl Threaded Pipe Fitting-3000 PSI 1" X 3/4" Pipe Size, Female Reducing Coupling	$6.34	4	$25.36
Blk Forged Stl Threaded Pipe Fitting-3000 PSI 1" X 1/2" Pipe Size, Female Reducing Coupling	$6.34	2	$12.68
Blk Forged Stl Threaded Pipe Fitting-3000 PSI 1-1/4" X 1" Pipe Size, Female Reducing Coupling	$7.41	2	$14.82
Blk Forged Stl Threaded Pipe Fitting-3000 PSI 2" X 1" Pipe Size, Female Reducing Coupling	$13.23	2	$26.46
Blk Forged Stl Threaded Pipe Fitting-3000 PSI 2" Pipe Size, 90 Degree Elbow	$17.84	4	$71.36
Blk Forged Stl Threaded Pipe Fitting-3000 PSI 2-1/2" X 2" Pipe Size, Female Reducing Coupling	$42.38	2	$84.76
Blk Forged Stl Threaded Pipe Fitting-3000 PSI 1/2" Pipe Size, Male X Female, 90 Degree Elbow	$6.24	2	$12.48
Blk Forged Stl Threaded Pipe Fitting-3000 PSI 1" Pipe Size, Male X Female, 90 Degree Elbow	$9.14	3	$27.42
Blk Forged Stl Threaded Pipe Fitting-3000 PSI 2" Pipe Size, Male X Female, 90 Degree Elbow	$29.20	5	$146.00
Blk Forged Stl Threaded Pipe Fitting-3000 PSI 1/2" Pipe Size, Tee	$4.27	2	$8.54
Blk Forged Stl Threaded Pipe Fitting-3000 PSI 2" Pipe Size, Tee	$22.73	2	$45.46
Grainger Ball Valve Carbon Steel, 2" NPT Female	$49.60	4	$198.40
Grainger Ball Valve Carbon Steel, 1/2" NPT Female	$11.71	6	$70.26
Grainger Ball Valve Carbon Steel, 1" NPT Female	$18.08	2	$36.16
General Purpose Stl Compression Tube Fitting Male Straight Adapter for 5/8" Tube, 1/2" NPTF	$4.88	1	$4.88
Smooth-Flow Reducing Pipe Nipple-Schedule 80 1" X 1/2" Pipe Size X 3-1/2" Length	$8.39	2	$16.78
Smooth-Flow Reducing Pipe Nipple-Schedule 80 1-1/4" X 3/4" Pipe Size X 4" Length	$13.03	2	$26.06
316 Stainless Steel Full-Port Ball Valve Lockable Lever Handle, 3/4" NPT Female	$28.85	1	$28.85
Black Welded Steel Pipe Nipple-Schedule 40 1-1/4" Pipe X 2" Length, Threaded Ends, 1" L Thread	$1.33	2	$2.66
316 Stainless Steel Full-Port Ball Valve Lockable Lever Handle, 1" NPT Female	$41.05	1	$41.05
Black Welded Steel Pipe Nipple-Schedule 40 2" Pipe X 8" Length, Threaded Ends, 1-1/16" L Thread	$6.26	1	$6.26
Blk Forged Stl Threaded Pipe Fitting-3000 PSI 2" Pipe Size, 45 Degree Elbow	$20.57	1	$20.57
Black Welded Steel Pipe Nipple-Schedule 40 2" Pipe X 12" Length, Threaded Ends, 1-1/16" L Thrd	$8.48	1	$8.48
Black Welded Steel Pipe Nipple-Schedule 40 2" Pipe X 5" Length, Threaded Ends, 1-1/16" L Thrd	$3.19	2	$6.38
Black Welded Steel Pipe Nipple-Schedule 40 1" Pipe X 5" Length, Threaded Ends, 1" Length Thread	$1.58	1	$1.58
Black Welded Steel Pipe Nipple-Schedule 40 1/2" Pipe X 5" Length, Threaded Ends, 25/32" L Thrd	$0.93	1	$0.93
Blk Forged Stl Threaded Pipe Fitting-3000 PSI 1/2" Pipe Size, 1-1/8" OD, Half Coupling	$0.83	6	$4.98
Standard Wall Black Welded Steel Pipe 1/2" Pipe X 24" L, Thrded Ends, 25/32" L Thrd, Sch 40	$4.67	1	$4.67
Blk Forged Stl Threaded Pipe Fitting-3000 PSI 1-1/4" Pipe Size, Union	$17.65	4	$70.60
PVC/Fiber-Reinforced Vibration Damping Pad 19.7" X 39.4" X 1/4" Thick, 174 PSI Maximum Load	$53.10	1	$53.10
60" of 1/4" Stainless Steel Hose with Stainless Steel Wire Braid for Vacuum Pump Connection	$44.00	1	$44.00
Blk Forged Stl Threaded Pipe Fitting-3000 PSI 3/8" X 1/4" Pipe Size, Hex Bushing	$0.87	1	$0.87

Brass Single-Barbed Tube Fitting Barbed X NPT Male for 3/32" Tube ID, 1/4" NPT	$7.18	1	$7.18
Tin-Plated Steel Pail With Cover 3 Gal Cap, 9" Top Dia, 13-3/4" HT	$15.92	1	$15.92
Low Pressure Blk Malleable Thrd Pipe Fitting 1/2" X 1/4" Pipe, Reducing Cplg, 1-1/4" L, 150 PSI	$1.42	1	$1.42
Loctite 7649 Structural Adhesives Container (Primer)	$19.74	1	$19.74
Low-Pressure Brass Threaded Pipe Fitting 1" X 3/4" Female Pipe Sz, Reducing Cplg, 1-15/32" L	$6.87	2	$13.74
All-Flow EPDM Rubber Multipurpose Hose With Brass Male X Female, 10', 3/4" ID, 200 PSI (Same as 5304K97)	$20.95	2	$41.90
All-Flow EPDM Rubber Multipurpose Hose With Brass Male X Female, 15', 1/4" ID, 200 PSI	$11.99	2	$23.98
Low-Pressure Brass Threaded Pipe Fitting 1/4" Pipe Size, Tee	$3.71	1	$3.71
Med Pressure Extruded Brass Hex Nipple 1/4" Pipe Size, 1-3/8" Length	$0.93	2	$1.86
Master-Flow Oil-Resistant Multipurpose Hose W/Brass Male X Male Fittings, 5', 1/2" ID, 250 PSI	$16.64	1	$16.64
Standard Wall Blk Steel Threaded Pipe Nipple 1/2" Pipe X 5" L, Thrded Ends, 25/32" L Thrd, Sch 40	$0.93	1	$0.93
Alloy Steel Flat Head Socket Cap Screw 1/4"-20 Thread, 3" Length, Packs of 5	$6.98	2	$13.96
Filter With Zinc Body and Bowl Manual Drain, 1/4" Pipe, 45 Scfm Max	$23.20	1	$23.20
Precision Thrd Hi-Pressure Brass Pipe Fitting 1/2" X3/8" NPT, Fem X Male Adapter, 3600PSI, 1-11/16" L	$6.32	1	$6.32
Med Pressure Extruded Brass Hex Nipple 1/2" Pipe Size, 1-13/16" Length	$2.40	1	$2.40
Med Pressure Extruded Brass Hex Nipple 1/4" Pipe Size, 1-3/8" Length	$0.93	1	$0.93
Blk Forged Stl Threaded Pipe Fitting-3000 PSI 1/2" Pipe Size, Cap	$1.42	1	$1.42
Loctite 5900 Silicone Flange Sealant 10.1-Ounce Cartridge, Black	$26.86	3	$80.58
Permatex No. 2 Form-A-Gasket Sealant 11-Ounce Tube, Black	$5.56	1	$5.56
Loctite 7649 Structural Adhesives Container (Primer)	$19.74	1	$19.74
Loctite 294- Action Bearing Company	$15.00	1	$15.00
D.L. Thurott Roper Pump parts for the Pressure Relief Valve	$15.00	1	$15.00
X-Pando Pipe Sealant from F.W. Webb and Company	$10.00	1	$10.00
Room Exhaust Fan 10" Diameter, 350 CFM, Vertical, Ceiling Mount	$74.77	1	$74.77
FLMH-1040AL-HT Flowmeter	$335.00	2	$670.00
Stainless Stl Horiz-Mount Liquid-Level Switch 316SS, 1/2"-13 Male Outside, 100 PSI	$68.31	2	$136.62
Aluminum Flexible-Sight Liquid-Level Gauge 12" Center-To-Center, 10.5" Sight Length	$22.92	1	$22.92
7671K24 Fixed-Angle ABS-Housed Glass Thermometer Angle Stem, 50 To 400 Deg F/10 To 204 Deg C	$33.62	1	$33.62
TC-K-NPT-G-72 Rugged Pipe Plug Probe with 1/4 NPT Fitting	$34.00	3	$102.00
PCI-6208 8/8 analog voltage/current output	$675.00	1	$675.00
Interface Cable and Termination Board	$79.00	1	$79.00

Standard to Mini-K Type Thermocouple Adapter	$5.00	3	$15.00
TC-(K)-NPT-G-36-DUAL 1/8" NPT Thermocouple from Omega.com	$60.00	1	$60.00
OMEGA Sensors for the Platens HKMTSS-032G-6	$31.00	6	$186.00
Light Switch Rocker, 20 Amps @ 277 Vac, SPST-No, Ivory (Same as 7030K52)	$9.24	1	$9.24
Thin-Wall Rigid Metal Conduit (EMT) Fitting Insulated Set Screw Connector, Steel, 3/4" Trade Sz	$1.57	2	$3.14
SOLDER-TYPE COMPUTER CONNECTOR, STANDARD DB25 MALE 1	$9.33	1	$9.33
SHIELDED STANDARD COMPUTER CABLE, MULTICONDUCTOR FOIL SHIELD, 25 CONDUCTOR, 0.37" OD 25	$20.25	1	$20.25
RadioShack Electronic Component Purchases	$24.00	1	$24.00
Cable Mount Adhesive Mount Strap, 1.25" Max Bundle Diameter	$13.48	1	$13.48
Indoor Steel Enclosure W/Knockouts (NEMA 1) 4" Height X 4" Width X 4" Depth	$8.69	1	$8.69
Stranded Single-Conductor Wire UL 1015, 24 AWG, 600 Vac, Blue	$6.23	2	$12.46
Thermocouple wire FF-K-20S-TWSH-25	$53.00	1	$53.00
Thermocouple Connectors (SMP-K-M)	$1.75	5	$8.75
Unistrut: 11 x 10' Green painted Carbon Steel Struts from Newman Associates	$20.00	11	$220.00
Steel Single Strut Channel Slotted, 1-5/8" X 1-5/8", Green-Painted, 10' Length (Same as 3310T3)	$25.67	5	$128.35
Corner Brace for Strut Channel Green-Painted Steel	$6.34	8	$50.72
Bracket for Strut Channel 5-Hole Connecting Plate, Green-Painted Steel	$5.56	8	$44.48
Grade 5 Zinc-Plated Steel Hex Head Cap Screw 1/2"-13 Thread, 1-1/4" Long, Fully Threaded, Packs of 50	$11.12	5	$55.60
Grade 5 Zinc-Plated Steel Hex Nut 1/2"-13 Screw Size, 3/4" Width, 7/16" Height, Packs of 100	$7.76	2	$15.52
Zinc-Plated Stl SAE High Strength Flat Washer 1/2" Screw, 17/32" ID, 1-1/16" OD, .097"-.121" Thk, Packs of 25	$4.52	6	$27.12
Strut Channel Nut W/Spring, Galv, for 1-5/8 X 1-5/8 Strut, 1/2"-13 Thrd, Packs of 5	$6.19	15	$92.85
Bracket for Strut Channel 90 Degree Angle, 4-Hole, Green-Painted Steel	$2.57	13	$33.41
Newman Associates UNISTRUT Fitting P1887GR	$12.00	4	$48.00
Newman Associates UNISTRUT Fitting P2225GR	$8.00	8	$64.00
Newman Associates UNISTRUT Fitting P2224GR	$7.30	4	$29.20
Newman Associates UNISTRUT Fitting P2341LRG	$5.50	6	$33.00
Newman Associates UNISTRUT Fitting P1031GR	$3.95	10	$39.50
Top-Mount Clamping Hanger for 3-1/2" OD, for 3" Pipe Size, 500 Pound WLL	$0.98	1	$0.98
Strut-Mount Clamp Zinc-Plated Steel, for 1-5/16" OD, 1" Pipe	$0.92	1	$0.92
Flexible Hanger Strap Galvanized Steel W/O Holes, 1" W, .036" Thk, 10'Coil	$3.97	1	$3.97
Strut-Mount Clamp Zinc-Plated Steel, for 4-1/2" OD, 4" Pipe	$2.63	1	$2.63

Top-Mount Clamping Hanger for 2-3/8" OD, for 2" Pipe Size, 275 Pound WLL	$0.55	5	$2.75
Top-Mount Clamping Hanger for 1-11/16" OD, for 1-1/4" Pipe Size, 275 Pound WLL	$0.42	2	$0.84
Strut-Mount Clamp Zinc-Plated Steel, 1/2" Tube OD	$1.12	1	$1.12
Strut-Mount Clamp Zinc-Plated Stl, for 1-1/4" Conduit, 600 lb WLL	$1.38	2	$2.76
Bracket for Strut Channel 90 Degree Angle, 2-Hole, Green-Painted Steel	$1.93	2	$3.86
Metric Blue Coated Socket Head Cap Screw M10 Thread, 35mm Length, 1.50mm Pitch, Packs of 25 (Same as 91303A900)	$8.70	1	$8.70
Metric Black-Oxide Stl Extra-Thk Flat Washer M10 Screw Size, 10.5mm ID, 23mm OD, 4.6-5.4 mm Thk, Packs of 5	$6.15	2	$12.30
Corner Brace for Strut Channel Green-Painted Steel	$6.34	8	$50.72
Bracket for Strut Channel 5-Hole Connecting Plate, Green-Painted Steel	$5.56	4	$22.24
PETG Sheet 1/8" Thick, 48" X 96"	$64.69	1	$64.69
Surface Hinge W/Holes Znc Pltd Fnsh, Removable Pin, 3" Leaf H, 2-1/2" Open W	$4.17	2	$8.34
Extruded Alum Pull Handle W/Threaded Holes Oval-Grip, Plain Finish, 3" Center To Center	$3.06	2	$6.12
ECONOMICAL PVC-COATED FIBERGLASS DUCT HOSE, 10" ID, 10-11/32" OD 10 FT	$70.20	1	$70.20
DRIE Mask	$950.00	1	$950.00
TO BE PURCHASED: Closed Cell Foam Glass w/ ASG Wrap for Carbon Steel Pipe in Hot Oil Application (Minimum 1.5" thick, Recommend: 2.0"). Fiberglass Insulation for hose areas because Foamglas is rigid.	$150.00	1	$150.00
Hand-Held Zinc-Plated Steel Plunger Drum Pump 16 Ounce/Stroke Flow Rate	$18.22	1	$18.22
Versa-Grip Strap Wrench 8" Alum Hndl, 3/4" Min Dia, 12" Max Dia, 36" Strap	$20.12	1	$20.12
Brass Single-Barbed Tube Fitting Barbed X NPT Male for 1/8" Tube ID, 1/4" NPT	$7.18	1	$7.18
Brass Single-Barbed Tube Fitting Barbed X NPT Male for 3/32" Tube ID, 1/4" NPT	$7.18	1	$7.18
Teflon Pipe Thread Tape 3/4" Width: 520" Length	$1.84	1	$1.84
6-Gallon Steel Pail with Lug Cover	$0.00	1	$0.00
Class ABC Dry Chemical Fire Extinguisher 3-A:40-B:C UL Rating, 5 lb Capacity, Wall Bracket	$30.38	1	$30.38
Light Duty Machinists' Vise 5-1/2" Jaw Width, 5" Max Opening, 3-3/16" D Throat	$59.43	1	$59.43
5 Gallons Of Mineral Spirits (Paint Thinner)	$34.18	1	$34.18
Solid-Carbide 2-Flute Twist Drill Bit Letter Size " H", 3-1/2" L O'all, 2-1/8" Flute L	$22.96	2	$45.92
Neoprene Gloves Size 9, 22 Mils Thk, 12-1/2" Length, Black, Flocked (Same as 5278T15)	$2.90	2	$5.80
Color-Coded Hygienic Scrub Brush Twisted Wire Hndl, 1-1/2" L Brush, 15" L O'all, Blue (Same as 63935T18)	$3.39	1	$3.39
All-Purpose Cleaning and Finishing Brush Polypropylene Bristle, Plastic Handle, 5/8" Bristle	$3.39	2	$6.78
Tube Fitting Brush Plumbing, 1/2" ID Tube/Fitting Size	$3.60	1	$3.60
Tube Fitting Brush Plumbing, 1" ID Tube/Fitting Size	$4.40	1	$4.40

Tube Fitting Brush Plumbing, 2" ID Tube/Fitting Size	$4.48	1	$4.48
Single-Spiral Wire Bristle Brush 302 SS, 1/2" Dia, 3" Brush L, 27" Overall L	$4.18	1	$4.18
Single-Spiral Wire Bristle Brush 302 SS, 1" Dia, 3" Brush L, 27" Overall Length	$4.45	1	$4.45
Single-Spiral Wire Bristle Brush 302 SS, 1-1/2" Dia, 3" Brush L, 27" Overall Length	$5.03	1	$5.03
Disposable Respirator Mask R95 Filter, for Nuisance Organic Vapors	$3.88	2	$7.76
Face Shield Clear, 8" H X 12" W Acetate Window, Pinlock Headgear	$12.50	1	$12.50
Color-Coded Flexible PVC Conduit (ENT) 1/2" Trade Size, 0.6" ID, 0.84" OD, Blue	$8.80	1	$8.80
Shank-Mounted Miniature Carbon Steel Brush Cup Type, 5/8" Dia, .003" Wire, 1/4" Wire Length	$2.51	1	$2.51
1/4" Shank-Mounted Crimped Wire Cup Brush Carbon Stl, 1-3/4" Dia, .006" Wire, 11/16" Wire L	$6.14	1	$6.14
Light Duty Hacksaw With 10" Long, 24 TPI Blade, 3-3/4" Throat Depth	$9.37	1	$9.37
Military Grade Teflon® Thread Sealant Tape Premium, 43'L X 3/4" W, .003" Thk, 1.2 G/CC Gravity	$3.60	1	$3.60
Graduated Glass Bottle 1 oz, 1-15/16" Dia Base, 2-13/16" Overall Height	$1.65	1	$1.65
Graduated Glass Bottle 2 oz, 1-11/16" Diameter Base, 3-5/16" Overall Height	$1.94	1	$1.94
Graduated Glass Bottle 4 oz, 2" Diameter Base, 4" Overall Height	$2.55	1	$2.55
Graduated Glass Bottle 8 oz, 2-1/2" Diameter Base, 5" Overall Height	$3.33	1	$3.33
Graduated Glass Bottle 16 oz, 3-3/16" Diameter Base, 6" Overall Height	$4.49	1	$4.49
Graduated Glass Bottle 32 oz, 3" Square, 8" Overall Height	$6.51	1	$6.51
Disposable Respirator Mask R95 Filter, for Nuisance Organic Vapors	$6.26	4	$25.04
Tin-Plated Steel Container Friction-Top Lid, Without Bail Handle, 32 Ounce	$10.81	1	$10.81
Light Duty Box Fan 20" Blade Diameter	$29.17	1	$29.17
Shank Mounted Abrasive Filament Cup Brush 2" Diameter, 80 Grit, 3/4" Bristle Length	$8.80	1	$8.80
Miniature Abrasive Filament Brush Cup Type, 9/16" Diameter, 3/8" Bristle Length	$2.67	1	$2.67
Miniature Abrasive Filament Brush Wheel Type, 1-1/4" Diameter, 3/8" Bristle Length	$3.96	1	$3.96
Double-Spiral Double-Stem Power Brush Stainless Steel, 1/4" Brush Dia, .005" Bristle Sz	$6.11	1	$6.11
Metal Handle Wire Scratch Brush .014" Steel Bristles, 5/8" X 1-3/8", 3/4" L Bristle	$5.33	2	$10.66
36" LG, 5" CAPACITY ALUMINUM PIPEWRENCHES	$90.25	1	$90.25
Three-Outlet Indoor/Outdoor Extension Cord NEMA 5-15, SJTW-Round, 14/3 AWG, 10'L, Orange	$11.90	2	$23.80
Low-Density Polyethylene Funnel 1-1/2 Gal Capacity, 9" Top OD, 10-1/2" O'all Height	$5.20	1	$5.20
Citrus Orange Soap With Scrubbing Grit 1 Gallon Pump Dispenser	$17.47	1	$17.47
Purchase Made by Matt: The small mirror, clips to secure plastic tubing, etc.			
Grainger Ball Valve Carbon Steel, 1/2" NPT Female	$11.71	1	$11.71

Grainger Ball Valve Carbon Steel, 3/4" NPT Female	$13.49	2	$26.98
Black Welded Steel Pipe Nipple-Schedule 40 2" Pipe X 2-1/2" L, Threaded Ends, 1-1/16" L Thread	2.29	3	$6.87
Black Welded Steel Pipe Nipple-Schedule 40 1" Pipe X 2" Length, Threaded Ends, 1" Thread Length	$1.02	1	$1.02
Grainger Ball Valve Carbon Steel, 1" NPT Female	$18.08	1	$18.08
Industrial-Shape Hose Coupling Push-To-Connect Socket, 1/2" NPTF Male, 3/8" Cplg Sz	$10.75	1	$10.75
Carbon Steel Hose With Galvanized Steel Braid W/Stl Male X Fem Fittings, 18" L, 2" ID, 300 PSI (Same as 56155K68)	$67.75	1	$67.75
Black Welded Steel Pipe Nipple-Schedule 40 1/2" Pipe X 1-1/2" L, Threaded Ends, 25/32" L Thread	$0.55	1	$0.55
Carbon Steel Hose With Galvanized Steel Braid W/Steel Male X Fem Fittings, 18" L, 1/2" ID, 300 PSI (Same as 56155K83)	$27.82	1	$27.82
Low Pressure Blk Malleable Thrd Pipe Fitting 1/2" X 1/4" Pipe, Reducing Cplg, 1-1/4" L, 150 PSI	$1.42	1	$1.42
Extra-Flex PTFE Hose With SS Wire Braid Znc-Pltd Rigid Male Fittings, 24" L, 1-1/4" ID, 1000PSI (Same as 54685K204)	$119.79	1	$119.79
Steel, 1/8" Pipe, Square Head Plug, 150 PSI	$0.07	1	$0.07
Brass Single-Barbed Tube Fitting Barbed X NPT Male for 1/8" Tube ID, 1/4" NPT	$7.18	1	$7.18
D.L. Thurott Roper Pump parts for the Pressure Relief Valve	$15.00	1	$15.00
POLYESTER BAG AIR FILTER, 90-95% EFFICIENCY, 5 POCKET, 24" X 20" X 22"	$33.42	1	$33.42
New High Speed Lower Accuracy PCI Board for Analog Input with Cable	$480.00	1	$480.00
Total			**$37,195.05**

References

1 "Manufacturing Processes, Equipment and Controls for the Production of Polymer-based Microfluidic Devices/Systems Research for Emerging Industries," Singapore-MIT Alliance Manufacturing Systems and Technology Research Program.

2 D. Erickson, "Towards Numerical Prototyping of labs-on-chip: Modeling for Integrated Microfluidic Devices," *Microfluid Nanofluid*, Received: 8 February 2005, Accepted: 14 March 2005, Published online: 14 July 2005, p. 301-318.

3 Larsson, O. "Biochips in Plastic-Future Technology Platforms for Drug Discovery," *Amic AB*, Business Briefing: Pharmatech 2002.

4 S. R. Quake, A. Scherer, "From Micro- to Nanofabrication with Soft Materials," *Science*, Volume 290, November 24, 2000, p. 1536-1540.

5 T. Thorsen, S. J. Maerk, S. R. Quake, "Microfluidic Large-Scale Integration," *Science*, Volume 298, October 18, 2002, p. 580-584.

6 M. Krishnan, V. Namasivayam, R. Lin, R. Pal, M. Burns, "Microfabricated Reaction and Separation Systems," *Analytical Biotechnology*, 2001, p. 92-98.

7 C. H. Ahn, J. Choi, G. Beaucage, J. H. Nevin, J. Lee, A. Puntambekar, J. Y. Lee, "Disposable Smart Lab on a Chip for Point-of-Care Clinical Diagnostics," *Proceedings of the IEEE*, Vol. 92, No. 1, January 2004, p. 154-173.

8 M. G. Alonso-Amigo, "Polymer Microfabrication for Microarrays, Microreactors and Microfluidics," Mildendo GmbH US Operations.

9 L. Eldada, "Microphotonics: Hardware for the Information Age," *MIT Microphotonics Center Industry Consortium*, The Microphotonics Center at MIT, 2005.

10 T. Otto, A. Schubert, J. Bohm, T. Gessner, "Fabrication of Micro Optical Components by High Precision Embossing."

11 M. Rossi, I. Kallioniemi, "Micro-optical modules fabricated by high-precision replication processes," *Presented at OSA topical meeting "Diffractive optics and micro-optics"* June 3-6, 2002; Tucson

12 J. R. Webster, M. A. Burns, D. T. Burke, C. H. Mastrangelo, "Monolithic Capillary Electrophoresis Device with Integrated Fluorescence Detector," *Analytical Chemistry*, Received on April 19, 2000, Accepted on December 17, 2000.

13 Z. Jia, Y. Lee, Q. Fang, C. W. Huie, "Fluorescence Imaging of Sample Zone Narrowing and Dispersion in a Glass Microchip: The Effects of Organic Solvent

(acetonitrile)-Salt Mixtures in the Sample Matrix and Surfactant Micelles in the Running Buffer," *Electrophoresis* 2006, 27, p.1104-1111.

14 H. Becker, C. Gartner, "Polymer microfabrication methods for microfluidic analytical applications," *Electrophoresis 2000*, 21, p.12-26.

15 N. Rana, S. Yau, "Construction of low-dimensional assemblies of nanoparticles," *Nanotechnology,* 15, 2004, p.275-278.

16 M. Satyanarayana, "Microfluidics: The Flow of Innovation Continues," *NCI Alliance for Nanotechnology in Cancer*, August 2005.

17 P. Mach, M. Dolinski, K. W. Baldwin, J. A. Rogers, C. Kerbage, R. S. Windeler, B. J. Eggleton, "Tunable microfluidic optical fiber," *Applied Physics Letters*, Volume 80, Number 23, 10 June 2002.

18 J. Ouellette, "A New Wave of Microfluidic Devices," *The Industrial Physicist*, August/September 2003.

19 P. F. Man, D. K. Jones, C. H. Mastrangelo, "Microfluidic Plastic Capillaries on Silicon Substrates: A New Inexpensive Technology for Bioanalysis Chips," *IEEE* 1997, p. 311-316.

20 P. Hadaegh, S. Lin, L. Schenato, C. W. Yiu, "The Global Pharmaceutical Market," May 15, 2002.

21 J. Clayton, "Go with the Microflow," *Nature Methods*, Vol.2 No.8, August 2005, p. 621-627.

22 G. T. A. Kovacs, *Micromachined Transducers Sourcebook*, WCB McGraw-Hill, 1998.

23 L. Lin, Y. T. Cheng, C. J. Chiu, "Comparative study of hot embossed micro structures fabricated by laboratory and commercial environments." *Microsystem Technologies*. Vol 4, 1998, p 113-116.

24 X.-J. Shen, L. Pan, L. Lin, "Microplastic embossing process: experimental and theoretical characterizations," *Sensors and Actuators* A (2002), p. 428-433.

25 C. Chen, F. Jen, "Fabrication of Polymer Splitter by Micro Hot Embossing Technique," *Tamkang Journal of Science and Engineering*, Vol. 7, No. 1, p. 5-9 (2004).

26 D. Hardt, M. Dirckx, G. Shoji, K. Thaker, W. Qi, "Process Control for Microembossing: Basic Characterization Studies," Laboratory for Manufacturing and Productivity.

27 Q. Wang, *Process window and variation characterization of micro embossing process*, S.M. Thesis, Massachusetts Institute of Technology, 2006.

28 Y. Xia, G. M. Whitesides, "Soft Lithography," *Annual. Rev. Material. Science*, 1998. 28:153–84.

29 M. Dirckx, *Design of a Fast Cycle Time Hot Micro-Embossing Machine*, S.M. Thesis, Massachusetts Institute of Technology, 2005.

30 M. Heckele, W. K. Schomburg, "Review on micro molding of thermoplastic polymers," *Journal of Micromechanics and Microengineering*, 14 (2004) R1-R14.

31 O. Rotting, W. Ropke, H. Becker, C. Gartner, "Polymer microfabrication technologies," *Microsystem Technologies*, 8 (2002), p. 32-36.

32 D. Hardt, B. Ganesan, M. Dirckx, G. Shoji, K. Thaker, "Process variability in micro-embossing." Singapore MIT Alliance Program in Innovation in Manufacturing Systems Technology, Singapore, Jan. 2005.

33 B. Ganesan, *Process control for micro embossing: Initial variability study.* S.M. Thesis, Massachusetts Institute of Technology, 2004.

34 C. Lu, Y. Juang, L. J. Lee, "Numerical Simulation of Laser/IR Assisted Micro-Embossing," The Ohio State University.

35 S. Liu, Y. Dung, "Hot Embossing Precise Structure Onto Plastic Plates by Ultrasonic Vibration," *Polymer Engineering and Science*, 2005.

36 J.-H. Chang, S.-Y. Yang, "Development of fluid-based heating and pressing systems for micro hot embossing," *Microsystem Technologies*, 11 (2005), p. 396-403.

37 Obducat Product Catalog. Retrieved on April 24, 2006 from http://www.obducat.com/pdf/Product_Catalog_2006_ver1.pdf

38 Jenoptik Product Website. Retrived on April 24, 2006 from http://www.jo-mt.de/cps/rde/xchg/SID-26EE34DB-B801E062/mikrotechnik/hs.xsl/2481.htm and http://www.jo-mt.de/cps/rde/xchg/SID-26EE34DB-B801E062/mikrotechnik/hs.xsl/2478.htm

39 EV Group Product Website. Retrieved on April 24, 2006 from http://www.evgroup.com/downloads/evg520he.pdf

40 *5800 Series: Materials Testing System for the Most Demanding Applications.* Instron Materials Testing Corporation. Canton, MA.

41 Control Valve Sizing for Water Systems. (2006, April 10). *Spirax Sarco Learning Centre*. Retrieved April 10, 2006 from http://www.spiraxsarco.com/learn/modules/6_3_01.asp

42 Valve Sizing and Selection. (2006, April 10). *CheResources*. Retrieved April 10, 2006 from http://www.cheresources.com/valvezz.shtml

43 *Pnematic Actuated Industrial Valves. Series 2800: Sizes ½ to 2 inches: Precision Globe Valves*. Warren Controls Product Specification Manual for Two-Way and Three-Way, Reciprocating Bronze or Stainless Steel Body Valves for Process and Utility Applications. March 2005.

44 Centrifugal Pumps: Basic Concepts of Operation, Maintenance, and Troubleshooting (Part- I) Page 2. (2006, April 10). *CheResources*. Retrieved April 10, 2006 from http://www.cheresources.com/centrifugalpumps5.shtml

45 Driedger, Walter. *Controlling Positive Displacement Pumps*. First published in *Hydrocarbon Processing* , May 1996. Retrieved April 10, 2006 from http://www.driedger.ca/ce2_pdp/CE2_PDP.html

46 External Gear Pump. (10 April 2006). *California State University, Fresno Agricultural Association*. Retrieved April 10, 2006 from http://cast.csufresno.edu/agedweb/agmech/graphics/Hydraulics6.gif

47 Centrifugal Pumps: Basic Concepts of Operation, Maintenance, and Troubleshooting (Part- I) Page 1. (2006, April 10). *CheResources*. Retrieved April 10, 2006 from http://www.cheresources.com/centrifugalpumps4.shtml

48 *Hitachi: L100 Series Inverter Instruction Manual: NB576XC*. Hitachi Industrial Equipment Systems Co., Ltd.

49 *Understanding SCR Power Controllers*. (10 April 2006). Avatar Instruments. Retrieved April 10, 2006 from http://www.avatarinstruments.com/scr.htm

50 *Liquid Phase Systems Design Guide*. Therminol Heat Transfer Fluids by Solutia. (1999): 9-10. Retrieved April 10, 2006 from http://www.therminol.com/pages/tools/liquid.asp

51 6208/6216 Series Multi-channel Analog Output Cards-User's Guide. (2006, April 11). *NuDAQ*. Retrieved April 11, 2006 http://www.adlinktech.com/PD/marketing/Manual/PCI-6208+6216Series/PCI-6208+6216Series_Manual_1.pdf

52 *2104 Chromalox Temperature Controller Technical Manual 0037-75276*. Chromalox Instrument and Controls. May 1996.

53 *1600 High-Low Limiter User's Manual 0037-75331*. Chromalox Instrument and Controls. October 2000.

54 Energy Conservation & Renewable Energy. (2006, April 10). *Kansas State University Engineering Extension*. Retrieved April 10, 2006 from http://www.engext.ksu.edu/henergy/envelope/ventilation.asp#winter

55 D. P. Campbell, *Dynamic Behavior of the Production Process..........Process Dynamics*, John Wiley and Sons, Inc., 1958.

56 W. S. Janna, *Design of Fluid Thermal Systems*. PWS Publishing Co. 1998.

57 F. P. Incropera, D. P. DeWitt, *Fundamentals of Heat and Mass Transfer*, Fifth Ed. John Wiley & Sons, Inc., 2002.

58 Maxchanger Product Specification Sheet

59 S. Kakac, H, Liu, *Heat Exchangers Selection, Rating, and Thermal Design*, 2nd Ed. CRC Press, 2002.

60 L, Thomas, *Heat Transfer*, Prentice-Hall, Inc., 1992.

61 R. Shah, D. Sekulic, *Fundamentals of Heat Exchanger Design*, John Wiley & Sons, Inc., 2003.

62 Control Valve Handbook. (2006, April 18). Emerson Process Management. Retrived April 18, 2006 from http://www.documentation.emersonprocess.com/groups/public/documents/book/cvh99.pdf

63 M. A. A. S. Choudhury, V. Kariwala, S. L. Shah, H. Douke, H. Takada, N. F. Thornhill, "A simple test to confirm control valve stiction," *IFAC World Congress,* July 4-8, 2005, Praha.

64 M. A. A. S. Choudhury, N. F. Thornhill, S. L. Shah, "Modelling Valve Stiction," *Control Engineering Practice 13*, 2005, p. 641-658.

65 J. Deschenes, A. Pomerleau, "Process Control Through a Case Study: A Mixing Process. I. SISO Case," Accepted April 29, 2005, p. 324-332.

66 N. Bonavita, J. C. Bovero, R. Martini, "Tuning Loop: Control performance and diagnostics," *ABB Process Solutions & Services SpA Via Hermada, 6-16154 Genoa.*

67 LabJack UE9 User's Guide, Revision 1.04, LabJack Corporation, January 9, 2006.

68 N. S. Nise, *Control Systems Engineering*, Third Edition, John Wiley & Sons, Inc., 2000.

69 K. Miyoshi, "Surface Characterization Techniques: An Overview," Glenn Research Center, July 2002.

70 FEI/Philips XL 30 FEG ESEM, with Electron Backscatter Diffraction analysis and Energy-Dispersive X-ray capability, retrieved on April 25, 2006 from http://prism.mit.edu/facilities/XL30/xl30home.htm.

71 M. Madou, L. J. Lee, K. W. Koelling, S. Daunert, S. Lai, C. G. Koh, Y.-J. Juang, L. Yu, Y. Lu, "Design and Fabrication of Polymer Microfluidic Platforms for Biomedical Applications," *ANTEC*, 2001.

72 J. Hruby, "LIGA Technologies and Applications," *MRS Bulletin*, April 2001.

73 E. Uhlmann, S. Piltz, U. Doll, "Machining of micro/miniature dies and moulds by electrical discharge machining-Recent development," *Journal of Materials Processing Technology*, 167 (2005), p. 488-493.

74 J. Zhang, K. L. Tan, G. D. Hong, L. J. Yang, H. Q. Gong, "Polymerization optimization off SU-8 photoresist and its applications in microfluidic systems and MEMS," *Journal of Micromechanics and Microengineering*, 11 (2001), p. 20-26.

75 R. Jurischka, Ch. Blattert, I. Tahhan, C. Muller, A. Schoth, W. Menz, "Rapid processing of replication tools with high-aspect-ratio microchannels for microfluidics," *Proc. of SPIE,* Vol. 5718, p. 65-72.

76 K. Thaker, *Design of a Micro-Fluidic Functional Testing System for Process Characterization of a Hot Micro-Embossing Machine*, S.M. Thesis, Massachusetts Institute of Technology, 2006.

77 N. Roos, M. Wissen, T. Glinsner, H. C. Scheer, "Impact of vacuum environment on the hot embossing process." Presented at SPIE's symposium Microlithography, Feb. 22-28, 2003, Santa Clara CA

2640 - 68